

AN INVESTIGATION ON THE PREPARATION AND PROPERTIES OF CERTAIN SEMICONDUCTING SULPHIDE THIN FILMS

Thesis submitted by

K. S. JOSEPH

*in partial fulfilment of the
requirements for the Degree of
Doctor of Philosophy*

**SOLID STATE PHYSICS LABORATORY
DEPARTMENT OF PHYSICS
UNIVERSITY OF COCHIN**

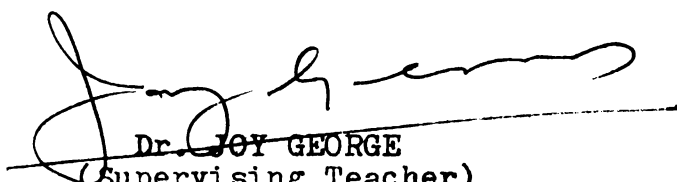
1983

To my parents

for imparting the best possible education
within their limited means to their son

CERTIFICATE

Certified that this thesis is based on the work done by Mr. K.S. Joseph under my guidance in the Department of Physics, University of Cochin and none of this has been presented by him for any other degree.



Dr. JOY GEORGE
(Supervising Teacher)
PROFESSOR IN INDUSTRIAL PHYSICS
DEPARTMENT OF PHYSICS,
UNIVERSITY OF COCHIN.

Cochin-22,
22nd December, 1983.

DECLARATION

Certified that the work presented in this thesis is based on the original work done by me under the guidance of Professor Joy George in the Department of Physics, University of Cochin, and has not been included in any other thesis submitted previously for the award of any degree.

Cochin-22,
22nd December, 1983.


K.S. JOSEPH.



SYNOPSIS

AN INVESTIGATION ON THE PREPARATION AND PROPERTIES OF CERTAIN SEMICONDUCTING SULPHIDE THIN FILMS

In this thesis the preparation and properties of thin films of certain semiconducting sulphides (sulphides of tin, copper and indium) are reported. As single source evaporation does not yield satisfactory films of these compounds for a variety of reasons, reactive evaporation of the metal in a sulphur atmosphere has been used for film preparation. It was found that for each metal sulphide a stoichiometric interval of fluxes and substrate temperature exists for the formation of the compound in accordance with the analysis of Guenther.

As the particles used for film formation in reactive evaporation are of low energy, chemical reaction rate is low and also because a high partial pressure of the volatile component is used, there is the possibility of the volatile component getting entrapped in the film which will adversely affect its properties. To avoid these difficulties the particles for film formation has been activated using a low pressure electric discharge obtained with the help of a low voltage electron gun and a magnetic field. This process known as

activated reactive evaporation increases chemical reactivity so that high deposition rates are possible and also eliminates the possibility of unreacted volatile component getting entrapped in the growing film. Activated reactive evaporation hitherto used only when the reactive substance is in a gaseous state at room temperature (eg. O_2 and C_2H_2) has been successfully extended to the case of a solid reactive substance like sulphur and sulphide films used in this study have been prepared using this technique also. Films with very good optical quality have been obtained by this method.

The formation of compound films in these evaporation techniques which is not well understood, has been discussed in terms of the kinetic energy of the particles used for film formation.

The films were characterized with respect to their structure and morphology by X-ray diffraction, scanning electron microscopy, and optical microscopy. It has been found that these films when deposited on to room temperature substrates are amorphous in nature. As the substrate temperature is increased, crystalline films with certain particular orientation have been obtained. It can be said that these methods of preparation of the films are very efficient for the preparation of amorphous sulphides.

Optical properties of the films have been studied in the UV-Vis-NIR region. Refractive index, absorption coefficient, and absorption edge of these films has been determined. The nature of the transition leading to the fundamental absorption is also discussed. It was found that the amorphous films crystallized when heated and their optical transmission changed due to crystallization. This was manifested as a shift in the absorption edge in the case of tin disulphide and in the case of CuS the golden yellow colour of the amorphous CuS changed to deep green.

Electrical conductivity, conductivity type, carrier concentration, activation energy for conduction etc. of these films have been studied. The effect of heating of this as prepared films, where the resistivity changes by different orders of magnitude due to crystallization, has also been discussed in detail.

Transparent conducting films of tin dioxide has been prepared by heating the as prepared tin disulphide films in air and their optical and electrical properties studied. It is found that the oxidation of these films obey an exponential rate law. Films of Cu_2O and CuO has also been prepared by heating CuS films in air.

ACKNOWLEDGEMENTS

I would like to express my sincere thanks and gratitude to Dr. Joy George, Professor in Industrial Physics for his able and inspiring guidance and continual assistance on all stages of my research work.

I also wish to express my thanks to the authorities of University of Cochin and particularly Dr. K. Sathianandan, Head of the Department of Physics, for providing laboratory and library facilities.

I acknowledge the cooperative and helpful attitude of all my fellow research scholars, especially Dr.(Fr.) E.C.Joy, Dr. M.K. Radhakrishnan, Mr. T.I.Palson, Mr. B.Pradeep, Mr.P.K.Sarangadharan, Dr.S.K. Premachandran, Mr. A.V.Alex, Mr.(Fr.) George Peter and Miss C.K. Valsala Kumari of our Solid State Physics group.

I am extremely thankful to all members of the faculty, office staff and technical personnel for the friendly assistance throughout the period of research work.

My thanks are also due to Dr. Jacob Chacko of Department of Marine Sciences, Dr. Sivasankara Pillai of Department of Applied Chemistry both of University of Cochin, Dr. P.K. Joy and V. Ramachandran Pillai of Travancore Titanium Products and Dr. Balakrishnan of USIC,

University of Kerala for providing various instrumentation facilities in the course of my work.

I also thank University of Cochin and Council of Scientific and Industrial Research, New Delhi for the award of fellowship during the tenure of my work.

Thanks are also due to Mr. Antony Wilfred for beautifully xeroxing the typescript and figures and Mr. Bhaskaran for his excellent typing.



CONTENTS

	INTRODUCTION	1
Chapter - I	SEMICONDUCTOR PHYSICS	7
1.1	Crystalline Semiconductors	7
1.2	Amorphous Semiconductors	37
	References	49
Chapter - II	REACTIVE EVAPORATION METHODS	50
	References	69
Chapter -III	EXPERIMENTAL TECHNIQUES	70
3.1	Determination of Optical Constants of Thin Films	70
3.2	Measurement of Electrical Resistance	77
3.3	Determination of Conductivity type	82
3.4	Measurement of Hall Voltage	83
3.5	X-ray Diffraction	85
3.6	Scanning Electron Microscopy	87
3.7	Thin Film Thickness Measurement	88
3.8	Set-up for the Oxidation of the Film	91
3.9	Preparation of the Film by Reactive Evaporation	93
	References	101
Chapter - IV	REACTIVELY EVAPORATED FILMS OF TIN DISULPHIDE	102
4.1	Experimental	107
4.2	Electrical Measurements	110
4.3	Optical Measurements	117
	References	130

Chapter - V	TRANSPARENT CONDUCTING FILMS OF TIN DIOXIDE PREPARED BY THE OXIDATION OF TIN DISULPHIDE FILMS	132
5.1	Experimental	136
5.2	Oxidation of the Film	137
5.3	Electrical Properties	141
5.4	Optical Properties	144
	References	150
Chapter - VI	REACTIVELY EVAPORATED FILMS OF COPPER SULPHIDE	153
6.1	Preparation of the film	156
6.2	Structural Studies	158
6.3	Electrical Properties of Crystalline CuS films	163
6.4	Optical Properties of Crystalline CuS films	164
6.5	Amorphous films of CuS	169
6.6	Electrical Properties of Amorphous CuS films	170
6.7	Optical Properties of Amorphous CuS films	172
	References	179
Chapter -VII	EFFECT OF HEATING ON THE PROPERTIES OF CuS FILMS	181
7.1	Experimental	182
7.2	Results and Discussions	182
	References	193

Chapter -VIII	OXIDE FILMS OF COPPER PREPARED BY THE	
	OXIDATION OF COPPER SULPHIDE FILMS	199
8.1	Experimental	200
8.2	Results and Discussions	201
	References	216
Chapter - IX	REACTIVELY EVAPORATED FILMS OF	
	INDIUM SULPHIDE	218
9.1	Experimental	220
9.2	Structural Studies	221
9.3	Optical Measurements	225
9.4	Electrical Studies	234
9.5	Stability of β - In_2S_3 Films	237
	References	243
Chapter - X	FILMS PREPARED BY ACTIVATED REACTIVE	
	EVAPORATION	245
10.1	Experimental	245
10.2	Films of Tin Disulphide	249
10.3	Films of Copper Sulphide	251
10.4	Films of Indium Sulphide	253
	References	254
Chapter - XI	FORMATION OF COMPOUND FILMS IN	
	EVAPORATION TECHNIQUES	255
11.1	Effect of Kinetic Energy and	
	Ionization	256
11.2	General Remarks	273
	References	278

INTRODUCTION

In general, any solid or liquid object with its one dimension very much less than the other two, may be called a thin film. Thin layers of oil, floating on the surface of water, with their fascinating colours, have attracted man's curiosity from time immemorial. The earliest application of thin films was the protective coatings in the form of paints. In India a thin layer of tin has been used from ancient times to protect copper utensils from corrosion. Thin films of metals were probably first prepared in a systematic manner by Michael Faraday using electrolysis. Scientific interest in thin films, both fundamental and applied, began with their application first in optics and later in electronics. Application of this technology has revolutionized both these fields - narrow band filters with a few nanometer bandwidth and structures with several thousand semiconductor elements in a square cm. area. Thin film technology has a whole variety of applications extending from protective coatings to epitaxial layers in semiconductor heterojunction lasers. In addition to this, basic physics and chemistry have also gained much from the study of thin films. Homo and hetero nucleation theories, heterogenous catalysis, optical absorption studies in the fundamental absorption region of solids, electrical conduction mechanisms in insulating and amorphous semiconductors

are a few to mention.

Interest in compound semiconductor thin films began with the realization of the fact that optimum material properties in device applications, which cannot be achieved in the case of a single element, can easily be achieved using a combination of two or more elements (i.e. alloys and compounds). Germanium, silicon and selenium, which were the earlier known and most used elemental semiconductors, had to make way for the semiconducting II-VI, III-V, and IV-VI compounds. As the range of applications increased, material properties had to meet stringent and wide ranging requirements. Silicon is of little use in high speed integrated circuits or in optoelectronic devices because of low carrier mobility and indirect gap. In these respects the members of the III-V family are far more superior. These compounds have a high carrier mobility, direct optical gap (except a few members) and hence their widespread application in high speed integrated circuits, Hall generators, semiconductor heterojunction lasers and high efficiency solar cells.

Another area where the properties of elemental films do not come anywhere near the mark is in the case of metallurgical and protective coatings. Except in the case of the so called diamond like carbon (i-carbon) compound films are the only hard coatings available with the required properties.

The deposition of compound films by single source evaporation is a rather difficult problem. Often a large fraction of the compound dissociates when heated. When the compound dissociates in vacuum, the volatile component will be given off first. This will result in layered films if all the evaporated material stick to the substrate surface; or a film of the non-volatile component, if the volatile component does not stick to the substrate at the substrate temperature used. The films of the former type may be annealed in an inert atmosphere (to prevent the evaporation of the volatile component and also to avoid any chemical reaction with the ambient gases) at a suitable temperature to reproduce the compound. This process, although successful in the case of certain compounds, is rather time consuming. Deposition of high melting point carbides and nitrides is another area where single source evaporation is not practicable because of the lack of suitable support materials for evaporation which can withstand the high temperatures needed for evaporation.

As a result of these difficulties a number of experimental techniques have been devised to synthesis the compound from their components, which on the one hand eliminates the decomposition problem and on the other hand eliminates the use of high temperature sources. The first method to appear in this context was Günther's 'Three Temperature Method' (TTM) and is based on the fact that continuous

condensation of a given vapour at a given deposition rate is possible only if the substrate temperature drops below a critical temperature. Differences in magnitude of these critical values make it possible to condense a given vapour or combination (i.e. a compound) preferentially on the substrate surface. This technique was the forerunner of modern day Molecular Beam Epitaxy (MBE). TTM has now been so perfected that it is now possible to deposit certain III-V compounds (InSb and InAs) at rates approaching $1 \mu \text{ min}^{-1}$, a rate which is comparable to vapour phase epitaxy.

One of the disadvantage of this process is the low chemical reactivity of the components and hence the need for high partial pressure of the volatile element. It is found that when high deposition rates are needed, the increased partial pressure affects film properties like hardness and refractive index, even though stoichiometry is maintained. To overcome these difficulties Prof. Bunshah of UCLA introduced the technique of Activated Reactive Evaporation (ARE) where the components are activated by an electric discharge. This allowed him to deposit TiC films by reactively evaporating Ti in an atmosphere of acetylene at high deposition rates. It must be mentioned that without the electric discharge, compound formation itself was not possible.

One further improvement in this type of techniques came as Reactive Ion Plating (RIP). Here the ionized components are accelerated to the negatively biased substrates

and films with good adhesion, high microhardness etc. could be formed by this technique.

In continuation of the work in this laboratory on the preparation and study of semiconducting compound thin films by the three temperature method, it has been thought fit to pursue the work on certain semiconducting compounds where component elements have widely different vapour pressures. And in this thesis is reported the work on the preparation and study of thin films of sulphides of tin, copper, and indium.

The first chapter of the thesis gives a resume of the basic principles of semiconductor physics relevant to the work reported here. In the second chapter is discussed in detail the reactive evaporation techniques like ordinary reactive evaporation, activated reactive evaporation and reactive ion plating. Third chapter deals with the experimental techniques used in this study for film preparation and characterization. In the next seven chapters is discussed the preparation and properties of the compound films studied. The last chapter gives a general theory of the formation of compound films in various deposition techniques in terms of the kinetic energy of the film forming particles. It must be mentioned here that this is of fundamental importance to thin film deposition and is virtually untouched in the literature.

Part of the work reported in this thesis is published in the form of the following papers:

- 1) "Absorption Edge Measurements in Tin Disulphide Thin Films" J. Phys. D: Applied Physics, 15 (1982) 1109
- 2) "Effect of Heating on the Electrical and Optical Properties of Tin Disulphide Thin Films" J. Phys. D: Applied Physics, 16 (1983) 33
- 3) "Transparent Conductive Films of Tin Oxide-Preparation and Properties" Solid State Communications, 46 (1983) 541
- 4) "Amorphous Films of CuS" Solid State Communications, 48 (1983) 601
- 5) "Reactively Evaporated Copper Sulphide Films" J. Phys. Chem. Solids, 44 (1984) (in press)

CHAPTER-I

SEMICONDUCTOR PHYSICS

1.1 CRYSTALLINE SEMICONDUCTORS

Crystalline material is one having their atoms arranged in a periodic manner. The first application of quantum mechanics to the motion of electrons in solids was the treatment of conduction of electricity in metals by A. Sommerfeld /1/. Here the electrons are assumed to move in a field free space, the fields of force due to the atomic cores and other electrons being smoothed out except at the boundary of the solid. These forces are supposed to attract the electron strongly if it moves outside the boundary. This theory enabled such phenomena as field emission and thermionic emission to be discussed in terms of potential barriers of finite height at the boundary of the solid. But this theory gives no explanation of the vast differences in the properties of metals, semiconductors and insulators.

The next step was to take into account the interaction of valence electrons with the atomic cores, assuming these to be placed at the lattice points of the crystal. These electrons are still assumed to move independently but the smoothed out potential used by Sommerfeld is replaced by a periodic potential (see figure 1). The particular feature of a potential of this form is that it is periodic having the same periodicity of the lattice. Motion of

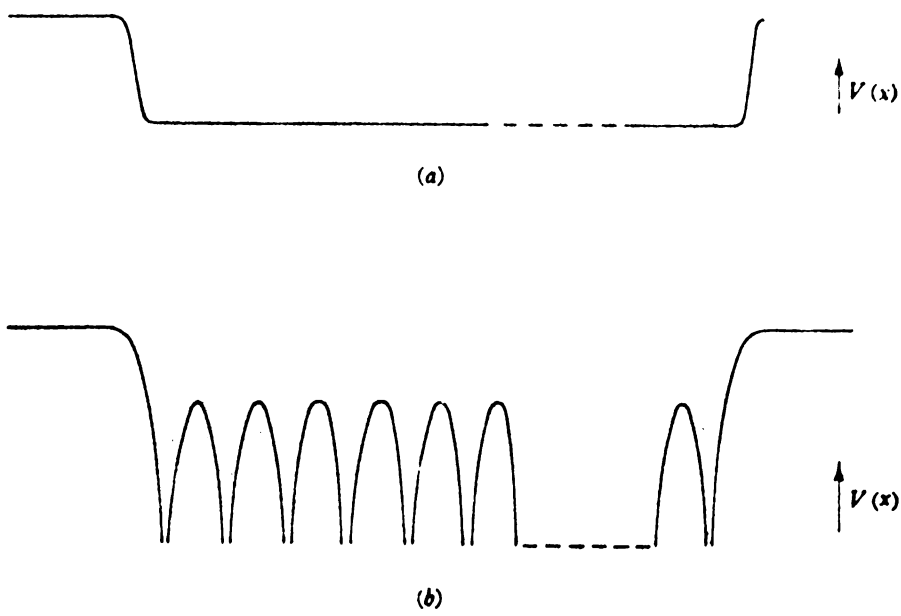


Figure 1: Potential energy of electron in crystalline solid a) Sommerfeld model
b) periodic potential.

electrons in such a potential was discussed by F. Bloch /2/ and a most fundamental result which was independent of the particular form of potential used came to light. It turns out that in a perfect periodic lattice an electron may move freely and is not scattered by the individual atoms of the lattice but only by imperfections in the periodicity of the potential. The effect of periodic potential is only to cause an apparent change in the mass of the charge carriers.

In Sommerfeld's theory, the allowed energy levels lie very close together and their values extend from nearly the bottom of the potential trough in which the electrons move to indefinitely high values. When the periodic potential is introduced, however, the energy levels are confined to certain allowed bands of energy, separated by regions in which no energy levels are allowed. For the inner electrons these allowed bands are extremely narrow and correspond to the atomic levels; for the valence electrons the bands are quite broad. The arrangement of levels is shown in figure 2. Each band consists of many closely spaced levels and for many purposes may be regarded as a continuum. When we come to allocate electrons to these levels, however, we must remember that they are discrete and that there exist a definite number of them. Just as the inner levels in a heavy atom are all filled with electrons, all the levels in the lower allowed bands are filled, and it is only the upper bands which

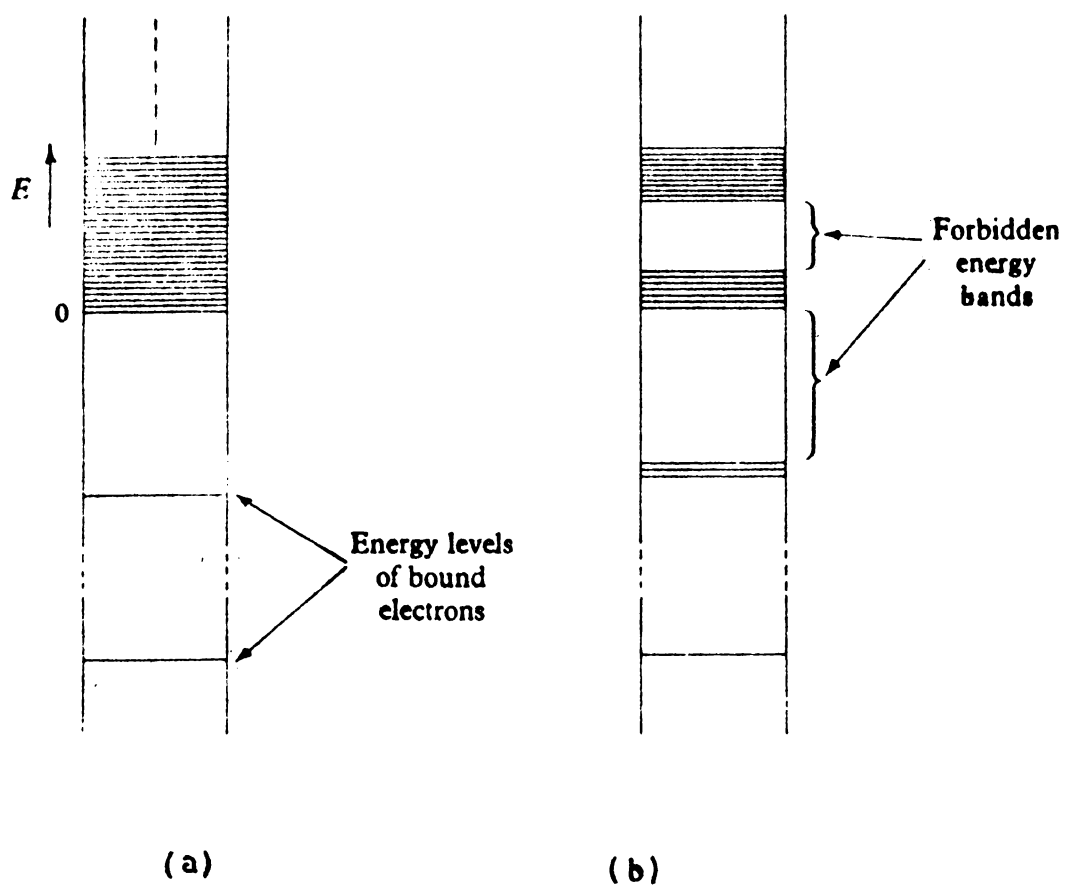


Figure 2: Energy levels of (a) Sommerfeld model of metal (b) periodic lattice.

may be wholly or partially unoccupied by electrons.

Energy band picture of a solid may be arrived in another way. Suppose we have N atoms of the same kind far apart and consider a single level of each of the atom. The allowed levels of the combined system consist of a single N -times degenerate level, i.e. each electrons has precisely the same energy. Now if we let the atoms approach, this degenerate level will be split into N by the interaction between the atoms. This will be a band of N closely spaced levels instead of a single degenerate level. For the deep-lying levels the perturbation will be very small compared with the attractive force of the nucleus and the splitting will be very small. But in the case of valence electrons, the splitting may be quite large and in fact neighbouring bands may overlap.

The bands corresponding to atomic levels in which there are paired electrons with opposite spins are completely filled. And also various filled closed shells in an atom correspond to bands in which all the levels are occupied. It is only bands corresponding to the outer electrons which may be partially filled. This distinction between completely filled bands and partially filled bands are used in the explanation of the electrical conductivity of solids. To produce conduction, an electron must receive energy from an electric field. In terms of quantum mechanics it must be raised to a higher level. If all the levels in a band are

occupied this cannot take place unless the electron is excited to a higher band in which there are free places. This is highly improbable as it requires energies of the order of electron volt. Thus electrons can contribute to current only if there are available neighbouring empty levels into which they can go. Such materials which have an incompletely filled band is known as metals.

If the forbidden energy gap E_g between the highest filled band and the next empty band is large, no electronic conduction can take place as no neighbouring empty levels exist into which electrons may be accelerated. These type of materials are known as insulators. If on the other hand, the value of E_g is small there is the possibility that electrons may be thermally excited into the band above and these excited electrons can conduct. The number of excited electrons would increase with temperature in a manner governed by a process having an activation energy of E_g and we should expect a rapid increase of conductivity with temperature. Substances behaving in this way was identified by Wilson as semiconductors /3/.

When an electron is excited from the full band to an empty band above, the level occupied by the electron is left vacant so that other electrons may move into it. In an applied electric field this position left unoccupied moves in the opposite direction to that in which an electron would move, and so appears to have a positive charge and is called

a 'hole'. Electrical conduction in an ideal semiconductor thus consists of motion of electrons in a nearly empty band, and of positive holes in a nearly full band. The top most filled band in a semiconductor is known as the valence band and the next highest one, the conduction band.

If we assume that the variation of mobility of electrons and holes in an electric field with temperature T is small, the conductivity σ is proportional to the number of carriers and hence a variation of the form

$$\sigma = \sigma_0 \exp(-E_g/2k_B T) \quad (1.1.1)$$

Such an exponential variation of conductivity had long been known for semiconductors at high temperature. At lower temperatures, however, a much less rapid increase in conductivity is observed and the value of conductivity may vary enormously from sample to sample. To explain this Wilson proposed that the low temperature behaviour was due to imperfections in the crystal due either to mechanical defects or to chemical impurities. Wilson showed that impurities may produce isolated levels in the forbidden energy gap, and it turns out that these levels may lie very near to the conduction band or very near to the full band. A simplified energy band diagram of a semiconductor is shown in figure 3.

If impurity levels are separated by only a small energy gap from the empty band, electrons may be readily

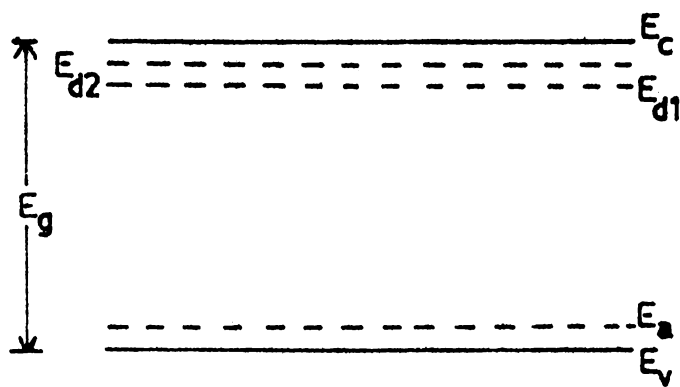


Figure 3: Simplified energy level diagram of a semiconductor. Two donor levels E_{d1} and E_{d2} and one acceptor level E_a are shown.

excited into this band. Such impurities are called donor or n-type impurities. If impurity levels lie near the full band (valence band), and can accept electrons, these may be readily excited from this band and leave holes behind which will conduct. Such impurities are called acceptor or p-type impurities.

The energy required to excite an electron into the conduction band from a donor level is sometimes so small that the electrons from all the donor levels are excited and are in the conduction band at room temperature. If the number of donors greatly exceeds the number of intrinsic electrons, the number of carriers will hardly vary at all with temperature and the variation of conductivity will be due only to the variation of mobility. Hence for a semiconductor in this condition the conductivity will decrease with increasing temperature till a temperature is reached at which intrinsic electrons begin to predominate. Then the conductivity will begin to rise exponentially. Similar considerations also apply to p-type semiconductors.

Intrinsic Carrier Concentration

The Fermi-Dirac distribution function for electrons in the conduction band is

$$f_e \approx \exp(E_F - E_g)/k_B T \quad \text{provided } E_g - E_F \gg k_B T \quad (1.1.2)$$

where E_F is the Fermi level.

This is the probability that a conduction electron orbital is occupied. The energy of an electron in the

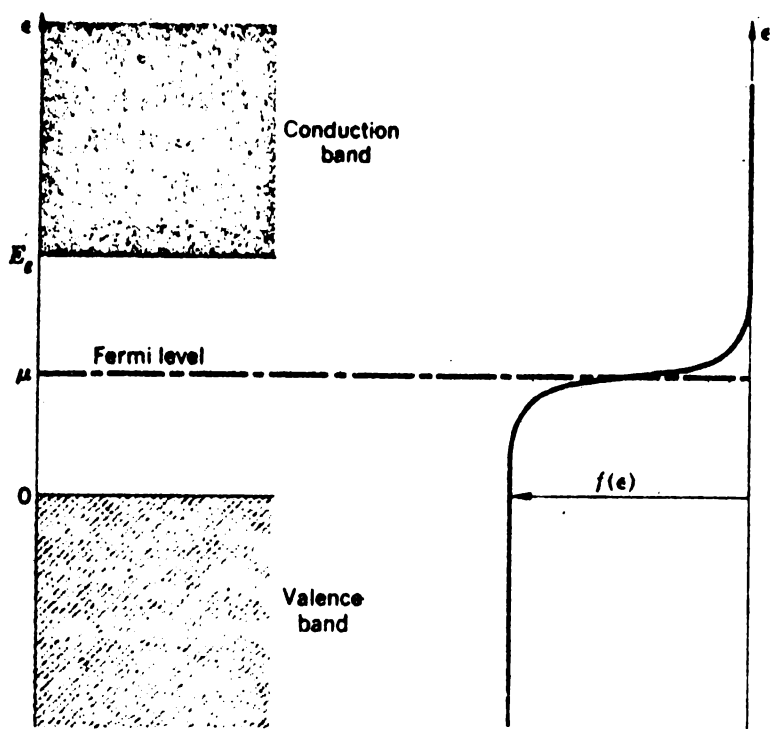


Figure 4: Energy scale for statistical calculations. The Fermi distribution function is shown on the same scale for a temperature $k_B T \ll E_g$.

conduction band is

$$E_K = E_g + \hbar^2 K^2 / 2m_e \quad (1.1.3)$$

where m_e is the effective mass of an electron and K the wave vector. The density of orbitals at E is

$$D_e(E) = \frac{1}{2\pi^2} (2m_e/\hbar^2)^{3/2} (E-E_g)^{1/2} \quad (1.1.4)$$

The concentration of electrons in the conduction band is

$$\begin{aligned} n &= \int_{E_g}^{\infty} D_e(E) f_e dE \\ &= \frac{1}{2\pi^2} (2m_e/\hbar^2)^{3/2} \exp(E_F/k_B T) \int_{E_g}^{\infty} (E-E_g)^{1/2} \exp(-E/k_B T) dE \\ &= 2(m_e k_B T / 2\pi \hbar^2)^{3/2} \exp(E_F - E_g) / k_B T \end{aligned} \quad (1.1.5)$$

similarly the equilibrium concentration of holes is given by

$$p = 2(m_h k_B T / 2\pi \hbar^2)^{3/2} \exp(-E_F/k_B T) \quad (1.1.6)$$

we multiply together the expressions for n and p to obtain the equilibrium relation

$$np = 4(k_B T / 2\pi \hbar^2)^3 (m_e m_h)^{3/2} \exp(-E_g/k_B T) \quad (1.1.7)$$

This result does not involve the Fermi level E_F and is known as the law of mass action. Since it is not assumed in the derivation that the material is intrinsic, the result holds good in the presence of impurities as well.

In an intrinsic semiconductor the number of electrons is equal to the number of holes. Thus we have from equation 1.1.7 letting i denote the intrinsic case,

$$n_i = p_i = 2(k_B T / 2\pi\hbar^2)^{3/2} (m_e m_h)^{3/4} \exp(-E_g / 2k_B T) \quad (1.1.8)$$

Impurity Conductivity

Certain impurities and imperfections drastically affect the electrical properties of a semiconductor as already mentioned. In a compound semiconductor a stoichiometric deficiency of one constituent will act as an impurity; such semiconductors are known as deficit semiconductors. The deliberate addition of impurities to a semiconductor is called doping.

The most striking difference between metals and semiconductors is that, in the former, the number of carriers is large and constant, whereas in the latter the number is smaller and variable. This variable characteristic suggests that, in semiconductors, the number of carriers and hence the conductivity may be controlled. This control may be effected by control of impurity content.

At absolute zero² a semiconductor may contain a certain concentration of occupied electronic levels which lie in the normally forbidden region between the valence and conduction bands. These electrons are localized in the vicinity of the impurities and therefore do not contribute to the conductivity unless they are excited to the conduction band. Similarly a semiconductor may contain a certain density of holes which at absolute zero of temperature are trapped in levels lying in the forbidden gap. These acceptor levels may become occupied by electrons excited from the filled band. These excited electrons leave a hole in the valence band and conduction become possible in this band.

The density of free electrons in the conduction band due to a donor with activation energy $E = E_c - E_i$ is given by

$$n_c = (2n_d)^{1/2} (2\pi m_e k_B T / h^2)^{3/4} \exp(-E / 2k_B T) \quad (1.1.9)$$

where n_d is the donor density and E_i the donor level. It is to be noted that n_c is proportional to the square root of donor concentration. A similar expression holds for the case of acceptors also.

The Hall Effect

When a magnetic field is applied to a conductor carrying a current, in a direction at right angles to the

current, an e.m.f. is produced across the conductor in a direction perpendicular to the current and to the magnetic field. This effect has become one of the most powerful tools for studying the electronic properties of semiconductors.

Let us consider an infinite semiconductor having an electric current density J in the x -direction and a magnetic field in the z -direction. If we consider the effect of the magnetic field on the drift velocity of electrons in an electric field in the x - y plane, we see that there must be a component of the field at right angles to the current flow to balance the transverse force due to the magnetic field. The drift velocity v_x is equal to $-J/ne$. The average transverse force on an electron in the y -direction is then eBv_x and the balancing field E_y is given by

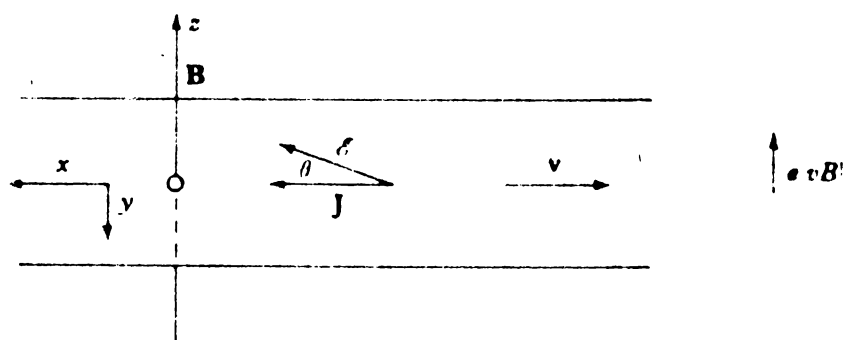
$$e E_y = eBv_x = -BJ/n \quad (1.1.10)$$

where B is the magnetic induction. The component of electric field E parallel to the current is given by the equation

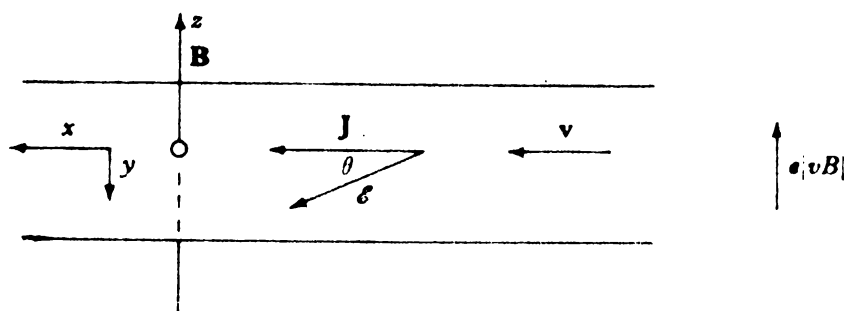
$$J = ne \mu_e E_x \quad (1.1.11)$$

The angle θ between the current and resultant electric field is then given by

$$\tan \theta = E_y/E_x = -B/\mu_e \quad (1.1.12)$$



(a) Electrons



(b) Holes

Figure 5:(a)Hall effect for electrons and holes.

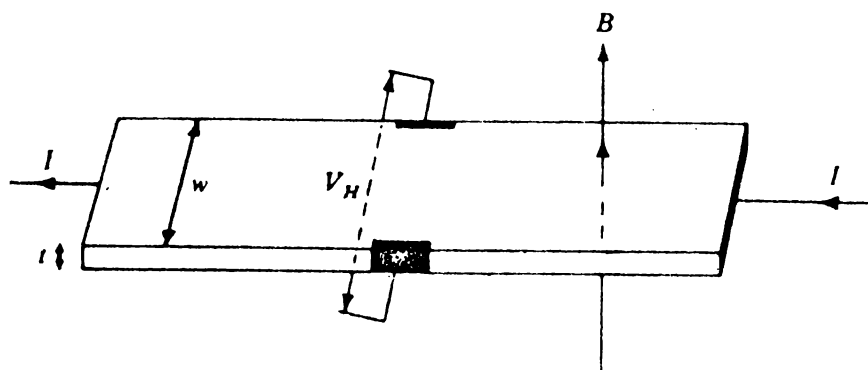


Figure 5:(b)Arrangement for Hall effect measurement.

angle θ is known as the Hall angle.

The Hall effect is described by the Hall constant R_H defined in terms of the current density J by the equation

$$E_H = R_H J B \quad (1.1.13)$$

where E_H is the Hall field. If t is the thickness of the film and W its width, if V_H is the Hall voltage and I the current,

$$V_H = R_H I B / t \quad (1.1.14)$$

therefore

$$E_H = R_H n e / \mu_e = -B / \mu_e E_x$$

$$R_H = -1 / n e \quad (1.1.15)$$

This equation holds exactly only when relaxation time is not a function of the velocity. We generally have to include a numerical factor r which varies between 1 and 2 according to the type of scattering which predominates. Apart from this uncertainty, we may obtain from a measurement of the Hall constant the important quantity n_e giving the electron concentration in the conduction band. The sign of the Hall constant tells whether we have an n-type or p-type semiconductor.

Since $\sigma = n_e e \mu$, by measuring the conductivity of the sample along with the Hall constant, we can determine μ , the mobility of the carriers.

Optical absorption in crystalline materials.

The various ways in which light interact with matter are of obvious practical interest, whether absorption, transmission, reflection, scattering or emission. The study of the optical properties of solids has proved to be a powerful tool in our understanding of the electronic and atomic structure of solids. Among the most important parameters characterizing a semiconducting material is the value of its fundamental energy gap as well as the position of the band extrema in momentum space. The measurement of optical absorption provides the most accurate way to determine the gap value. It is also possible to get information about the relative position of the extrema, although for the evaluation of the absolute position, cyclotron resonance must be used.

A plane electromagnetic wave travelling in an absorbing medium can be represented by the equations for electric and magnetic field

$$E = E_0 \exp - i (K \cdot r - \omega t) \quad (1.1.16)$$

$$H = H_0 \exp - i (K \cdot r - \omega t) \quad (1.1.17)$$

where K is the complex propagation vector $K = K_1 + i K_2$

The above equations are solutions of Maxwell's equations for the electromagnetic field in a medium with magnetic permeability unity.

The complex dielectric constant

$$\epsilon = \epsilon_1 + i \epsilon_2 = \epsilon_1 + i \frac{4\pi\sigma}{\omega} \quad (1.1.18)$$

with the frequency dependant conductivity σ describes the response of the medium to the driving field $D = \epsilon E$. The complex refractive index is defined as

$$N = n + ik = \epsilon^{1/2} \quad (1.1.19)$$

where n is the real refractive index and k , the extinction coefficient. The optical constants n and k are real positive numbers and can be determined by optical measurements.

From these we obtain

$$\epsilon_1 = n^2 - k^2 \quad (1.1.20)$$

$$\epsilon_2 = \frac{4\pi\sigma}{\omega} = 2nk \quad (1.1.21)$$

For homogenous plane waves

$$|K_1| = \frac{n\omega}{c}, \quad |K_2| = \frac{k\omega}{c} \quad (1.1.22)$$

Inserting these in the equation for the electric component of the wave, we get,

$$E_x = E_{0x} \exp i\omega(nxc^{-1} - t) \exp(-\omega Kxc^{-1}) \quad (1.1.23)$$

This form represents a wave travelling in x-direction with velocity (c/n) which is attenuated by $\exp(-\omega kx/c)$. The absorption coefficient \mathcal{L} , defined by the relative decrease of the intensity per unit distance in the propagation direction through $I = I_0 \exp(-\mathcal{L}x)$, is then

$$\mathcal{L} = 4\pi k/\lambda \quad (1.1.24)$$

A survey of photon absorption processes in solids

Figure 6 shows the absorption spectrum of a hypothetical solid - a semiconductor to which a magnetic field may be applied and is antiferromagnetic at some low temperature. Semiconductors show all the optical properties of insulators and metals though not to the same degree. The main features are as follows:

- (a) In the UV, and sometimes in the visible or IR, is a region of intense absorption which arises from electronic transitions between the valence and conduction bands. Such transitions generate mobile electrons and holes which results in photoconductivity. The absorption coefficient is typically in the range 10^5 to 10^6 cm^{-1} . On the high energy side of the band (around 20 eV) there is a smooth fall in absorption over a range of several electron volts. On the low energy side the absorption coefficient falls more rapidly and may fall as much as six orders of magnitude within a few

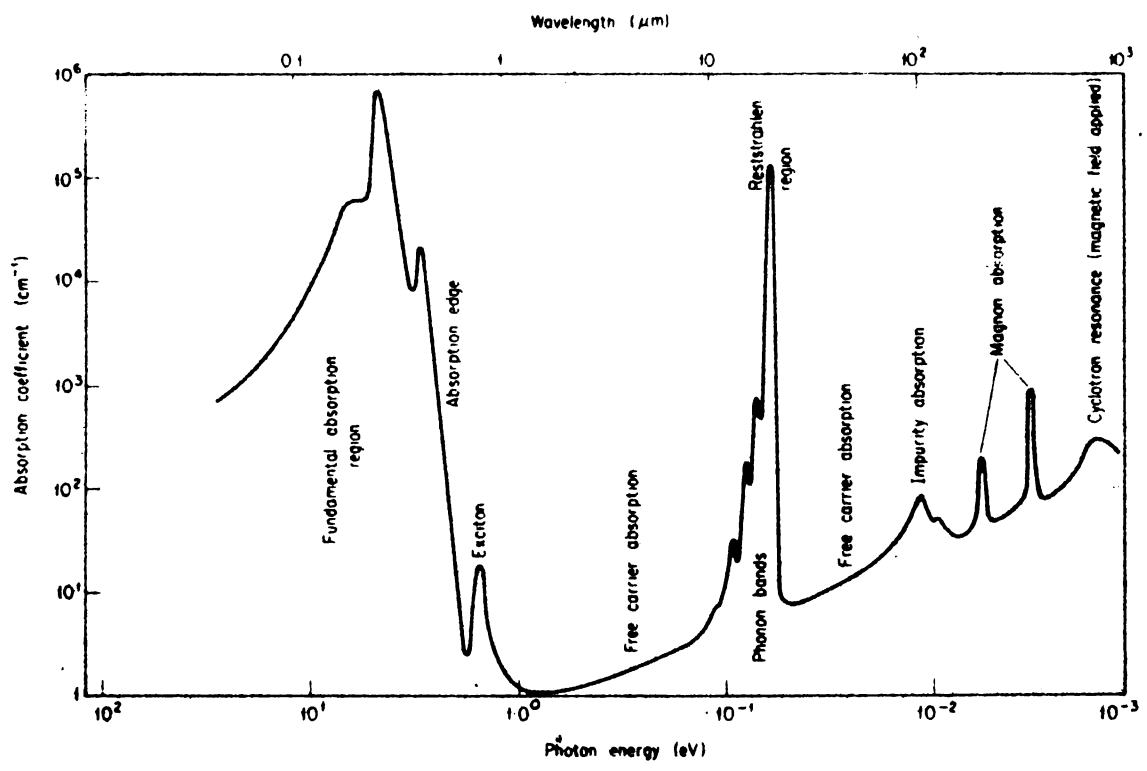


Figure 6: Absorption spectrum of a hypothetical semiconductor.

tenths of an eV. This low energy boundary of the fundamental absorption is referred to as the absorption edge. The limit of the absorption edge corresponds to the photon energy required to promote electrons across the minimum energy gap E_g .

- (b) The absorption edge region often show some structure, in particular that due to excitons. Exciton absorption is more pronounced in insulators, particularly in ionic crystals, and can lead to strong narrow-line absorption as in atomic spectra.
- (c) As the wavelength is increased beyond the absorption edge, the absorption starts to rise slowly again. This increase is due to electronic transitions within the conduction or valence bands and is known as free carrier absorption and extends throughout the infrared and microwave regions of the spectrum. Its magnitude is a function of the mobile electron (hole) density.
- (d) In the 20-50 μ region, due to the interaction between the incident photons and the vibrational modes of the lattice a new set of absorption peak occurs. If the crystal is ionic the absorption coefficient may reach 10^5 cm^{-1} and strong reflection occurs. Homopolar crystals show such features but with much lower absorption coefficients.

- (e) Impurities give rise to absorption. Absorption due to a shallow impurity with an ionization energy 0.01 eV is shown in the figure and the absorption will be observable at low temperatures.
- (f) Absorption may occur in solids due to electron spin reversal. Thus a solid containing paramagnetic impurities will show absorption lines in the presence of an external magnetic field which splits otherwise degenerate spin levels. In an antiferromagnetic material where there is a substantial internal field, the spins are coupled together and there is the possibility of the collective excitation of the spins. Such collective excitations are called spin waves or magnons.
- (g) Enhanced absorption by mobile carriers in the presence of a magnetic field may occur and is referred to as cyclotron resonance.

The fundamental absorption

We now consider transitions in which an electron is excited from the valence band to the conduction band with absorption of a photon of energy approximately equal to E_g , the energy of the forbidden gap. Here we must distinguish two types of transitions, those involving only one (or more) photons and those involving also lattice energy in the form of phonons. Transitions involving no phonons we call

direct transitions and those involving phonons indirect transitions. We must also distinguish between two types of semiconductors since their behaviour is rather different; the first type consists of semiconductors which have the same value of K_{\min} of the wave-vector K (usually $K=0$) for the lowest energy state in the conduction band, as for the highest state in the valence band (K_{\max}): the second type consists of those semiconductors for which this is not so. (See figure 7)

Direct transitions

In an absorption process, crystal momentum must be conserved. The momentum P_p given by the incident photon, is equal to $(h/\lambda)\mathbf{i}$, where \mathbf{i} is unit vector along the direction in which the photon is travelling before it is absorbed and λ is the wavelength of the incident radiation. The equation expressing the conservation of momentum is then

$$P_2 - P_1 = (h/\lambda)\mathbf{i} \quad (1.1.25)$$

where P_1 and P_2 are the crystal momenta associated with the states occupied by the electron before and after absorption. The probability of a transition taking place under a perturbing potential F is proportional to the matrix element $|M_{if}|^2$, where

$$M_{if} = \int \psi_i F \psi_f \, dr \quad (1.1.26)$$

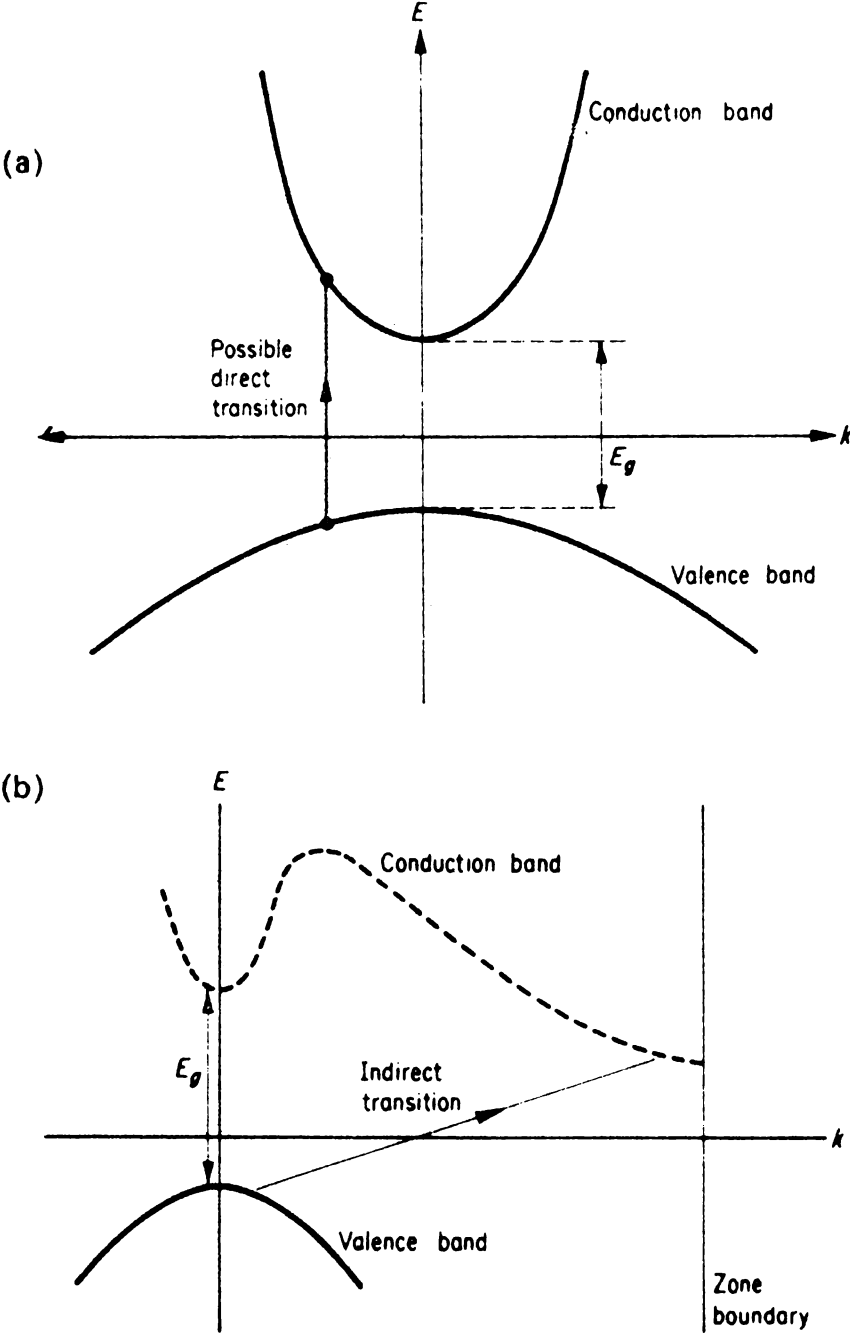


Figure 7: Valence and conduction band edges of the two types of semiconductors. (a) direct gap semiconductor (b) indirect gap semiconductor.

and ψ_i and ψ_f are the initial and final wave-functions.

In this case F has the form

$$F = A \exp [2\pi i(r \cdot j)/\lambda]$$

and

$$\psi_i = U_{K_1}(r) \exp[i(K_1 \cdot r)]$$

$$\psi_f = U_{K_2}(r) \exp[i(K_2 \cdot r)]$$

the integral therefore contains the factor

$$\exp[i(K_1 - K_2 + 2\pi j/\lambda) \cdot r]$$

which varies rapidly and periodically unless

$$K_1 - K_2 + 2\pi j/\lambda = 0 \quad (1.1.27)$$

Unless this equation is satisfied the matrix element will be very small. In transitions from one band to another, we thus see that only vertical transitions are allowed and we may have a selection rule $\Delta K = 0$. This is illustrated in figure 7(a). If an electron is in a state with crystal momentum P_1 in the full band, it goes into a state with crystal momentum P_1 in the conduction band leaving behind a hole in the full band. The velocity of hole is equal to $-P_1/m_h$ so that the electron and hole move off in opposite directions. In this case the minimum frequency for which such a transition will take place is given by $h\nu = E_g$, so that absorption edge begins at this frequency.

It is of considerable interest to determine the form of the absorption curve as a function of wavelength immediately on the short wave side of the edge. The form depends on whether the transition is allowed or not, apart from the momentum condition, i.e. on the form of the functions $U_{K1}(r)$, $U_{K2}(r)$. If these are such as to give an allowed transition then the probability of transition between two such states is very nearly independent of K .

Let us consider transitions from the valence band originating from states having values of K in the interval K to $K + dK$. The energy of a photon required to induce a transition is then given by

$$h\nu = E_c(K) - E_v(K) \quad (1.1.28)$$

The probability of absorption of a quantum in the frequency interval $d\nu$ is then proportional to the number of states in the valence band with energies lying between $-E_g - E'$ and $-E_g - E' - dE'$. Let us assume for the moment that the conduction band is flat near $K = 0$, i.e. $E_c(K)$ is a constant. Then if we write

$$E_v(K) = -E_g - E' \text{ we have,}$$

$$h d\nu = dE'$$

The number of transitions $N_t d\nu$ in the interval $d\nu$ is then given by

$$N_t d\nu = P_K N(E') dE' \quad (1.1.29)$$

where $N(E')$ dE' is the number of states with E' in the interval E' to $E'+dE'$ and P_K is the probability of transition.

But

$$N(E') = AE'^{1/2} \quad (1.1.30)$$

where A is a constant. Absorption coefficient \mathcal{L}_d may therefore be written in the form

$$\begin{aligned} \mathcal{L}_{da} &= A'P_K (h\nu - E_g)^{1/2}, \quad h\nu > E_g \\ &= 0, \quad h\nu \leq E_g \end{aligned} \quad (1.1.31)$$

where A' is a constant.

Allowed transitions take place, for example, if the valence band wave functions are derived from s-states of the individual atoms, and the conduction band wave functions from p-states; if the latter were derived for example, from d-states the transition would not be allowed. In this case it may be shown that when $K = 0$, $P_K = 0$, but as K departs from zero, the transition probability is proportional to K^2 , i.e. to $(h\nu - E_g)$. Thus we may write

$$P_K = \text{const.} (h\nu - E_g) \quad (1.1.32)$$

so that the absorption coefficient \mathcal{L}_{df} is given by the equation

$$\mathcal{L}_{df} = C(h\nu - E_g)^{3/2} \quad (1.1.33)$$

where C is a constant.

Indirect Transitions

Let P_1 be the crystal momentum of an electron before transition and P_2 the momentum after transition. To conserve the momentum an amount $(P_1 - P_2)$ must be supplied by the lattice. This may be achieved in two ways, either by absorption of a phonon of momentum $-(P_1 - P_2)$ or by emission of a phonon of momentum $(P_1 - P_2)$. Let us take $K_1 = 0$, $K_2 = P_2/\hbar = K_{\min}$, then a phonon whose wave number is K_{\min} must be absorbed or emitted. The minimum frequency for which a transition may take place is now given by

$$h\nu = E_g - E_p \quad (1.1.34)$$

for absorption of a phonon, and by

$$h\nu = E_g + E_p \quad (1.1.35)$$

for emission of a phonon. E_p is the energy of the phonon. The lowest value of $h\nu$ for this type of transition is given by equation 1.1.34, which defines the edge of the fundamental absorption band.

If the wave-vector K_{\min} is well separated from $K = 0$, the transition probability between a state with a small value of K situated near the top of the valence band

and a state with $K = K_{\min} - K'$ situated near the bottom of the conduction band will not vary very rapidly with K and K' , and may as a first approximation be taken as a constant. The absorption coefficient then depends on the density of states from which transitions may take place and on the relative probability of emission and absorption of phonons.

The number of states in the interval dE is,

$$N_c(E) dE = aE^{1/2}dE = a(h\nu - E_g \mp E_p - E')^{1/2}dE$$

where a is a constant. To find the total number of pairs of states between which transitions corresponding to a frequency between ν and $\nu + d\nu$ may take place, we must integrate with respect to E' over the portion of the valence band for which the relation $h\nu = E_g \pm E_p + E + E'$ can be satisfied. The largest possible value E'_m of E' is given by

$$E'_m = h\nu - E_g \pm E_p \quad (1.1.36)$$

the negative sign being for phonon emission and the positive sign for phonon absorption.

The total number of pairs of states $Nd\nu$ between which transitions may take place is given by

$$N(\nu)d\nu = aa'h d\nu \int_0^{E'_m} (E'_m - E')^{1/2} E'^{1/2} dE' = DE_m^2 d\nu \quad (1.1.37)$$

where D is a constant and $a'E'^{1/2}dE'$ the density of states in the valence band in the interval dE' . The absorption coefficient for transitions with phonons is therefore

proportional to $(h\nu - E_g + E_p)^2$. It is also proportional to the number N_p of phonons of energy E_p present, which is given by

$$N_p = 1 / \exp(E_p/k_B T) - 1 \quad (1.1.38)$$

The contribution to the absorption coefficient \mathcal{L} is therefore given by

$$\begin{aligned} \mathcal{L}_{ia} &= \frac{A(h\nu - E_g + E_p)^2}{\exp(E_p/k_B T) - 1} & h\nu > E_g + E_p \\ &= 0 & h\nu \leq E_g + E_p \end{aligned} \quad (1.1.39)$$

where A is a slowly varying function of ν . The ratio of the probabilities for emission and absorption is equal to $(N_p + 1)/N_p$.

The contribution \mathcal{L}_{ie} to the absorption coefficient is given by

$$\begin{aligned} \mathcal{L}_{ie} &= \frac{A(h\nu - E_g - E_p)^2}{1 - \exp(-E_p/k_B T)} & h\nu > E_g + E_p \\ &= 0 & h\nu \leq E_g + E_p \end{aligned} \quad (1.1.40)$$

In the case of forbidden transition, it may be shown that the absorption coefficient is given by

$$\mathcal{L}_{if} = \frac{B(h\nu - E_g + E_p)^3}{1 - \exp(-E_p/k_B T)} \quad (1.1.41)$$

Thus an experimental determination of the functional dependence of absorption coefficient \mathcal{L} on photon energy $h\nu$ at the absorption edge can give information about the relative positions of conduction band minima and valence band maxima and also information about the individual atomic wave functions from which the valence band or conduction band wave functions are derived. Knowledge of the type of wave functions from which valence and conduction band wave functions are derived together with a structural knowledge of individual atomic positions can be used in theoretical band structure calculations to get a full picture of the band structure of the material.

1.2 AMORPHOUS SEMICONDUCTORS.

The ideal, infinite crystal is characterized by the regular arrangement of the atoms in the lattice. Two aspects of this order are important. (1) Short range order; this is due to the regular arrangement of lattice atoms in the immediate vicinity of the particular atom considered. It determines the crystal field in which the atom is embedded. (2) Long range order; this is due to the strict periodicity and hence the translational invariance of the crystal lattice. Long range order connects the short range order in such a way that atoms at equivalent lattice have the same surroundings in the same orientation.

Long range order is very important for the theory of band model. But strict long range order scarcely influences the physical properties of the solid. In reality a crystal is always perturbed, be it by the finite extent of the crystal or by the elementary excitations as dynamic perturbations and by point imperfections as static perturbations. A lattice is referred to as ordered if it is possible to explain the characteristics by starting with an infinite lattice with ideal long range order as the zeroth approximation and to include the dynamic and static perturbations by perturbation theory. An arrangement of atoms is called disordered when this approximation is not meaningful.

The two dimensional cubic point lattice shown in figure 8(a) has three important signs of order. All lattice atoms are equal, the neighbours of a particular lattice atom are arranged in a geometrically fixed short range order, and the coordination number, i.e., the number of nearest neighbours, is the same for all atoms. The first sign of order is absent in figure 8(b): two sorts of atoms are statistically distributed over the available lattice sites. This type of disorder is called compositional. Figure 8(c) illustrates another type of disorder: positional disorder. Here all the lattice atoms are same as in the ordered lattice, but the geometric arrangement is statistically disturbed. Positional disorder is the characteristic of amorphous solids. A further sign of disorder can be

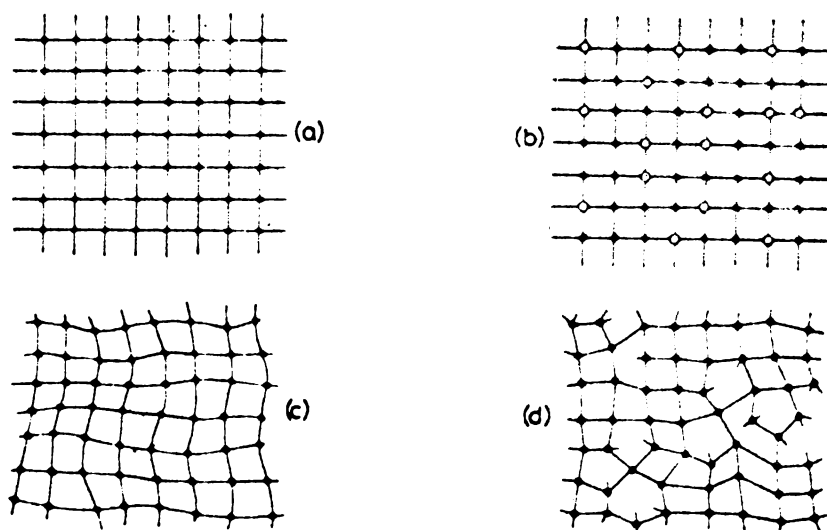


Figure 8: Possible types of lattice disorder: (a) orderd lattice, (b) mixed crystal formation by statistical distribution of two sorts of atoms over the lattice sites: compositional disorder, (c) positional disorder by distortion of the lattice, (d) topological disorder with simultaneous formation of dangling bonds.

added to positional disorder, namely topological disorder. Here the topology of the lattice is perturbed. In addition to the four-atom rings which are characteristic for the cubic net, figure 8(d) shows the appearance of rings with five or six atoms. If the coordination number is not maintained, individual valences remain unsaturated (dangling bonds). These form additional localized defects and are similar to vacancies in an ordered lattice.

In the disordered solid, in contrast to crystalline infinite medium, localized states can occur. In crystalline media a single imperfection leads to the splitting-off and simultaneous localization of a state from the band edge. With increasing number of imperfections the number of localized states outside the band increases. The defect levels combine into a band (impurity band) which can overlap with the band of the delocalized states if the defect concentration is sufficiently high. We can imagine that the same phenomenon occurs with increasing disorder of a lattice. The states at the edge of an energy band become localized first, and simultaneously shift into the energy gap. The bands thus acquire tails with localized states at its top and bottom edges. A distinct energy E_d separates localized and extended states. If one approaches from the extended state side, the mean free path becomes smaller. However, since the mean free path cannot become smaller than a lattice constant, a minimum conductivity σ_{E_d} remains.

Below E_d the states are localized. The conductivity at absolute zero of temperature is then zero. At E_d an abrupt step occurs in σ and hence in mobility. Accordingly E_d is referred in the literature as mobility edge.

In energy ranges where the one-electron states E_i are localized, the wave-vector K is no longer a good quantum number. A band structure function $E(K)$ can then not be introduced, nor can the derived concepts like effective mass, crystal momentum, etc. As long as the one electron states can be defined, the density of states concept is valid. Its general definition is

$$g(E) = \frac{1}{V_g} \sum_i \delta(E - E_i)$$

Both experiment and theory show that, as in the crystalline case, bands of delocalized states can exist. Tails with localized states are attached to their edges. Between the tails of two adjacent bands a region without states, a gap, can occur, or the tails can overlap (pseudo-gap). Models for density of states in amorphous semiconductors are given in figure 9.

Temperature variation of D.C. conductivity

In an amorphous semiconductor, three mechanisms of electrical conduction can be distinguished /4/.

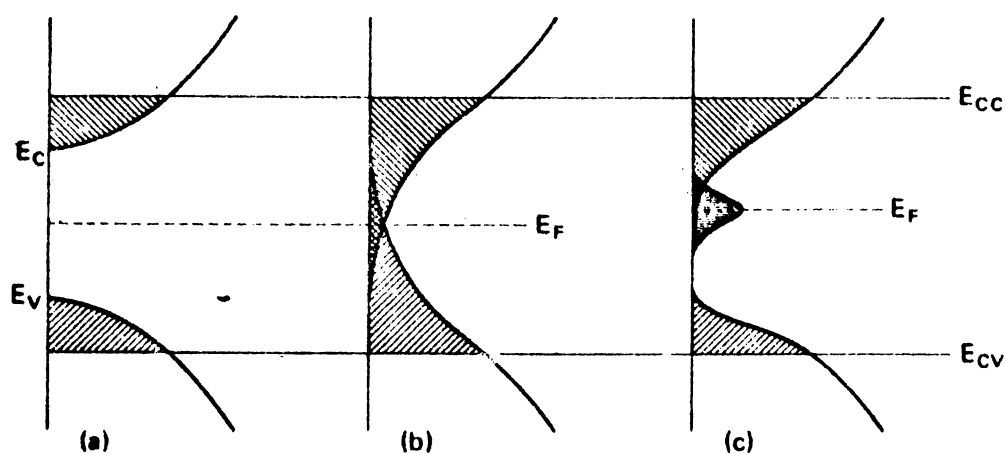


Figure 9: Possible density of states in amorphous semiconductors (a) localized states at the edges of the valence and conduction bands, (b) overlap of the tails of the localized states, (c) additional impurity band of local defects.

- a) Conduction due to carriers excited beyond the mobility shoulders into extended states. If the main current is carried by holes, we expect

$$\sigma = \sigma_0 \exp(-(E_F - E_V)/k_B T) \quad (1.2.1)$$

the pre-exponential factor σ_0 is expected to be given by

$$\sigma_0 \approx \frac{0.06 e^2}{\hbar a_E}$$

for a coordination number 6 and a_E is the distance between the localized states. In general σ_0 may lie between 100 and 500 $\Omega^{-1} \text{cm}^{-1}$ in most materials.

- b) Conduction due to carriers excited into the localized states at the band edges, i.e. at E_C or E_V . If the main current is carried by holes, and conduction is by hopping,

$$\sigma = \sigma_1 \exp(-(E_F - E_B + \Delta W_1)/k_B T) \quad (1.2.2)$$

where ΔW_1 is the activation energy for hopping and E_B is the energy at the band edge.

An estimate of σ_1 is not easy to make, but is expected to be a factor of 10^2 - 10^4 less than σ_0 . This is partly due to an effective density of states lower by a factor $\approx (E_B - E_V)/k_B T$, but mainly by a lower mobility

μ_1 .

Conduction due to carriers tunnelling between localized states near the Fermi energy. This is the process analogous to impurity conduction in heavily doped semiconductors, and we may write

$$\sigma = \sigma_2 \exp(-\Delta W_2/k_B T) \quad (1.2.3)$$

where $\sigma_2 \lesssim \sigma_1$ and ΔW_2 is the hopping energy of the order of half the width of the defect band shown in figure 9(c). A straight line in a plot of $\ln \sigma$ against $1/T$ is expected only if hopping is between nearest neighbours. As the temperature is lowered, it may become favourable for the carriers to tunnel to more distant sites, ΔW_2 will fall and ultimately the conductivity is expected to behave like

$$\ln \sigma = A - BT^{-1/4} \quad (1.2.4)$$

Knowledge of activation energy needed for conduction and the value of the pre-exponential factor at different temperature ranges provide us information on the type of conduction occurring in the concerned temperature range.

Optical absorption in amorphous semiconductors

In disordered solids we can distinguish three characteristically different regions of absorption (Table I, figure 10 and 11) /5/.

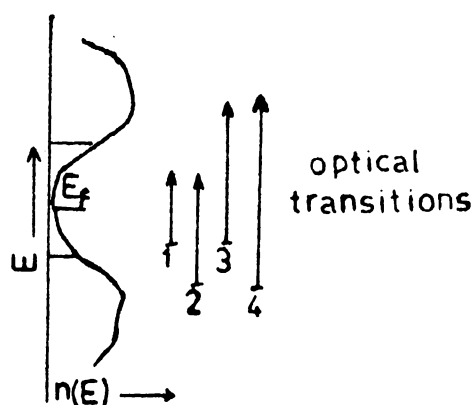


Figure 10: Optical transitions in disordered materials (see Table I).

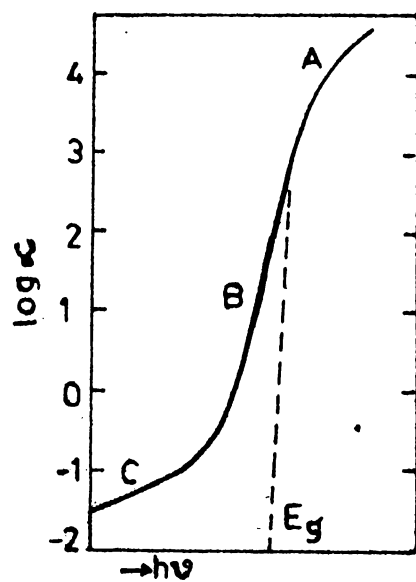


Figure 11: Shape of the optical edge of disordered material (see Table I).

TABLE I

Optical transitions in disordered semiconductors

notation in figure 11	notation in figure 10	γ_i	γ_f	$\omega^2 \epsilon_2(\omega)$
C	1	Localized	Localized	$\exp(\omega/E_1)$
B	2	Extended	Localized	$\exp(\omega/E_2)$
	3	Localized	Extended	
A	4	Extended	Extended	$(\omega - E_g)^r$
$r > 0$				

The transitions from localized into localized states are important in explaining the shape of the ϵ_2 curve for small photon energies. This region is very difficult to treat theoretically and experimentally. Using exponential valence and conduction band tails one can estimate the absorption coefficient.

$$\omega \mathcal{L}(\omega) \sim \exp(\omega/E_1) \quad (1.2.5)$$

where E_1 is some characteristic temperature dependant parameter, ($E_1 \approx 0.1$ eV). For transitions between localized and delocalized states (and vice versa) one can also derive an exponential law, by using exponential density of states for the localized states and a free electron density of states for the extended states.

$$\omega \mathcal{L}(\omega) \sim \exp(\omega/E_2) \quad (1.2.6)$$

For transitions between extended valence states and extended conduction states we can assume a power law to hold, i.e.

$$\begin{aligned} n_v(E) &\sim (E_v - E)^{r_v} \\ n_c(E) &\sim (E - E_c)^{r_c} \end{aligned}$$

Then with constant matrix elements,

$$\omega \mathcal{L}(\omega) \sim (E - E_g)^{r_v + r_c + 1} \quad (1.2.7)$$

with a phenomenological optical energy gap E_g . For

$r_v = r_c = 1/2$ we obtain

$$\omega \mathcal{L}(\omega) \sim (E - E_g)^2 \quad (1.2.8)$$

This is the so called non-direct transition law.

References:

1. A. Sommerfeld, Z. Phys., 47 (1928) 1.
2. F. Bloch, Z. Phys., 52 (1928) 555.
3. A.H. Wilson, Proc. Roy. Soc. A, 133 (1931) 458.
A.H. Wilson, Proc. Roy. Soc. A, 134 (1931) 277.
4. N.F. Mott and E.A. Davis "Electronic Processes
in Non-Crystalline Materials" Clarendon
Press, Oxford (1971).
5. B. Kramer in Physics of Structurally Disorderd
Solids; Ed. S.S. Mitra, Plenum Press,
New York 1976, p 374.

CHAPTER-II

REACTIVE EVAPORATION METHODS

Reactive evaporation is a variant of Günther's Three Temperature Method (TTM) /1/ and is based on the fact that continuous condensation of a given vapour at a given deposition rate takes place only if the substrate temperature drops below a critical value. Differences in magnitude of these critical values, which are functions of the interfacial energies, make it possible to condense a given vapour type or a combination (i.e. a compound) preferentially on the substrate surface.

The condensation flux N_K of a given vapour on a given substrate, exceeds zero only if the ratio p/p_e of the actual vapour pressure p and the equilibrium pressure p_e exceeds a critical value q_c .

$$\text{i.e. } N_K > 0 \text{ if } (p/p_e) > q_c \quad (2.1.1)$$

since this pressure may be related to the substrate temperature, it can be shown that the condition for progressive condensation at a given substrate temperature involves exceeding a critical incident flux, i.e.,

$$N_K = 0 \text{ if } N_+ \leq N_{+c} (T) \quad (2.1.2)$$

$$N_K > 0 \text{ if } N_+ > N_{+c} (T) \quad (2.1.3)$$

where N_+ is the incident flux and N_{+c} is the critical value of incident flux. If the flux exceeds N_{+c} , the condensation flux rises rapidly and approaches a maximum value given by

$$N_K \text{ max} = \mathcal{L} (N_+ - N_e) \quad (2.1.4)$$

where \mathcal{L} is the condensation coefficient and N_e the number of reevaporated atoms.

The state of affairs described above and illustrated in figure 1 may be represented in terms of a critical temperature T_c assuming a constant incident flux N_+

$$N_K = 0 \text{ if } T \geq T_c(N_+) \quad (2.1.5)$$

$$N_K > 0 \text{ if } T < T_c(N_+) \quad (2.1.6)$$

Thus by analogy with figure 1, the condensation can be represented schematically as a function of substrate temperature as in figure 2, i.e., after dropping below the critical temperature T_c , condensation sets in spontaneously and quickly approaches a maximum.

Suppose the vapour phase consists of two components A and B and both being incident on the substrate under consideration. If the vapour density is low enough, we may neglect collisions between particles

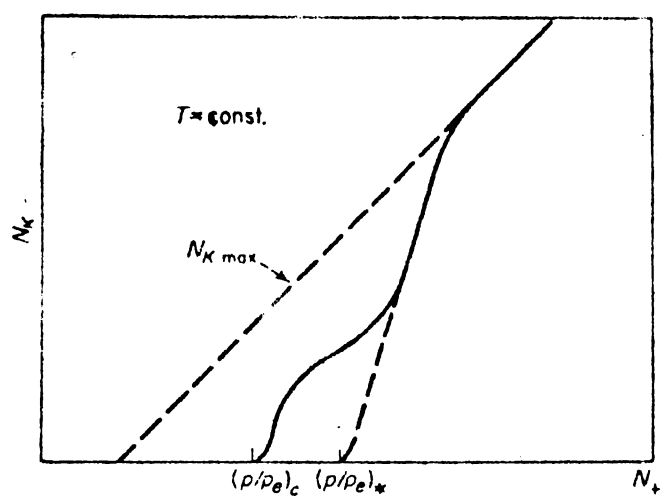


Figure 1: Variation of condensation flux N_K with flux N_+ of incident particles.

of the components A and B in the vapour phase. However interactions can take place between such particles within the adsorbed stage on the substrate surface. These interactions may lead to the formation of molecules



where AB stands for all possible compounds $A_n B_m$. A rough estimate of the interaction probability on the surface gives a density

$$n_{AB} = \text{const. } n_A n_B \bar{D} \quad (2.1.8)$$

where n_A and n_B are the number of adsorbed atoms A and B and \bar{D} the mean diffusion coefficient. This estimate is rough because we are not considering the energies of the particles and we know that only if the particles collide with sufficient translational energy they will react to form the compound molecule. Since the number of adsorbed atoms is proportional to actual vapour pressure p , or the incident flux N_+ of the particular vapour, the density n_{AB} should also be proportional to the product of incident fluxes ($N_{+A} N_{+B}$) or vapour pressures ($p_A p_B$).

In order to estimate the critical values which now apply, the equilibrium pressures p_{eA} , p_{eB} of the components and p_{eAB} of the compound must be considered. p_{eAB} usually corresponds to the dissociation pressure of

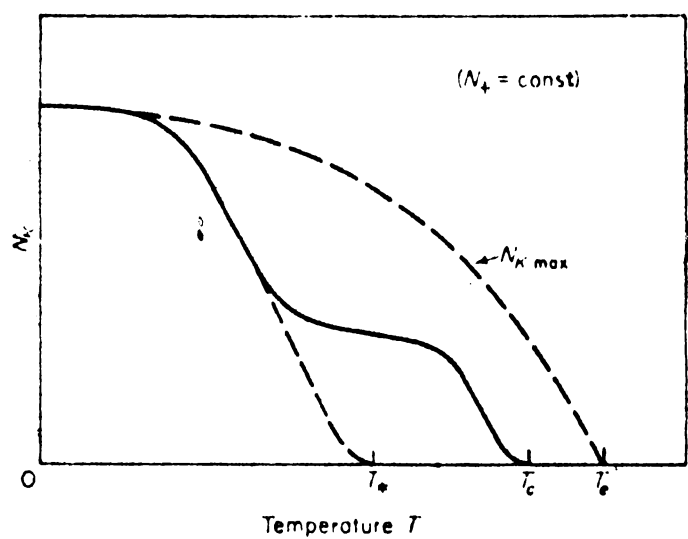


Figure 2: Variation of condensation flux N_K with substrate temperature T .

the compound and is equivalent to the pressure of the more volatile component (say, A) in equilibrium with the compound. In most cases, this value is much lower than the equilibrium pressure p_{eA} of the pure component A. Thus the critical values of one component A in the presence of the other component B should vary as follows:

$$N_{+cA}(B) \ll N_{+cA} \quad (2.1.9)$$

$$T_{cA}(B) > T_{cA} \quad (2.1.10)$$

This means that it will be possible to condense A (in combination with B, of course) at a lower critical flux in the presence of B for a given substrate temperature. Or in terms of substrate temperature it means that a higher substrate temperature may be used to deposit A in combination with B for a given flux of A.

At a given substrate temperature T and for incident fluxes $N_{+B} < N_{+cB}$, no condensation of any kind is possible while the incident rate N_{+A} is low. However, at a critical value $N_{+cA}(B)$, sufficient molecules AB are formed on the substrate, and nucleation and progressive condensation of AB starts. This critical value $N_{+cA}(B)$ itself depends on the incident flux of the component B. With further increase of N_{+A} , no increase of condensation flux N_K is possible until, with $N_{+A} > N_{+cA}$,

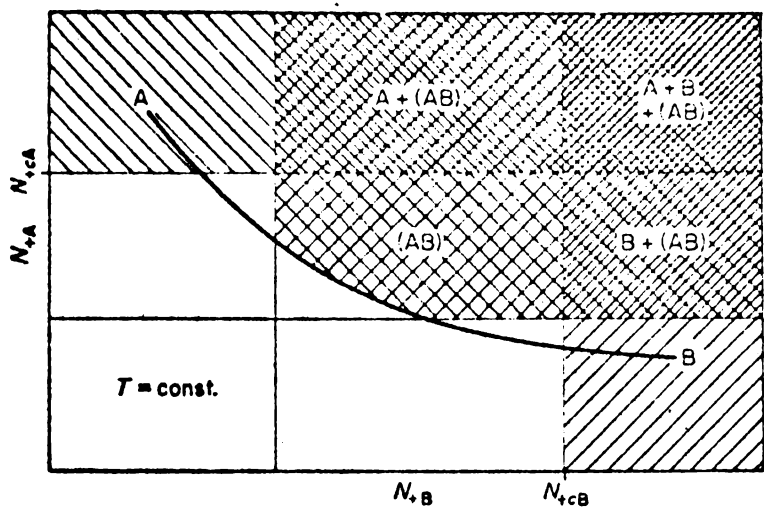


Figure 3: Condensation diagram for two incident components A and B.

condensation of unreacted A takes place. Figure 3 shows the condensation diagram for two incident components A and B for a given substrate temperature .

The plus points of reactive evaporation include the following.

- (1) Elimination of the synthesis of the compound prior to deposition. This is advantageous because the tedious and sometimes expensive metallurgical process which needs high temperature rocking furnaces and facilities to seal the ampoule containing the reactants at high vacuum (10^{-5} Torr), is eliminated.
- (2) High temperatures ($> 2000^{\circ}\text{C}$) are frequently needed to evaporate high melting point carbides, nitrides, and oxides. If resistive heaters are used, the film will get contaminated because of the evaporation of the heater itself. And also it may not be possible to get high evaporation rates which are essential in industrial processes. Reactive evaporation overcomes this defect, because almost all the metals evaporate below 1500°C with sufficient vapour pressure, so that high deposition rates of the compounds are possible.
- (3) The decomposition of the compound on heating in vacuum and consequent loss of the original composition in the films are inherently not present. It must be mentioned that TTM and reactive evaporation

were originally developed to overcome this disadvantage in ordinary evaporation technique.

- (4) The lowest substrate temperature possible is dictated by the condensation temperature of the more volatile component and is usually low (eg. O_2 , S_2 , and Se_2) and consequently this method can be used as an efficient technique for the preparation of amorphous films.
- (5) Dopants can be evaporated simultaneously at a suitable rate and thus a uniform dispersal of the dopant can be easily achieved.
- (6) Film growth can be started and stopped abruptly and hence abrupt interfaces are possible.
- (7) In general, different compounds in a binary or ternary system may be prepared by adjusting the evaporation rate of the individual components and substrate temperature.

The technique has now been so perfected that it is possible to deposit epitaxial films of certain compounds (InAs and InSb) at rates approaching that of vapour phase epitaxy ($0.5 - 1 \text{ micron min}^{-1}$) with excellent carrier mobilities /2/. If this high rate of deposition can be extended to other III-V compounds like GaAs and InP, it will be possible to dispense with UHV conditions, where it is solely used for preventing the incorporation of

impurities in the growing film. This will certainly give a boost to semiconductor heterojunction laser technology which now requires costly and time consuming MBE.

This technique which has been so successfully used in the case of many technologically important compounds suffers from the following drawbacks which arise from the low chemical reactivity of the particles used for film formation as discussed in chapter XI.

- (1) The use of large volatile flux and consequent wastage of the volatile element.
- (2) When high deposition rates are needed, large volatile flux leads to the use of high volatile partial pressure (10^{-4} to 10^{-2} Torr) which reduces the mean free path and also scatters the non-volatile beam away from the substrate surface. Also the high pressure in the vacuum system reduces the evaporation rate of the non-volatile component.
- (3) Because of the high volatile elemental pressure, some unreacted volatile flux may get entrapped in the growing film which will have drastic effects in the film properties. It has been reported that refractive index, hardness etc. of TiO_2 films prepared by this technique decreases as the oxygen partial pressure is increased to

get high deposition rates /5/. Though this has been explained as due to the large number of collisions TiO molecules suffer in the gas phase and consequent lack of energy of the particles, it seems that this is due to the entrapment of unreacted volatile element (here oxygen) in the growing film. And that explains why the films have a lower hardness and refractive index.

Chemical reaction rate may be increased in two ways. The first method is by increasing the translational energy of the particles so that they can overcome the potential barrier and the second method is by lowering the potential barrier itself so that particles with very low energies can react.

It may not be easily possible to enhance reaction rate by increasing the substrate temperature so as to increase translational energy, as this will lead to increased dissociation of the compound formed and also increase chemical reactions with the underlying substrate. Stability of the substrate at high temperature is another problem which has to be taken into consideration. One way to increase the translational energy of the particles is by increasing the source temperature. But the associated increase in rate of evaporation must be prevented and this can be achieved by using flash

evaporation like techniques. But the practical kinetic energies attainable by this technique is limited to 0.2 to 0.3 eV. The most versatile way of increasing the kinetic energy of the particles is by ionizing the particles with electron beams or suitable radiations and accelerating them in electric fields.

Historically the first method which used some of these techniques to increase chemical reaction rate is the activated reactive evaporation /4/ of Bunshah and Raghuram. Their original set up is shown in figure 4. The secondary electrons from the molten pool of the metal is attracted by a low voltage probe (biased positively around 100 V) and these electrons ionize the reactive gas atoms generating a thick plasma. Because of the presence of the plasma, chemical reaction rate is very much increased and Bunshah and Raghuram could deposit TiC at a rate of $12 \mu \text{ min}^{-1}$ at a source substrate distance of 15 cm using this technique. It may be mentioned that using ordinary reactive evaporation, titanium and the reactive gas used, acetylene, do not react to form the compound.

Let us analyze this process in some detail. It will be shown in Chapter XI that the reacting species must possess a certain amount of translational energy to overcome the potential energy barrier for reaction. It is also shown there that the reaction rate should increase if we increase particle energies. In ARE the ions are

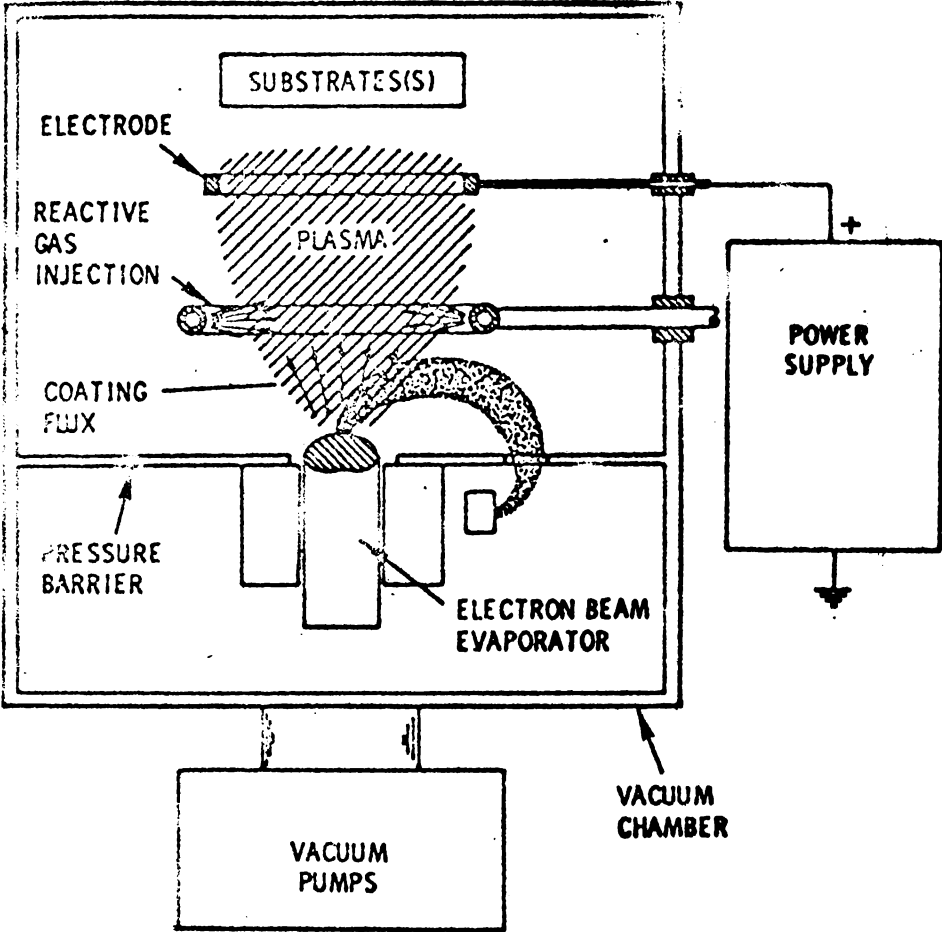


Figure 4: Set-up for ARE used by Bunshah and Raghuram.

not accelerated to the substrate as may be seen from Figure 4. This is because usually ions are positively charged and will be attracted only to the negatively charged pool of the metal and this is in a direction opposite to that of the substrate. Moreover, the applied electric field is confined to a small region above the source of secondary electrons and ionization of the atoms predominantly take place beyond this field. Hence the only increase in translational energy of the atoms is from collisions with electrons. Consider, for simplicity, an electron colliding head-on with a gas atom at rest. From the principle of conservation of momentum,

$$mv + MV = mv_1 + MV_1 \quad (2.1.11)$$

where m and M are the electronic and ionic mass and v , v_1 and V , V_1 are the initial and final electron and ion velocities respectively.

From the principle of conservation of energy,

$$\frac{1}{2} mv^2 = \frac{1}{2} mv_1^2 + \frac{1}{2} MV_1^2 + W_p \quad (2.1.12)$$

where W_p is the ionization energy of the atom. Solving these equations for V_1 , we get,

$$V_1 = \frac{Mv + \sqrt{M^2 v^2 - 2M \left(1 + \frac{M}{m}\right) W_p}}{\frac{M}{2} \left(1 + \frac{M}{m}\right)} \quad (2.1.13)$$

Since $\frac{M}{m}$ is a large quantity, V_1 can be approximated to

$$V_1 = 2m \left[v \pm \sqrt{v^2 - 2W_p/m} \right] / M \quad (2.1.14)$$

Substituting typical values, it may be seen that, the increase in kinetic energy of the particle is approximately equal to 0.1 eV which is less than the thermal energy of the particle.

Hence we have to look for other causes for a very large increase in chemical reaction rate. In ordinary reactive evaporation, the particles are not ionized and they have to collide with sufficient translational energy to overcome the potential barrier (see Chapter XI). But when one of the particles is ionized, the activation energy necessary for chemical reaction become very low or equal to zero. In other words for ion molecule reactions, the potential barrier is very low or does not exist at all. This is because of an inverse fifth power attractive force arising from point charge-induced dipole interaction between the ion and the molecule /5/. This long-range attraction, greatly increases the rate of collisions above what would usually obtain if both the particles were ground state neutrals, and is responsible for the very large cross sections ($10^{-14}/\text{cm}^2$) of many ion-molecule reactions at thermal energies. So collision rate is increased and almost all collision leads to a

reaction and also the reaction rate is nearly independent of temperature. In the case of a plasma as used in ARE, the velocities of ionized and neutral particles obey the Maxwellian distribution of velocities (because due to collision with electrons, the velocities of the atoms or molecules are not changed much) and the rate constant is approximated by Gioumousis and Stevenson's formula /6/

$$k = 2\pi e (\alpha_o / \mu_r)^{1/2} \quad (2.1.15)$$

where α_o is the polarizability of the molecule, μ_r the reduced mass of the colliding pair and e the electronic charge. From this expression, a rate constant of about $10^{-9} \text{ cm}^3 \text{ sec}^{-1}$ can be predicted for most collisions of ion with non-polar molecules. In order to get an idea of the increase in reaction rate due to ionization, this rate constant must be compared with bimolecular reactions involving atoms and radicals which have rate constants of the order of only $10^{-11} - 10^{-14} \text{ cm}^3 \text{ sec}^{-1}$.

Though chemical reaction rate is tremendously increased, making it possible to get high deposition rates by the use of ARE, there is still the problem of amorphous areas and unreacted species getting entrapped in the growing film. This, as we know, will adversely affect film properties. It is well known that if the substrate temperature is so chosen that the reevaporation of amorphous

and unreacted areas are favourably increased, high quality films can be obtained. It is also found that if the ratio of substrate temperature T to the normal boiling point of the compound T_b is approximately 0.33, films with optimum properties are obtained /7,9/. This particular substrate temperature will also increase diffusion into the reevaporated areas and microhole free films with good carrier mobility etc. can be obtained. If too high a substrate temperature is chosen, the crystalline areas of the film itself will reevaporate and film quality will be poor.

If high substrate temperature is not practicable for any reason, another way to obtain almost all the beneficial effects of high substrate temperature is by giving additional kinetic energy to the ionized and neutral particles by accelerating the ionized particles to the substrate and making it collide with neutral particles before they reach the substrate surface. Such a method is known by various names like Biased Activated Reactive Evaporation (BARE) /10/ or Reactive Ion Plating (RIP) /11/. In this method, the substrate is kept at a high negative potential (around 3KV) and the ions are accelerated to the substrate. An analysis by Teer /12/ showed that for a typical system with an applied voltage of 3KV and a gas pressure of 10^{-2} Torr, the ions lose almost 90% of the energy by transferring their energy to

neutral atoms in traversing the cathode dark space. If the mean free path λ_0 and the length Z_c of cathode dark space are assumed to be 0.5 cm and 10 cm respectively under the conditions given above, a total number $(Z_c/\lambda_0)N_0 = 20 N_0$ of energetic neutrals are produced, where N_0 is the number of ions leaving the edge of the cathode dark space towards the cathode in unit time. The average energy of the ions arriving at the cathode is approximately $(V_c/Z_c) \cdot 2 \lambda_0 = 300$ eV and of the neutral particles is $V_c(Z_c - 2 \lambda_0) (\lambda_0/Z_c)/Z_c = 135$ eV, for the same conditions, assuming they suffer no collisions after gaining their energy. From this it can be seen that energetic neutral atoms (less than 135 eV) are in the majority and ions with moderately high energy (about 300 eV) are in the minority for film formation.

The most important physical process which occur during ion-plating and allied techniques are

- (1) ion induced (and energetic atom induced) desorption of adsorbed impurities from substrate surface. This cleaning effect gives excellent adhesion of the film to the substrate.
- (2) ion penetration and entrapment in the substrate and coating.

- (3) ion induced sputtering of substrate and coating. If the energy of the ions are properly adjusted, this backspattering effect can be used to sputter away amorphous and disordered regions leaving the crystalline region intact. This process may be used to get films with optimal properties.
- (4) recoil displacement of substrate and coating atoms. This leads to good intermixing and improvement in adhesion and microhardness results.

References:

1. K.G. Gunther in 'The Use of Thin Films in Physical Investigations', J.C. Anderson Ed., Academic Press, New York, 1966.
2. H. Freller, Thin Solid Films 58 (1979) 49.
3. E. Ritter, J. Vac. Sci. Tech. 3 (1966) 225.
4. R.F. Bunshah and A.C. Raghuram, J. Vac. Sci. Tech. 9 (1972) 1389.
5. E.W. McDaniel, Collision Phenomena in Ionized Gases, Sect 3-6 and 6-3, Appendix II, Wiley, New York (1964).
6. G. Gioumousis and D.P. Stevenson, J. Chem. Phys., 29 (1958) 294.
7. P.S. Vincett, W.A. Barlow, and G.G. Roberts, J. Appl. Phys., 48(1977) 3800.
8. P.S. Vincett, Z.D. Popovic and L. McIntyre, Thin Solid Films, 82 (1981) 357.
9. P.S. Vincett, Thin Solid Films, 100 (1983) 371.
10. R.F. Bunshah, Physical Vapour Deposition of Metals, Alloys and Compounds, New Trends in Materials Processing, American Society for Metals, Metals Park, OH, 1976, p 200.
11. M. Kobayashi and Y. Doi, Thin Solid Films 54(1978) 67.
12. D.G. Teer, Proc. Ion Plating and Allied Techniques 1PAT-77, Edinburgh, 1977, CEP Consultants, Edinburgh 1977, p 13.

CHAPTER-III

EXPERIMENTAL TECHNIQUES.3.1 DETERMINATION OF OPTICAL CONSTANTS OF THIN FILMS

The measurement of the optical constants, refractive index n and extinction coefficient k of a solid is of crucial importance from the point of view of basic and applied research. This is because, these constants are determined by the structure and bonding of atoms in solids and hence measurement of these quantities as a function of wavelength can give valuable information regarding structure and bonding. And also in any application of solids in optics or in optoelectronics n and k are the most important quantities.

The usual methods used to measure these quantities as a function of wavelength are spectroscopic ellipsometry, simultaneous measurement of transmission and reflection, and the measurement of reflection/transmission only. Spectroscopic ellipsometry which is the most precise technique, is applicable only in the regions of wavelength where polarizers and analyzers are available. This and the lengthy mathematical calculations involved restrict somewhat its application. One great advantage of this technique is that the material need

not be transparent to the radiation used. Simultaneous measurement of transmission and reflection is the most used method for the measurement of n and k . This method is applicable in any region of the spectrum if suitable light sources and detectors are available and also if the material is fairly transparent. In the highly absorbing regions of the spectra of a material, measurement of reflectivity is the only method available. This region for most semiconductors and insulators lie above 10 eV where ellipsometry is not applicable because of the lack of suitable analyzers and polarizers and also the use of vacuum spectrographs.

Recently it was shown by Manifacier et al /1/ that the measurement of transmission through a parallel faced film in the region of transparency is sufficient to determine the real and imaginary parts of the complex refractive index. This method, because of its extreme simplicity and the availability of commercial scanning spectrophotometers in the UV, Vis, NIR, and IR regions of wavelength, was used in all the studies reported in this thesis.

Figure 1 shows a film with complex refractive index $\eta = n - ik$ bounded by two transparent media with refractive indices n_0 and n_1 . Considering a unit amplitude for the incident light wave, in

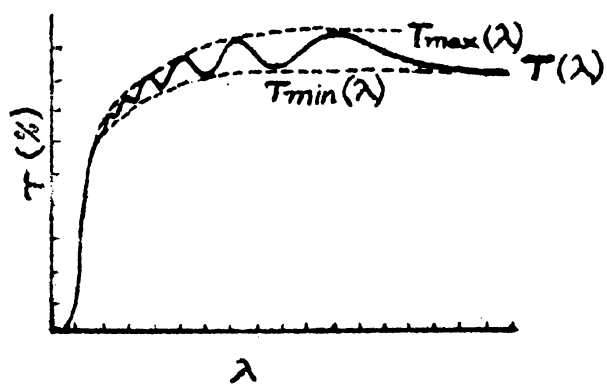
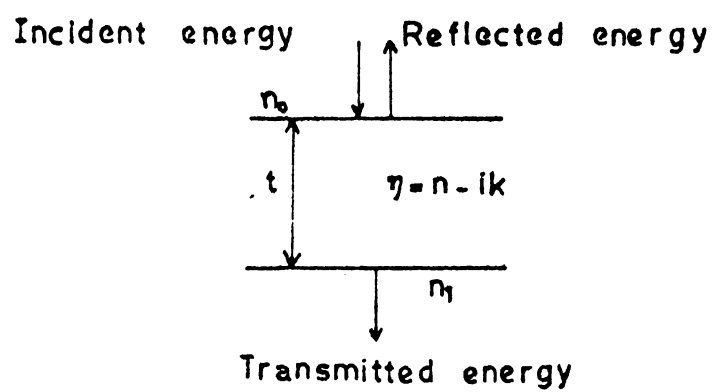


Figure 1: Reflection and transmission of light by a single film along with a typical transmission spectrum.

the case of normal incidence, the amplitude of the transmitted wave is given by

$$A = \frac{t_1 t_2 \exp(-2\pi i \eta t / \lambda)}{1 + r_1 r_2 \exp(-4\pi i \eta t / \lambda)} \quad (3.1.1)$$

in which t_1, t_2, r_1, r_2 are the transmission and reflection coefficients at the front and rear faces. The transmission of the layer is given by

$$T = \frac{n_1}{n_0} |A|^2 \quad (3.1.2)$$

In the case of weak absorption with $k^2 \ll (n - n_0)^2$ and $k^2 \ll (n - n_1)^2$,

$$T = \frac{16n_0 n_1 n^2 \mathcal{L}'}{C_1^2 + C_2^2 \mathcal{L}'^2 + 2C_1 C_2 \mathcal{L}' \cos \left(\frac{4\pi n t}{\lambda} \right)} \quad (3.1.3)$$

where $C_1 = (n + n_0)(n_1 + n)$, $C_2 = (n - n_0)(n_1 - n)$

and $\mathcal{L}' = \exp(-4\pi k t / \lambda) = \exp(-\mathcal{L} t)$

The extreme values of transmission are given by the formulae

$$T_{\max} = 16 n_0 n_1 n^2 \mathcal{L}' / (C_1 + C_2 \mathcal{L}')^2 \quad (3.1.4)$$

$$T_{\min} = 16 n_0 n_1 n^2 \mathcal{L}' / (C_1 - C_2 \mathcal{L}')^2 \quad (3.1.5)$$

Considering T_{\max} and T_{\min} as continuous functions of λ through $n(\lambda)$ and $\mathcal{L}'(\lambda)$, which will be the envelopes of the maxima $T_{\max}(\lambda)$ and the minima $T_{\min}(\lambda)$, and forming the ratio of equations (3.1.4) and (3.1.5),

$$\mathcal{L}' = \frac{C_1 [1 - (T_{\max}/T_{\min})^{1/2}]}{C_2 [1 + (T_{\max}/T_{\min})^{1/2}]} \quad (3.1.6)$$

Then from equation (3.1.4),

$$n = [N + (N^2 - n_o^2 n_1^2)^{1/2}]^{1/2} \quad (3.1.7)$$

$$\text{where } N = \frac{n_o^2 + n_1^2}{2} + 2n_o n_1 \frac{(T_{\max} - T_{\min})}{T_{\max} T_{\min}}$$

From these equations refractive index n , extinction coefficient k and absorption coefficient \mathcal{L} was determined.

The following conditions have to be satisfied for getting good results.

1. To obtain good fringe pattern, which is necessary for the precise measurement of refractive index, the difference between film refractive index n and the substrate refractive index n_1 should be as great as possible.

2. Effective bandwidth of the spectrophotometer should be kept smaller than the half width of the interference maximum.
3. The sample must be homogeneous and parallel faced.
4. Variation of n and k with wavelength should be small; this condition fails in the vicinity of fundamental absorption.

In the region of fundamental absorption, another simpler method may be used to measure \mathcal{L}

Transmission through a film on a transparent substrate in a medium of refractive index n_0 is given by

$$T = \frac{16 n_0 n_1 (n^2 + k^2)}{[(n_0 + n)^2 + k^2] [(n_1 + n)^2 + k^2]} \exp(-\mathcal{L}t) \quad (3.1.8)$$

In weakly absorbing regions of the spectra, $n^2 \gg k^2$, this equation approximates to

$$T = \frac{16 n_0 n_1 n^2}{(n_0 + n)^2 (n_1 + n)^2} \exp(-\mathcal{L}t) \quad (3.1.9)$$

If we have two samples with thickness t_1 and t_2 and if the samples are put in the sample and reference beam of the spectrophotometer,

$$T_1 = \frac{16 n_0 n_1 n^2}{(n_0 + n)^2 (n_1 + n)^2} \exp(-\mathcal{L}t_1) \quad (3.1.10)$$

for the specimen in the sample beam

$$T_2 = \frac{16 n_o n_1 n^2}{(n_o + n)^2 (n_1 + n)^2} \exp(-\mathcal{L} t) \quad (3.1.11)$$

for the specimen in the reference beam.

The spectrophotometer displays the log of the ratio of the two transmissions, and hence for any particular wavelength

$$\ln (T_2/T_1) = \mathcal{L} t \quad (3.1.12)$$

where $t = t_1 - t_2$. From this equation \mathcal{L} may be determined.

The advantage of this method is that only simple calculations are needed and one does not have to know the refractive index of the film. The only disadvantage is that a precise knowledge of film thickness is necessary as \mathcal{L} is dependant on the differences in sample thickness, which is a small quantity.

For measurements in the UV-Vis region, mostly a Hitachi 200-20 UV-Vis spectrophotometer was used. This instrument can cover the wavelength range from 900 nm to 200 nm with a light source change at 370 nm. For measurements in the NIR region, a Cary 17D or Carl Zeiss DMR 21 which can cover wavelengths from 2500 nm to 200 nm was used. All these instruments have fairly

high resolution and a spectral bandwidth of 1 or 2 nm was used in the measurements. After switching on the instrument, before taking the spectra, 15 minutes were allowed for the instrument to stabilize.

Measurements were made in the transmission mode of the spectrophotometer for the calculation of refractive index and extinction coefficient. In the fundamental absorption region, when the two specimen comparison technique was used, spectra was taken with the spectrophotometer in the absorption mode. The base line of the spectrophotometer was periodically adjusted, so that measurements could be made with 1% accuracy in transmission. The wavelength accuracy of the spectrophotometers were within 0.2 nm.

Films were deposited on optically flat glass substrates of dimension 3cm x 1cm x 0.1cm when the measurements were to be made in the visible region of wavelength and on quartz, when the measurements were to be made in the UV or NIR region.

3.2 MEASUREMENT OF ELECTRICAL RESISTANCE.

Electrical resistance of a semiconductor is controlled by the number of charge carriers available for conduction. As temperature increases from absolute zero, electrons from the closest defect level get excited

to the conduction band. This will be manifested as an exponential rise in conductivity and the activation energy needed for the process will be equal to the depth in energy level diagram of the particular level from the conduction band. As the temperature is further increased, electrons from the next level closest to the conduction band get excited and this process continues until all such levels in the forbidden gap are exhausted. Similar considerations hold true in the case of holes also. Each level will show up as a change of slope of the straight line portions in a $\ln \rho$ versus $\frac{1}{T}$ curve, where ρ is the resistivity of the film. At sufficiently high temperatures, the number of electrons excited from the valence band to the conduction band will come into prominence and the activation energy for conduction is then equal to the band gap of the semiconductor.

Thus, in principle, the measurement of electrical resistance as a function of temperature can yield information regarding levels in the forbidden gap and also the value of the band gap. But in practice, the material has to be highly purified and fairly free of structural defects to get the successive levels experimentally. Otherwise the level which is closest to the conduction band (valence band in the case of holes) will control the conductivity if it is sufficiently populated.

Also if this level lies very close to the band, resistance may increase with temperature after a certain temperature. This is because all the carriers from the level is already excited at that temperature and ~~any~~ further increase in temperature decreases mobility and hence the increase of resistance. Only at very high temperatures the intrinsic conductivity will set in (but at that temperature the semiconductor may have melted and vapourised!).

Measurement of electrical resistivity of highly insulating samples are rather difficult. This is because of the small value of currents ($\sim 10^{-15}$ A) encountered in these measurements. To measure such currents, good quality electrometers have to be used. When electrometers are used for measurements, it is not safe to increase the measuring voltage to more than 10V, as any short circuiting will damage the electrometer. As the currents are small, electrometer has to be worked at its maximum sensitivity and this calls for heavy shielding of specimen and electrometer cable from electrical disturbances. For this purpose an all metal cell was fabricated which could be evacuated to better than 10^{-2} Torr. High resistance measurements should be conducted in vacuum, otherwise water vapour present in the atmosphere may short circuit the specimen and give a false low resistance. The measuring cell and a typical

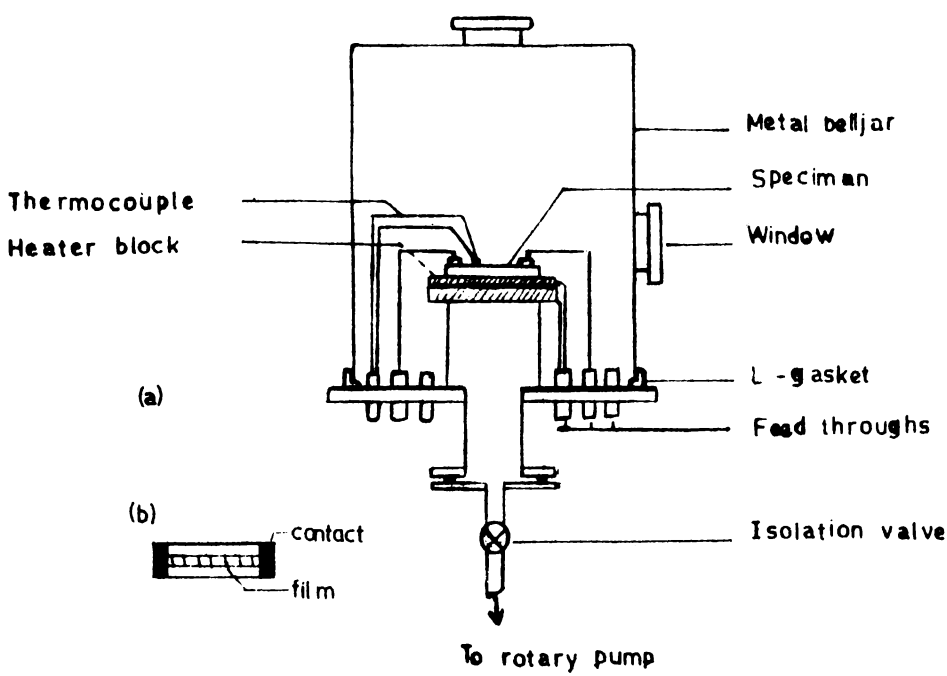


Figure 2:(a) Measuring cell for high resistance specimens (b) Typical specimen geometry.

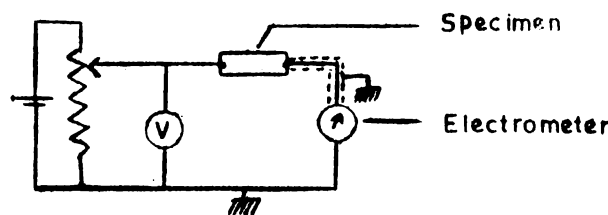


Figure 3: Electrical circuit for measurement of resistance.

specimen is shown in figure 2.

Current to the heater block on which the specimen is mounted for varying the specimen temperature, should be well smoothed DC and one terminal of it should be earthed. This is because any ripple present in the DC will induce large currents in the film or contacts which will completely mask the required signal. When the resistance is measured as a function of temperature, sufficient time should be given for the specimen to take up the heater block temperature.

The metal contact made to the film must be ohmic in characteristic. Substrate on which film is coated should be atleast hundred times more resistive than the film. Otherwise film will be electrically short circuited by the substrate. It must be noted that all electrical insulations in the cell should be made of teflon. The electrical circuit used for measuring the specimen resistance is shown in figure 3.

The potentiometer is a 10 K helical potentiometer and V is a digital multimeter. Since the voltage drop across the electrometer is negligible, the voltmeter reading may be taken as the true voltage applied to the specimen. Model EA 815 electrometer of ECIL has been used for current measurement. The temperature (thermocouple output) was measured using a

4½ digit, 200 mV full scale DPM. The potentiometer output was measured using an Hewlett Packard 3465 A digital multimeter.

3.3 DETERMINATION OF CONDUCTIVITY TYPE.

It is often convenient to have a means for determining whether a sample is p - type or n - type; the Hall effect is one means of doing this, but it requires a good deal of sample preparation and is not applicable when the sample is of high resistivity. A simple and convenient technique to test the type of carriers make use of the thermoelectric properties of semiconductors and is known as the hot probe method.

When one end of the sample is heated by the hot probe, carriers there get a high velocity and drift to the colder end. This produces a disturbance in the equilibrium distribution of carriers and sets up an electric field which opposes the flow of carriers. This electric field will be +ve with respect to the cold end if the carriers are electrons and negative if the carriers are holes.

One probe of a microvoltmeter is heated with a soldering iron for a few minutes and both the probes (hot and the other cold one) are touched to the sample and the meter deflection is observed. If the hot probe

voltage is +ve with respect to cold probe, the sample is n - type and if the voltage is -ve, the sample is p - type.

3.4 MEASUREMENT OF HALL VOLTAGE.

The measurement of Hall voltage gives the carrier concentration. This information together with the electrical conductivity can be used to get the mobility of the carriers. Hence measurement of Hall effect in conjunction with conductivity measurements may in principle be used for the complete electrical characterisation of the material.

The measurement of Hall effect using ordinary techniques is practicable only when the carrier mobility is atleast a few $\text{cm}^2/\text{volt sec}$ (upto $10^{-3} \text{cm}^2/\text{volt sec}$ using special techniques like single or double AC methods). This is because of three reasons; (1) the inverse proportionality of Hall voltage and carrier concentration (2) if the specimen resistance is high it will be difficult to send a current through the specimen which will give a reasonable Hall voltage (atleast a few microvolts) without appreciably joule heating the specimen (3) as the sample resistance increases, specimen noise also increases and this will mask whatever small Hall voltage that has developed.

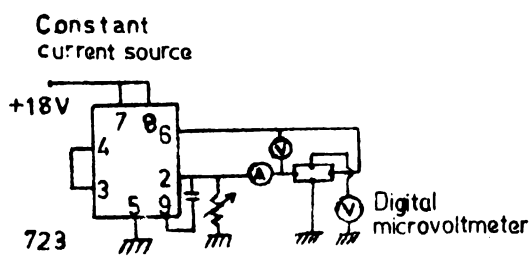


Figure 4: Circuit for measuring Hall Voltage.

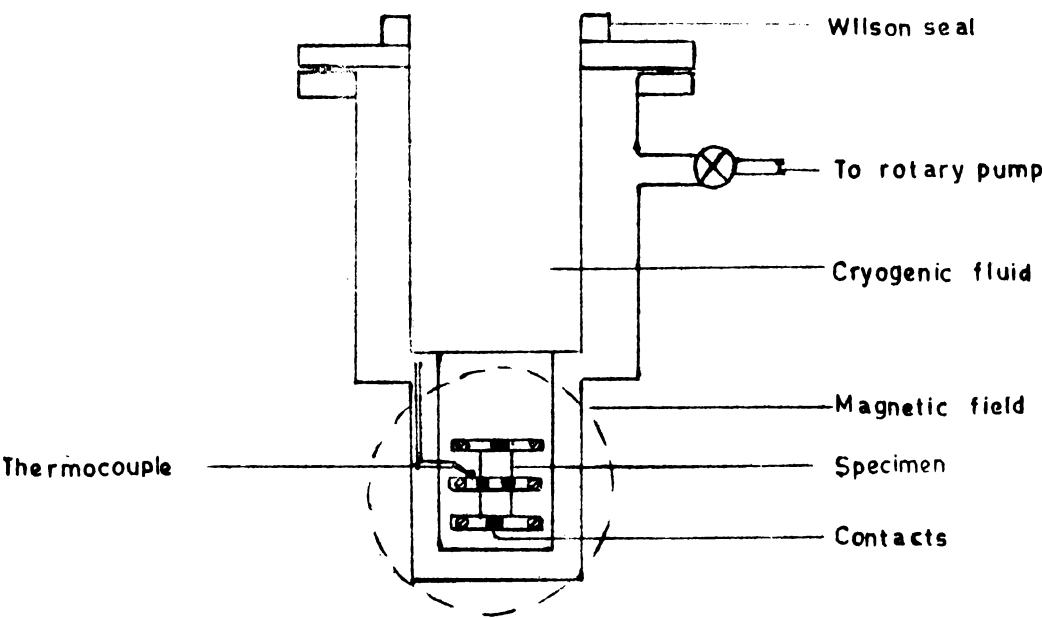


Figure 5: Cross section of Hall Effect measurement cell.

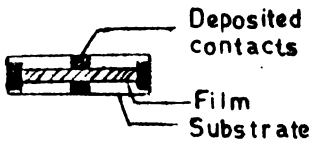


Figure 6: Specimen for Hall Effect measurement.

The circuit used for measuring Hall voltage is shown in figure 4. Current through the specimen was kept below 10mA and was measured by a digital multimeter. The Hall voltage developed was measured using a Hewlett Packard 3465 A digital multimeter which has a resolution of 1 μ V. Magnetic fields upto 10K gauss was applied, and all measurements were made in an evacuated cell made of copper which can go in between the pole peices of the magnet. A cross section of the cell is shown in figure 5 and is fully described in /2/.

The films for measurement were deposited on 4 x 1cm glass substrate with the aid of suitable masks. A typical specimen is shown in figure 6. Readings were taken with the direction of the current normal and reversed and the average of two readings was taken as the true Hall voltage. The carrier concentration was calculated using the formula

$$\text{Hall voltage } V = 10^{-8} RIH/t \quad (3.4.1)$$

where $R = -1/nq$, I , current in ampere, H , magnetic field in gauss and t , specimen thickness in cm.

3.5 X-RAY DIFFRACTION.

In preparing compound films using reactive evaporation, it is necessary to identify the compound formed and also its structure unambiguously. For this

X-ray diffraction is a non-destructive technique if the film thickness is greater than about 2000 Å . Electron diffraction is more sensitive and can be used even if the film is very thin, but suffers from the drawback that the film has to be detached from the substrate.

In usual X-ray diffractometers the Bragg-Brentano geometry is used, where the X-ray beam falls at an angle θ to the substrate and the detector is placed at an angle 2θ . The specimen and the detector are rotated at angular velocities ω and 2ω to get the various diffracting planes. In this geometry, when thin films are used, the effective thickness the X-ray beam sees at any angle of incidence will be $t/\sin \theta$, where t is the film thickness and θ the angle of incidence of the X-ray beam. Consequently scattered intensities will be angle dependant (enhanced by a factor $t/\sin \theta$) and this must be borne in mind when comparing the intensities with ASTM cards. If proper care is taken, X-ray diffraction can yield good results and any particular compound in the binary or ternary system can be identified without difficulty.

A Philips PW 1140/90 X-ray unit fitted with Philips PW 1050/70 goniometer was used in these studies. The detector was a proportional counter connected to a pulse height analyzer. Filtered $\text{Cu K}\alpha$ radiation was used. The accelerating potential applied to the X-ray tube was

35 KV and the tube current 18 mA. The specimens/were at least 2000 Å⁰ thick films coated on glass substrates of 3.5 cm x 2.5 cm. The X-ray beam was scanned from θ values of 10⁰ to 25⁰. The spectra (intensity of the reflected beam versus 2 θ) were recorded on a chart recorder running in synchronization with the goniometer.

3.6 SCANNING ELECTRON MICROSCOPY

Scanning electron microscopy is a useful tool for observing the surface features of the films. From the micrographs, grain size and their orientation relative to the substrate surface can be obtained. Scanning electron microscopical studies in conjunction with X-ray diffraction can be used to get a complete understanding of the structural properties of the films.

In an SEM a finely focused electron beam (energy of the beam may be varied from 1 to 35K eV) scans the specimen surface. The secondary or backscattered electrons are detected using properly mounted electron detectors. The output of the detector is displayed on a cathode ray tube which is scanned in synchronization with the electron beam. Resolutions of the order of 10 nm and magnifications more than 10⁵ are possible using SEMS.

A JEOL JSM 35 electron microscope was used in this study. The acceleration voltage and beam current was selected to give the maximum contrast.

The films were at least 3000 Å thick coated on 1cm x 1cm glass substrates. The films should be electrically conducting and earthed to prevent the accumulation of charges which will repel the electron beam. If the specimen is insulating a thin coating of gold should be given on top of the surface to be observed, and this thin coating should be earthed for the above mentioned reason.

3.7 THIN FILM THICKNESS MEASUREMENT /3/.

Multiple beam interferometry offers a direct accurate method for measuring the thickness of thin films. The film to be measured is deposited on an optically flat glass slide with part of the film removed along a straight edge so that film forms a step on the glass surface. An opaque highly reflecting film of aluminium or silver is then deposited over the surface of the film and bare glass. A second silvered optical flat is then brought near to the filmed surface and clamped on a specially made jig with three tilt adjustment screws as shown in figure 7, with the silvered surfaces facing each other. When the interferometer is illuminated with a parallel monochromatic beam at normal incidence and viewed with a low power microscope, dark interference fringes can be observed which trace out the points of equal air gap thickness. By adjusting the relative

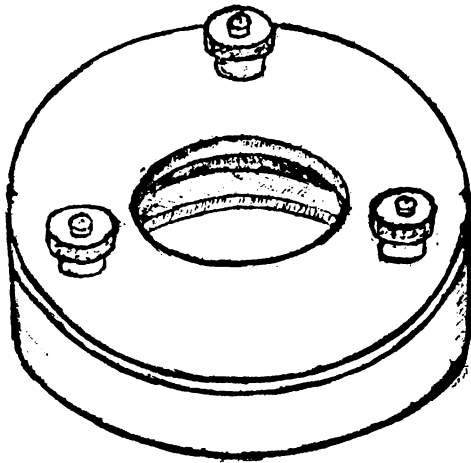
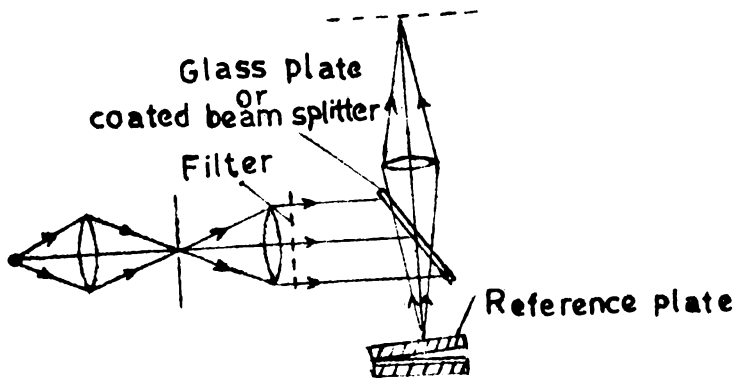


Figure 7: (a) Set-up for multiple beam interferometry (b) jig for multiple beam interferometry.

positions to form a wedge shaped air gap, the fringes can be made to run in straight lines perpendicular to the steps on the opaque film. The fringes show a displacement as they pass over the step edge. The difference in the air gap spacing for the two adjacent fringes is $\lambda/2$ and the displacement of any fringe expressed as a fraction of the fringe spacing gives the film thickness in units of $\lambda/2$. The film thickness is given by

$$t = \frac{d}{D} \frac{\lambda}{2} \quad (3.7.1)$$

where d is the fringe shift, D the fringe spacing and λ the wavelength of the monochromatic light used.

It is essential that the specimen film and the bare glass substrate are coated with the reflecting film, otherwise the phase changes suffered by the light on reflection from the two sides of the step edge would not be due solely to the difference in air gap spacing but also depend in an unknown manner on the phase changes for the two materials.

For the production of sharp fringes the following conditions must be taken care of:

- 1) The surfaces must be coated with highly reflecting films. A reflectivity of 0.94 has been found to be optimum.

- 2) The reflecting film must be of uniform thickness over the specimen and the distance between the plate surfaces must be as small as possible (preferably less than 0.01 mm).
- 3) The divergence of the incident parallel beam should be less than 1° to 3° .
- 4) The incidence should be normal.

If narrow, well separated fringes can be produced, film thickness can be measured to an accuracy of $\pm 20\text{\AA}$.

3.8 SET-UP FOR THE OXIDATION OF THE FILM.

Films were heat treated or oxidized in air in the set-up shown in figure 8. The set-up consists of a large heater block made of aluminium on which there was provision for clamping two substrates simultaneously close together, one with the film on it and the other a dummy substrate. The block was heated by means of a coil of nichrome heating wire placed inside the split block. A chromel-alumel thermocouple was fixed on the dummy substrate to measure the temperature. The output of the thermocouple was read on a digital panel meter with 10 microvolt resolution. Power was supplied to the heater through a dimmerstat from a servo-voltage stabilizer. The rate of heating and the final temperature

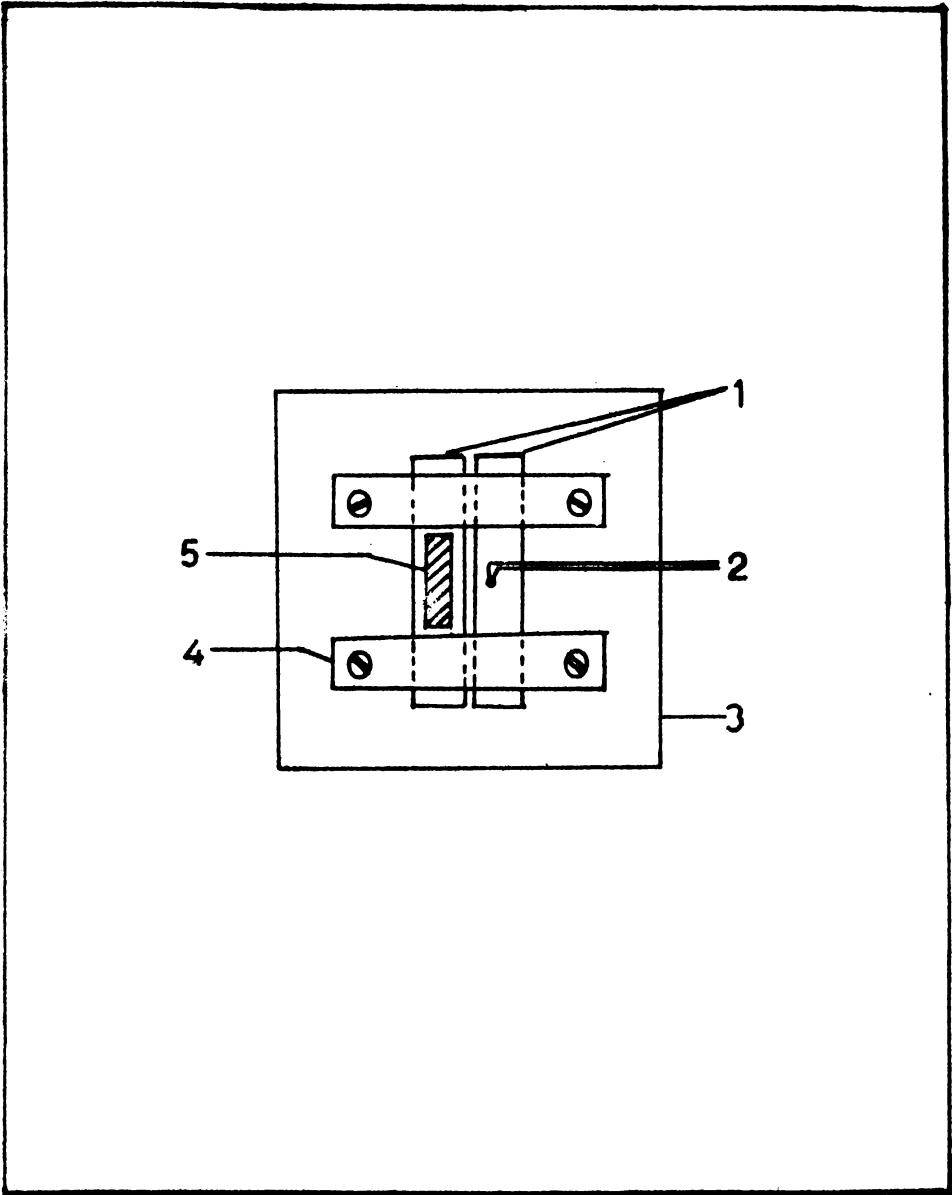


Figure 8: Heat-treatment set-up (1) substrates; (2) thermocouple; (3) heater block; (4) clamping arrangement; (5) film.

attained were controlled manually by adjusting the dimmerstat carefully. The temperature could be controlled only to an accuracy of $\pm 2\text{K}$ around 400K and $\pm 7\text{K}$ around 600K. This uncontrollability was mainly due to air currents over the completely exposed heated surface. Average heating rate could be controlled from a few degrees per minute to a few degrees per second.

3.9 PREPARATION OF THE FILM BY REACTIVE EVAPORATION.

All the films reported in this study were prepared mainly by the reactive evaporation of the metal in an atmosphere of sulphur. By adjusting the temperature of the sulphur source, it was possible to maintain an atmosphere of sulphur vapour in the chamber. This is easily achieved with sulphur for the low partial pressures needed ($\sim 10^{-4}$ Torr), because inside the chamber as the surfaces are clean and the supersaturation of sulphur vapours is not large, a sulphur film will not form on the walls of the chamber and also the loss of sulphur vapour through the pumping port is small. Usually for the preparation of sulphides by the reactive evaporation techniques, H_2S has been used as the reactive gas. But H_2S is a poisonous gas and its preparation and purification to the level needed in thin film work is rather difficult. The controlled evaporation of sulphur itself for the creation of sulphur atmosphere

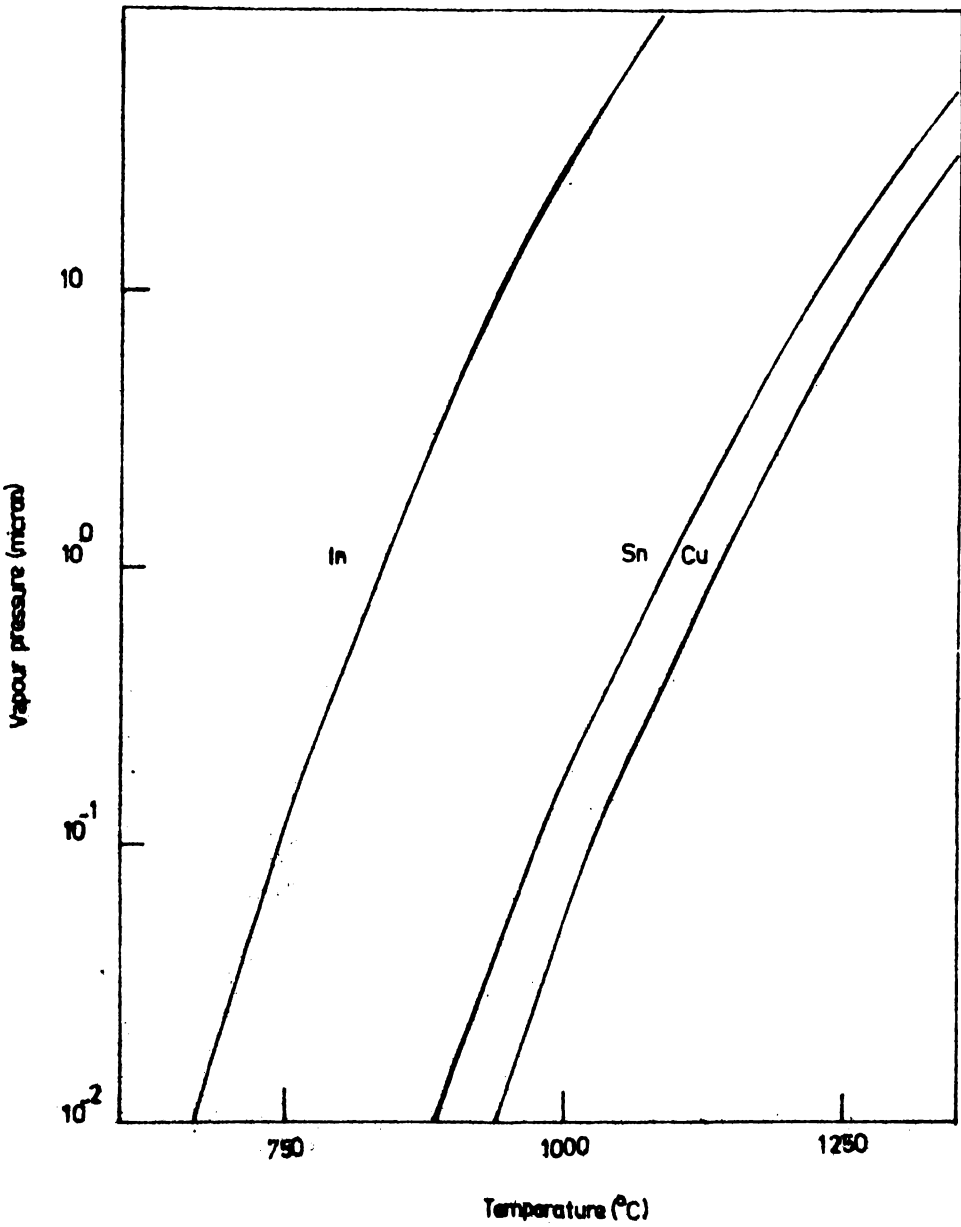


Figure 9: Variation of vapour pressure with temperature for In, Sn, and Cu.

overcomes this difficulty.

The rate of evaporation G from a surface at a temperature T is given by the Langmuir expression,

$$G = p \sqrt{M/2\pi RT} \quad (3.8.1)$$

where p is the vapour pressure and M the molecular weight of the material, R is the gas constant per mole. The relationships between p and T have been published by various authors for a wide variety of materials /4/. Figure 9 shows the variation of vapour pressures of tin, copper, and indium with temperature. A temperature which is normally considered suitable for evaporation is that at which the vapour pressure of the material is equal to 10^{-2} Torr.

For purposes of reactive evaporation, the rate at which metal atoms arrive at a substrate is best expressed in terms of the deposition rate as observed from the same source at the same temperature and substrate to source distance, but in the absence of reactive element flux /5/

$$\frac{dN_m}{A_r dt} = N_a \int_m d'/M_m \text{ atoms/cm}^2 \text{sec} \quad (3.8.2)$$

where \int_m is the density of the metal film in g cm^{-3} , M_m is the molar mass of the metal film in g cm^{-3} , d' is the pure metal condensation rate in cm sec^{-1} and A_r the receiving surface area in cm^2 .

The impingement rate of sulphur molecules is given by

$$\frac{dN_{S_2}}{A_r dt} = 3.513 \times 10^{22} (M_{S_2} T)^{-1/2} p_{S_2} \text{ molecules/cm}^2 \text{sec} \quad (3.8.3)$$

where M_{S_2} is the mass of S_2 . T is the vapour temperature, which is approximately 450K and p_{S_2} is the partial pressure in Torr.

Equation (3.8.2) and (3.8.3) can be used to calculate the number of atoms/molecules impinging on the substrate for given deposition rates/partial pressures.

Experimental details of the preparation of the films by activated reactive evaporation is given in Chapter X.

Substrate Cleaning

Optically flat glass or quartz slides of the required dimension were first cleaned with an industrial detergent (Teepol). After this the substrates were washed in tap water followed by distilled water. The substrates were then cleaned in analytical reagent grade acetone followed by twenty minute cleaning in distilled water in an ultrasonic cleaner. They were then dried in a flow of hot air and loaded in the vacuum system. In the vacuum system the substrates were further cleaned by ion-bombardment for ten minutes prior to the actual film deposition.

This cleaning procedure was satisfactory and allowed us to get films with good adhesion to the substrate surface.

Vacuum system

Preparation of the films were carried out in a conventional vacuum system with a 14 inch glass bell jar. The system was pumped by a 6 inch diffusion pump backed by a 500 liters/min rotary pump. Without the use of a liquid nitrogen trap, pressures down to 9×10^{-6} Torr could be achieved with care, but routinely it was 2×10^{-5} Torr. The evaporation chamber had provisions for three independent resistively heated sources with two transformers capable of supplying 200A each and one 10A. One 200A transformer was used to evaporate the metal and the smaller 10A source was used to evaporate sulphur. There were also provision in the chamber for ion-bombardment cleaning, substrate heating and substrate temperature measurement. For pressure measurements the chamber had one Pirani gauge and one Penning gauge. The normal pumping down time to get the ultimate vacuum was around 45 minutes.

Deposition of the Film

The system was first pumped to the ultimate low pressure obtainable and the substrates heated to the required temperature. Temperature was measured by a chromel-alumel thermocouple placed in contact with the

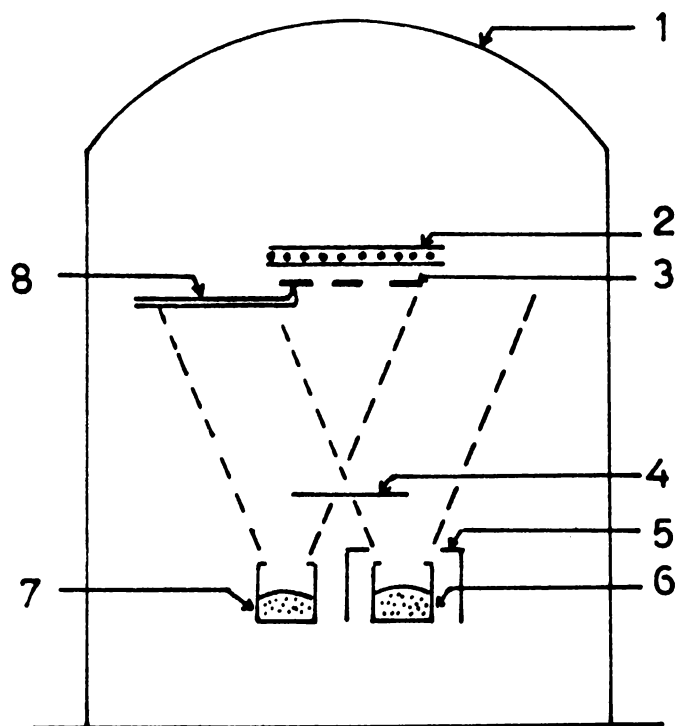


Figure 10: Schematic diagram of the experimental set-up.
1. bell jar, 2. substrate holder, 3. substrates,
4. shutter, 5. heat shield, 6. copper source, 7. sulfur
source, 8. thermocouple.

substrate. High purity metal (5N) and sulphur (4N) was used as evaporants. A glass crucible placed in a conical basket of molybdenum wire was used as the sulphur source (S_1). The temperature of the source and hence the flux could easily be controlled by adjusting the current through the molybdenum wire. A helical filament or a boat (S_2) made of molybdenum wire or sheet, as the case may be, was used to evaporate the metal. The metal source was covered with stainless steel heat shields to minimise substrate heating due to radiations from the high temperature ($\sim 1000^\circ\text{C}$) source. This meant that we could control the temperature within 2 - 4K. A schematic diagram of the set-up is shown in figure 10.

When the substrate had attained and stabilized at the required temperature, with a shutter placed over the sulphur and tin sources, the current through S_1 was switched on. The sulphur melted and the current through S_1 was adjusted such that a sulphur partial pressure of 10^{-4} Torr was maintained in the chamber. The current through S_2 was then switched on and increased to a preset value which gave a deposition rate of 0.1-0.2 nm sec^{-1} of the metal film. The shutter was then withdrawn and the deposition of the compound film allowed to take place.

At the substrate temperatures and partial pressures used in these experiments, the supersaturation



of sulphur atoms is not sufficient to form a film by itself. Only the metal/compound film forms at this temperature. When the shutter was withdrawn, the metal atoms reaching the substrate react with the sulphur atoms present on the substrate and the compound film was deposited.

References:

1. J.C. Manificier, J. Gasiot and J.P. Fillard,
J. Phys. E, 9 (1976) 1002.
2. V.J. Sebastian, M.Sc. Project, Department of Physics,
University of Cochin (1982).
3. S. Tolansky, "An Introduction to Interferometry,
Longmans, London, 1955, p 170.
4. S. Dushman, "Scientific Foundations of Vacuum
Technique", John Wiley, New York 1962, p 696.
5. R. Glang in "Handbook of Thin Film Technology"
eds. L.I. Maissel and R. Glang, McGraw Hill,
New York, 1970, p 1-81.

CHAPTER-IV

REACTIVELY EVAPORATED FILMS OF TIN DISULPHIDE

Tin disulphide is a layer compound which crystallizes in the CdI_2 crystal structure. These compounds are characterised by strong bonding in the layers and weak bonding between the layers. The chalcogenide atoms form densely packed hexagonal layers and the metal atoms are arranged in layers with the same hexagonal structure to give a stacking sequence X-M-X, X-M-X, etc. in the c-direction of the crystal. Bonds between these sandwich layers are weak and thought to be of van-der-Waal's type. But within the layers the bonding is mainly covalent. Because of their layered nature these crystals exhibit strong anisotropy in their physical properties. Polytypism is another interesting phenomena exhibited by these crystals. Eventhough the reason for the existence of polytypes is still unknown, it is known that polytype periodicity affect the width of the forbidden energy gap.

Optical properties of tin disulphide near the fundamental absorption edge was first reported by Greenaway and Nitsche /1/. They reported that tin disulphide is an indirect band gap semiconductor with a band gap of 2.21 eV and the optical transition leading to this is an indirect allowed one. Domingo et al /2/

studied the optical properties of these crystals and concluded that the fundamental gap of tin disulphide is an indirect one at 2.07 eV and the transition leading to this is a forbidden one. Moreover they showed that there is a direct gap at 2.88 eV. Further studies were made by Lee et al /3/ on the optical properties in the solid solutions of tin disulphide and tin diselenide. Results of Lee et al are similar to that reported by Greenaway and Nitsche but with a slight difference in the reported value of band gap. Powell and Grant /4/ from the pressure dependence of absorption coefficient reported that the value of indirect energy gap is 2.15 eV.

Photoconductivity in tin disulphide was first studied by Domingo et al /2/ and they observed a photoconductivity peak around 2.3 eV. Subsequent studies by Patil and Tredgold /5/, Nakata et al /6/, Bletsan et al /7/ also reported a photoconductivity peak around 2.3 eV. Usually photoconductivity peak coincides with the absorption edge and as is seen from what is given above, there is disagreement between the photoconductivity peak and absorption edge. The photoconductivity peak neither coincides with the indirect gap at 2.07 eV or the direct gap at 2.88 eV. This disagreement between the photoconductivity data and the lowest band gap was recently

resolved using high resolution absorption edge measurements by George, Valsala Kumari and Joseph /8/. They showed that the valence band in tin disulphide is split into three, by crystal field splitting and spin-orbit interaction. The lowest band gap found in this case was 2.07 eV in agreement with Domingo et al /2/ and the transition leading to this is shown to be an indirect forbidden one. It was also shown that the photoconductivity maxima obtained at 2.3 eV is due to transitions from the third valence band.

Electrical properties of tin disulphide has been studied by Said and Lee /9/. Current controlled negative resistance and bistable switching were observed in this material by Lee et al /10/. Gowers and Lee /11/ have shown that AC conductivity as a function of frequency and temperature, is similar to that found in some amorphous materials. Measurement of electron mobility by the same authors /11/ showed that the electrons in the planes (i.e. \perp to the c-axis) have a mobility

$\approx 30 \text{ cm}^2/\text{volt sec}$ whereas mobility perpendicular to the planes was only $10^{-4} \text{ cm}^2/\text{volt sec}$. These authors interpreted these results by assuming that electrons has to tunnel between sandwiches when conduction is perpendicular to the planes and hence the very low mobility in that direction. But recent measurement of mobility perpendicular to the planes using MIM structures in

crystals grown by physical transport by George and Valsala Kumari /12/ showed that this mobility may be as high as $\approx 10 \text{ cm}^2 / \text{volt sec}$ which is approximately equal to the value given by Gowers and Lee for conduction along the planes. The results of Gowers and Lee for conduction perpendicular to the planes may be due to contamination of the crystals grown by iodine vapour transport. The presence of adsorbed iodine in between the layers can certainly decrease the mobility perpendicular to the planes.

Acharya and Srivastava /13/ studied the activation energy needed for electrical conduction as a function of polytype periodicity and concluded that activation energy (equal to the band gap) decreases with increasing polytype periodicity.

Raman spectra of these crystals were studied by Mead and Irwin /14/ and they reported phonon energies of 0.04 eV and 0.025 eV. Infra-red reflectivity measurements were made by Lucovsky and White /15/ to investigate the nature of the interlayer bonding forces in a variety of layered crystals including tin disulphide.

Theoretical band structure calculations for tin disulphide have been performed by empirical pseudopotential method by Fong and Cohen /16/ and by Schluter and Schluter /17/. The band structure of tin disulphide

was calculated using tight-binding method by Murray and Williams /18/. An a priori pseudopotential band structure calculation was made by Mula et al /19/. The pseudopotential calculation made by Powell et al /20/, has been experimentally varified (qualitatively) by the work of George et al /8/.

All these experimental work mentioned above were made on single crystals of tin disulphide grown by either vapour transport (both physical and chemical) or Bridgman method. As is known, single crystals are expensive to prepare and it is not easy to prepare large single crystals. For the economic utilization of materials in device applications where polycrystallinity is not a severe problem, it is better to prepare the material in thin film form as it offers advantages of easy preparation, large area and material saving. Tin disulphide is a material which can transmit almost all of the visible spectra without much attenuation when the thickness of the deposited layer is low and hence this material has potential applications as a window material in heterojunction solar cells, or if it can be made sufficiently conducting, as a transparent conductor. This chapter presents work on thin films of tin disulphide prepared for the first time. The films are prepared by evaporating tin in an atmosphere of sulphur.

4.1 EXPERIMENTAL

Because of the thermal instability of the compound above 900°C , it is impossible to evaporate tin disulphide as such and get good quality films. Above 900°C , the compound dissociates and sulphur evaporates preferentially. The evaporation temperature of tin is $\sim 1150^{\circ}\text{C}$ and hence after some time all the sulphur will be evaporated leaving tin alone in the boat. This will give rise to a final film which is almost metallic in nature.

In this study films of tin disulphide were prepared by evaporating tin in an atmosphere of sulphur. In this fashion it is possible to get an excess partial pressure of sulphur molecules which will produce stoichiometric films of the compound. It has been found that a stoichiometric interval exists for the reactive evaporation of tin disulphide from its individual components with the following deposition parameters:

metal film deposition rate = $0.1 - 0.2 \text{ nm sec}^{-1}$
 chalcogen partial pressure = $5 \times 10^{-5} - 9 \times 10^{-5} \text{ Torr}$
 substrate temperature = $295 - 335 \text{ K}$

The corresponding metal atom flux and chalcogen flux calculated using equations (3.8.2) and (3.8.3) of chapter III gives

metal atom flux = 4×10^{14} - 1.5×10^{15} atoms $\text{cm}^{-2} \text{sec}^{-1}$

chalcogen flux = 1.5×10^{16} - 2.8×10^{16} molecules $\text{cm}^{-2} \text{sec}^{-1}$

Evaporation was carried out in a conventional vacuum system as discussed in Chapter III. 5 N purity tin and three times recrystallized sulphur was used as evaporants. A glass crucible placed in a conical basket of molybdenum wire was used as the sulphur source. The temperature of the source and hence the flux could be easily controlled by adjusting the current through the molybdenum wire. A helical filament made of molybdenum wire was used to evaporate tin. The helical filament was covered with stainless steel heat shields to minimise substrate heating. This meant that we could control the temperature within 2 K.

When the substrate had attained and stabilized at the required temperature, with a shutter placed over sulphur and tin sources, the current through the sulphur source was switched on. The sulphur melted and the current was adjusted such that a sulphur partial pressure of 5×10^{-5} to 9×10^{-5} Torr was maintained in the chamber. The current through the tin source was then switched on and increased to a preset value which gave a deposition rate of 0.1 to 0.2 nm sec^{-1} of the metal film. The shutter was then withdrawn and the

deposition of the compound films allowed to take place.

At the substrate temperature and partial pressures used in these experiments, the supersaturation of sulphur atoms is not sufficient to form a film by itself. Only the metal / compound film form at this temperature. When the shutter is withdrawn, the metal atoms reaching the substrate react with the sulphur atoms present on the substrate and the compound film is deposited. Films thus obtained are golden yellow in colour and extremely transparent. Highly reproducible films were obtained under **these** conditions. Films prepared with the substrate temperature lower than 295 K were found to contain some sulphur-rich regions when the sulphur flux was maximum. These patches of sulphur films form because at low substrate temperature, the reevaporation of sulphur atoms from the substrate become lower and hence nucleation of the sulphur film become possible. At substrate temperature higher than 345 K, the films tended to be of chocolate brown colour and their optical transmission was very poor. Moreover at high substrate temperatures a dust like coating was found on the top of the films. This dust-like coating could be easily wiped out using a paper, but the underlying compound film had good adhesion to the substrate.

It was also found that if the sulphur flux was decreased for a given metal deposition rate, films

tended to become chocolate brown in colour and also if the sulphur flux was increased for a given deposition rate, the films became more and more yellow till regions containing exclusively of sulphur appears.

4.2 ELECTRICAL MEASUREMENTS

Electrical measurements were performed on films deposited on highly insulating quartz substrates after depositing two metallic electrodes on either end of the film. The set-up used for electrical measurements and the specimen geometry are as discussed in Chapter III. The specimens were immediately transferred to the measuring cell and evacuated after taking them out from the electrode coating chamber. This was to reduce adsorption of water vapour by the film which may affect the electrical properties. After evacuating the measuring cell to a pressure of 10^{-2} Torr for one hour, the film resistance at room temperature was measured with enough time given for the electrometer reading to stabilize. The film was then heated and allowed to stabilize at a temperature which was higher than about 15 K from the previous value and once again the resistance of the film was measured. The measurement was continued till the required temperature range is covered. The temperature of the sample was measured using a chromel-alumel thermocouple to an accuracy of 1K.

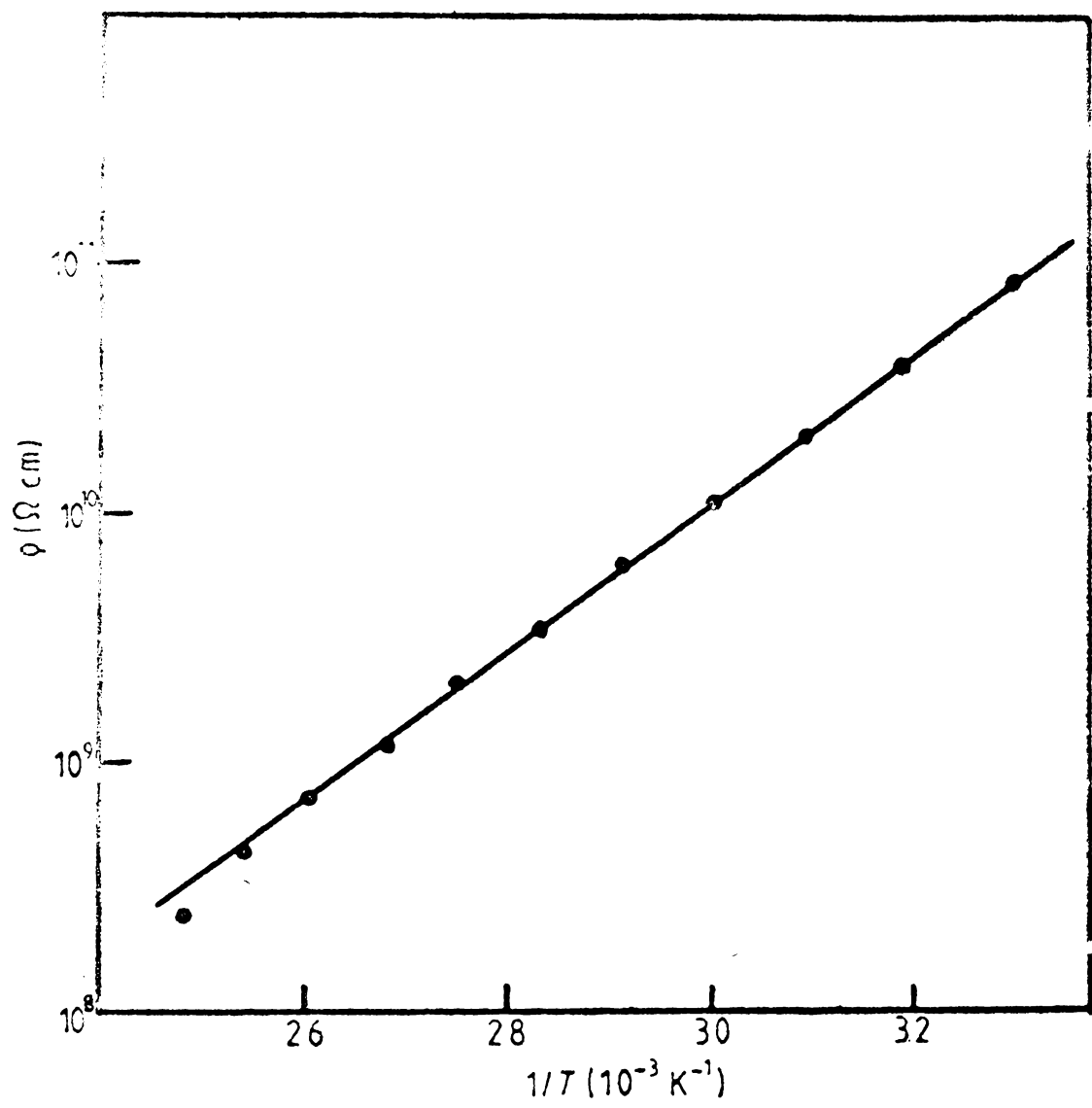


Figure 1: Resistivity versus inverse temperature of the as prepared film. Film thickness 2 μm , deposition rate 2.5 nm sec⁻¹.

Variation of $\ln \rho$ with inverse temperature for a typical film of thickness 2 micron is shown in figure 1. The straight line curve immediately suggests a relationship of the form

$$\rho = \rho_0 \exp(E_a/k_B T) \quad (4.2.1)$$

which is obviously due to a thermally activated process. Here ρ is the resistivity, E_a , the activation energy needed for conduction, ρ_0 a constant and k_B , the Boltzman constant. The activation energy for conduction for different films was found to be within 0.65 ± 0.05 eV. The films can be repeatedly heated and cooled between room temperature and 400K without any appreciable change in the value of resistance at any particular temperature during the cycle. However when the films were heated to a steady temperature of 410K the resistance began to drop sharply to a steady low value, the time taken for the process being about 30 minutes. This change was found to be irreversible. The resistivity value drops about ten orders of magnitude in this process (i.e. from $10^{11} \Omega \text{cm}$ to $10^1 \Omega \text{cm}$).

These results can be explained as, the films are amorphous in nature when prepared and hence their very high resistance; but when they are heated to 410K the films crystalizes. The variation of resistivity of

the as prepared film is similar to that observed in many amorphous semiconductors. In our case when the films are heated to 410K, the films crystallizes and their resistance falls sharply. Such large change in resistivities when films crystallizes can be explained as due to the increase in grain size and consequent increase in mobility of the charge carriers. Another reason for the fall in resistivity is that in amorphous state even if there are chemical impurities in the film, their effect will not be pronounced since in amorphous structures impurities can be accommodated with all their valencies filled because of the flexibility of the structure.

This type of large resistivity change found when amorphous films are crystallized has earlier been observed in $\text{Ge}_{1-x}\text{SnTe}$ alloy films where the resistivity decreased from 10^3 to 10^{-3} ohm cm /21/ and also in undoped ZnSe films where the resistivity decreased from 10^{11} ohm cm to 10 ohm cm on crystallization /22/.

Hot probe measurements show that crystallized films exhibit n-type conductivity. The variation of electrical resistivity of the recrystallized films are shown in figure 2. Two straight line portions are seen in the figure. Activation energies obtained for two

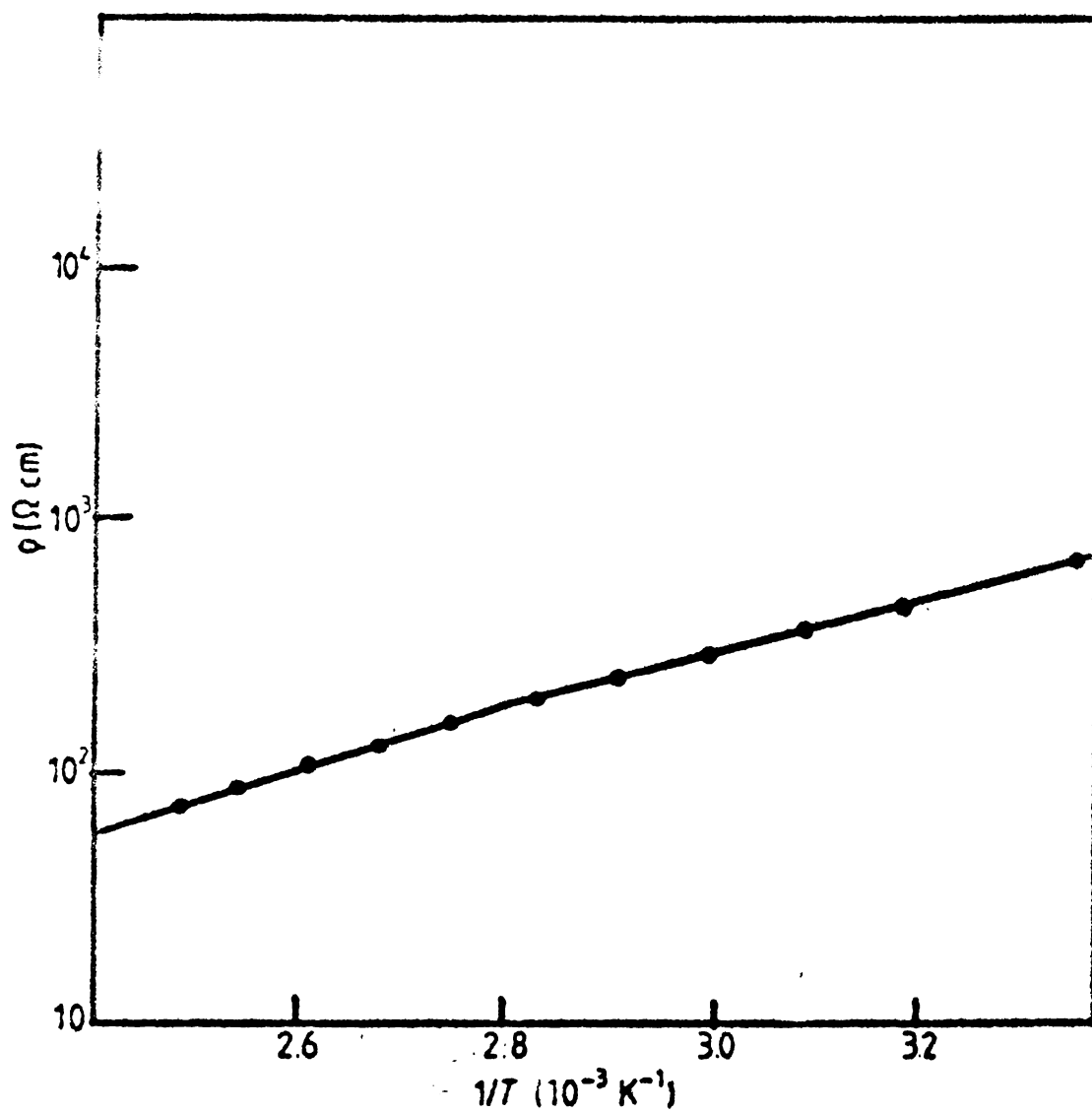


Figure 2: Resistivity versus inverse temperature of the recrystallized film.

TABLE I

Author and year	Type of material	Technique used	Resistivity Ω cm	Activation energy eV	Mobility $\frac{\text{cm}^2}{\text{Volt sec}}$	Carrier concentration cm^{-3}
1	2	3	4	5	6	7
Gowers and Lee (1970)	Single crystal			0.18		
	to c	Hall effect			10^{-4}	
	\perp to c				20	
Patil and Tredgold (1971)	Single crystal					
	\perp to c	Electrical conductivity	$4 \times 10^7 - 10^9$	0.61-0.4		
	to c		$10^{12} - 10^{14}$	0.79-0.57		
Ishizawa and Fujiki (1973)	Single crystal	Hall effect	3.00	0.19	6.3	
		Electrical conductivity				4×10^{16}
						(Contd.)

1	2	3	4	5	6	7
Said and Ioe (1973)	Single crystal to c	NIM structure	4×10^{-1}	0.4		
			1×10^6	0.11		
			4×10^7	0.05		
Present work (1982)	Thin film amorphous crystalline	Electrical conductivity "	1×10^{11} 5×10^2	0.65 0.25 0.20		
George and Valsala Kumari (1983)	Single crystal to c	NIM structure	5×10^6	0.4	6	2.3×10^{11}

regions of temperature, from 300K to 365K (0.20 ± 0.02 eV) and from 365K to 400K (0.25 ± 0.02 eV) can be explained by assuming the existence of two different donor levels situated very close to the conduction band. Said and Lee /9/ also report in their study of electrical conductivity in tin disulphide single crystals two such levels (0.22 eV and 0.1 eV). These levels can originate due to doubly ionizable sulphur vacancies. In tin dioxide, which is a chemically analogous compound, two levels exist below the conduction band due to doubly ionizable oxygen vacancies /23/. Table I gives the electrical properties reported by various authors for tin disulphide.

4.3 OPTICAL MEASUREMENTS

Optical measurements were made using a Hitachi model 200-20 UV-Vis spectrophotometer. A spectral bandwidth of 2nm was used. Two films of nearly equal thickness were made in a single run. One film was placed in the reference beam and the other in the sample beam of the spectrophotometer for absorption measurements in the fundamental absorption region. For transmission measurements, the film was placed only in the sample beam of the spectrophotometer. Absorption coefficient, refractive index and extinction coefficient was determined as described in Chapter III.

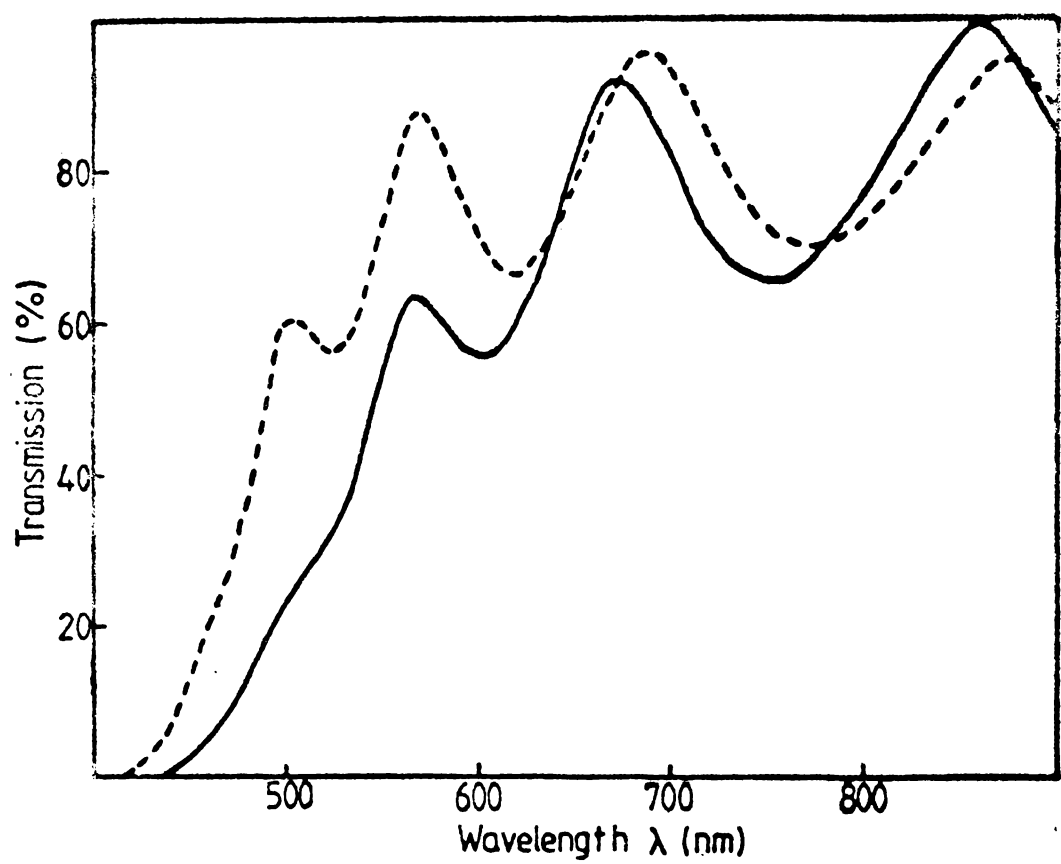


Figure 3: Transmission spectra of the as-prepared (full curve) and recrystallized film (broken line).

Transmission spectra of a typical film in as-prepared and crystallized conditions are shown in figure 3. It can be seen that films have an average transmission of 80%. The crystallized films have a reduced transmission at higher wavelengths and the threshold of absorption shifts to lower wavelengths compared to the as prepared films. The decrease in transmission of the recrystallized films in the long wavelength region can be attributed to absorption by free carriers in the degenerate films. The shift in absorption edge may be due to two reasons. In amorphous films some sort of band tailing exists and this may cause the absorption to start at higher wavelengths compared to crystallized films. Another reason could be that the bottom of the conduction band becomes filled to rather high energy states in degenerate films and the allowed transition from valence band begins at a correspondingly higher energy than in the forbidden gap /24/.

Refractive index and extinction coefficient of the as-prepared and recrystallized films are shown in figure 4 and figure 5 respectively. The values of refractive index for both as-prepared and recrystallized films are less than the bulk value of 2.8 /2/. This could possibly be due to the presence of voids, impurities

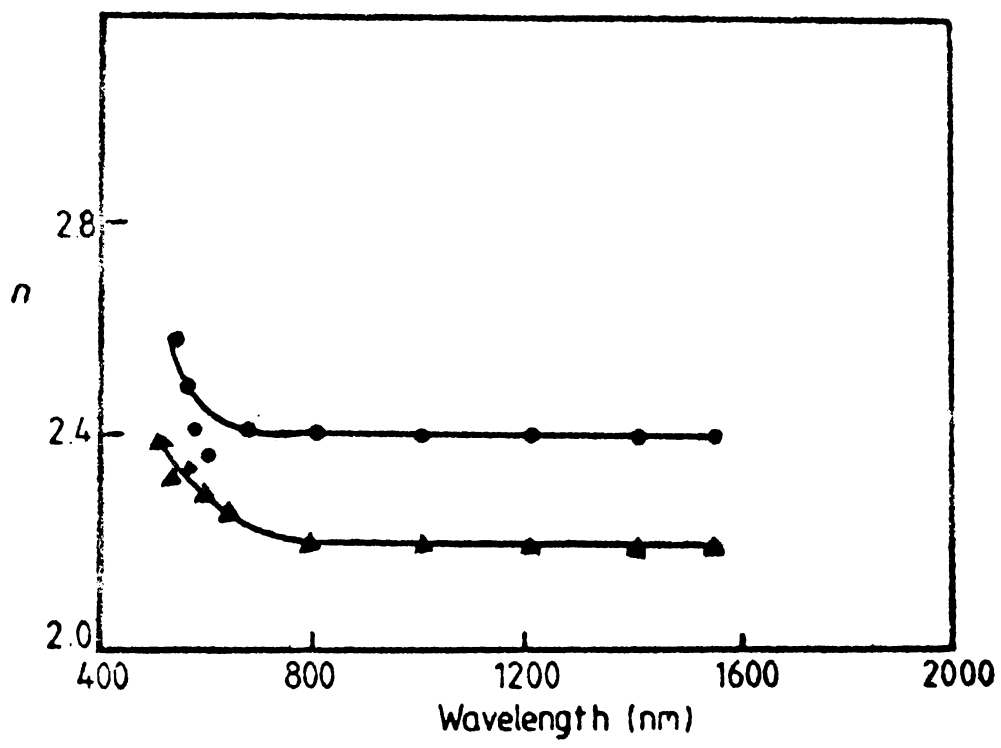


Figure 4: Refractive index of the as-prepared (●) and recrystallized film (▲).

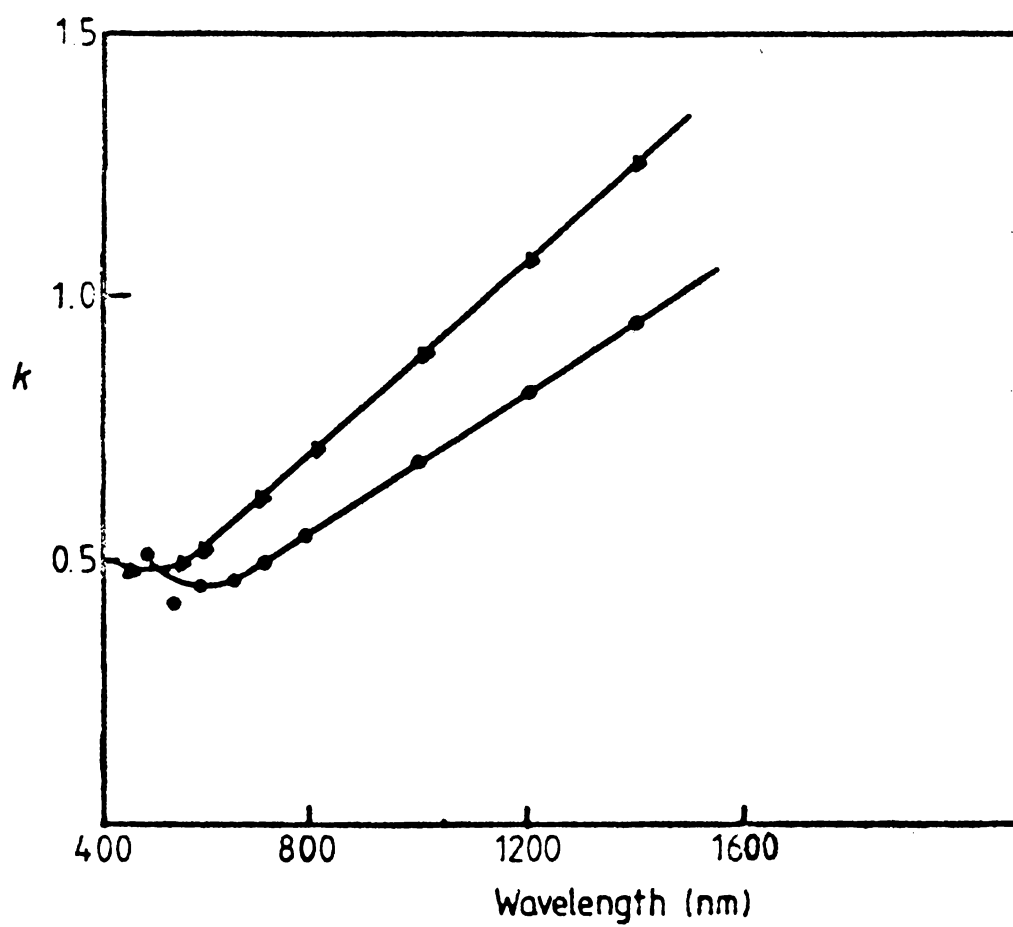


Figure 5: Extinction coefficient of as-prepared (●) and recrystallized film (▲).

and imperfections in large numbers in the film material. It may also be noticed that the refractive index of the annealed film is slightly lower than the as-prepared film. This type of behaviour is reported in tin dioxide (conducting glass) where highly conducting films have a lesser refractive index than non-conducting films /25/.

Figure 6 shows the dependence of absorption coefficient on photon energy at room temperature. The optical absorption data of tin disulphide films were investigated for evidence of either indirect or direct transitions in accordance with the theory of Bardeen et al /26/. For such transitions

$$\alpha = \frac{A(h\nu - E_g' \pm E_p)^r}{h\nu} \quad (4.3.1)$$

where $r = 3$ for forbidden indirect transitions and $r = 2$ for allowed indirect transitions; E_g' is the indirect band gap and E_p the absorbed (+) or emitted (-) phonon energy.

Both $(\alpha h\nu)^{1/3}$ and $(\alpha h\nu)^{1/2}$ versus photon energy $h\nu$ have been plotted and the plot of $(\alpha h\nu)^{1/2}$ versus $h\nu$ (figure 7) gives two straight line portions. The one at low photon energies extends from 2.25 eV to 2.45 eV and the energy intercept gives a band gap of

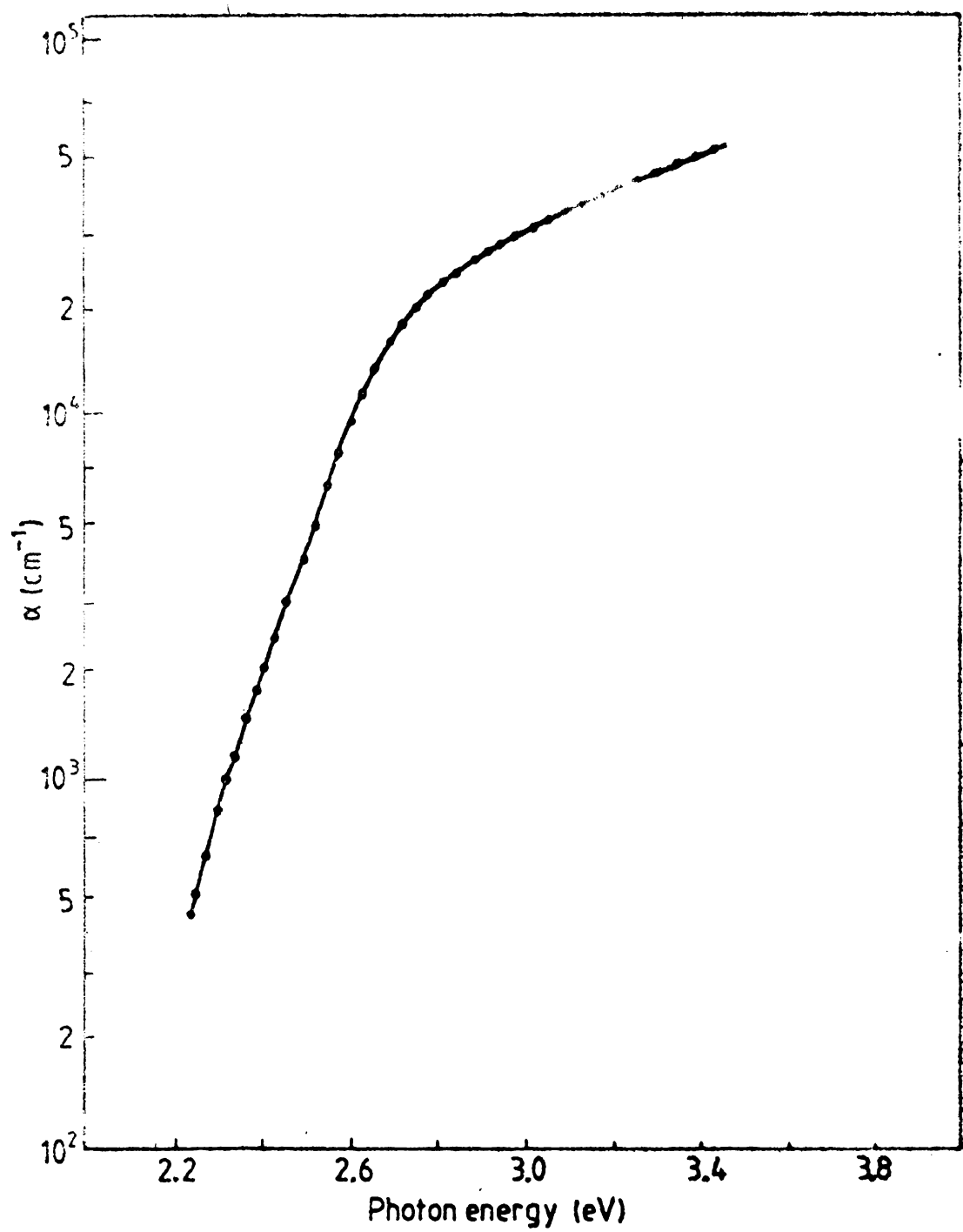


Figure 6: Absorption coefficient versus photon energy.

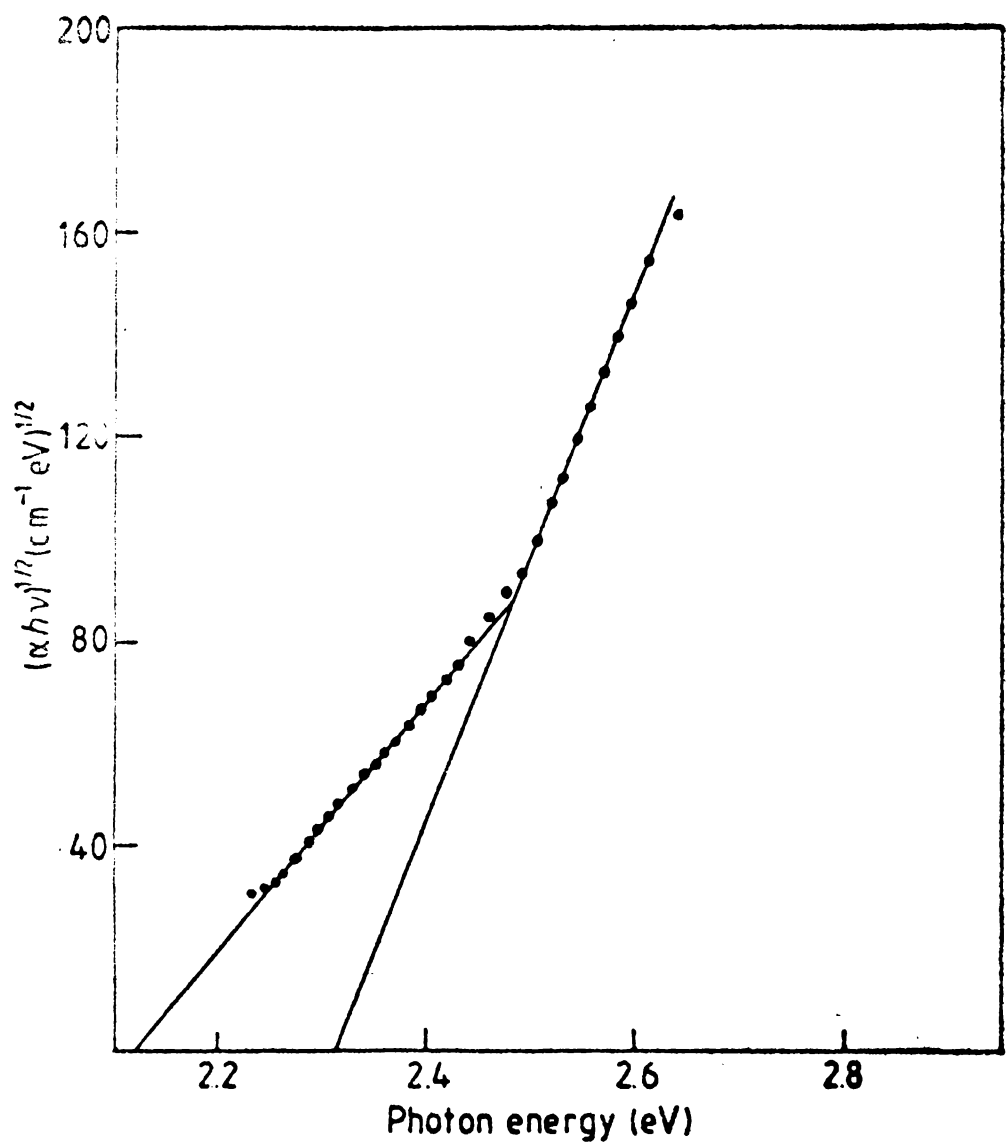


Figure 7: $(\alpha h\nu)^{1/2}$ versus $h\nu$.

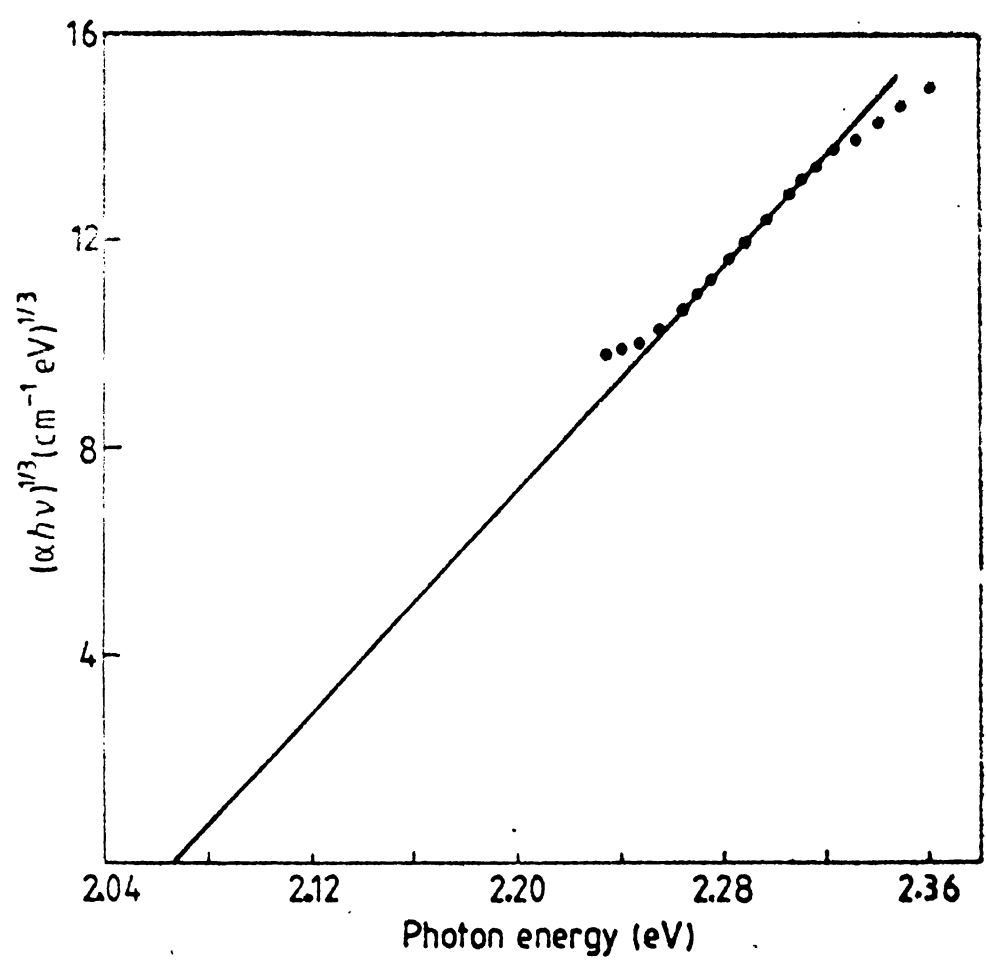


Figure 8: $(\alpha h\nu)^{1/3}$ versus $h\nu$.

2.12 ± 0.02 eV. In this region $(\alpha h\nu)^{1/3}$ versus $h\nu$ also gives a straight line (figure 8) but only over a narrow region of 0.07 eV, and the intercept of the straight line along the energy axis gives a value of 2.07 eV, in excellent agreement with Domingo et al /2/ and George et al /8/. Since the plot of $(\alpha h\nu)^{1/2}$ versus $h\nu$ gives a wider region of agreement, it is concluded that the transition leading to the fundamental absorption edge take place at 2.12 ± 0.02 eV and the transition is an indirect one.

For photon energies from 2.45 to 2.65 eV, another straight line portion is seen in figure 7 and gives an energy intercept of 2.31 ± 0.02 eV. Greenaway and Nitsche /1/ and Lee et al /3/ both reported the value of band gap from the mean of the intercepts on the energy axis in their respective square root of absorption versus energy plots. But the difference in energy intercepts (which should give twice the phonon energy) in both cases do not seem to agree with the phonon energies reported in tin disulphide /14/. It may be seen that in both cases the intercepts compare well with the present work. Also photoconductive studies made by Domingo et al /2/, Patil and Tredgold /5/, Nakata et al /6/, Bletskan et al /7/ indicate a peak photoconductive response at 2.3 eV. Hence the transition found at 2.31 ± 0.02 eV must be intercepted as a new transition which was not recognised

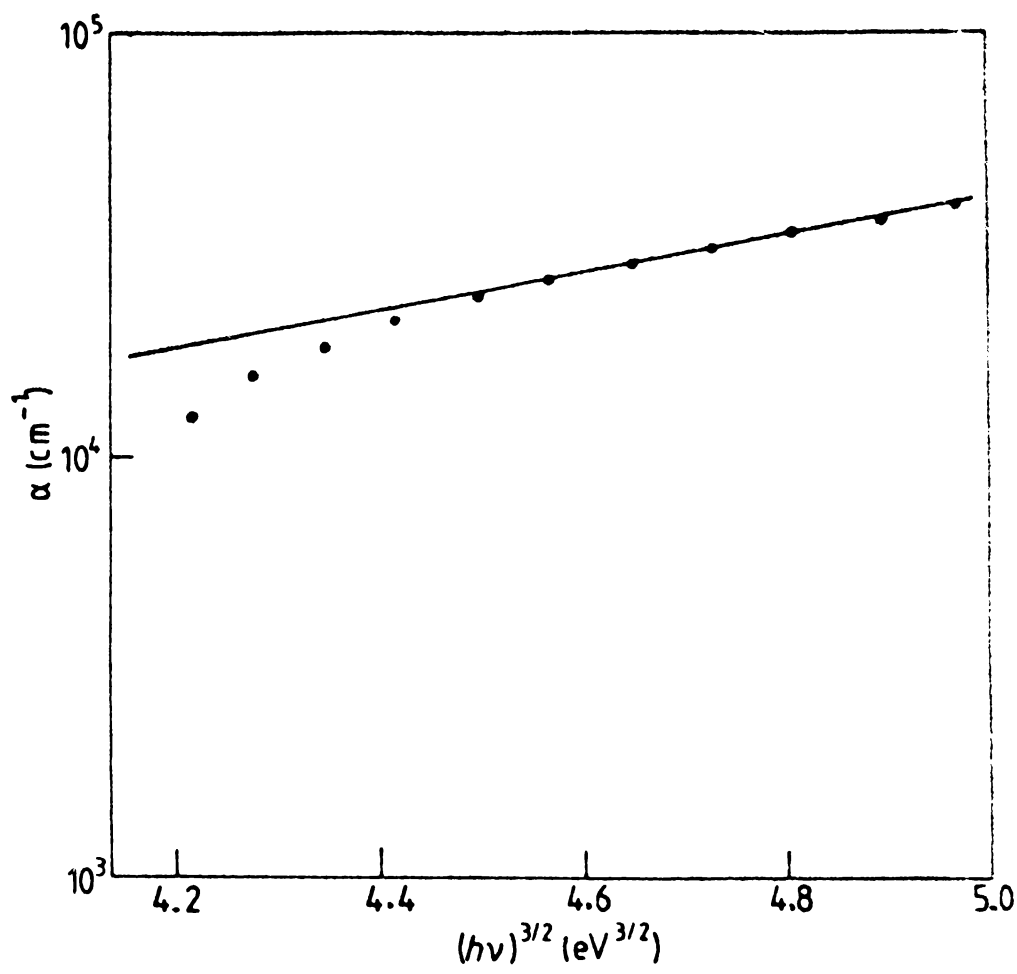


Figure 9: Absorption coefficient versus $(h\nu)^{3/2}$.

TABLE II
Energy gap of tin disulphide(eV)

Authors and year	Optical Methods			Photocon- ductive methods	Electrical Methods
	Indirect forbidden	Indirect allowed	Direct forbidden		
Greenaway and Nitsche (1965)		2.21			
Domingo et al (1966)	2.07		2.88	2.3	
Lee et al (1969)		2.21			
Patil and Tredgold (1971)				2.3	
Nekata et al (1972)				2.3	
Bletskan et al (1976)				2.296	
Powell and Grant (1977)		2.15	2.34		
Acharya and Srivastava (1979)					2.18
Nozaki and Imai (1981)		2.14			
Present work (1982)		2.12			
		2.31			
George et al (1983)	2.07				
	2.228				
	2.300				
George and Valsala Kumari (1983)			2.40		

in earlier optical absorption studies.

For photon energies from 2.7 to 2.9 eV there is Franz-Keldysh line broadening /26,27/ and the absorption data gives a good fit when α is plotted against $(h\nu)^{3/2}$ (figure 9). This may be due to strong electron/phonon interaction. Beyond 2.9 eV, the absorption coefficient shows an exponential dependence on photon energy, and the direct forbidden transition reported at 2.88 eV by Domingo et al /2/ could not be observed. There is, however, a change in the slope of the absorption curve at 2.8 eV.

The reported values of band gaps for tin disulphide are given in Table II.

CONCLUSION

Thin films of tin disulphide were prepared by reactive evaporation for the first time. It is found that the as-prepared films are amorphous in nature. Heating above 410K converts these into crystalline films. Electrical resistivity of the films changes by about ten orders of magnitude (from 10^{11} ohm cm to 10 ohm cm) due to crystallization. The crystallized films are degenerate and show n-type conductivity. The refractive index of both the as-prepared and crystallized films is less than that of single crystals. Optical absorption studies show indirect allowed transitions at 2.12 eV and 2.31 eV.

References:

1. D.L. Greenaway and R. Nitsche, J. Phys. Chem. Solids 26 (1965) 1445.
2. G. Domingo, R.S. Itoga and C.R. Kannewurf, Physical Review 143 (1966) 536.
3. P.A. Lee, G. Said, R. Davis and T.H. Lim, J. Phys. Chem. Solids 30 (1969) 2719.
4. M.J. Powell and A.J. Grant, Il. Nuovo Cimento 38B (1977) 486.
5. S.G. Patil and R.H. Tredgold, J. Phys. D: Appl. Phys 4 (1971) 718.
6. R. Nakata, M. Yamaguchi, S. Zembutsu and M. Sumita J. Phys. Soc, Japan 32 (1972) 1153.
7. D.I. Bletskan, I.F. Kopinets, I.M. Migolinets and S.V. Mikulaninets, Neorganicheskie Materially 12 (1976) 2138.
8. J. George, C.K. Valsala Kumari and K.S. Joseph, J. Appl. Phys. (in press).
9. G. Said and P.A. Lee Phys. Stat. Sol (a) 15 (1973) 99.
10. P.A. Lee, G. Said and R. Davis, Solid State Communications, 7 (1969) 1359.
11. J.P. Gowers and P.A. Lee, Solid State Communications, 8 (1970) 1447.
12. J. George and C.K. Valsala Kumari, Solid State Communications (in press).

13. S. Acharya and O.N. Srivastava, Phys.Stat. Solidi (a) 56 (1979) KI.
14. D.G. Mead and J.C. Irwin, Solid State Communications, 20 (1976) 885.
15. G. Lucovsky and R.M. White, Il Nuovo Cimento, 38B (1977) 290.
16. C.Y. Fong, and M.L. Cohen, Phys. Rev. B 5 (1972) 3095.
17. C. Schluter and M. Schluter, Phys. Stat. Solid 57 (b) (1973) 145.
18. R.B. Murray and R.H. Williams, J. Phys. C, 6 (1973) 3643.
19. G. Mula and F. Aymerich, Phys. Stat. Col. 51(b), (1972) K35.
20. M.J. Powell, E.A. Marseglia and W.Y. Liang J. Phys. C 11 (1978) 895.
21. P. Mascheretti, R. Giorgi and A. Borghesi, Thin Solid Films 34 (1976) 61.
22. R. Rentzsch, I.S. Shlinmak and H. Berger, Phys. Stat. Solidi (a) 54, (1979) 487.
23. S. Samson and C.G. Fonstad, J. Appl. Phys. 44 (1973) 4618.
24. H.Y. Fan and W.G. Spitzer, Phys. Rev. 106 (1957) 882.
25. T. Arai, J. Phys. Soc. Japan 15 (1960) 916.
26. W. Franz, Z. Naturf 13a (1958) 484.
27. L.V. Keldysh, Zh. Eksp. Teor. Fiz, 34 (1958) 1138 (Sov. Phys. JETP 7, 788)

CHAPTER-V

TRANSPARENT CONDUCTING FILMS OF TIN DIOXIDE
PREPARED BY THE OXIDATION OF TIN DISULPHIDE
FILMS

The occurrence of high optical transparency in the visible region and low electrical resistivity makes the so called transparent conductors extremely interesting from the stand point of technology. These group of materials, which are oxides of low melting point metals, include tin oxide, indium oxide, cadmium oxide, zinc oxide, and cadmium stannate. A large number of electronic, opto-electronic and mechanical applications based on transparent conductors has emerged in the industry. High stability resistors, transparent heating elements used in aircraft and automobile windows, antistatic coating for instrument windows, touch sensitive switches, heat reflecting mirrors, antireflection coatings, electrodes for liquid crystal displays, solar cells, gas sensors and protective and wear resistant coatings for glass containers are some of the application of these materials. With increasing sophistication of active and passive devices based on transparent conductors, the need for improved properties and their understanding became a necessity and this justifies the great amount of work still going on in these materials.

The first transparent conductor was prepared by thermal oxidation of sputtered cadmium by Badeker in 1907 /1/ and ever since this discovery technological interest in these materials has gone high. Numerous techniques have been developed for the deposition of these materials which include evaporation techniques like direct evaporation of the compound /2/ post oxidation of the respective metal films /3/, reactive evaporation in oxygen atmosphere /4/, activated reactive evaporation /5/, ion plating /6/, sputtering techniques like reactive sputtering of metallic targets in oxygen atmosphere /7/, sputtering from oxide targets /8/, ion beam sputtering /9/ and also chemical vapour deposition /10/ and spray pyrolysis /11/. Many of these methods have been developed to large scale production stages.

In 1942 Mc Masters of Libbey Owens - Ford-Glass Company synthesized good quality tin oxide films for the first time on a commercial scale /12/. The next significant improvement in film properties came when J.L. Vossen of RCA Laboratories in 1971 synthesized tin doped indium oxide films with transmission averaging 90% and sheet resistivities as low as 15 ohm/square /13/. The best films to date have been prepared by R.F. Bunshah of UCLA with transmission over 90% and 2 ohm/square resistivity by using activated reactive evaporation in 1980 /14/.

TABLE I

Deposition Technique	Deposited	Carrier concentration (cm ⁻³)	Mobility (cm ² volt ⁻¹ sec ⁻¹)	Resistivity (ohm cm)	Average Transmittance
Spray Pyrolysis /16/	-	9.5 x 10 ¹⁹	13	5 x 10 ⁻³	0.82-0.9
Chemical vapour deposition /17/	-	9 x 10 ¹⁸	10	7 x 10 ⁻²	0.9 -0.95
ARE /5/	Antimony	-	-	~8x10 ⁻⁵	0.85
Spray Pyrolysis /18/	Antimony	5 x 10 ²⁰	~10	~10 ⁻³	0.85-0.9
Chemical vapour deposition /19/	Antimony	1.2 x 10 ²⁰	23	~2 x 10 ⁻³	0.85-0.9
Spray Pyrolysis /20/	Flourine	5 x 10 ²⁰	23	5 x 10 ⁻⁴	0.85
Ultrasonic Spray /21/	Flourine	-	-	6 x 10 ⁻⁴	0.84
Chemical vapour deposition /22/	Phosphorous	6.5x10 ¹⁹	26	~3 x 10 ⁻³	>0.95

The phenomena of conductivity and transparency are quite strongly interrelated, leading to a trade-off between the two. The high optical transparency of these oxides in the visible and NIR region of the spectrum is a direct consequence of them being wide band gap materials ($E_g \geq 3\text{eV}$). Their fundamental absorption edge lies in the UV and shifts to shorter wavelengths with increasing carrier concentration due to the well known Moss-Burstein shift [15]. Electron-hole generation due to fundamental absorption limits transparency at short wavelengths and the steep increase in free carrier absorption limits it at long wavelengths. As the number of free carriers is directly related to the conductivity, increase in conductivity tends to decrease transmission. Table I summarises properties of tin dioxide films prepared by various techniques.

In this chapter a new method for the preparation of transparent conducting films of tin oxide is reported. The films are prepared by thermal oxidation in air of reactively evaporated tin disulphide films. This method is in a way analogous to the oxidation of thin metal films as both use thermal oxidation. But it differs from the oxidation of the metal film in a significant way; when the sulphide film is oxidized it involves only the replacement of sulphur atoms by oxygen atoms, the required lattice structure being present there

already; when a metal film is oxidized, the required lattice structure is not present. Tin oxide films prepared in this manner has a resistivity of 800 ohm/square and an average transmission of 87% in the visible region. The films have good adhesion to the substrate and will tolerate heating in air and cold acids.

5.1 EXPERIMENTAL

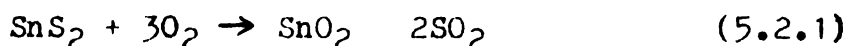
Tin disulphide films were deposited on optically flat glass/quartz slides of dimension 2cm x 2cm x 0.2cm as described in Chapter III. After deposition, the films are taken out of the deposition chamber and oxidized in air in the set-up described in Chapter III. The temperature of the film is measured using a chromel-alumel thermocouple and a digital microvoltmeter. The final oxidation temperature was manually controlled and because of small air-currents the controlling was accurate only to $\pm 7\text{K}$. The heating rate was approximately 0.5K sec^{-1} . All the sulphide films used in these investigations were of thickness between 250 and 400 nm. The deposition rate of the sulphide films was 1 nm sec^{-1} . The substrate temperature during evaporation of the sulphide films was $325 \pm 4\text{K}$.

Electrical resistance of the oxidized films were measured using a Hewlett-Packard 3465A digital multimeter after depositing silver electrodes on either ends

of the film. Transmission measurements were made using Hitachi 200-20 UV-Vis spectrophotometer.

5.2 OXIDATION OF THE FILM.

The reaction leading to the thermal oxidation of the sulphide film may be represented as



Oxidation of the films was monitored by observing the colour of the film in reflected light. As prepared tin disulphide films are amorphous in nature. These films have a low reflectivity and hence in the initial stages of heating the reflectivity was poor. Reflectivity increased with temperature as the sulphide film crystallized. At the instant the oxidation began, an abrupt change in the colour of the film was observed. The time taken for this abrupt change in colour to occur after the film has attained the particular temperature used for oxidation was taken as the time required for oxidation at that particular temperature. It has been found that the time t taken for the onset of oxidation at different temperature T can be represented by a simple rate relationship of the form

$$t = t_0 \exp\left(\frac{E_a}{k_B T}\right) \quad (5.2.2)$$

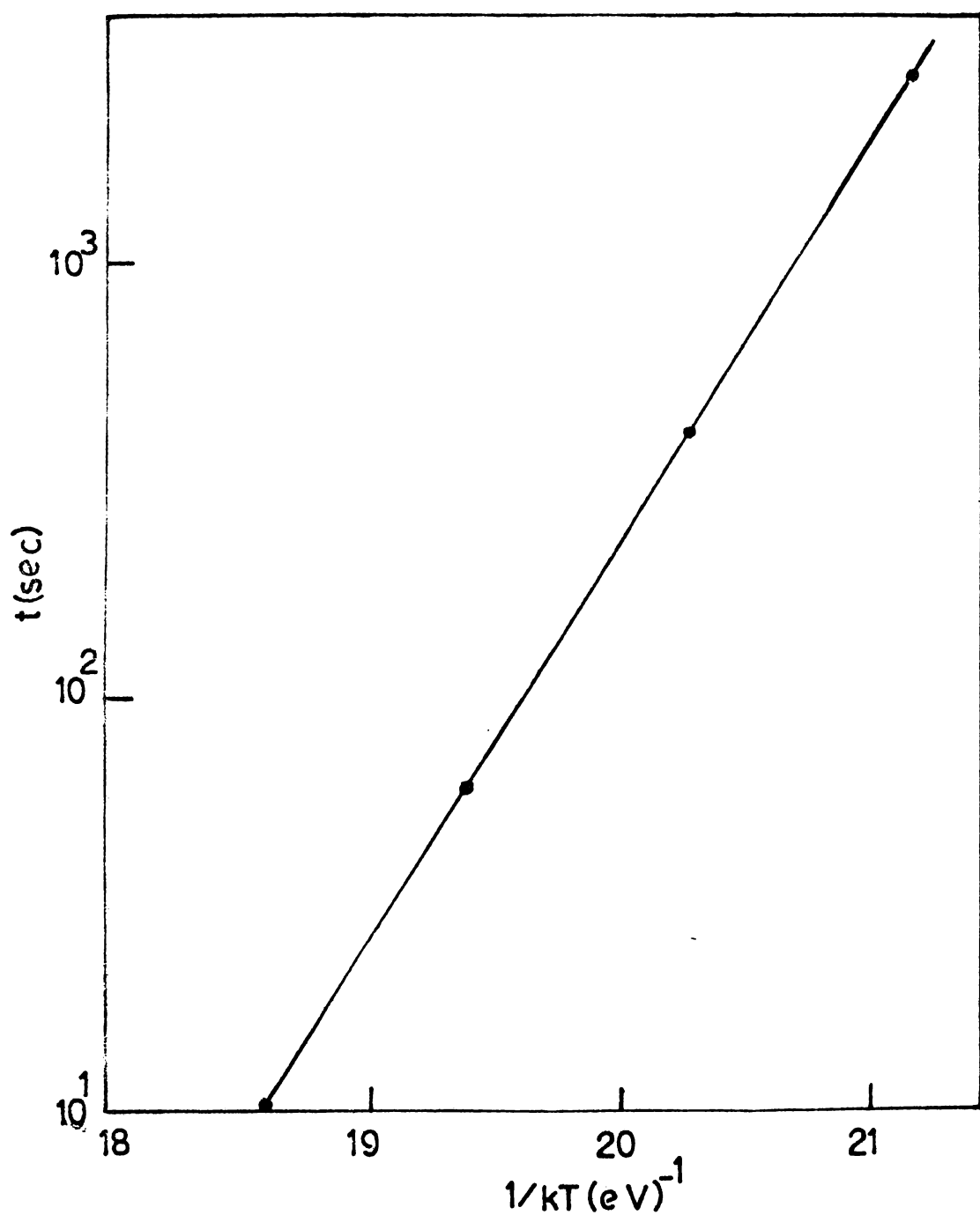


Figure 1: Plot of $(1/k_B T)$ versus time taken for the onset of oxidation (t) at different oxidation temperatures (T) for a typical set of samples.

where t_0 is a constant, k_B the Boltzmann constant and E_a may be identified with the activation energy needed for the process.

The plot of the time taken for the onset of oxidation (t) and the temperature T is shown in figure 1 for a typical set of samples, all prepared in the same deposition run. The activation energy needed for oxidation obtained from the plot is $2.25 \pm 0.1\text{eV}$. It has been found that activation energy varies for different sets of specimens by about 0.2eV . This may have been caused by several factors like rate of deposition, variation in thickness of the sulphide films etc. Though the monitoring technique used may seem crude, the results obtained are quite consistent and reasonable.

Homogenous and good quality films were obtained only when the thickness of the starting sulphide films were less than 300 nm . It is found that with thicker films, because of the different thermal expansion coefficients of film and substrate material, the sulphide films always cracked when suddenly heated in air. Eventhough these thick sulphide films may be converted fully to oxide films, the quality of the films suffered with increasing thickness. When the starting sulphide film thickness was more than one micron,

oxidation of the films was incomplete, i.e. only certain areas were oxidized. This suggests that diffusion is the mechanism by which oxygen is penetrating the film. In thicker films it takes more time for oxygen to diffuse into the substrate side of the film and by that time the surface of the film may become completely oxidized and may perhaps create a diffusion barrier which impedes further flow of oxygen into the film and sulphur or sulphur dioxide out of the film.

A simple phenomenological theory may be developed for the oxidation process and can be used to derive (5.2.2). If the volume of the film in the oxidized state is V_c and the volume transforming is proportional to the untransformed volume, then the rate of transformation is

$$\frac{dV_c}{dt} = k_o (V - V_c) \quad (5.2.3)$$

so that

$$V_c = V [1 - \exp(-k_o t)] \quad (5.2.4)$$

where V is the total volume and k_o the rate constant

$$k_o = \nu \exp(-E_a/k_B T) \quad (5.2.5)$$

where ν is a constant and E_a the activation energy

needed for the process.

From (4), the fraction which is unoxidized at a time t_c is,

$$g = \frac{V - V_c}{V} = \exp(-k_o t_c) \quad (5.2.6)$$

The time t_c corresponds to the observed optical criterion for oxidation (the sudden change in the colour of the film) at a temperature T and thus determines some untransformed fraction g ; this constant fraction may be combined with (5.2.5) to give

$$t_c = t_o \exp(E_a/k_B T)$$

Equation (2) has a form common to many polymorphic transformations which do not include nucleation. A similar relationship has been observed in the crystallization of amorphous silicon films /23/. The constant t_o has been identified in certain cases as the time taken for the microscopic interaction between the atoms.

5.3 ELECTRICAL PROPERTIES

Tin dioxide films prepared by this method show n-type conductivity. We say a film is a low resistivity type if its resistivity is less than 10 ohm cm.

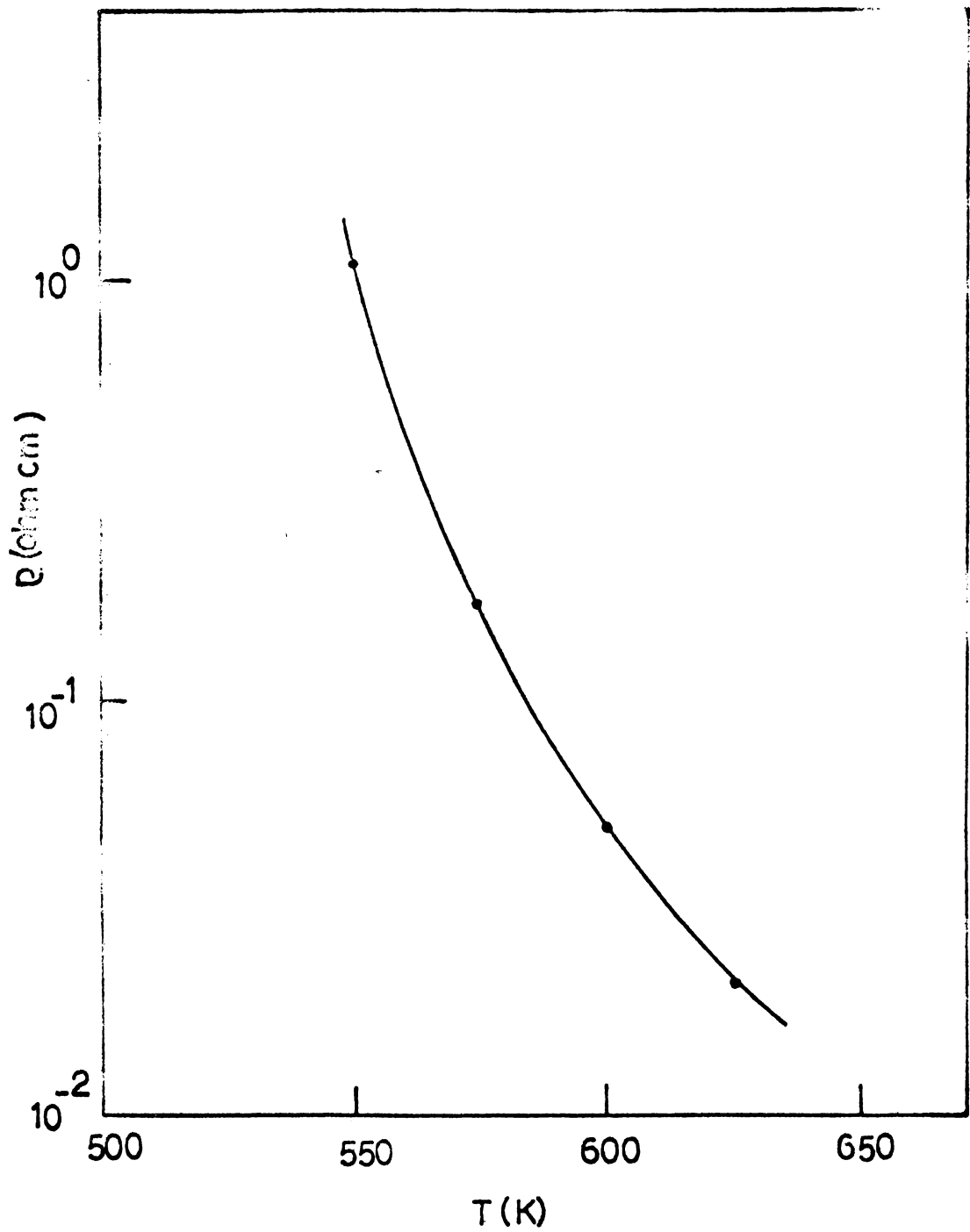


Figure 2: Variation of resistivity with oxidation temperature for the same set of samples as shown in figure 1.

The variation of film resistivity with oxidation temperature for the same set of samples shown in figure 1 is shown in figure 2. From the figure it can be seen that the films oxidized at the highest temperature (625K) have the lowest resistivity. At this temperature it took only 30 sec for the oxidation to be completed with the rate of heating we used and so heating beyond 625K was not attempted. It was also observed that high heating rates of about 0.5K sec^{-1} had to be used to get low resistivity films. With low heating rates only high resistivity films were obtained even at the highest temperature of 625K.

On heating the amorphous sulphide films, the amorphous to crystalline transition take place around 410K and then the grains of the sulphide film begin to grow with time. At low heating rates the small crystallites will have sufficient time to grow into larger crystallites as the rate of crystallization of the amorphous films far exceeds the rate of oxidation at low temperatures. On oxidation of such large crystallites it is possible that the bulk of the SO_2 formed will sublime away resulting in tin oxide crystallites and small amounts of SO_2 and free S. This is similar to the oxidation behaviour reported in many II-VI compound crystals /24-26/. The free S atoms may modify

the conductivity of the films in two ways depending on whether the S atoms are inside the crystallites or are adsorbed in grain boundaries. It has been reported in the literature that the conductivity of undoped tin dioxide arises due to oxygen vacancy /27-28/. If the S atoms are inside the crystallites, these atoms can substitutionally occupy oxygen vacancies thereby decreasing the carrier concentration. In the other case the S atoms adsorbed in the grain boundaries can modify the barrier at the grain boundaries thereby decreasing the mobility of the carriers. It is not clear at present which of these mechanisms is responsible for the decreased conductivity. The role of SO_2 is also not understood.

But when the films are oxidized at high temperatures and high heating rates, the oxidation rate is almost comparable to the crystallization rate and the oxidation is completed much quicker depending on the temperature of the film. Also there is enhanced probability for the highly volatile S and SO_2 to escape from the film at high temperatures, thereby making it electrically more conductive.

5.4 OPTICAL PROPERTIES.

Figure 3 shows the transmission spectra of a typical oxidized film. For comparison purposes the

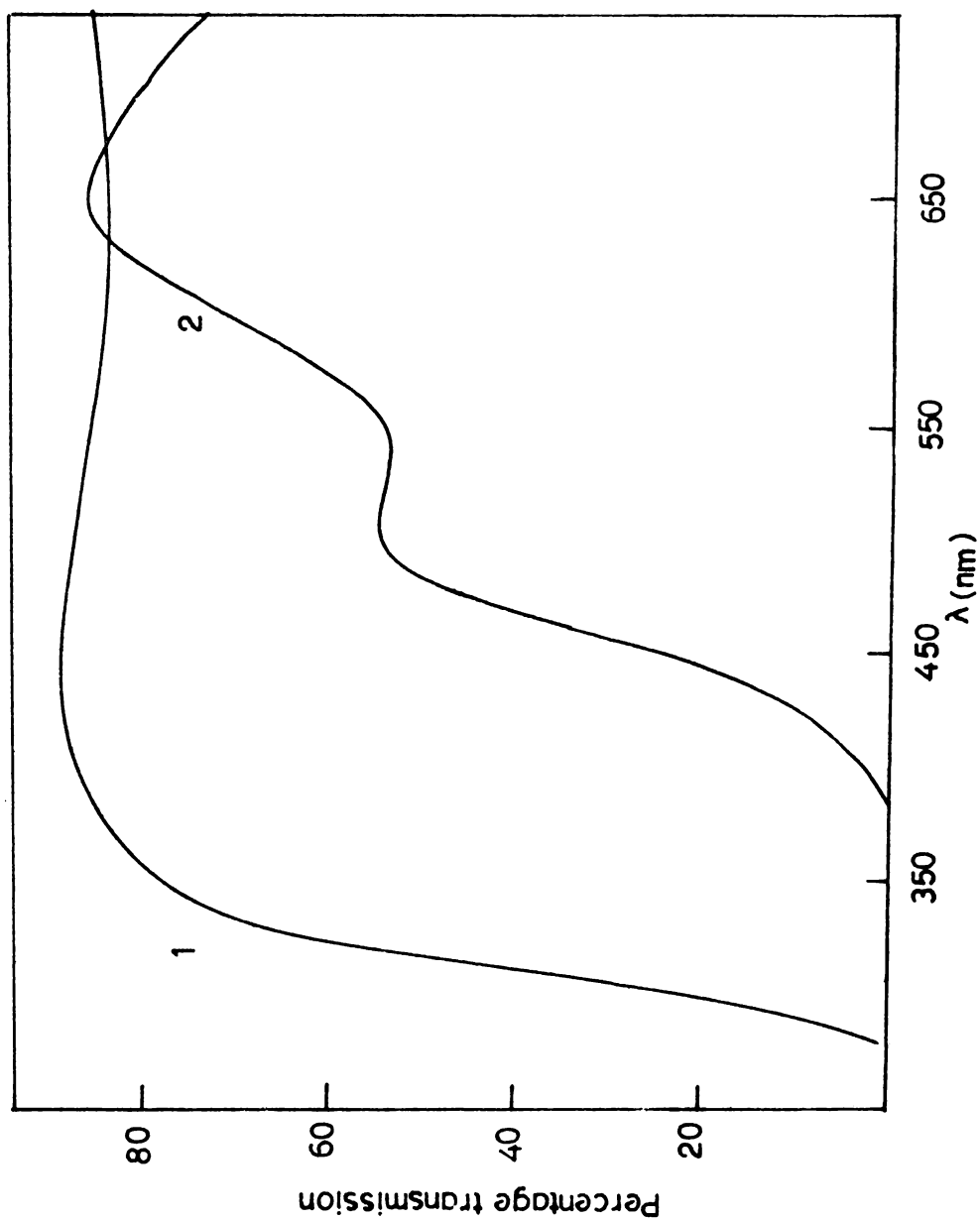


Figure 3: Transmission spectra of the oxidized film (curve 1) and of as-prepared sulphide film (curve 2). Oxidation temperature 600K, film thickness 250 nm.

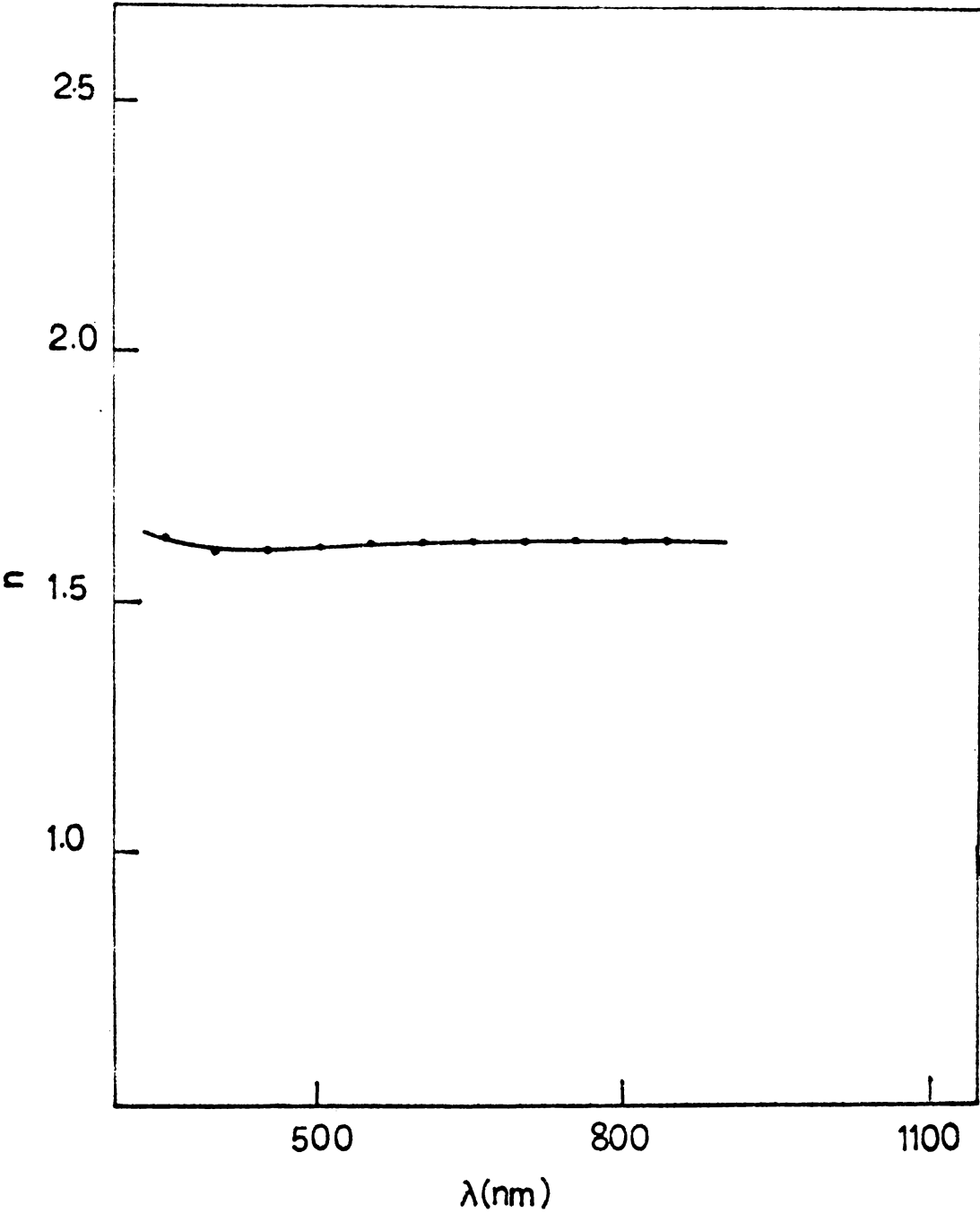


Figure 4: Variation of refractive index n with wavelength.

transmission spectra of an as prepared tin disulphide film is also included. It can be seen that the tin dioxide film has an average transmission of 87%. The transmission spectra was recorded without a compensating blank substrate in the reference beam of the spectrophotometer and hence include any absorption due to the quartz substrate of the sample film. It can be inferred from the transmission spectra that the films are of good optical quality as they show interference fringes. The variation of refractive index with wavelength is shown in figure 4. The refractive index was calculated as described in Chapter III. The value obtained here agrees well with that reported in the literature /11/. This value is slightly less than that reported for tin dioxide crystals ($n=1.9$) /29/.

Absorption coefficient of the film was calculated as described in Chapter III. The absorption data was analyzed in terms of the theory of Bardeen et al /30/. For a direct transition the theory gives

$$\alpha = \frac{A(h\nu - E_g)^r}{h\nu} \quad (5.4.1)$$

$r = 1/2$ for an allowed transition

$r = 3/2$ for a forbidden transition

where A is a constant, $h\nu$ photon energy and E_g the

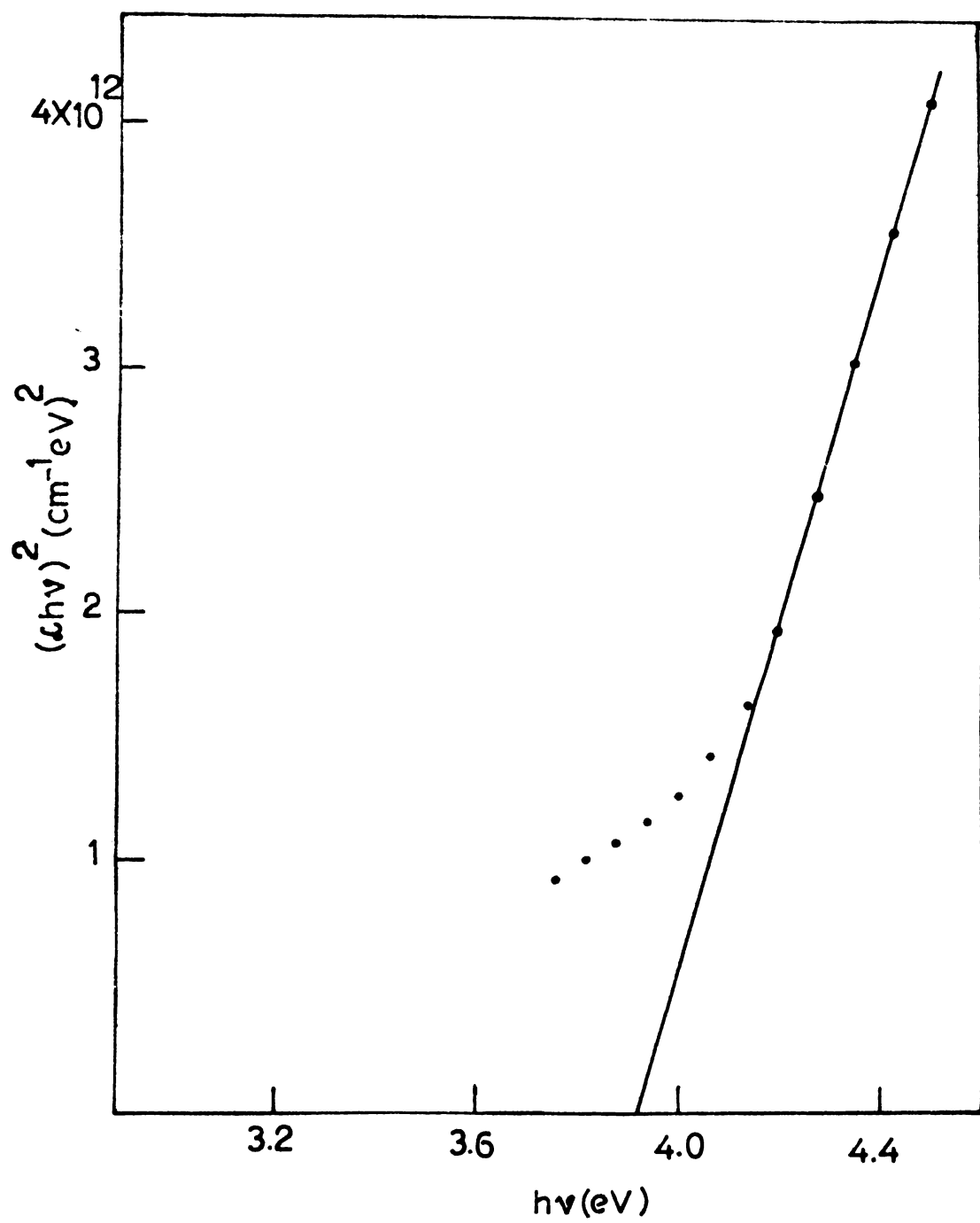


Figure 5: Plot of $(\alpha h\nu)^2$ versus $h\nu$ for a typical film.

direct band gap. It has been generally reported that tin dioxide is an indirect band gap semiconductor. Because of the thinness of the samples and also due to the low absorption coefficients ($\alpha < 10^3 \text{ cm}^{-1}$) associated with indirect transitions, the indirect transition could not be observed. In figure 6, $(\alpha h\nu)^2$ is plotted against $h\nu$ for a typical film and gives an intercept of $3.93 \pm 0.01 \text{ eV}$ corresponding to a direct transition. The intercepts obtained for different films range from 3.9 to 4.1 eV. This large scatter in the value of the band gap is due to the different amounts of carrier concentration in the film material which shifts the absorption edge to shorter wavelengths. Values reported in the literature for this transition varies from 3.7 to 4.3 eV/31-33/.

CONCLUSION

Transparent conducting films of tin oxide ($T = 87\%$, $\rho = 2 \times 10^{-2} \text{ ohm cm}$) have been prepared by the oxidation in air of reactively evaporated tin disulphide films. It has been found that the time taken for the onset of oxidation at different temperatures can be represented by a simple rate relationship. Low resistivity films are obtained with oxidation temperature around 625K and heating rate around 0.5 K sec^{-1} . The films are n-type and have strong adhesion to the substrate.

References:

1. K. Badeker, Ann. Phys. (Leipzig), 22 (1907) 749.
2. M. Mizuhashi, J. Non-Cryst. Solids, 38-39 (1980) 329.
3. M. Watanabe, Jpn. J. Appl. Phys., 9 (1970) 1551.
4. S. Muranaka, Y. Bands and T. Takada, Thin Solid Films 86, (1981) 11.
5. H.S. Randhawa, M.D. Mathews and R.F. Bunshah, Thin Solid Films 83 (1981) 267.
6. R.P. Howson, J.N. Avaritsiotis, M.I. Ridge and C.A. Bishop, Appl. Phys. Lett., 35(1979) 161.
7. M. Hecq and E. Portier, Thin Solid Films, 9 (1972) 341.
8. S. Yamanaka and T. Oohashi, Jpn. J. Appl. Phys. 8 (1969) 1058.
9. E. Giani and R. Kelley, J. Electrochem. Soc. 121 (1974) 394.
10. T. Muranoi and M. Furukoshi, Thin Solid Films 48 (1978) 309.
11. J.C. Manificier, M. de Murcia, J.P. Fillard and E. Vicario, Thin Solid Films, 41 (1977) 127.
12. British Patent 632, 256 to H.A. McMasters, Libely Owens - Ford Glass Co. (1942).
13. J.L. Vossen, R.C.A.Rev.32(1971) 289.

14. P. Nath and R.F. Bunshah, Thin Solid Films
69 (1980) 63.
15. E. Burstein, Phys. Rev., 93 (1954) 632.
16. J.C. Manifacier, L. Szepessy, J.F. Bresse,
M Perotin and R. Stuck, Mater. Res.
Bull. 14 (1979) 163.
17. J. Kane, H.P. Schweizer and W. Kern, J. Electro-
chem. Soc., 122 (1975) 1144.
18. E. Shanthi, V. Dutta, A. Banerjee and K.L. Chopra,
J.Appl.Phys. 51 (1980) 6243.
19. J. Kane, H.P. Schweizer, and W. Kern, J. Electro-
chem. Soc., 123 (1976) 270.
20. E. Shanthi, A. Banerjee, V. Dutta and K.L. Chopra,
J. Appl. Phys. 53 (1982) 1615.
21. G. Eblendenent, M. Court and Y. Lagarde, Thin Solid
Films 77 (1981) 81.
22. Y.S. Hsu and S.K. Ghandi, J. Electrochem. Soc.,
127 (1980) 1592, 1595.
23. N.A. Blum and C. Feldman, J. Non-Cryst. Solids,
11 (1972) 242.
24. P. Pianetta, I. Lindaw, C.M. Garner and W.E. Spear,
Phys, Rev. B., 18 (1978) 2792.
25. A. Ebina, K. Asano, Y. Suda and T. Takahashi,
J. Vac. Sci. Technol., 17 (1980) 1074.
26. A. Ebina, Y. Suda, T. Takahashi, Int. J. Elec.,
52 (1982) 77.

27. S. Samson and C.G. Fonstad, J. Appl. Phys.,
44 (1973) 4618.
28. J. Aboof, V.C. Marecotte and N.J. Chow, J. Electro-
chem. Soc., 120 (1973) 701.
29. S.F. Redaway and D.A. Wright, British J. Appl.
Phys. 16 (1965) 195.
30. J. Bardeen, F.J. Blatt and L.H. Hall, Photocond.
Conf., Atlantic City p. 146, Wiley, New York
1956.
31. T. Arai, J. Phys. Soc. Jap., 15 (1960) 916.
32. W. Spence, J. Appl. Phys., 38 (1967) 3767.
33. K.B. Sundaram and G.K. Bhagavat, J. Phys. D.,
14 (1981) 921.

CHAPTER-VI

REACTIVELY EVAPORATED FILMS OF COPPER SULPHIDE

In recent years there has been much interest in copper sulphide films because of its use as absorber material in CdS:Cu₂S thin film solar cells which still hold promise for large scale terrestrial power generation. The photovoltaic conversion efficiency in these cells depends markedly on the composition of the Cu_{2-x}S layer /1/. It is reported that chalcocite phase gives the maximum short circuit current and efficiency followed by djurleite phase. Other than this particular interest, copper sulphide in itself is an important material from the point of view of basic research, because this material is known to exist in several crystallographic phases. The number of independent chemical phases which exist at room temperature is still a matter under discussion. There are at least five known phases in the Cu_xS system at room temperature when x varies from 1 to 2. These are, in the copper rich region, orthorhombic chalcocite (γ -Cu₂S), djurleite (orthorhombic, x = 1.96 - 1.94), low temperature dignite (pseudocubic, x = 1.79 - 1.765), anilite (orthorhombic, x = 1.75) and in the sulphur rich region, covellite (CuS, hexagonal). When the temperature increases, the new phases which exist are mid temperature form of chalcocite (β -Cu₂S)

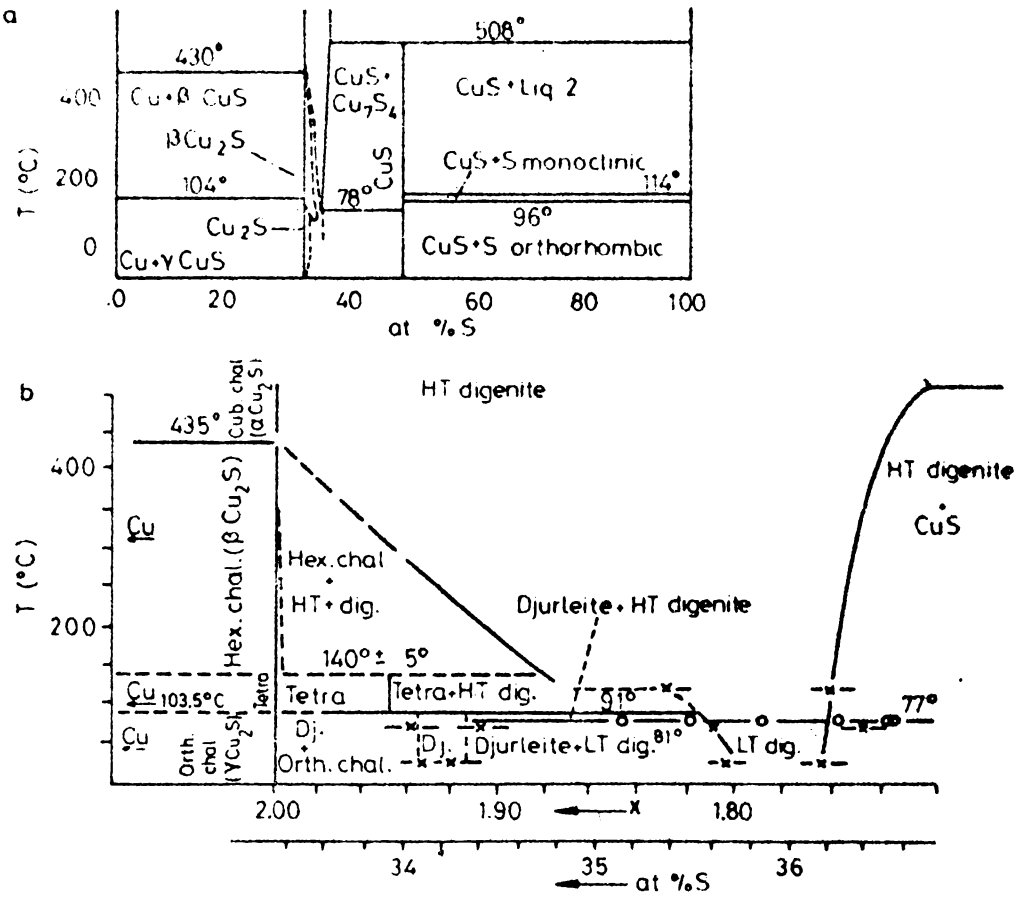


Figure 1: Phase diagram of Cu-S system.

between 103.5°C and 435°C , and the high temperature form (δ - Cu_2S). Another phase, the tetragonal, exists from $x = 1.8$ to $x = 2$. This phase was supposed to be metastable until Cook /2/ showed that it forms a solid solution between Cu_2S and $\text{Cu}_{1.95}\text{S}$ at temperatures from 94°C to 140°C . This is also the domain of high temperature form of dignite. Figure 1 shows the phase diagram of the Cu-S system; the upper figure showing all compositions between 0 and 600°C and the lower figure showing compositions involved in $\text{CdS}:\text{Cu}_x\text{S}$ solar cells. The present view is that a stoichiometric Cu_2S crystal consist of a highly orderd S-sublattice and a disorderd Cu-sublattice. The S-sublattice being the rigid armature of the crystal. The Cu ions are mobile and can occupy a large number of equivalent sites thus giving rise to different phases atleast in the vicinity of the region where $x \approx 2$.

Optical and electrical properties of the different phases in the Cu-S system has not been investigated thoroughly. Only properties of the composition relevant to application in $\text{CdS}:\text{Cu}_2\text{S}$ solar cells has been studied in some detail. Here too, the results obtained by different groups of workers vary to a considerable extent. For example the value of the forbidden energy gap reported by various authors for γ - Cu_2S vary from

1.05 to 2.50 eV/3-7/. Electrical properties also show large scattering. It is reported that the carrier concentration varies from $\sim 10^{15}$ to $\sim 10^{21} \text{ cm}^{-3}$ and hole mobility varies from 1 to $15 \text{ cm}^2/\text{volt sec}$. These scattering are primarily due to the existence of different phases in the same stoichiometric interval and also due to the non-stoichiometries of the phases themselves. In the sulphur rich region of the Cu-S phase diagram, electrical properties of pressed samples of CuS (Covellite) has been reported /8/ and it is also reported here that CuS exhibits metallic conductivity.

Copper sulphide (Cu_2S) films had in the past been prepared in a number of ways. Carlson prepared copper sulphide films by vacuum evaporation /9/, Ellis used flash evaporation /10/, Jonath et al used reactive sputtering /11/ and Islam and Haque used coevaporation /12/. A number of chemical methods are also available to deposit Cu_2S on CdS for solar cell applications /13-15/.

It was thought that reactive evaporation of copper in a sulphur atmosphere which was not yet reported, is a promising technique for the preparation of copper sulphide films and this method was used for preparing films reported in this chapter.

6.1 PREPARATION OF THE FILM.

Films were prepared in a conventional vacuum

system as described in Chapter III. The system was first pumped to 2×10^{-5} Torr and the optically flat substrate heated to the required temperature. Doubly electrolyzed copper and three times recrystallized sulphur were used as evaporants. A glass crucible placed in a conical basket made of molybdenum wire was used as the sulphur source. A molybdenum boat was used to evaporate copper. The boat was covered with stainless steel heat shields so that the substrate temperature could be kept within 4K of the required temperature.

It is found that a stoichiometric interval exists for the reactive evaporation of copper in a sulphur atmosphere with the following parameters:

metal atom flux = $1-2 \times 10^{14}$ atoms/cm²/sec
 chalcogen flux = $1-2 \times 10^{16}$ molecules/cm²/sec
 substrate temperature = 295-440K

It is also found that films prepared with substrate temperatures from 295K to 315K have a golden yellow colour and films prepared from 325K to 440K have a deep green colour. The deposition rate of the films were 0.2 - 0.5 nm/sec.

Composition of the films were determined by taking the X-ray diffraction pattern of the films prepared at various temperatures. For these measurements films were not detached from the substrate. A Philips PW 1140/90 X-ray unit fitted with PW 1050/70 goniometer was

used for X-ray diffraction studies. Filtered Cu K α radiation ($\lambda = 1.5405\text{\AA}$) was employed. Thickness of the films used for X-ray diffraction studies were between 300 and 500 nm.

Optical measurements were made using a Carry 17D double beam spectrophotometer which can cover the wavelength region from 2500 nm to 200 nm. Refractive index and absorption coefficient of the films were determined as described in Chapter III.

Electrical conductivity and Hall effect measurements were made after depositing gold electrodes to the film. It was found that copper and aluminium electrodes does not give an ohmic contact to these films; only gold electrodes give an ohmic contact. Electrical conductivity and Hall effect of the films were measured in the set-up described in Chapter III.

6.2 STRUCTURAL STUDIES

The X-ray diffraction pattern of the film-substrate system prepared at various substrate temperatures are shown in figure 2. It can be seen that films prepared at the higher substrate temperatures are crystalline in nature. From the colour of the films crystalline and amorphous films can be easily distinguished. Crystalline films have a deep green colour and amorphous ones a golden yellow colour. From the colour of the films it was inferred that films prepared above a substrate temperature of 320K are crystalline in nature

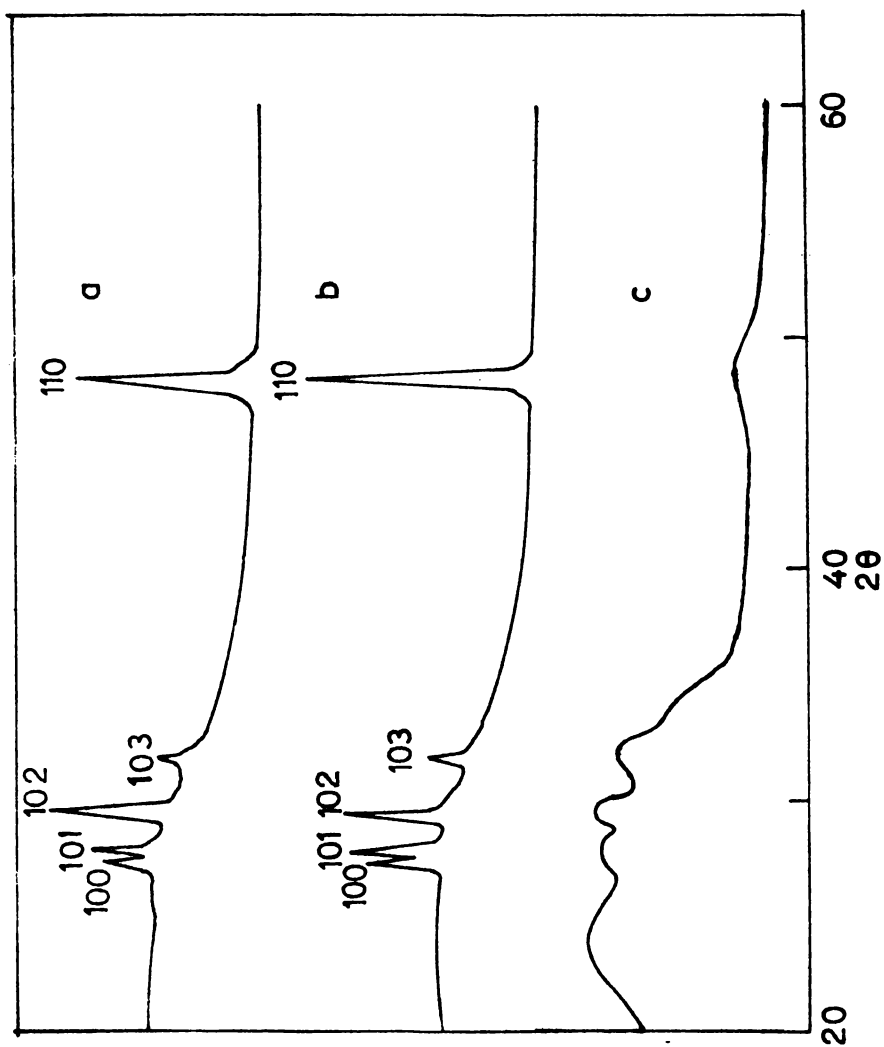


Figure 2: X-ray diffractograms of films prepared at various substrate temperature T_s : (a) 440K, (b) 345K, (c) 305K. The amorphous nature of the film prepared at 305K is evident. The background is due to the glass substrate.

TABLE I

hkl	JCPDS		FILM-A		FILM-B	
	d A.U.	I/I ₁	d A.U.	I/I ₁	d A.U.	I/I ₁
002	8.180	7				
100	3.287	11	3.269	11	3.258	11
101	3.223	16	3.207	15	3.205	15
102	3.050	47	3.034	16	3.028	27
103	2.815	100	2.803	7	2.795	5
006	2.726	44				
105	2.319	9				
106	2.099	4				
008	2.045	4				
110	1.898	53	1.891	51	1.888	60

and films prepared below 315K are amorphous in nature. The d-spacings calculated for films with well-defined diffraction peaks (a and b) agrees with that given for covellite (CuS) in JCPDS cards /16/. The d-spacings and relative intensities given in JCPDS card for covellite along with our results are given in Table I.. This table is obtained after normalizing the intensities obtained from the films to the 100 line of the JCPDS card and also taking into consideration the fact that in the diffractometer with Bragg-Brentano geometry, at any incident angle θ , the films gives an effective thickness of $t/\sin \theta$ and consequently the reflected intensity will be angle dependant. Films prepared at room temperature (305K) does not show any sharp peaks (film c). It can be concluded that these films are amorphous in nature. The diffused back-ground exhibited by all films is due to the glass substrate.

Referring to Table I it can be seen that reflections from planes having Miller indices 00l are missing in crystalline films. From this it can be concluded that the grains are oriented with 00l planes perpendicular to the substrate surface. Scanning electron microscopic observations also confirmed this. An SEM micrograph of a film prepared at 440K is shown in figure 3. This is rather surprising, because when materials with hexagonal structure grow with



Figure 3. SEM micrograph of a c-CuS film

preferred orientation on amorphous surfaces, they usually have a columnar growth with 001 planes along the substrate surface; a well known example being the columnar growth of CdS.

From the X-ray diffraction pattern, no other phases in the Cu-S system is detected. Taking into consideration the deposition condition (chalcogen flux to metal flux ratio greater than hundred) it can be seen that if there are enough sulphur molecules present for reaction, only covellite phase is formed. There has not yet been any report of covellite formation in evaporation of bulk Cu_2S . The formation of covellite phase in this case is highly probable because in the initial stages of evaporation when the bulk Cu_2S melts, a large proportion of Cu_2S molecules may dissociate causing preferential evaporation of sulphur. This excess partial pressure at the initial stages of evaporation will assist in the formation of covellite.

6.3 ELECTRICAL PROPERTIES OF CRYSTALLINE CuS films.

Hot probe measurement showed that the film is p-type. Electrical conductivity of the films were measured after depositing gold electrodes on either end of the film. Electrical measurements showed that films were highly conducting with a resistivity of 10^{-4} ohm cm. The variation of resistivity of the film with temperature was positive and very small down to liquid nitrogen

temperature. No significant information could be obtained from these measurements. The positive temperature coefficient of resistance and the very low film resistivity shows that the films are degenerate. Electrical resistivity measurements reported by Okomoto et al /8/ on pressed samples of CuS are very similar to this.

Hall effect measurements showed that the carrier concentration in these films was 10^{22} cm^{-3} and the mobility $2.5 \text{ cm}^2/\text{volt sec}$. Because of the high carrier concentration and the low mobility of the carriers, the Hall voltage developed was only a few microvolts, typically 6 to 8 microvolts for a current of 10mA and a magnetic field of 7K gauss. The temperature variation of this small Hall voltage, if any, could not be determined because of the lack of resolution of the measuring instrument used (maximum resolution of the digital meter was only one microvolt).

6.4 OPTICAL PROPERTIES OF CRYSTALLINE CuS FILMS.

The transmission spectra of crystalline CuS films are shown in figure 4. It can be seen that the spectra is characteristic of a semiconductor. Absorption at wavelengths less than 500 nm is due to the onset of band to band transitions in the semiconductor. Increasing absorption beyond 550 nm to the long wavelength side is due to free carrier absorption or due to transitions taking place from a filled acceptor level situated

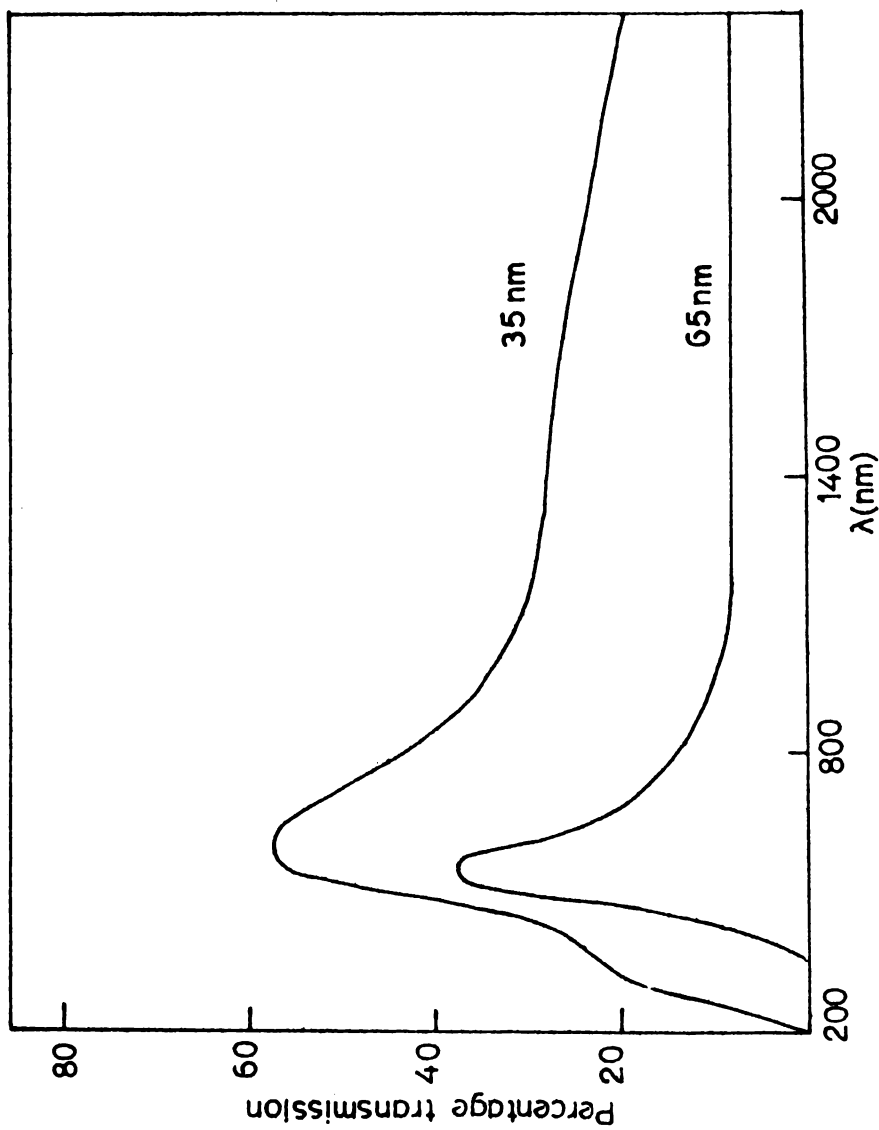


Figure 4: Transmission spectra of crystalline CuS films. Film thickness is indicated.

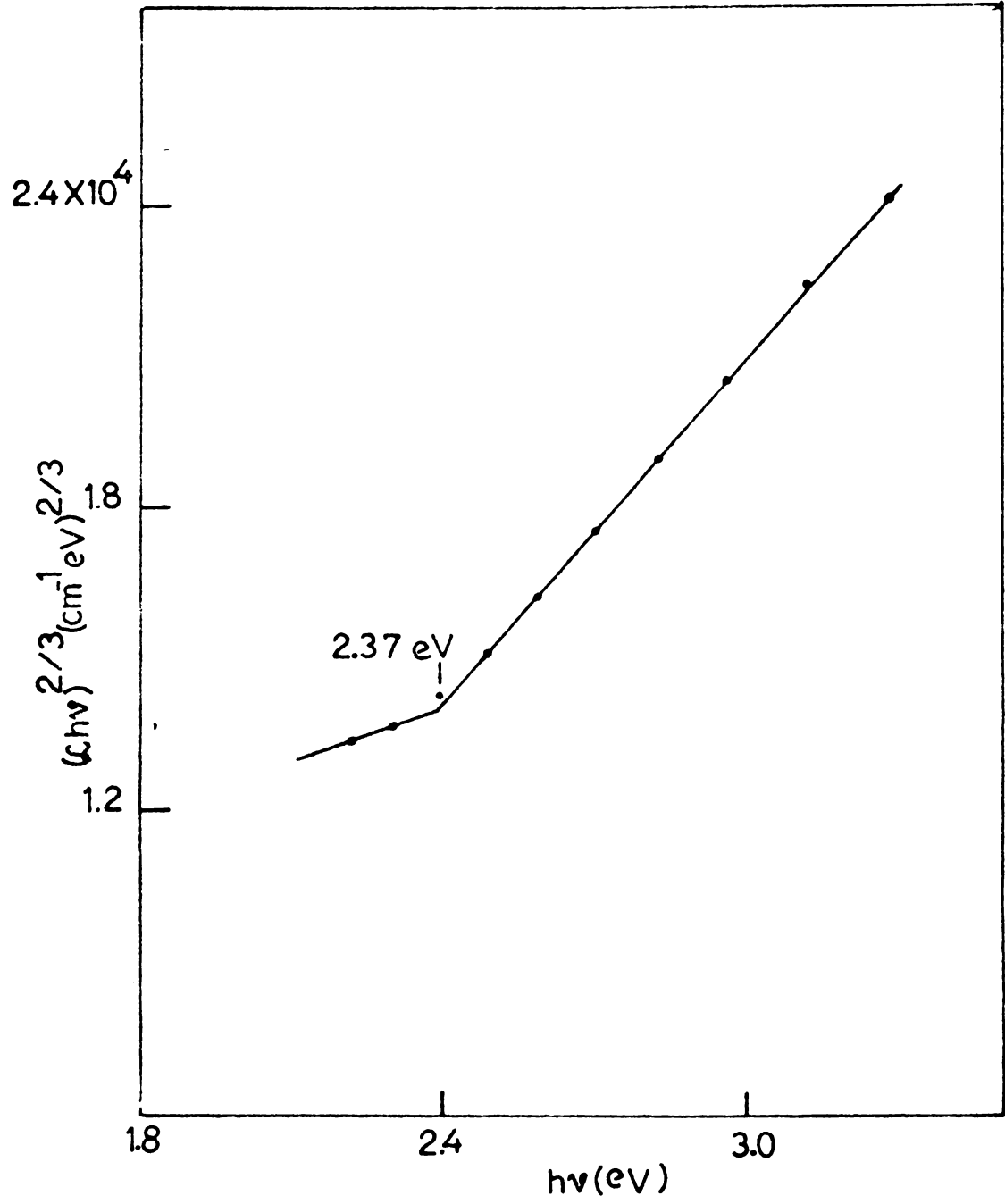


Figure 1: $(\alpha h\nu)^{2/3}$ versus $h\nu$.

just above the valence band to the conduction band. The large absorption ($\alpha \sim 10^5 \text{ cm}^{-1}$) shown by the films before the onset of fundamental absorption is due to the degenerate nature of the films.

Absorption data in the fundamental absorption region was analyzed in terms of the theory of Bardeen et al /17/. This theory gives for a direct transition

$$\alpha = \frac{A(h\nu - E_g)^r}{h\nu} \quad (6.4.1)$$

$r = 1/2$ for an allowed transition

$r = 3/2$ for a forbidden transition

The plot of $(\alpha h\nu)^{2/3}$ versus $h\nu$ is shown in figure 5. This gives a band gap of $2.37 \pm 0.01 \text{ eV}$ and the transition leading to this is a direct forbidden one. This value of band gap is only a representative one, since in degenerate materials, the value of band gap obtained can vary somewhat depending on the carrier concentration. The exact band gap of the material can only be obtained when high quality defect free films of CuS are available. This also holds true for the determination whether CuS is a direct or indirect band gap semiconductor. In the films used in the present study any indirect transition occurring before the direct transition will be masked by the high absorption coefficient of the film before the onset of band to band transitions.

Mooser and Pearson /18/ have introduced the concept of semiconducting bond, which has proved valuable in analyzing and predicting semiconducting properties of compounds and in particular in differentiating between metallic alloys and semiconductors. According to the concept of the semiconducting bond, the solid is a semiconductor if all the possible valence structures lead to filled sub-shells, whereas the metallic state is characterized by partially filled valence orbitals of the component atoms. This valence bond rule was successfully applied to many intermetallic compounds which are formed by s or p electrons of each atoms. But this rule was not applicable to compounds which contain transition elements or rare earths. Hullinger and Mooser /19/ extended the bond treatments of intermetallic compounds to the criterion where d-orbitals as well as s- or p-orbitals concern to the valencies of the compounds. They established that semiconductivity occurs if cation d-electrons are assumed to be localized, while if sub-shells are less than half filled, metallic conduction results.

Mooser and Pearsons' expression for the condition of occurrence of semiconductivity in solids is

$$\frac{n_e}{n_a} + r b_a - b_e = 8 \quad (6.4.2)$$

where n_e is the number of valence electrons (not counting any unshared electrons on the cations) per unit formula, n_a is the number of anions per unit formula,

b_a is the average number of anion-anion bonds and b_e is the average number of cation-cation bonds. If the above condition is not satisfied, the solid is a metallic conductor.

Application of the above rule to CuS predict that it is a semiconductor. From the results of their electrical measurements, Okomoto et al concluded that CuS is metallic in nature and as such Mooser and Pearsons rule does not hold in this case. But results reported in this chapter confirms that CuS is a semiconductor and that Mooser and Pearsons rule hold in this case also. Magnetic susceptibility data given by Okomoto et al indicates the presence of partially localized 3d electrons in CuS which is a necessary condition for the occurrence of semiconductivity in compounds where d-orbitals as well as s- or p- orbitals concern to the valencies of the compound according to Hullinger and Mooser . From what is given above it can be safely concluded that CuS is a semiconductor with a band gap of 2.37 eV.

6.5 AMORPHOUS FILMS OF CuS

It was found that when copper is reactively evaporated in an atmosphere of sulphur, and when the substrate temperature is lower than 315K, the films are amorphous in nature (see figure 2). These films have a golden yellow colour and highly transparent before the onset of fundamental absorption. Since crystalline CuS films have a deep green

colour, amorphous CuS films with their golden yellow colour can be easily distinguished. Films prepared with substrate temperature between 315K and 320K has a colour in between golden yellow and green and with a slight increase in temperature the films turned to the crystalline deep green colour. Obviously films prepared at these temperatures contain amorphous and crystalline regions.

6.6 ELECTRICAL PROPERTIES OF AMORPHOUS CuS FILMS

Hot probe measurements show that amorphous CuS films exhibit n-type conductivity. It is interesting to note that all the other compounds in the copper-sulphur system are p-type semiconductors, including crystalline CuS. Electrical measurements show that films are fairly resistive (room temperature resistivity $\sim 10^5$ ohm cm). The variation of resistance of the films with temperature is shown in figure 6. The activation energy for conduction calculated on the basis of the equation

$$\rho = \rho_0 \exp(E_a/k_B T) \quad (6.6.1)$$

is 0.26 eV. This indicates a thermally activated process and is exhibited by many amorphous semiconductors in this temperature range.

When these films are heated to above 220K, these films crystallize and their resistivity falls by about nine orders of magnitude (from 10^5 ohm cm to 10^{-4} ohm cm). The variation in resistivity of these crystallized films

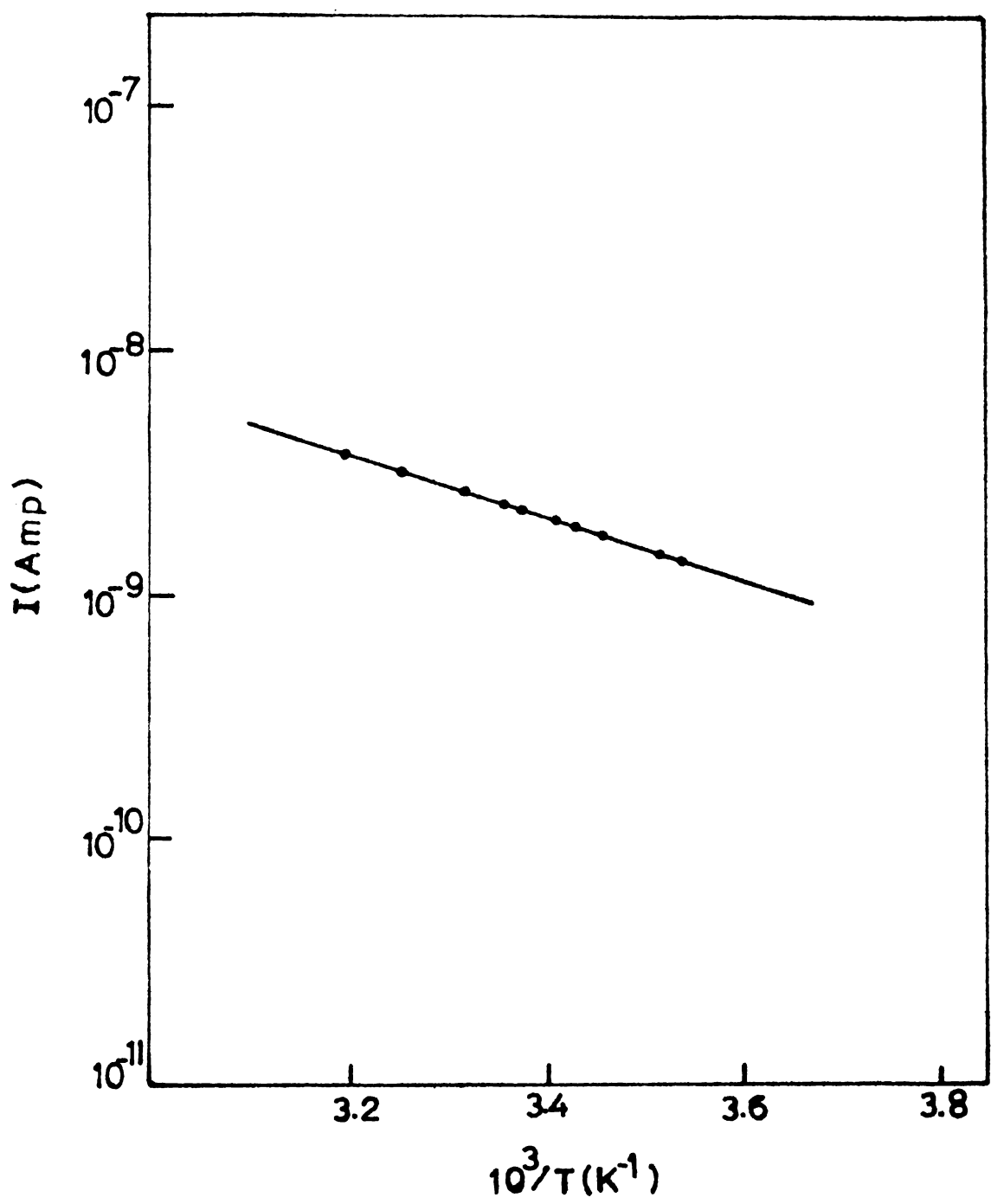


Figure 6: Current versus temperature
($V = 1V$) $E_a = 0.26$ eV.

with temperature, is very low as in the case of crystalline CuS films. Both exhibit positive temperature coefficient of resistance. The overall behaviour exhibited by CuS films are similar to that for tin disulphide films as discussed in Chapter IV. The only difference being, amorphous films of tin disulphide are more stable, as they crystallize only when heated to 410K, whereas amorphous films of CuS crystallize when heated to 320K.

6.7 OPTICAL PROPERTIES OF AMORPHOUS CuS FILMS

Figure 7 shows the transmission spectra of an amorphous CuS film of thickness 390 nm. It can be seen that films are fairly transparent before the onset of band to band transitions **except** for a slight decrease in transmission around 1200 nm. Electrical data given above (negative temperature coefficient of resistance) and the transmission spectra conclusively establish that amorphous CuS is a semiconductor.

The variation of refractive index of the films with wavelength is shown in figure 8. The refractive index of crystalline CuS films and also of amorphous films recrystallized could not be determined as they exhibited no interference fringes.

In many amorphous materials in the photon energy region where $\alpha \sim 10^5 \text{ cm}^{-1}$, the absorption coefficient is found to obey a law of the form /20/

$$\alpha \propto (h\nu - E_g)^r \quad (6.7.2)$$

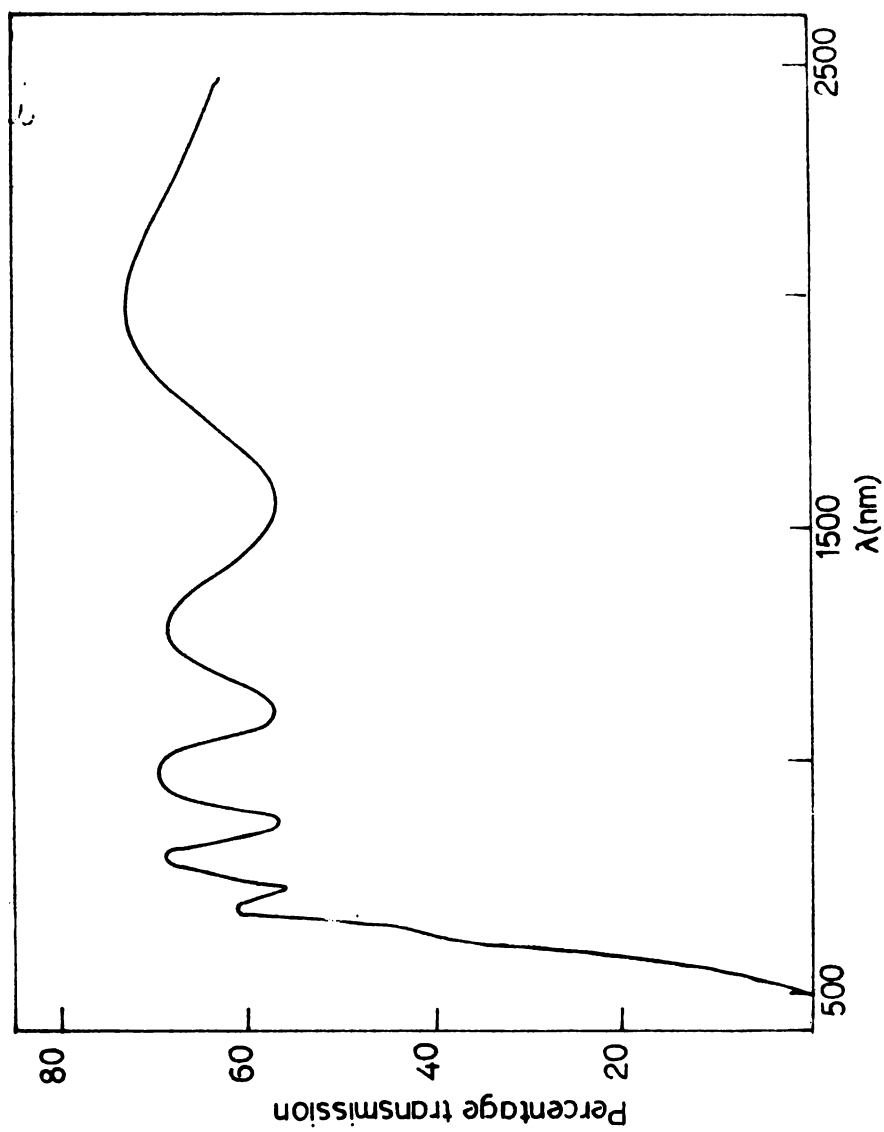
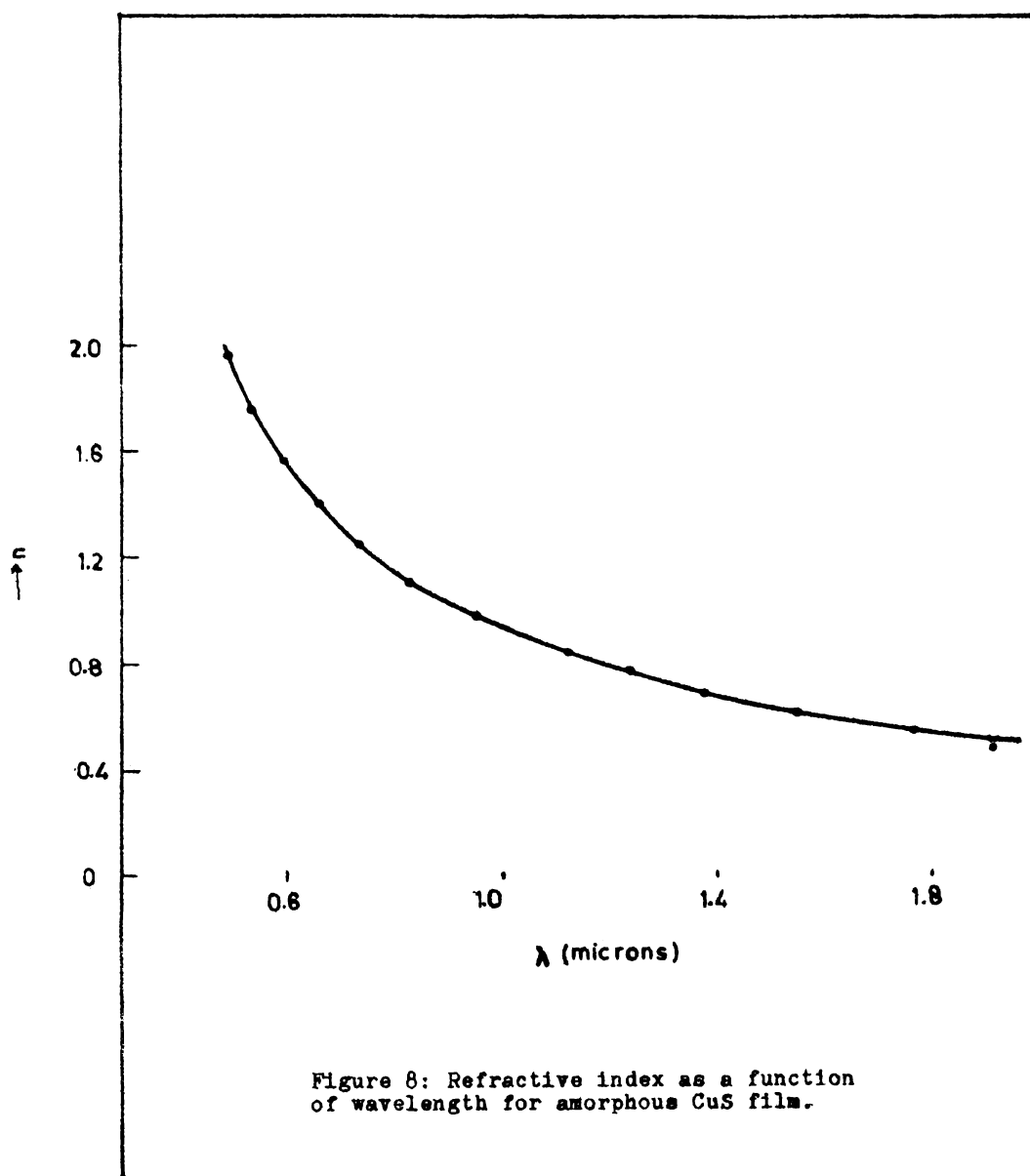


Figure 7: Transmission spectra of amorphous CuS film. Thickness 390 nm.



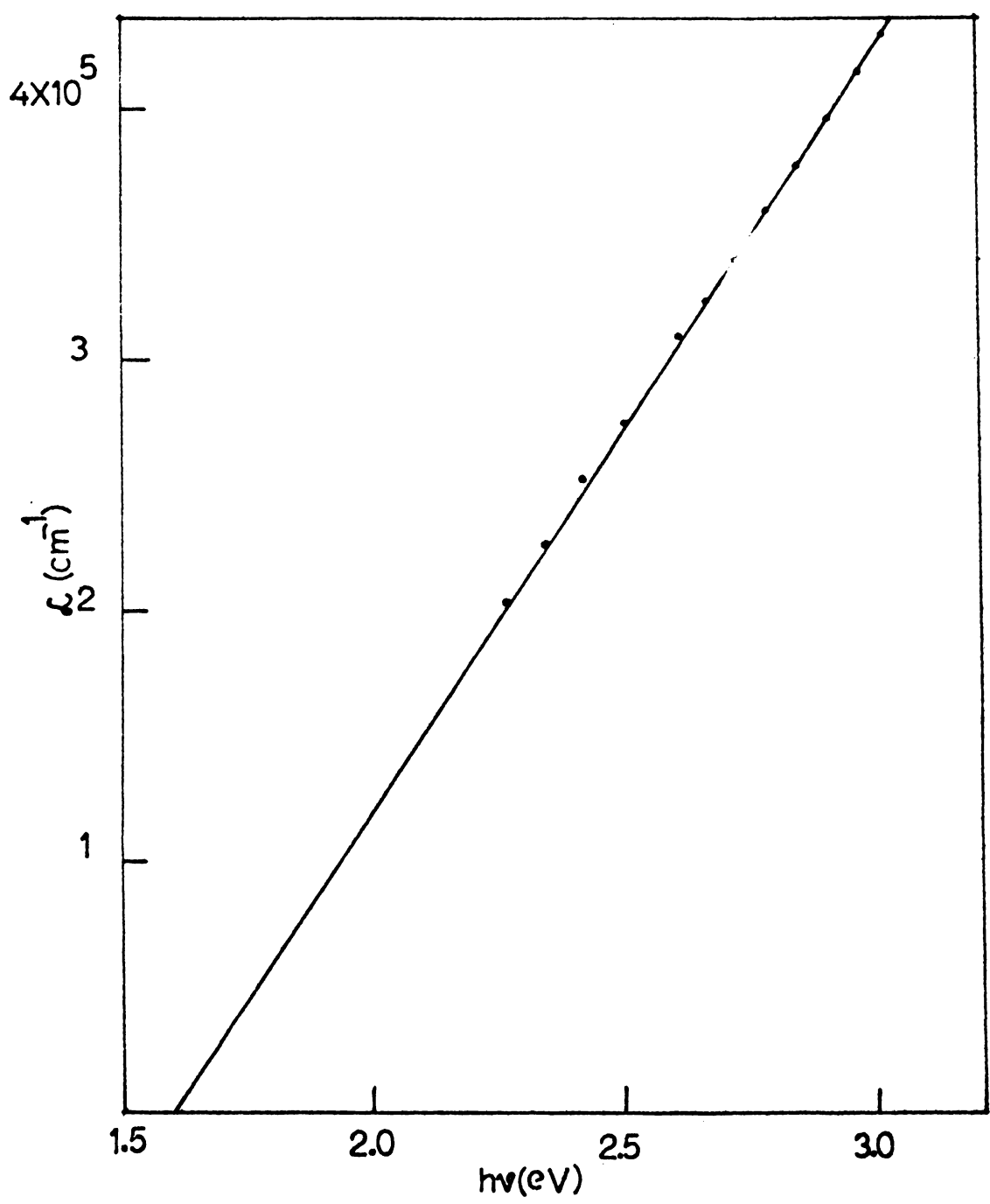


Figure 9: L versus $h\nu$ in the fundamental absorption region. The intercept gives an optical band gap of 1.60 ± 0.02 eV.

values of r between 1 and 3 have been observed. The constant E_g can be used to define an optical gap although it may represent an extrapolated rather than a real zero in the density of states.

The plot of \mathcal{L} versus $h\nu$ is shown in figure 9. The value of E_g obtained 1.60 eV is in agreement with the transmission data. The plot of $(\mathcal{L} h\nu)^{1/2}$ versus $h\nu$, which is the more commonly observed relationship ($r=2$), gives an energy gap of 1 eV which obviously is not in agreement with the transmission data. The unity value obtained for r indicates a sharp rise in the density of states at the band edges. This type of behaviour ($\mathcal{L} \propto (h\nu - E_g)$) was earlier reported in the case of amorphous selenium /21/.

In amorphous materials when a law of the form given by equation (6.7.2) holds, transitions are believed to take place between the extended states of the valence band and the extended states of the conduction band and hence the band gap in the crystalline and amorphous phases must be approximately equal /22/. But it can be seen that in the case of covellite, the value of the band gap for the crystalline material is 0.77 eV higher than that for amorphous material. This high value may be due to the top of the valence band being empty of electrons and transitions taking place from deeper lying levels in the valence band to the conduction band. This emptying

of the valence band is highly probable because of the high p-type conductivity ($\rho \sim 10^{-4}$ ohm cm) exhibited by the crystalline samples.

CONCLUSIONS

When copper is evaporated in an atmosphere of sulphur vapour, films of covellite (CuS) are formed. Films prepared below a substrate temperature of 315K are amorphous in nature, whereas films prepared above 320K are crystalline in nature. Films prepared in the transition region (i.e. substrate temperature between 315 and 320K) exhibit both crystalline and amorphous areas. Crystalline films have their grains oriented with 001 planes perpendicular to the substrate surface. Crystalline films show p-type conductivity with a room temperature resistivity of $\sim 10^{-4}$ ohm cm and positive temperature coefficient of resistance down to liquid nitrogen temperature. Amorphous films of CuS exhibit n-type conductivity with a room temperature resistivity of $\sim 10^5$ ohm cm. Activation energy for electronic conduction in amorphous CuS films is 0.29 ± 0.05 eV. The amorphous films crystallize when heated to 320K and their resistivity changes by nine orders of magnitude (i.e. from $\sim 10^5$ ohm cm to $\sim 10^{-4}$ ohm cm). Crystalline films have a deep green colour and amorphous films, a golden yellow colour. Crystalline films exhibit large

absorption ($\alpha \sim 10^5 \text{ cm}^{-1}$) before the onset of band to band transitions. This together with the positive temperature coefficient of resistance indicate that the crystalline films are degenerate. The forbidden band gap obtained for crystalline films from optical studies is 2.37 eV. This establishes that CuS is a semiconductor contrary to what was believed earlier. Amorphous films of CuS are fairly transparent before the onset of band to band transitions and are of good optical quality. The band gap obtained for amorphous CuS is 1.60 eV. The absorption coefficient in the fundamental absorption region in these films obey a law of the form $\alpha \propto (h\nu - E_g)$ which indicates a sharp rise in density of states at the band edges.

References:

1. W. Palz, J. Besson and J. Veden, Proc. 10th IEEE Photovoltaic. Specialists. Conf. Palo Alto, IEEE, New York (1973).
2. W.R. Cook Jr., Thesis, Case Western University USA (1971).
3. L. Eisenmann, Ann. Physik 10 (1952) 129.
4. G.P. Sorokin, Yu M. Papshierand P.T. Oush, Sov. Phys. Sol. State 7 (1966) 1810.
5. G.B. Abdullaev, Z.A. Aliyarova, E.H. Zamanova and G.A. Asadov, Phys. Status. Sol., 26(b) (1968) 65.
6. L.R. Shiozawa, F. Augustine, G.A. Sullivan, J.M. Smith and W.R. Cook Jr., Research on the Mechanism of the Photovoltaic Effect in High Efficiency CdS Thin Film Solar Cells, Clevite Corp., Contract AF 33 (615) - 5224 Proj. No.7885, Final Rep. (Oct. 1969).
7. N. Nakayawa, J. Physc Soc. Japan 25 (1968) 290.
8. K. Okomoto, S. Kawai and R. Kiriyama, Jap. J. Appl. Phys. 8 (1969) 713.
9. A Carlson, Research in Semiconductor Films. WADC Tech. Report. 56-52 AD 97494, Clevite Corp.(1956).
10. S.A. Ellis, J. Appl. Phys. 38 (1967) 2906.
11. A.D. Jonath, W.D. Anderson, J.A. Thornton and D.G. Cornog, Proc. 13th Photovoltaic. Spic. Conf. 1978 IEEE, New York (1978).

12. M.M. Islam, M.A. Haque, Thin Solid Films 94 (1982) 15.
13. F.A. Shirland, Advan, Energy. Convers. 6 (1966) 201.
14. N. Nakayama, Jap. J. Appl. Phys. 8 (1969) 450.
15. S. Martinuzzi, M. Gaign and W. Palz, Phys. Stat. Solidi 2(a) (1970) K9.
16. JCPDS Card No.24-60 (1974).
17. J. Bardeen, F.J. Blatt and L.H. Hall, Proc. Photocond. Conf., Atlantic City, Wiley, New York 1956.
18. E. Mooser and W.E. Pearson, Prog. Semicond. 5 (1960) 103.
19. F. Hullinger and E. Mooser, J. Phys. Chem. Solids 24 (1963) 283.
20. M. Zavetova and Velicky, Optical Properties of Solids, New Developments, Edited by B.O. Seraphin, p 386, North Holland, Amsterdam 1976.
21. E.A. Davis, J. Non-Cryst. Solids 4 (1970) 107.
22. J. Tauc, Optical Properties of Solids, Edited by F. Abels, p 279, North Holland, Amsterdam 1972.

CHAPTER-VII

EFFECT OF HEATING ON THE PROPERTIES OF CuS FILMS

It has already been shown that CuS films prepared below 315K are amorphous in nature and those prepared above 320K are crystalline in nature. In this chapter is reported the changes taking place as these films are gradually heated in air. This study is important because any application of these films in practical devices require a thorough knowledge about its high temperature behaviour and stability. Amorphous CuS films and crystalline CuS films prepared at low substrate temperatures ($T_s < 375K$) were used in this study. CuS films prepared at high substrate temperature ($T_s > 375K$) tended to behave in a different manner from that of films prepared at lower substrate temperatures. Whereas films prepared at low substrate temperatures went through a series of phase transitions to form Cu_2O and CuO , the films prepared at high substrate temperatures tended to get oxidized into Cu_2O and CuO without undergoing any other phase transformations. This is not surprising if we take into consideration the fact that when films are prepared at low substrate temperatures, they are effectively being quenched from the high source temperature to the low substrate temperature. Hence films prepared at low substrate temperatures will be too much strained

and these strained films can be more easily converted to different phases by giving sufficient thermal energy. But when films are prepared at high substrate temperature, the film forming particles get good mobility on the substrate surface and the films will be strain free to a large extent. Because of the lack of strains these films will be structurally more stable.

7.1 EXPERIMENTAL

Films of amorphous CuS and crystalline CuS were deposited as described in Chapter VI. These films were heated in air in the set-up described in Chapter III. Extremely low heating rates (1-2K/min) were used. The resultant films were characterized by X-ray diffraction and optical absorption studies. Both amorphous and crystalline films prepared at low temperatures were heat treated and amorphous films gave essentially the same results after their crystallization.

7.2 RESULTS AND DISCUSSIONS

When gradually heated in air at $320 \pm 3\text{K}$, the golden yellow colour of the amorphous films changed suddenly to the deep green colour of the crystalline phase. This is certainly due to the crystallization of the amorphous film. The X-ray diffraction pattern of such a crystallized film together with the X-ray diffraction

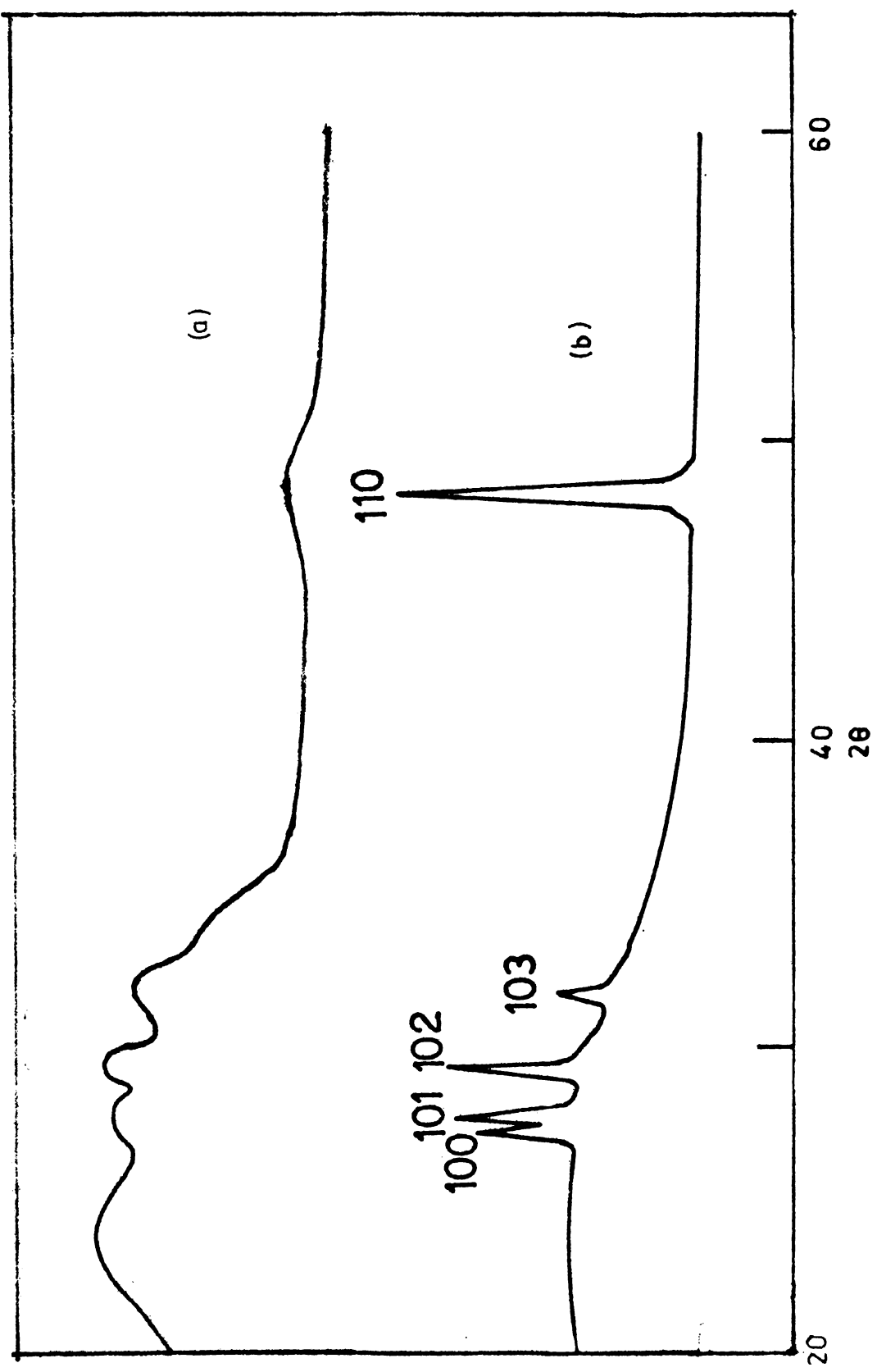


Figure 1: X-ray diffraction pattern of crystallized and amorphous CuS films (a) amorphous (b) crystallized.

pattern of an amorphous film is shown in figure 1. In the crystallized film only lines due to the phase coexistence is observed and is identical to the X-ray diffraction pattern given by CuS films prepared at substrate temperatures greater than 320K.

The transmission spectra of the amorphous and crystallized CuS films are shown in figure 2. It may be seen that crystallization reduces the transmission of the amorphous film considerably. The absorption coefficient exhibited by these films is of the same order as that of crystalline CuS films. The plot of $(\alpha h\nu)^{2/3}$ versus $h\nu$ for a typical crystallized film is shown in figure 3. This gives a forbidden gap value of 2.37 ± 0.02 eV which is in agreement with that of the crystalline CuS films.

When these films are further heat treated without increasing the temperature, gradually spherulites of sulphur begin to appear on the surface of the film. These spherulites have a flower like appearance and have dimensions as large as a few mm. But if a higher temperature is used for heat treatment, a large number of small spherulites are formed. Figure 4 shows a large spherulite grown at low temperature. Figure 5 shows a film which was heat treated at a slightly higher temperature and a large number of small spherulites could be seen.

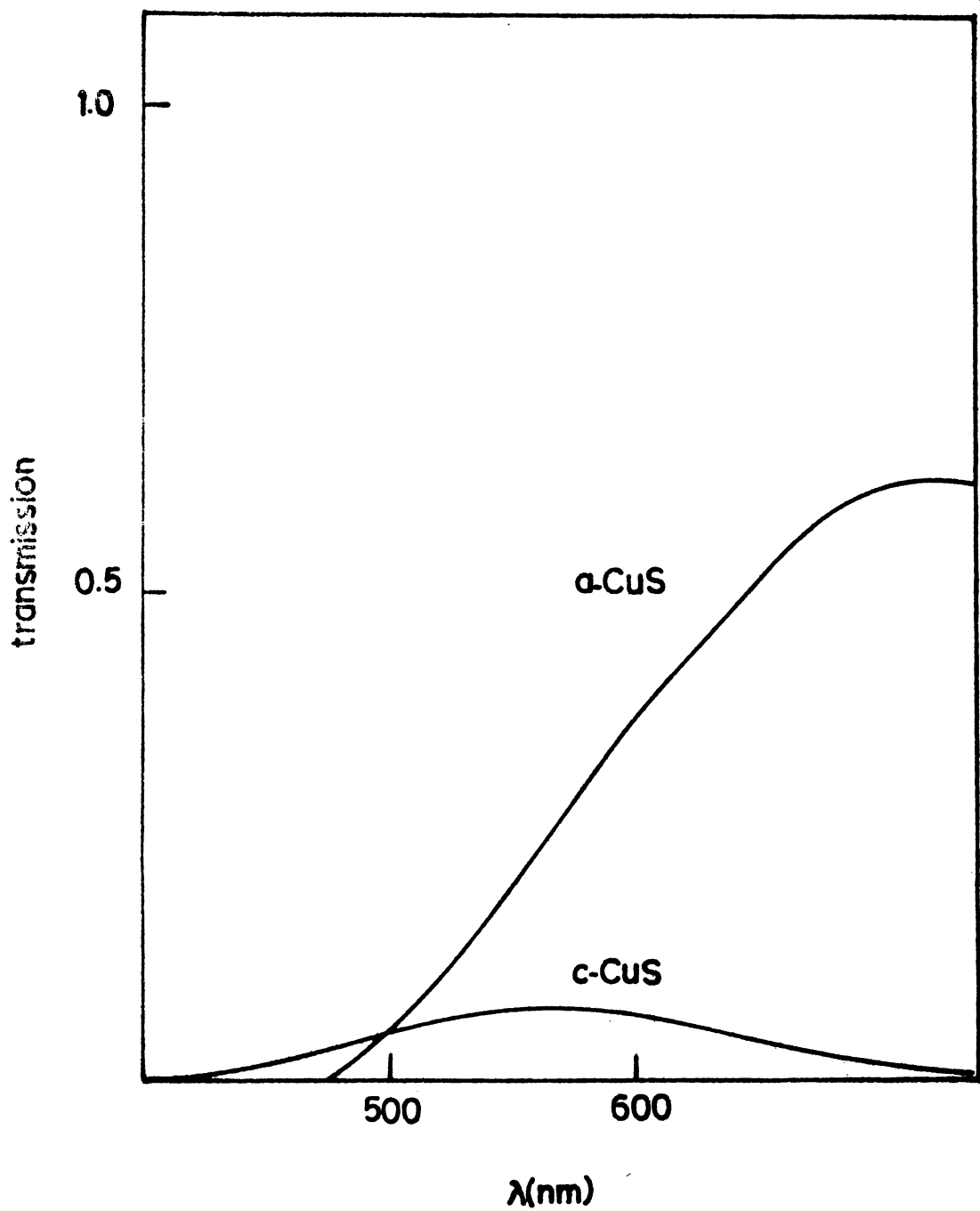


Figure 2: Transmission spectra of amorphous and crystallized CuS films

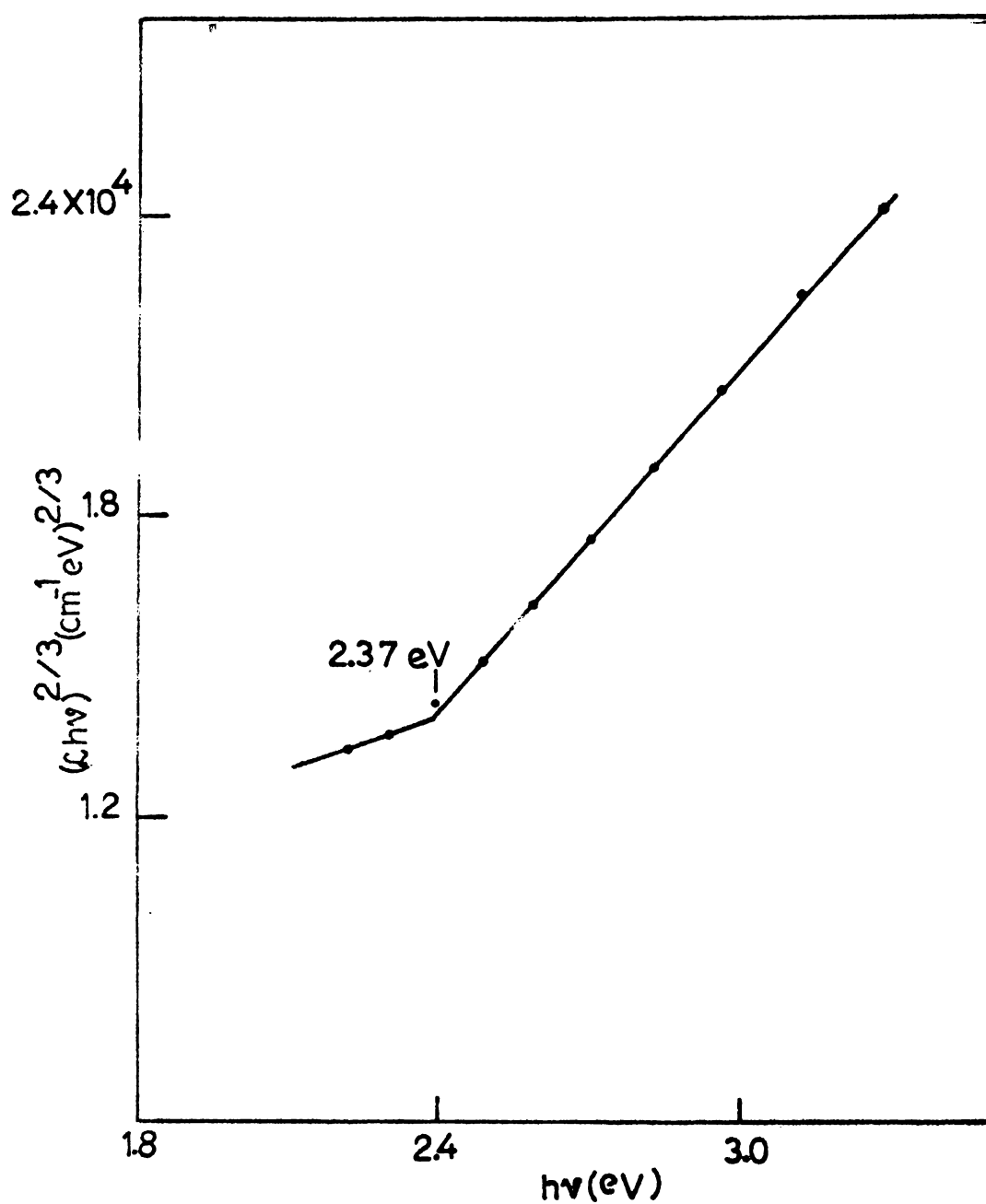
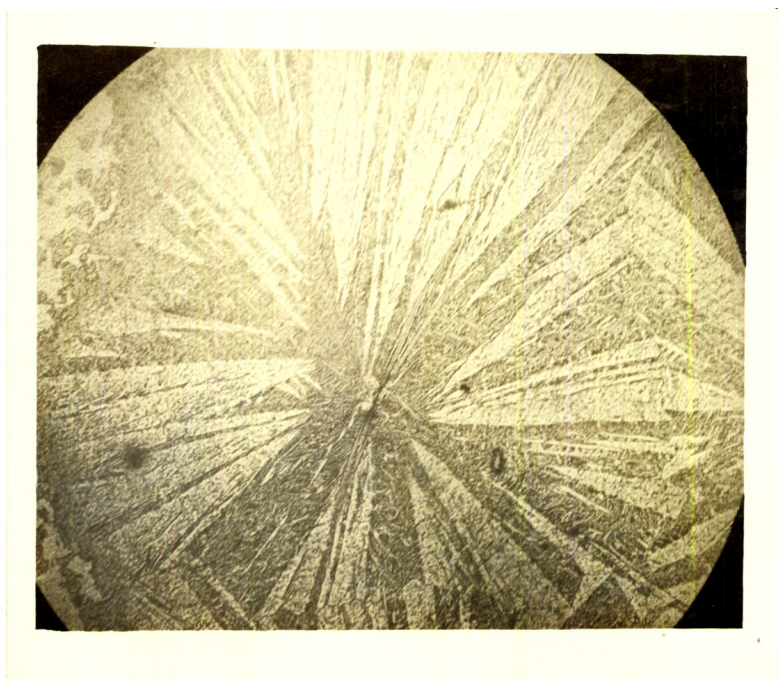
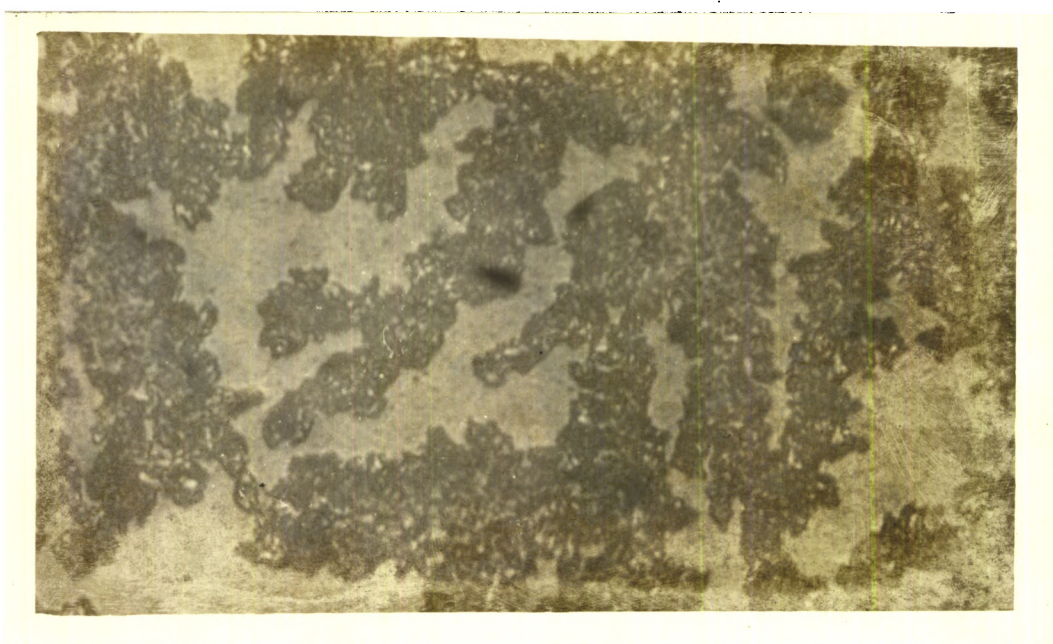


Figure 3: $(\alpha h\nu)^{2/3}$ versus $h\nu$ for a typical crystallized film. Band gap = $2.37 \pm 0.02 \text{ eV}$.



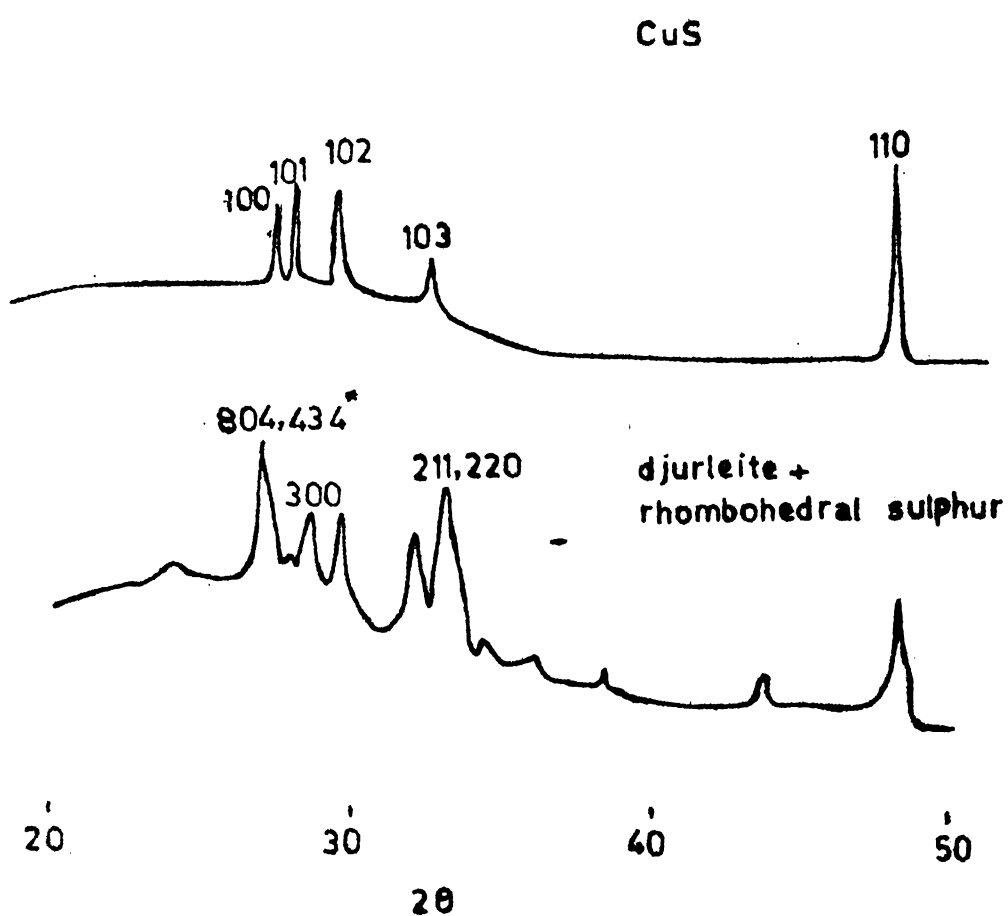
X25

Figure 4. A large spherulite grown at low temperature



X500

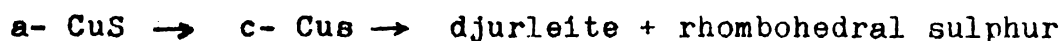
Figure 5. A large number of small spherulite



*identification line of djurleite

Figure 6: X-ray diffraction pattern of a djurleite film with sulphur spherulites on its surface.

X-ray diffraction pattern of a film with spherulites on it is shown in figure 6. Diffraction pattern of covellite films are also shown for comparison. It can be seen that lines due to covellite phase has completely disappeared. Lines of rhombohedral sulphur together with lines of another phase is seen. In the Cu-S phase system both chalcocite and djurleite has almost the same diffraction lines. The distinguishing lines of chalcocite are $d = 2.942\text{\AA}$, $d = 2.207\text{\AA}$ and that of djurleite is $d = 3.39\text{\AA}$. Because of the presence of the distinguishing line for djurleite together with other lines which are common to djurleite and chalcocite phase, it may be concluded that when CuS films prepared at low substrate temperatures is heated the following reaction takes place:



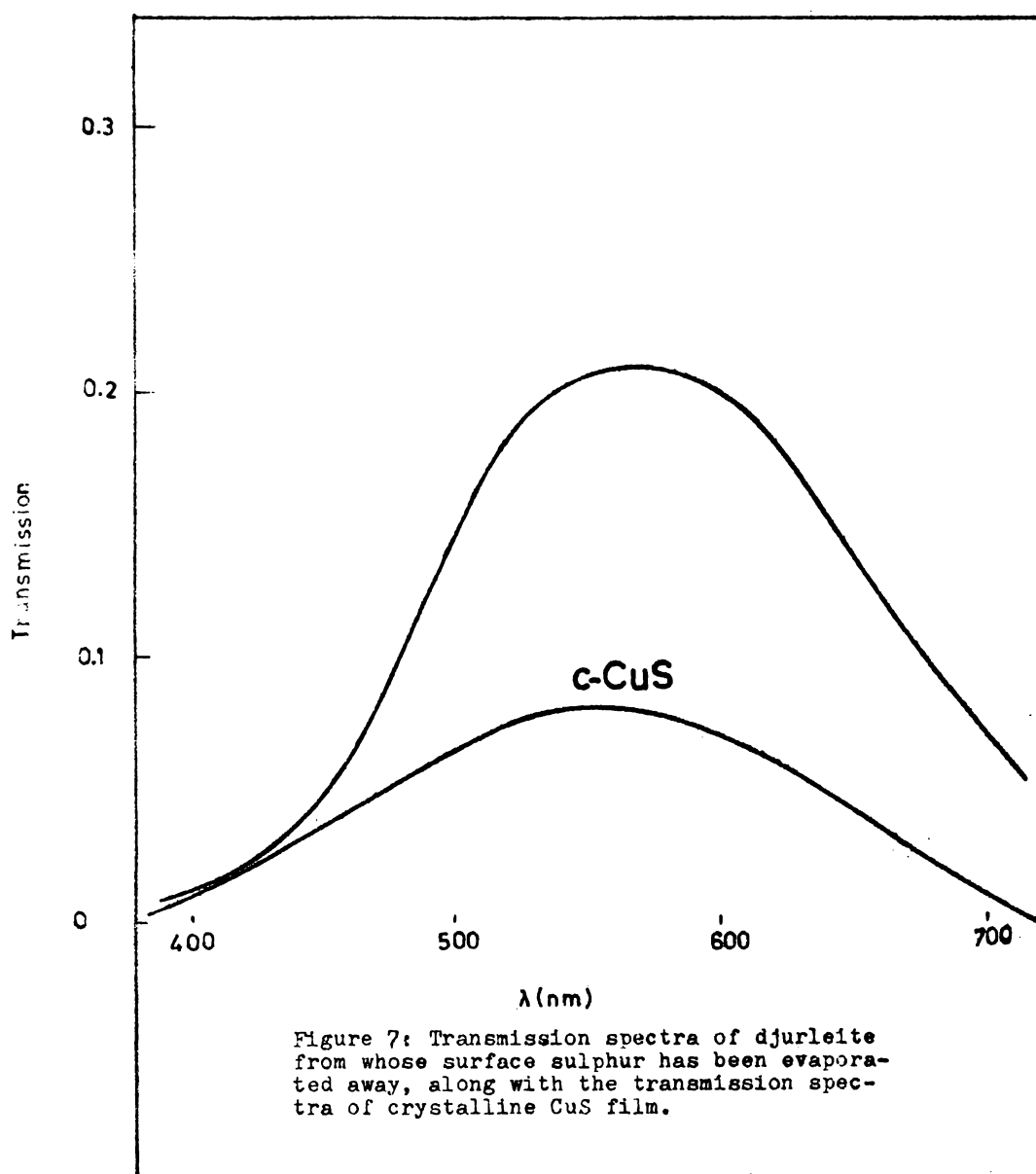
Because the films are heated in air, the atmospheric pressure prevents the evaporation of sulphur and also since the temperature is low, the formation of the much volatile SO_2 is also minimised. Hence the sulphur liberated due to the decomposition of the CuS film segregates out and because of the large undercooling ($\Delta T \sim 150\text{K}$) the sulphur grows in the form of spherulites. In most examples of crystal growth one finds that, after attaining a stable size, a typical primary nucleus grows into a crystallite having a discrete crystallographic orientation.

Generally speaking, this continues to develop as a single crystal until it impinges either upon external boundaries or upon other similar crystallites advancing from neighbouring nuclei. Certain systems are known, in which primary nuclei are seemingly incapable of such development /1/, each one giving rise instead to a more complicated structure of the kind shown in figure 4. This consist of radiating array of crystalline fibers all having the same fiber axis and possessing, therefore, the unusual property of branching in such a way that the crystallographic orientation of a branch departs appreciably from that of its parent fiber.

It is interesting to note that sulphur spherulites grow with the rhombohedral modification of sulphur. This may possibly be an epitaxial growth on the underlying CuS film which too has a closely related hexagonal structure. Since CuS grains grow with their c-axis along the glass surface, rhombohedral sulphur growing on the surface of these crystals may also take such an habit. X-ray data is not sufficient to find the growth axis of the sulphur spherulites in the present case. The presence or absence of reflections from planes of the form 00l would have confirmed the growth axis. But JCPDS data on rhombohedral sulphur /2/ does not list any lines from the planes of the form 00l. This prevented the determination of the growth axis from X-ray diffraction studies.

When these djurleite films are heated to about 370K, sulphur evaporates away from the film giving the characteristic odour of SO_2 . So the mechanism by which sulphur evaporates is not the usual melting and evaporation, but formation of highly volatile SO_2 . It is tentatively assumed that evaporation of sulphur does not bring about any phase transitions in the underlying material. The colour of the film does not change by this evaporation and the assumption is somewhat justified. Such films were used for optical studies. Transmission spectra of a film, from whose surface sulphur has been evaporated away is shown in figure 7. Figure shows the transmission spectra of a crystalline CuS film also. It may be seen that transmission increases due to the change from CuS to djurleite. Refractive index of the films could not be determined as the transmission spectra exhibited no interference fringes. For the calculation of absorption coefficient, refractive index of thin crystals of djurleite given by Mulder /3/ ($n = 2.4$) was used. The plot of $(\alpha h\nu)^{2/3}$ versus $h\nu$ is given in figure 8. This give a direct band gap of 1.94 ± 0.02 eV. From the functional dependence of absorption coefficient on photon energy, it can also be inferred that the direct transition is a forbidden one.

As the films are further heated to 425K, the colour of the film changes to yellow. The X-ray



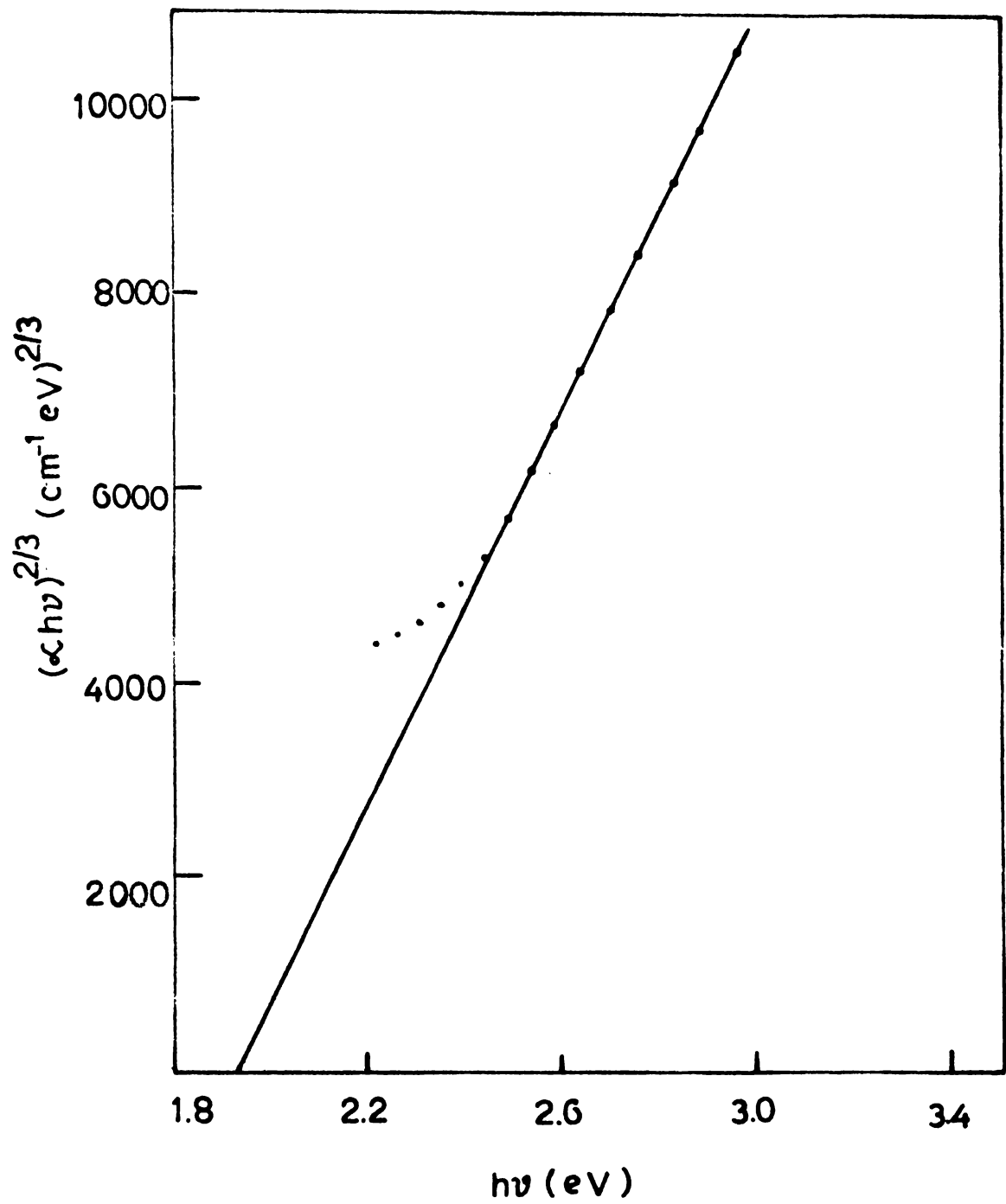


Figure 8: $(\alpha h\nu)^{2/3}$ versus $h\nu$ of d,l-uric acid film. Band gap = 1.94 ± 0.02 eV.

diffraction pattern of such a film is shown in figure 9. This diffraction pattern also shows almost all of the lines which are common to djurleite and chalcocite. But here the identification line of djurleite phase has disappeared indicating that the film is pure chalcocite.

Transmission spectra of a chalcocite film is shown in figure 10. This spectra is similar to that reported in the literature for thin layers of chalcocite. The absorption coefficient was calculated with n value taken from the literature ($n = 2.6$) /3/. The plot of $(\alpha h\nu)^{2/3}$ versus $h\nu$ is shown in figure 11. The value of the direct band gap obtained is 1.84 ± 0.02 eV. The functional dependence of α on $h\nu$ shows that the transition is a forbidden one. This value of the band gap is in agreement with that reported in the literature/4-6/. An indirect gap around 1 eV has been reported in the literature for chalcocite. Because of the thinness of the samples used in the present study ($t = 1000 \text{ \AA}$) the existence of such an indirect transition could not be verified.

The path of the transformation of CuS to Cu_2S may be represented as



There is not much meaning in assigning any particular temperature to these transformations. Because

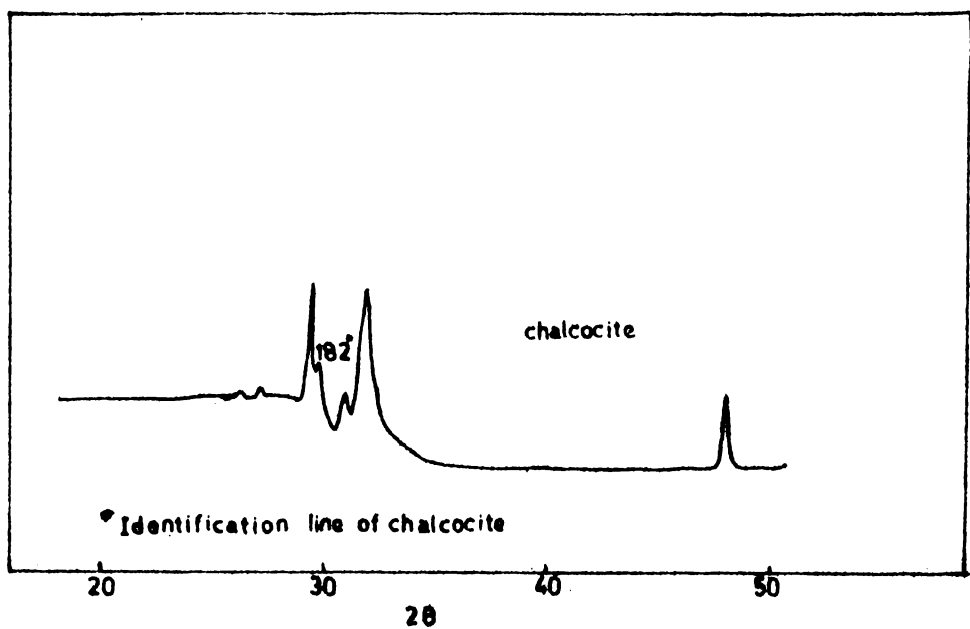


Figure 9: X-ray diffraction pattern of chalcocite film.

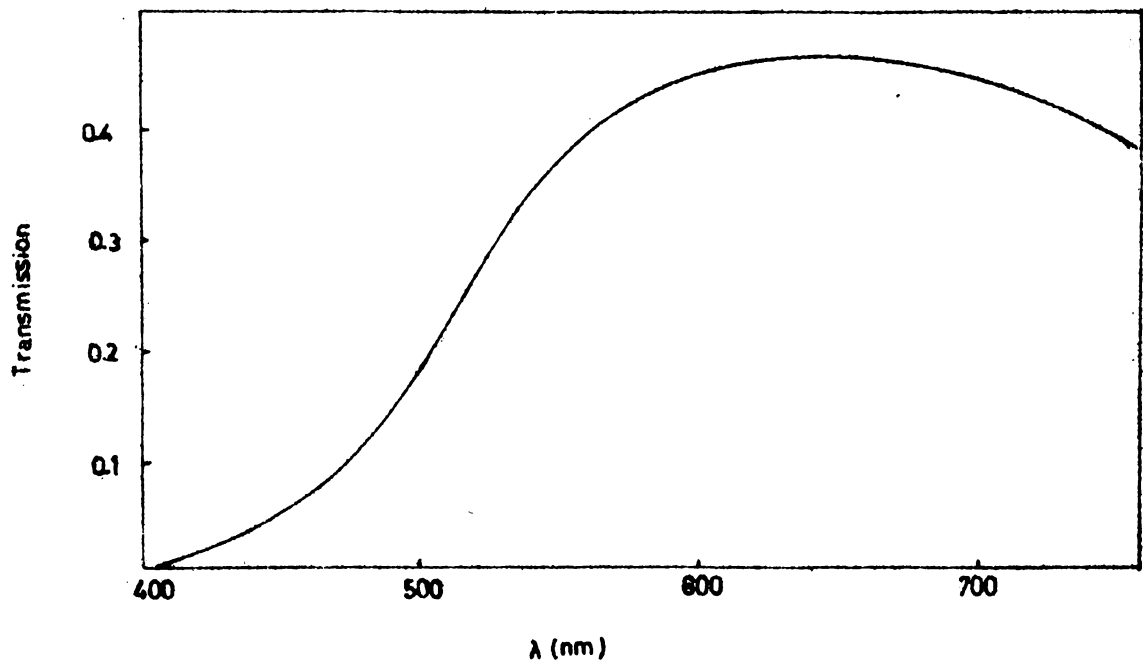


Figure 10: Transmission spectra of a chalcocite film.

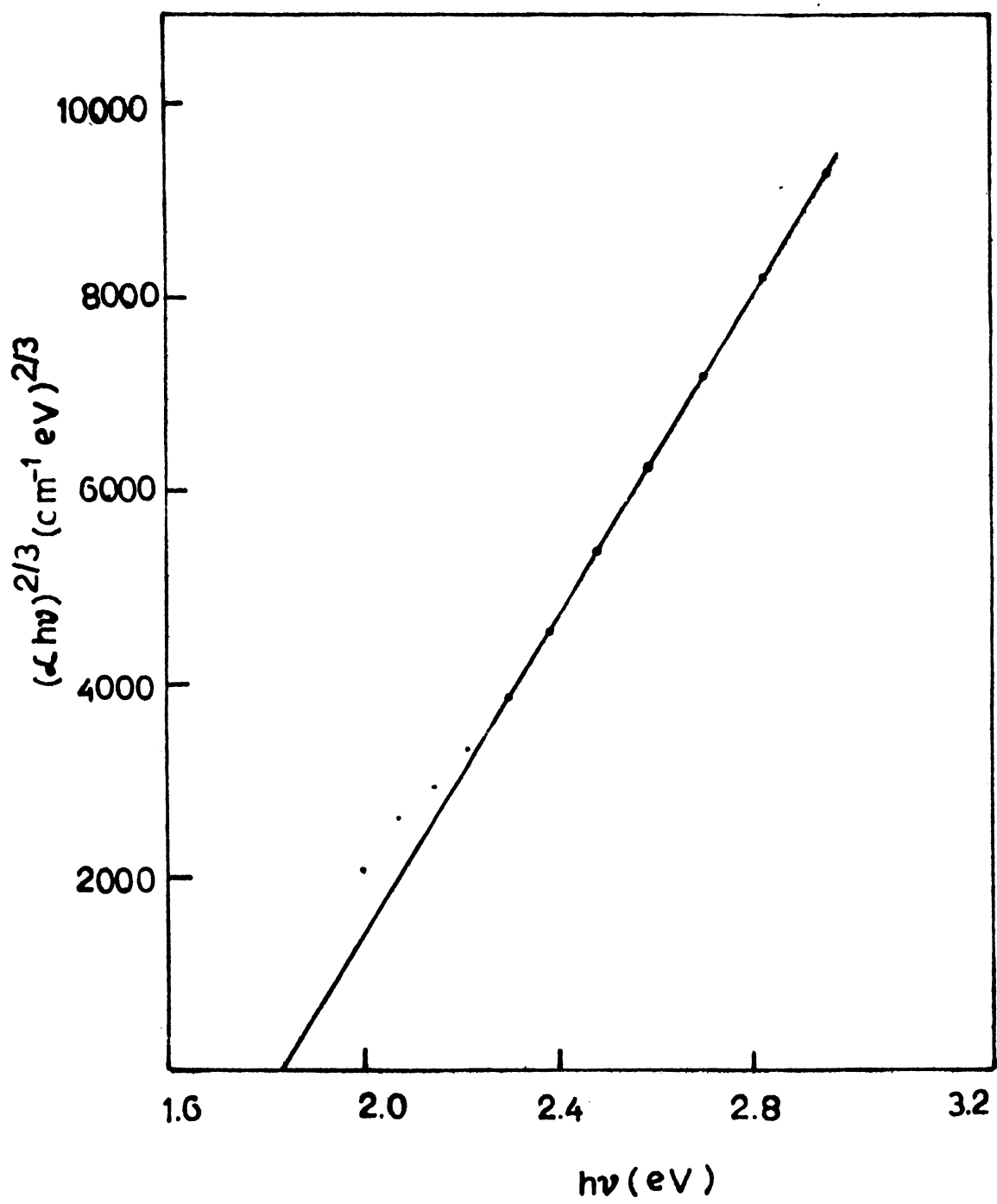


Figure 11: $(\alpha h\nu)^{2/3}$ versus $h\nu$ of chalcocite film. Band gap = 1.84 ± 0.02 eV.

these transformations will proceed at any finite temperature, the higher the temperature, the higher the transformation rate. One inference which may be taken from these chain of phase transformation is that the most stable phase in the Cu-S phase diagram is chalcocite and intermediate phases tend to attain this phase, if given enough freedom.

CONCLUSIONS

Amorphous films of CuS crystallizes when heated to 320K. When the heating is continued at 320K, amorphous and crystalline films prepared at low substrate temperatures get decomposed to djurleite and rhombohedral sulphur. As the evaporation of sulphur is prevented because of the large undercooling ($\Delta T \approx 150K$) spherulites of sulphur are formed. The spherulites grow with the rhombohedral modification of sulphur possibly because of an epitaxial ordering it gets from the underlying CuS film which also has a hexagonal crystal symmetry. When the temperature is raised, sulphur forms volatile SO_2 and gets evaporated. On continued heating of the films, djurleite gets converted to chalcocite.

References:

1. Keith and Padden, J. Appl. Phys. 34 (1963) 2409.
2. JCPDS Card No.13-144.
3. B.J. Mulder Phys, Status Solidi 13(a) (1972) 79; 15 (1973)409; 18 (1973) 633.
4. L. Eisenmann, Ann. Physik 10 (1952) 129.
5. G.P. Sorokin, Yu. M. Papshiev and P.T. Oush, Sov. Phys. Sol. State 7 (1966) 1810.
6. G.B. Abdullaev, Z.A. Aliyarova, E.H.Zamanova and G.A. Asadov, Phys. Status. Sol., 16(b) (1968) 65.

CHAPTER-VIII

OXIDE FILMS OF COPPER PREPARED BY THE OXIDATION
OF COPPER SULPHIDE FILMS

Copper oxide (Cu_2O) is a well known semiconductor that is finding renewed interest in the search for low cost materials for solar cell application /1/. It is a defect semiconductor with p-type conductivity and through the work carried out in the 1920s and 1930s, this became one of the first semiconducting materials to be investigated. Cuprous oxide layers on Cu have been known for many years to be photoconducting and to show photovoltaic effect. The first investigation on photoconductivity of these materials were made by Pfund /2/. More precise photoconductivity study began with the work of Schönwald /3/. He showed that p-type conduction in Cu_2O occurs through the presence of copper ion vacancies. Switching phenomena, similar to that observed in the case of many chalcogenide glasses was observed in Cu_2O crystals by Wang and Weichman /4/. Electrical /5-7/ and optical /8-11/ properties of Cu_2O has been reported in the literature by various authors. But reports on the electrical and optical properties of CuO are rare.

For use in thin film solar cell technology it must be possible to prepare low resistivity films of

Cu_2O with good optical properties in a reproducible manner on a variety of substrates. Preparation methods that are currently being investigated are thermal oxidation /12-14/, electrodeposition /15/ and reactive sputtering /16/. A problem common to oxidation and electrodeposition methods is that the resulting Cu_2O material tends to be of high resistivity, namely $10^2 - 10^4$ ohm cm in the thermal case /14/ and $10^4 - 10^6$ ohm cm in the electrodeposited case /15/. Best films are formed by reactive sputtering of copper in an oxygen-argon mixture which gives films with controlled resistivity over the range 25 to 10^4 ohm cm /16/.

In this chapter the preparation and optical properties of Cu_2O and CuO films prepared by the oxidation of copper sulphide films in air are discussed.

8.1 EXPERIMENTAL

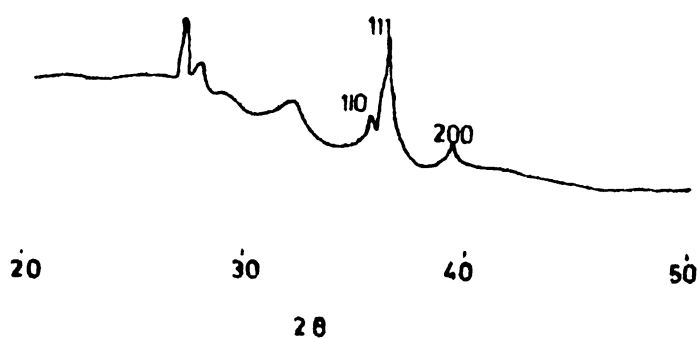
Oxidation of the film was carried out by heating the films to a high temperature in air as in the case of tin disulphide. The heating set-up is as described in Chapter III. Both amorphous and crystalline films of CuS were used in these experiments. Since CuS films underwent a series of phase transformations before it reached the oxidized state, the activation energy for oxidation could not be determined by the method used for tin disulphide. The criterion used for the oxidation

of the final phase of Cu-S (chalcocite, colour yellow) to Cu_2O was the sudden change in the colour of the film to golden yellow. And the criterion used for the further oxidation of Cu_2O into CuO was the change of golden yellow colour to a foggy appearance. These oxidized films was not as perfect as that of tin dioxide described in Chapter V and contained pin holes and non-uniformities. This was especially severe in the case of thicker films.

Optical measurements of these films were made by using a Hitachi 200-20 UV-Vis spectrophotometer. Films used in the optical study had a thickness around 100 nm. X-ray diffraction measurements were carried out in a Philips PW 1140/90 X-ray diffractometer. About 300 nm thick films were used in X-ray diffraction study.

8.2 RESULTS AND DISCUSSIONS

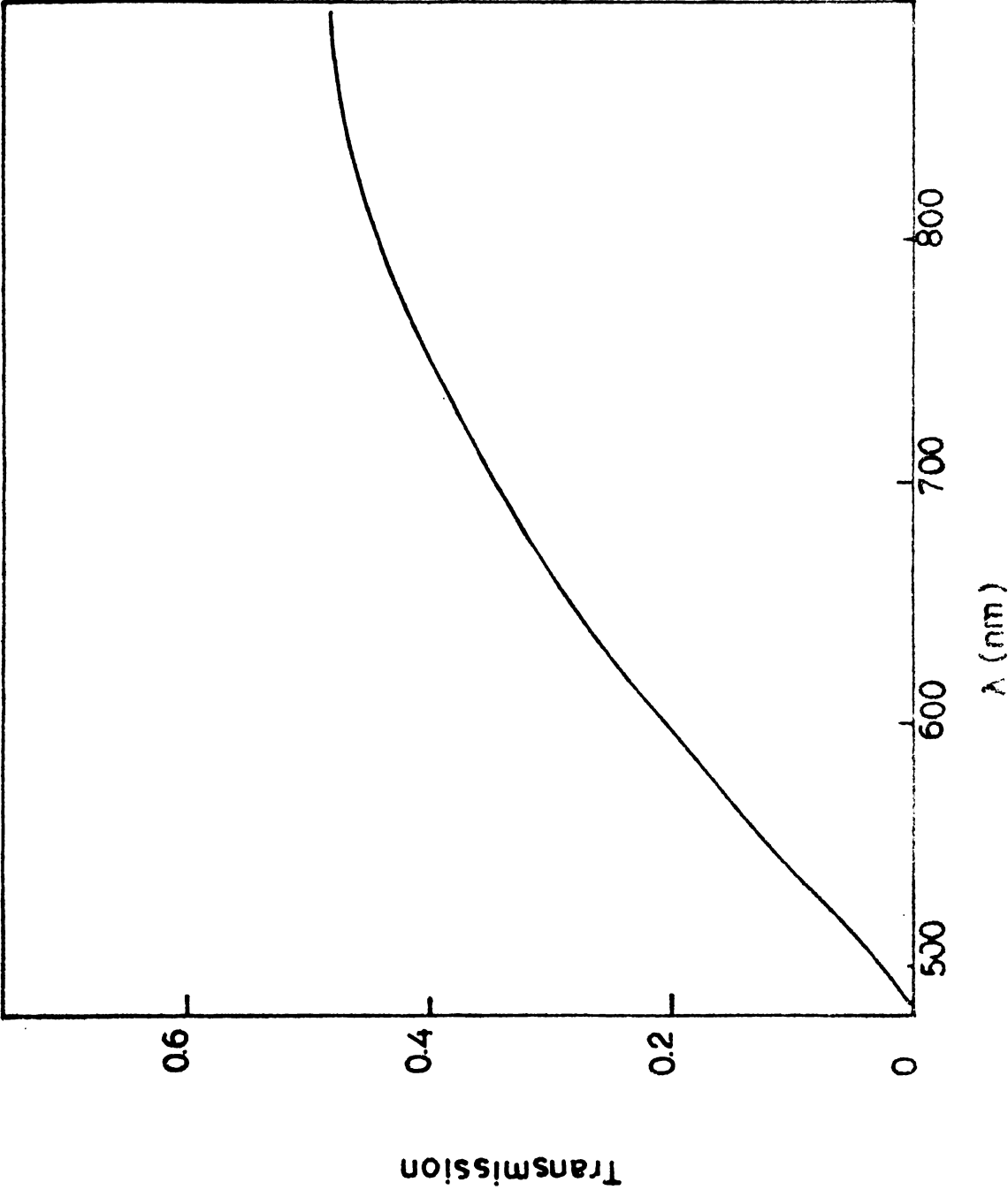
When CuS films are heated beyond 500K, after the series of phase transformations described in Chapter VII, the films get oxidized. This oxidation of the film is characterized by a sudden change in the colour of the film from yellow of **chalcocite** to the golden yellow of Cu_2O . The X-ray diffraction pattern of a film so oxidized, is given in figure 1. The table given along with the figure lists the d-spacings given in JCPDS card and our results. It can be seen that after a 'd' value of 3.173\AA , every lines in the JCPDS card and our results are



JCPDS		Present results	
$d(\text{\AA})$	I/I_0	$d(\text{\AA})$	I/I_0
3.020	9	3.175	8
2.265	100	2.256	50
2.154	57	2.296	7
1.745	11		

JCPDS card No.5-667

Figure1.X-ray diffraction pattern of Cu_2O



the same. The unidentified lines are not listed in the JCPDS card. It is not clear at present whether these lines are due to the presence of any other unknown phase or it was simply left unlisted in the JCPDS card because of the low inherent accuracy of these lines (low angle diffractions). The uniform colour of the film and the failure to detect two or more phases under crossed polaroids in an optical microscope and also the fact that the unlisted lines are not due to CuO almost rule out the first possibility.

From X-ray diffraction study no preferred orientation of the grains in the films could be found.

The samples obtained show p-type conductivity and were of high electrical resistivity. This is in general agreement with earlier reported data in the literature.

Transmission spectra of a Cu_2O film of thickness $\approx 100\text{nm}$ is shown in figure 2. It may be seen that this film shows a high absorption ($\alpha \sim 10^4 \text{ cm}^{-1}$) before the onset of band to band transitions. A visual inspection of the film shows that the film is not clear i.e. they scattered light too much. The absence of interference fringes also shows that films are not optically perfect. It may also be noted that transmission decreases continuously from 900 nm. This may be due to the existence of large number of levels in the forbidden gap just below

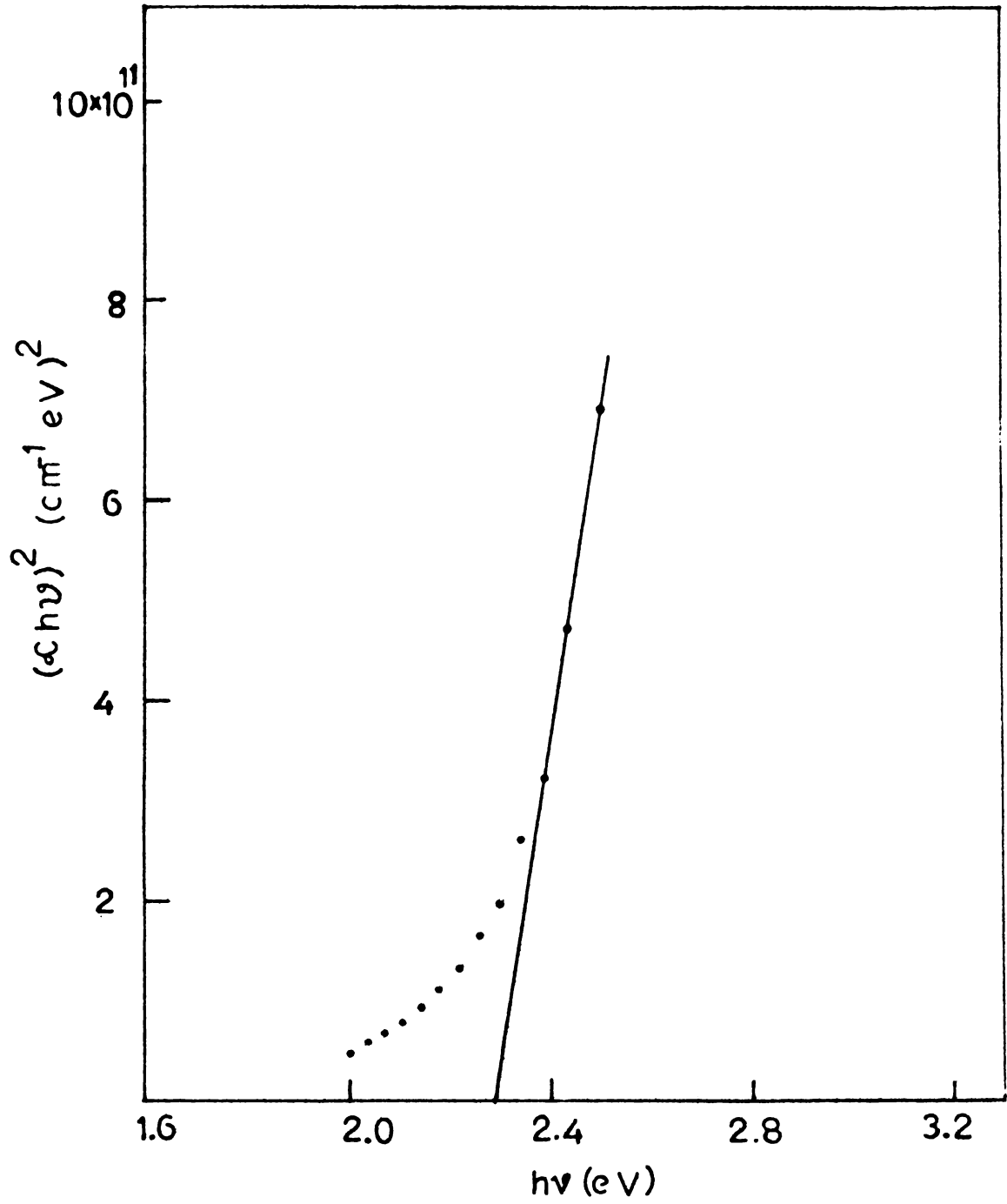
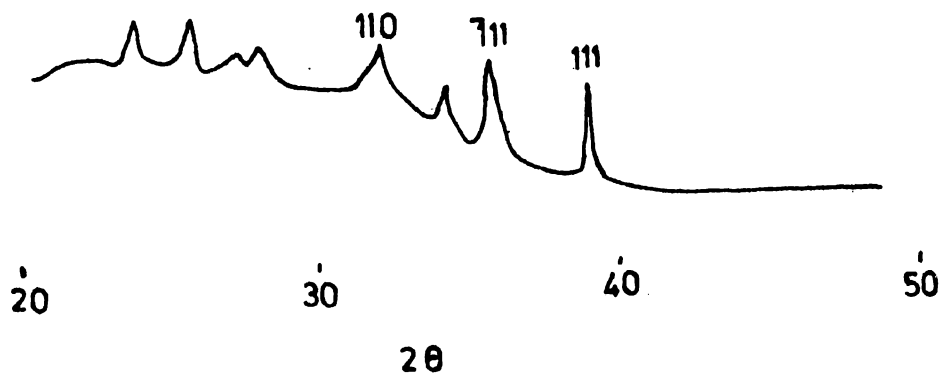


Figure 3. Plot of $(\alpha h\nu)^2$ versus $h\nu$ for a Cu_2O film

the conduction band or just above the valence band which merges to these bands. Weichman and Reyes /17/ report that copper inclusions are responsible for absorption peaks in the 1.1 eV to 2.0 eV range. In the present case these absorption peaks may have merged into a single one due to the large number of defects present causing high absorption before the onset of band to band transitions.

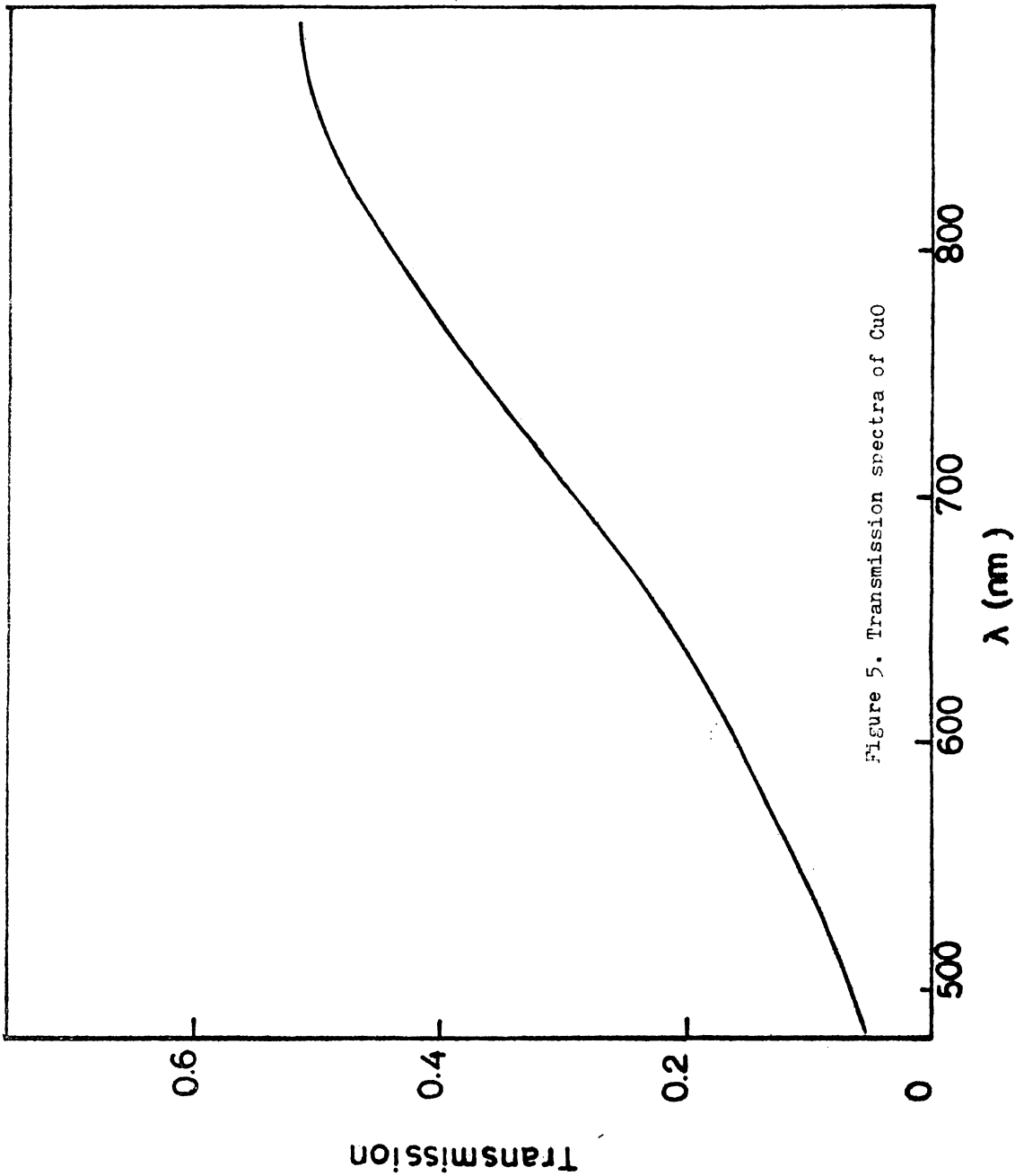
Because of the large absorption before the absorption edge, interference fringes were absent and consequently refractive index of the film could not be determined. For the calculation of absorption coefficient, refractive index data given in reference 16 was used. The plot of $(\alpha h\nu)^2$ versus $h\nu$ is shown in figure 3. This gives a band gap of 2.29 ± 0.02 eV and the transition leading to this is a direct allowed one. The reported band gap of Cu_2O polycrystalline specimens from photoconductivity data lies between 1.94 eV and 2.14 eV. This 'band gap' corresponds to transitions from valence band to exciton levels /18/ just below the conduction band. Since the samples used in the present study show no structure in the transmission curve due to exciton absorption and because of the large absorption coefficients ($\alpha \sim 10^5 \text{ cm}^{-1}$) characteristic of direct transitions, the band gap obtained in the present case may be taken as due to transitions taking place from valence band to conduction band and the band gap obtained as the true gap.



JCPDS		Present results	
d(A°)	I/I ₀	d(A°)	I/I ₀
2.751	12	2.803	9
		2.623	12
2.530	49		
2.523	100	2.520	22
2.323	96	2.320	18
2.312	30		
1.959	3		
1.866	25		

JCPDS card No.5-661

Figure4.X-ray diffraction pattern of CuO.



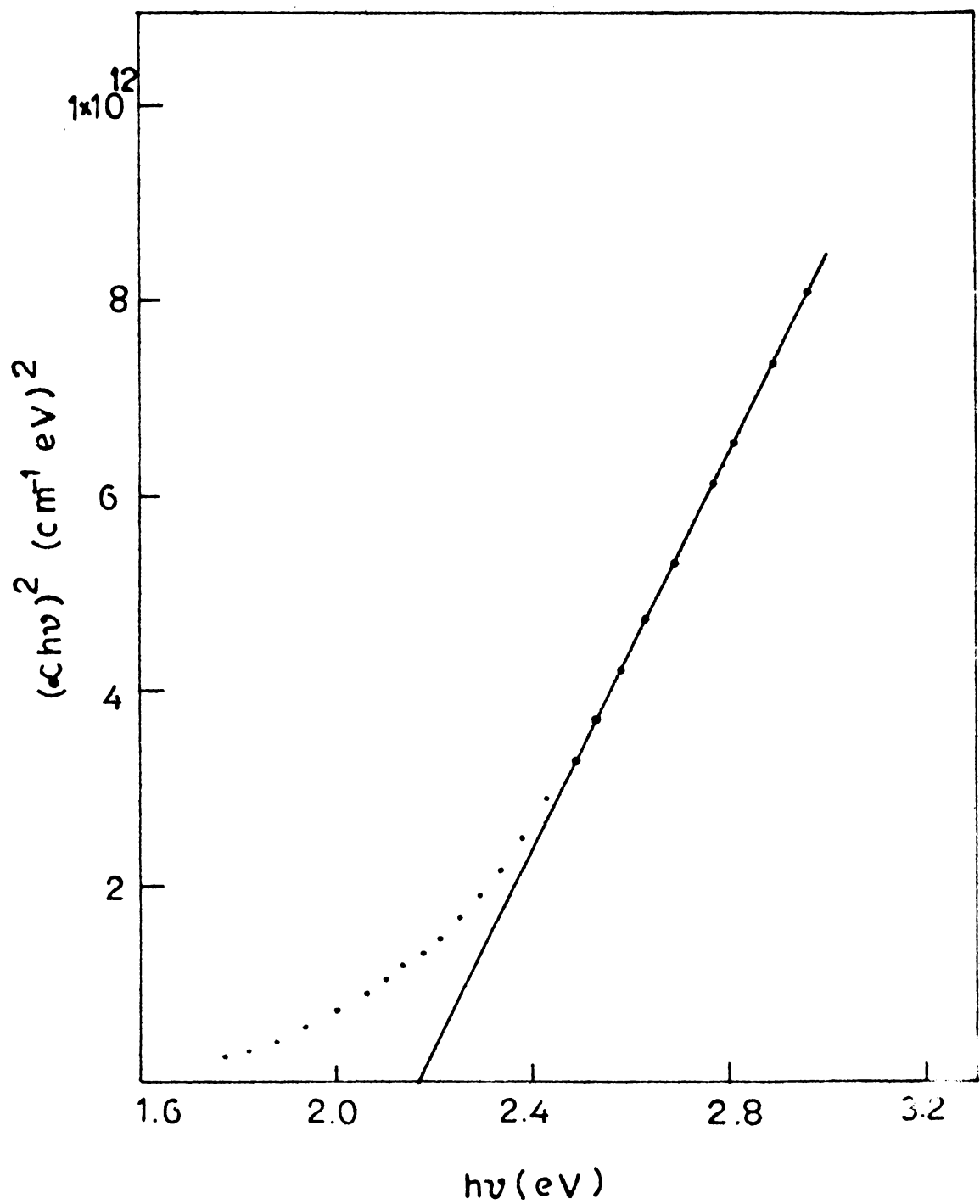


Figure 6. Plot of $(\alpha h\nu)^2$ versus $h\nu$

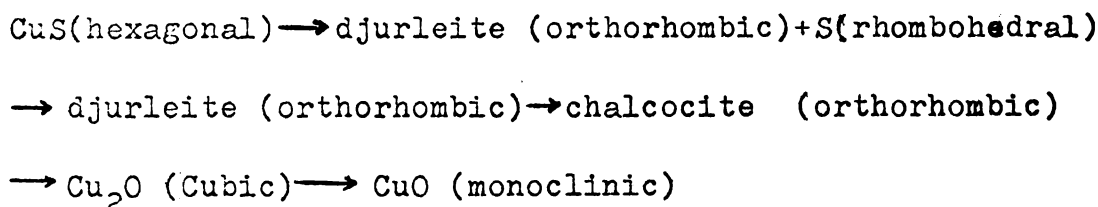
This is in agreement with the energy level diagram given in reference 19 for Cu_2O , where a band gap of 2.3 eV is taken.

When the Cu_2O films are maintained at 500K for some length of time, the characteristic golden yellow of Cu_2O disappears and a film with a transparent foggy appearance is obtained. X-ray diffraction pattern of such a film is shown in figure 4. The diffraction data shows lines due to monoclinic CuO together with three other lines which are unidentified. It is not clear at present whether this is due to the presence of any other phase.

The transmission spectra of a CuO film of $\approx 100\text{nm}$ thickness is shown in figure 5. It may be seen that as in the case of Cu_2O films, these films also show high absorption before the absorption edge. Because of the absence of interference fringes, refractive index in this case also could not be obtained. For the calculation of absorption coefficient, refractive index data given in reference 16 was used. The plot of $(\alpha h\nu)^2$ versus $h\nu$ for a typical CuO film is shown in figure 6. This gives a direct band gap value of 2.17 ± 0.02 eV and the transition leading to this is an allowed one. Band gap value of CuO films has apparently not been reported in the literature and hence a comparison is not possible. The band gap value obtained in the present case for CuO

film is less than that obtained for Cu_2O films. A film of a material with a band gap of 2.17 eV should have appeared yellow in transmission as it cuts off wavelengths lesser than yellow. But CuO films obtained in the present case, it seems, does not do this; as mentioned earlier they haveⁿ foggy transparent appearance. The apparent transparency suggests a band gap more than 3 eV. The apparent 'fundamental absorption' show by these films may be due to a large number of structural and stoichiometric defects which causes band tailing, i.e. impurity bands merging with conduction or valence bands. Evidently more work is needed to clarify these points.

So it can be seen that the effect of heating CuS films in air upto a temperature in excess of 500K is a series of chemical changes taking place in the structure and composition of the film:



It may have been clear from now that films of Cu_2O and CuO prepared by oxidation in air of the corresponding sulphide films are not of good quality; i.e. they showed too much optical absorption. But when tin dioxide was prepared by the oxidation in air of tin disulphide, highly transparent and good optical quality

films were obtained (see chapter V). Let us compare the oxidation of tin disulphide with that of copper sulphide in some detail. An important factor is the grain size of the films. It was found in the case of tin disulphide that the as prepared films were amorphous in nature and when the films were heated they crystallized at 410K. It was also found that if the oxidation of tin disulphide films were carried out at low temperatures, the conductivity of the films decreased considerably and optical transmission became poor and was explained as due to the incomplete oxidation of the large grains of tin disulphide formed due to prolonged heating at low temperatures.

In the case of CuS and Cu_2S films used in this study, the grain size was greater than 1 micron (see figure 3 of Chapter VI). In the case of amorphous films of CuS also when they underwent all the chemical transformations and finally reached Cu_2S , their grain size was at least one micron. It is highly probable that these large grains will not get completely oxidized when heated in air. When these large grains are oxidized, the surface of the grains will get oxidized first. This oxide layer may inhibit further diffusion of oxygen in and sulphur and sulphur dioxide out resulting in incomplete oxidation. The incomplete oxidation of grains can certainly make the films too defective causing poor

optical and electrical properties.

Another important point is that tin being a low melting point element (in that case all the respective metal elements of all known transparent conducting oxides) will get good mobility on the high temperature substrate (relative to the melting point of the element). This high mobility may be essential because a structural rearrangement of lattice is to take place. But in the case of copper, its melting point is 1356K and its mobility will be very low on the relatively cold substrate (temperature \approx 500K).

It is quite clear that either of these factors or both contribute to the quality of the films. More work is needed to determine the following:

- 1) Whether during the conversion from metal sulphide to metal oxide a complete decomposition of the sulphide take place followed by oxidation. In this case low melting point metals have a definite advantage as they will get good mobility on the substrate surface.
- 2) Whether only a chemical displacement of atoms take place with a **minor structural** rearrangement. In this case small grained films will be in an advantageous position, because oxygen will be able to diffuse

into the interior of the crystallite
thus producing complete oxidation of the
crystallite.

Data from the present work regarding the oxidation of
the films is given in Table I

Table I

Material oxidized	Melting point of the respective metallic compo- nent	Grain size of the initial film	Film quality
tin disulphide	505K	very small	good
copper sulphide	1356K	large (~ micron)	poor

Further work is to be done on other compounds
with low melting point metallic components to further
clarify these points.

CONCLUSION

Films of CuS when heated in air at 500K, after
a series of intermediate chemical transitions, get oxidi-
sed to Cu_2O . These Cu_2O films have a golden yellow colour
and show large absorption before the fundamental absorption

edge. The band gap obtained (2.29 ± 0.02 eV) from optical studies agrees with that reported in the literature for Cu_2O layers. When these Cu_2O films are further heated they get converted to CuO films. These films also show large optical absorption before the absorption edge. The band gap obtained for CuO films is 2.17 ± 0.02 eV. The quality of the films obtained by this method are rather poor.

References:

1. F.A. Shirland and P. Rai-Choudury, Rep. Progress in Phys. 41 (1978) 1839.
2. A.H. Pfund, Phys. Rev. 7 (1916) 289.
3. B. Schonwald, Ann. Phys. Lpz., 15 (1932) 395.
4. C.J. Wang and F.L. Weichman, Can. J. Phys. 60 (1982) 1648.
5. J.S. Anderson and N.N. Greenwood, Proc. Roy. Soc. (London) A215 (1952) 353.
6. O. Bottger, Ann. Phys. 10 (1952) 232.
7. W. Juse and B.W. Kurtchatow, Physik. Z.Sowjetunion 2 (1932) 453.
8. T.F. Gross and N.A. Karryev, Doklady Akad. Nauk. U.S.S.R. 84 (1952) 471.
9. S. Nikitine, L. Couture, M. Seiskind, and G. Perny, Comp. rend 238 (1954) 1786.
10. J.H. Apfel and L.N. Hadley, Phys. Rev. 73 (1948) 749.
11. M. Hayashi and K. Katsuki, J. Phys. Soc, Japan 7 (1952) 599.
12. L.C. Olsen and R.C. Bohara, Proc. 11th IEEE Photo. Spec. Conf., 1976, IEEE, New York, 1976 p.875.
13. D. Trivich, E.Y. Wang, R.J. Komp and F. Ho, Proc. 12th IEEE Photo. Spec, Conf., 1978, IEEE, New York 1978 p.174.

14. G. Noguet, M. Tapiero, C. Schwab, J.P. Zielinger, D. Trivich, in Proc. 1st Photovoltaic Solar Energy Conference of the Commission of European Communities, D. Reidel, Dordrecht, 1977, p 1180.
15. N.A. Economiu, R.S. Toth, R.J. Koump and D. Trivich, in Proc. 1st Photovoltaic Solar Energy Conference of the Commission of European Communities, D. Reidel, Dordrecht, 1977 p 1180.
16. V.F. Drobny and D.L. Pulfrey, Thin Solid Films 61 (1979) 89.
17. F.L. Weichman and J.M. Reyes, Can. J. Phys. 58 (1980) 325.
18. R.J. Elliot and A.F. Gibson "An Introduction to Solid State Physics and its Applications" McMillian, London, 1978 p 213.
19. G.F.J. Garlick in Encyclopedia of Physics 19(1956) 379 Springer-Verlag, Berlin 1956.

CHAPTER-IX

REACTIVELY EVAPORATED FILMS OF INDIUM SULPHIDE

From a II-VI compound, such as ZnS, a variety of semiconductors may be built up by replacing the divalent metal by other metals or combinations of them /1/. If we replace the divalent metal by one of the III-B-group elements, in most cases it leads to a defect structure of the formula M_2X_3 in which the non-metallic constituent X forms a cubic or hexagonal close packed structure, whereas part of the cation sites, normally occupied in the zincblende, wurtzite or similar lattices in which II-VI compounds crystallizes remain empty. These compounds should be similar in some respects to other zincblende and wurtzite type materials. But the defect structure gives rise to certain unusual properties such as a very strong scattering probability arising from the defect concentration /1/. Most of the III-VI compounds exist in several modifications. Some of these show an ordered arrangement of the cation vacancies possibly resulting in different carrier transport properties in the ordered and disordered form. The difference in electronegativity /2/ of 1.2 for the sulphides, 0.9 for the selenides and 0.8 for the tellurides of indium and gallium indicates a considerable amount of ionic contribution to the binding. The expected influence of

all these properties was demonstrated in the case of In_2Te_3 /3/ and In_2S_3 /4/, where a low value of electron mobility with an exponential temperature dependence was found.

It was thought worthwhile to study the properties of the sulphides of indium in thin film form, as indium is similar to tin in many respects (difference in atomic weight equals one, low melting points, high evaporation temperatures /5/ and also the oxides of tin and indium are well known transparent conductors). Moreover In_2S_3 is known to be photoconducting.

Three well defined modifications of In_2S_3 have been reported in the literature. The cubic α -form /7/ is stable above 693K and crystallizes in a defect spinel structure ($a = 10.77\text{\AA}$) in which one third of the tetrahedral metal sites remain empty. These metal vacancies are randomly distributed. But below 693K, these vacancies order into a 4_1 screw and a tetragonal super cell ($a = 7.61\text{\AA}$, $c = 32.32\text{\AA}$) consisting of three spinel blocks /8/. This ordered modification is termed β - In_2S_3 . The 693K transition is often suppressed in In rich material and the α -modification persists down to room temperature. A third modification (γ - In_2S_3) with trigonal symmetry has been reported above 1047K /9-11/. This modification can be stabilized to room temperature by the addition of 5 to 10% As or Sb /10/.

The first optical measurements of In_2S_3 was reported by Kauer and Rabenau /12/. Investigations by Bube and McCaroll /6/ and by Gilles et al /13/ were mainly concerned with photoconduction in indium sulphide. Garlick et al /14/ reported on the IR emission and luminescence properties. Repwald and Harbeke /4/ reported on electrical and optical properties. Bube and McCaroll /6/ also reported that In_2S_3 can be made to have high dark conductivity by incorporation of halogen donors, as from CdCl_2 or NH_4Cl or by heating the pure material in nitrogen to temperature above 1000K. They also showed that elements of groups I, II, and IV behaves as donor impurities.

9.1 EXPERIMENTAL

To prepare the indium sulphide films, indium was reactively evaporated in a sulphur atmosphere as described in Chapter III. A sulphur partial pressure of 10^{-4} Torr was maintained in the chamber during evaporation. The deposition rate of the sulphide films were around $200\text{--}300\text{\AA}/\text{min}$. Higher deposition rates decreased the optical transmission of the films considerably. This is possibly due to the incorporation of unreacted indium in the growing film. Substrate temperature was measured with a chromel/alumel thermocouple and was varied between room temperature and 575K. The films obtained have a

golden yellow colour and this colour is almost independent of the substrate temperature used.

Films thus obtained were characterized with X-ray diffraction, optical microscopy, electrical and optical studies.

9.2 STRUCTURAL STUDIES

X-ray diffraction pattern of the films prepared at two substrate temperatures are shown in figure 1. It may be seen that except for a slight change in the d-values, which is due to the different amount of strain present in the films, there is no qualitative difference between the patterns. The diffraction pattern obtained is identical with that given for β - In_2S_3 in JCPDS cards. Since every line in the JCPDS card with moderate intensity could be identified ($(I/I_0) > 5$), it must be concluded that the grains in the film possess no particular orientation. It may here be noted that In_2S_3 is formed in this process rather than the sulphur rich phase InS . In all the other phase systems investigated in the present study (Sn-S , Cu-S) the most sulphur rich phases are formed (SnS_2 , CuS).

An optical micrograph of a film prepared at 500K is shown in figure 2. It may be seen that the grains are large and have dimensions of the order of microns. Films prepared below a substrate temperature

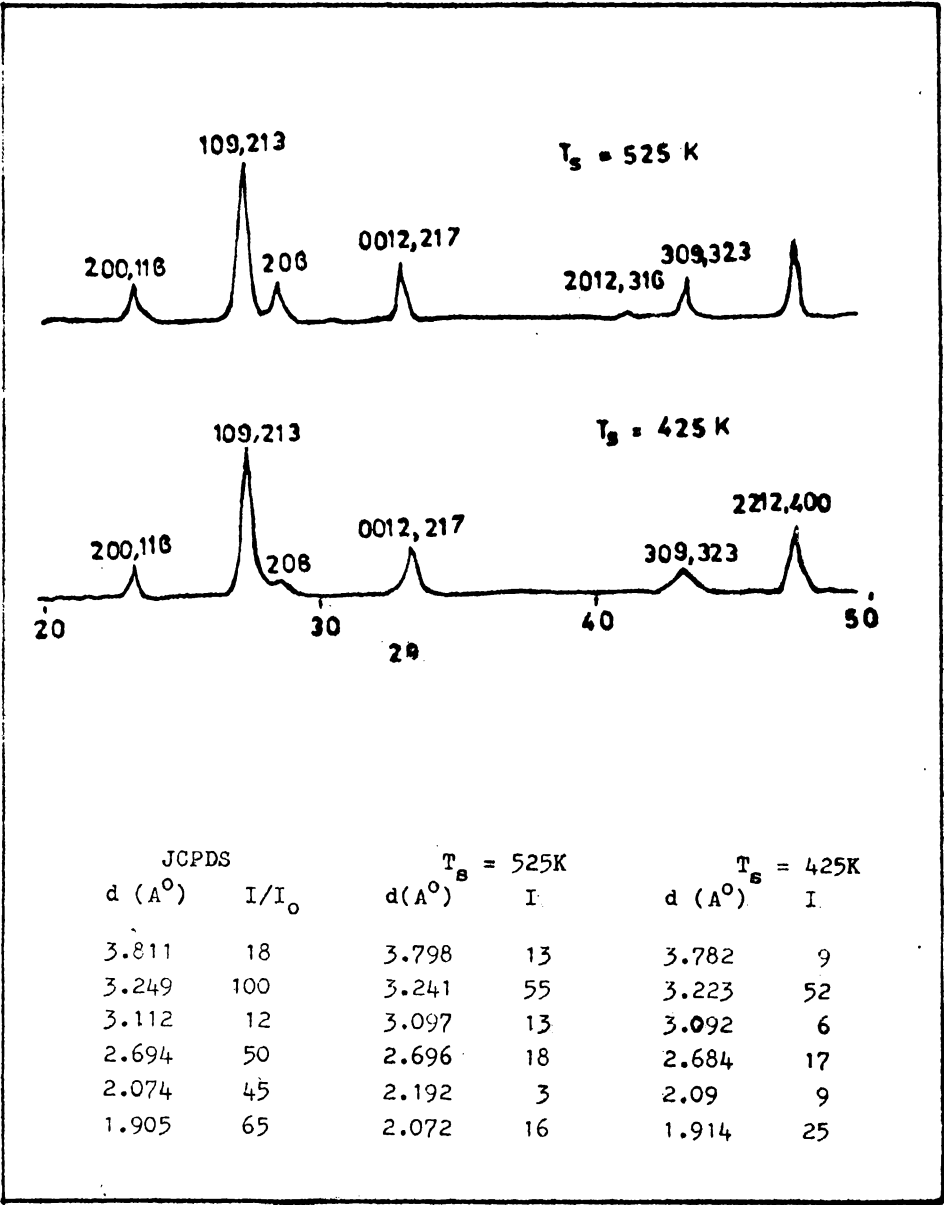
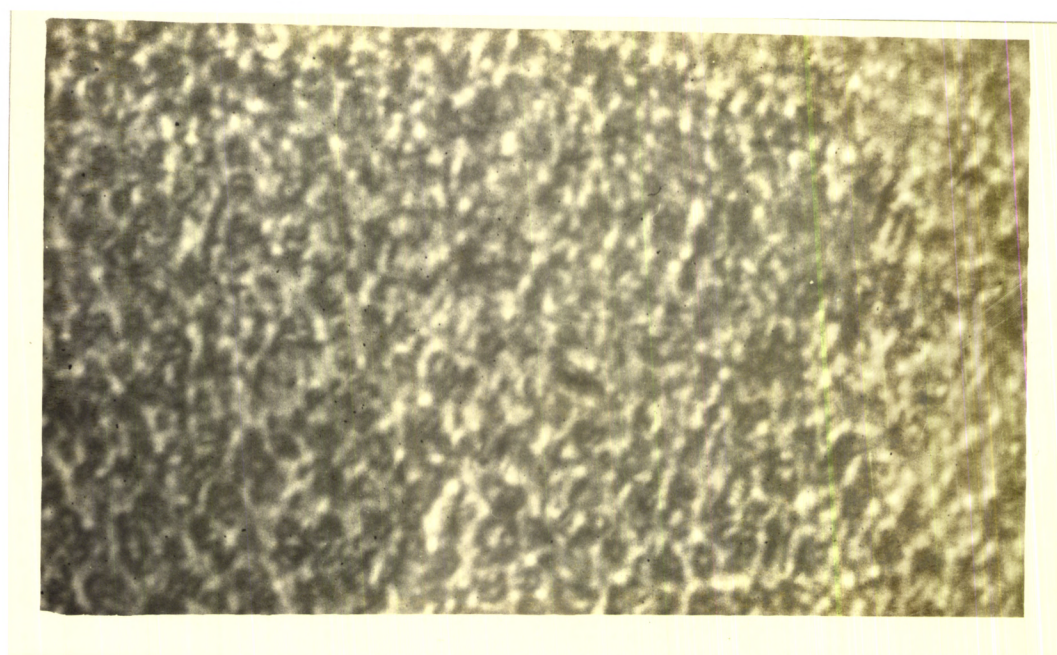


Figure 1: X-ray diffraction pattern of the indium sulphide films at two substrate temperatures.



X 2000

Figure 2. Optical micrograph of a β -In₂S₃ film ($T_s = 500K$)

of 450K are smooth, i.e., they showed no surface features when viewed through an optical microscope at X 1000 magnification. This can be qualitatively explained in terms of the concept of critical optimization of Vincett /15/. He has concluded from many experimental results that when the substrate temperature approaches about 0.33 of the boiling point of the material, the film qualities (surface smoothness, optical transmission, carrier mobility etc.) improve considerably. According to Vincett, when the substrate temperature is low, disordered as well as crystalline regions condense on the substrate surface. When the substrate temperature is increased to approximately 1/3 of the boiling point of the substance, preferential reevaporation of disordered regions in the growing film take place, resulting in a film of good quality. Why it is the boiling point rather than the melting point may be explained as follows. It may be recalled that, by definition, boiling point of a substance is the temperature at which the vapour pressure of a substance equals atmospheric pressure. Hence boiling point is a measure of the vapour pressure of the substance and gives a qualitative idea of the vapour pressure to be expected at any temperature; higher is the vapour pressure, lower is the boiling point. But melting point is not a true measure of the vapour pressure, because many low melting point substances

(e.g. tin and indium) have a very low vapour pressure after melting.

But when the substrate temperature is increased to more than $1/3$ of the boiling point of the substance evaporation of crystalline regions of the growing film also take place, resulting in films of poor quality.

The melting point of In_2S_3 is 1323K and one third of this value is 441K and hence the sudden smoothness of the film prepared at these substrate temperatures. Results of optical measurements given below also supports this view.

9.3 OPTICAL MEASUREMENTS

Transmission spectra of $\beta\text{-In}_2\text{S}_3$ films prepared at various substrate temperatures are shown in figure 3. Film thickness is approximately 600 nm. It is well known that the 'amplitude' of the interference fringes is a measure of film quality; the larger the amplitude, the better the film. This is because only if the film surface is highly reflecting and there is not much internal scattering/absorption, the films will show large amplitude interference fringes. If this is used as a criterion for film quality, it may be seen that films prepared with a substrate temperature around $425 \pm 50\text{K}$ are the best films. When the substrate temperature is lowered the amplitude of the fringes become smaller and

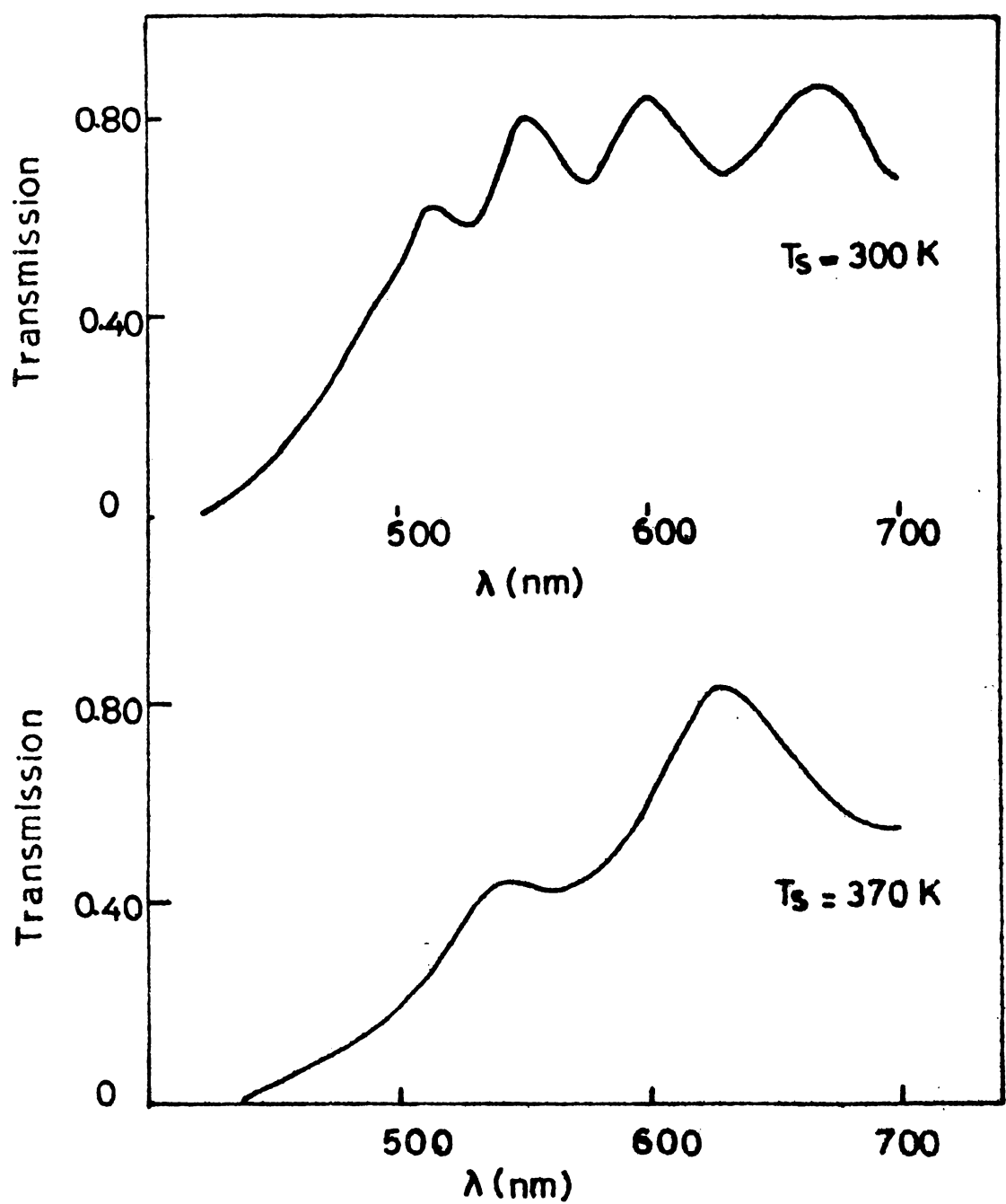


Figure 3: Transmission spectra of $\beta\text{-In}_2\text{S}_3$ films prepared at various substrate temperatures. Film thickness is $\approx 600\text{nm}$.

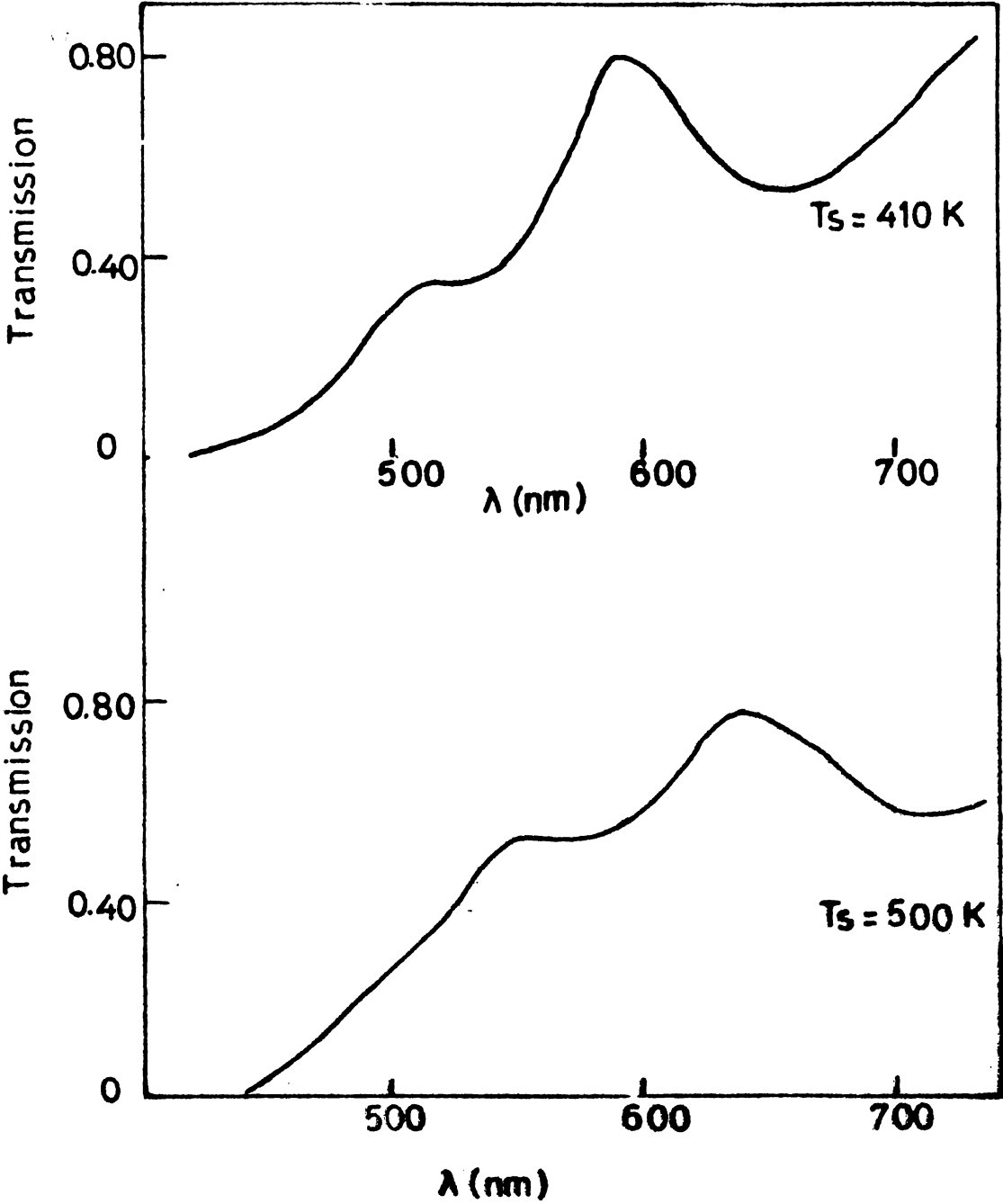


Figure 3: Transmission spectra of In_2S_3 film prepared at various substrate temperatures. Film thickness is $\approx 600\text{nm}$.

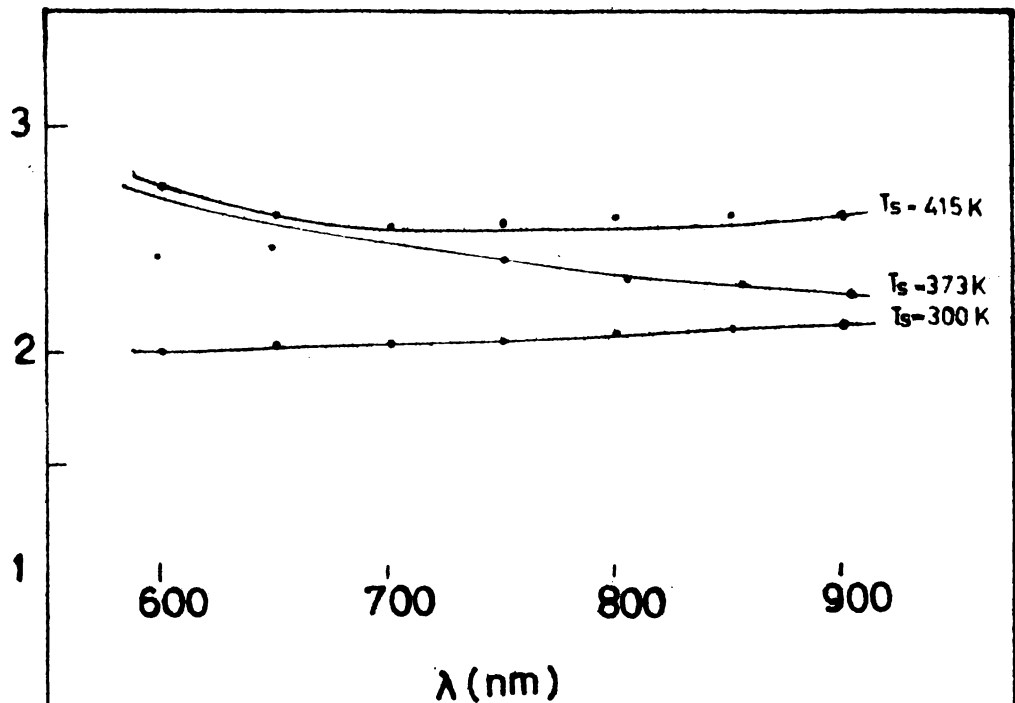


Figure 4(a): Refractive index as a function of wavelength for films prepared at various substrate temperatures.

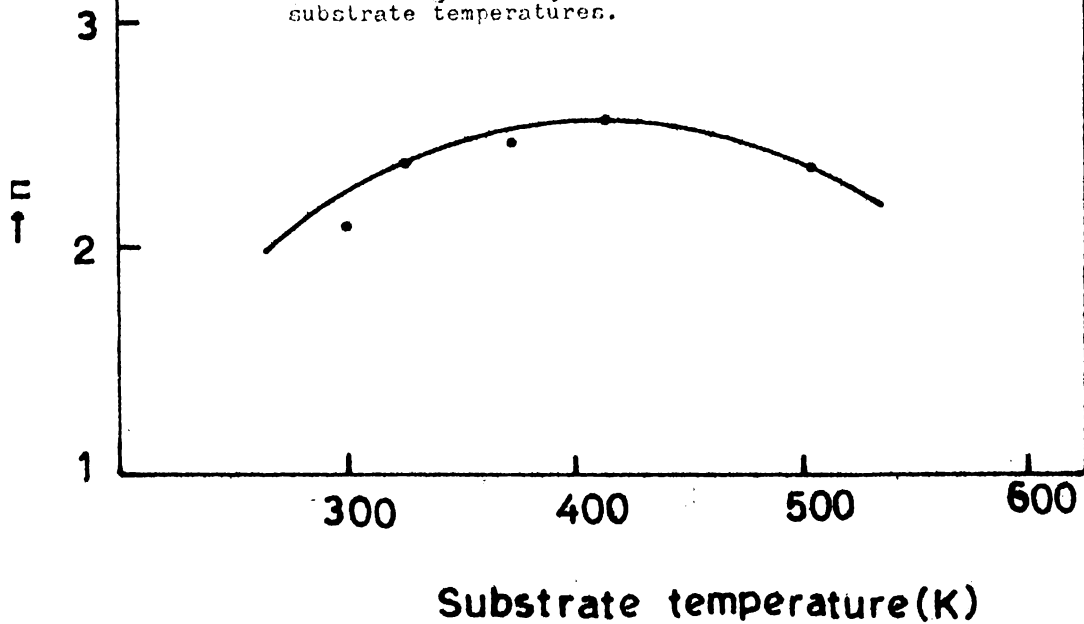


Figure 4(b): Refractive index of the films at a wavelength of 750nm as a function of substrate temperature.

at room temperature, which is the lowest substrate temperature used, it becomes the smallest. When the substrate temperature is raised to 500K, transmission decreases. This is certainly due to absorption by sulphur vacancies in the film. Because at this substrate temperature reevaporation of sulphur from the growing film will be considerable. Moreover the film surface is 'grainy' and will scatter light (see figure 7 also).

From transmission measurements it may be seen that the film quality goes through a maximum at a substrate temperature of $425 \pm 50\text{K}$. This also supports the concept of critical optimization discussed in the section on structural studies.

Figure 4a shows the refractive index as a function of wavelength for films prepared at various substrate temperatures. It may be seen that at a substrate temperature of 410K, the film refractive index is 2.56, which is the value reported for $\beta\text{-In}_2\text{S}_3$ single crystals /14/. Figure 4b shows the refractive index of the films at a wavelength of 750 nm as a function of substrate temperature. It may be seen that the refractive index goes through a maximum for substrate temperature predicted by the concept of critical optimization /15/.

Figure 5 shows $(\alpha h\nu)^{2/3}$ as a function of $h\nu$ for a film prepared at 410K. This gives an energy gap of $2.01 \pm 0.01 \text{ eV}$, which is in excellent agreement with the

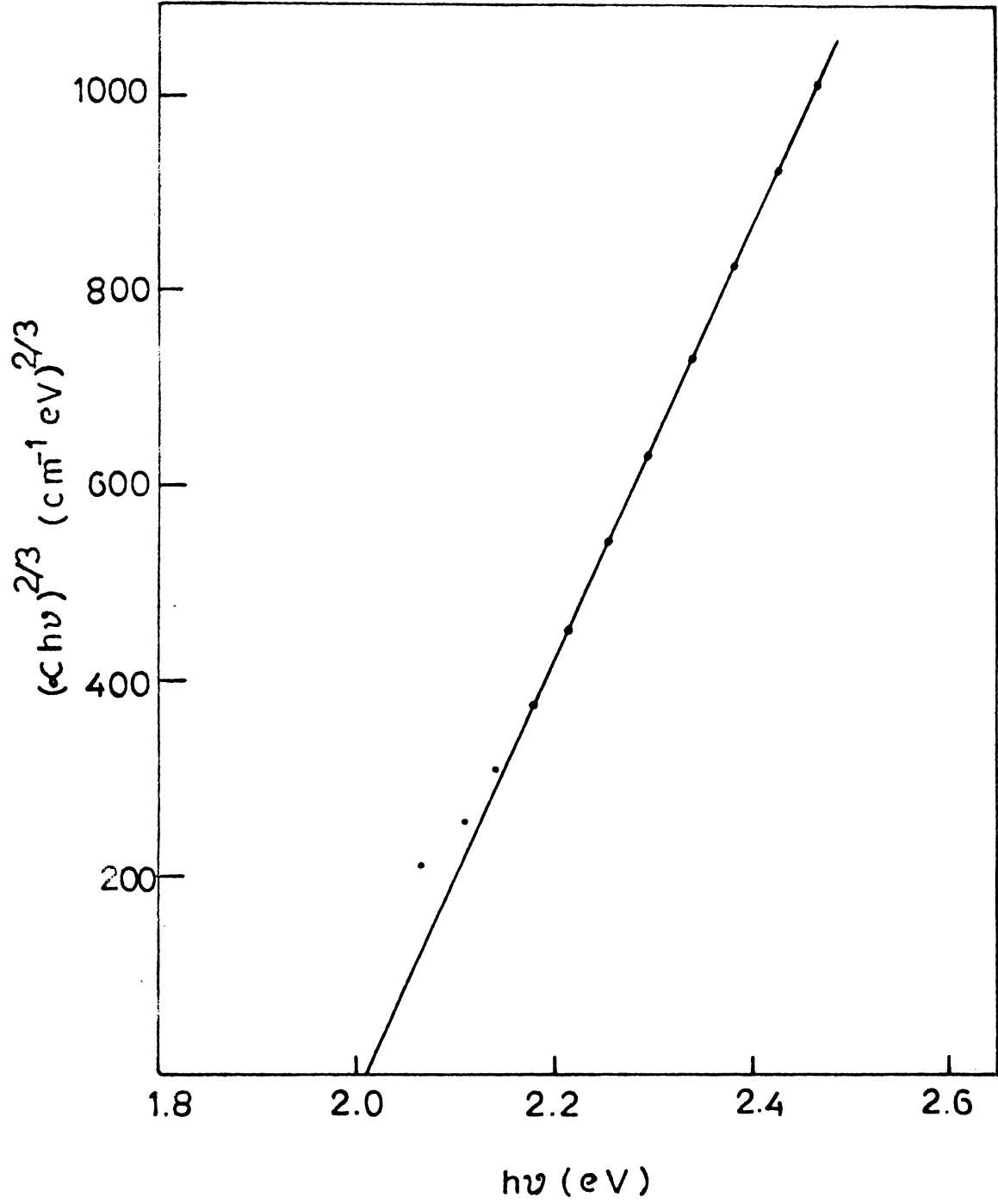


Figure 5. Plot of $(\alpha h\nu)^{2/3}$ versus $h\nu$ for a p - In_2S_3 film

published data for single crystals of β - In_2S_3 /4/. This functional dependence also shows that the transition is a direct forbidden one. Measurement of photoconductivity as a function of wavelength on β - In_2S_3 specimens also give a band gap around 2 eV /6, 3/.

From figure 3 it may be noted that for films prepared on room temperature substrate the absorption edge is shifted to shorter wavelengths and the fall in the transmission curve is different from that of films prepared above this temperature. Electrical measurements (to be discussed) also show that films prepared below a substrate temperature of 350K behave in a different manner from that of films prepared above that substrate temperature. Figure 6 shows $(\alpha h\nu)^{1/2}$ versus $h\nu$ for a film of thickness about 2 μ prepared at room temperature. It may be seen that this gives a band gap of 1.95 ± 0.01 eV, which is less than the band gap obtained for films prepared above a substrate temperature of 350K. The functional dependence of α on $h\nu$ is that of an indirect transition, but the magnitude of α ($> 10^3 \text{ cm}^{-1}$) in the present case rules out this possibility because for indirect transitions it is well known that α should be less than 10^3 cm^{-1} . The only other possibility which is there, is the case of the non-direct transition law which is obeyed by amorphous solids (see section 1.2 and equation 1.2.9). From what is given above, it may be concluded

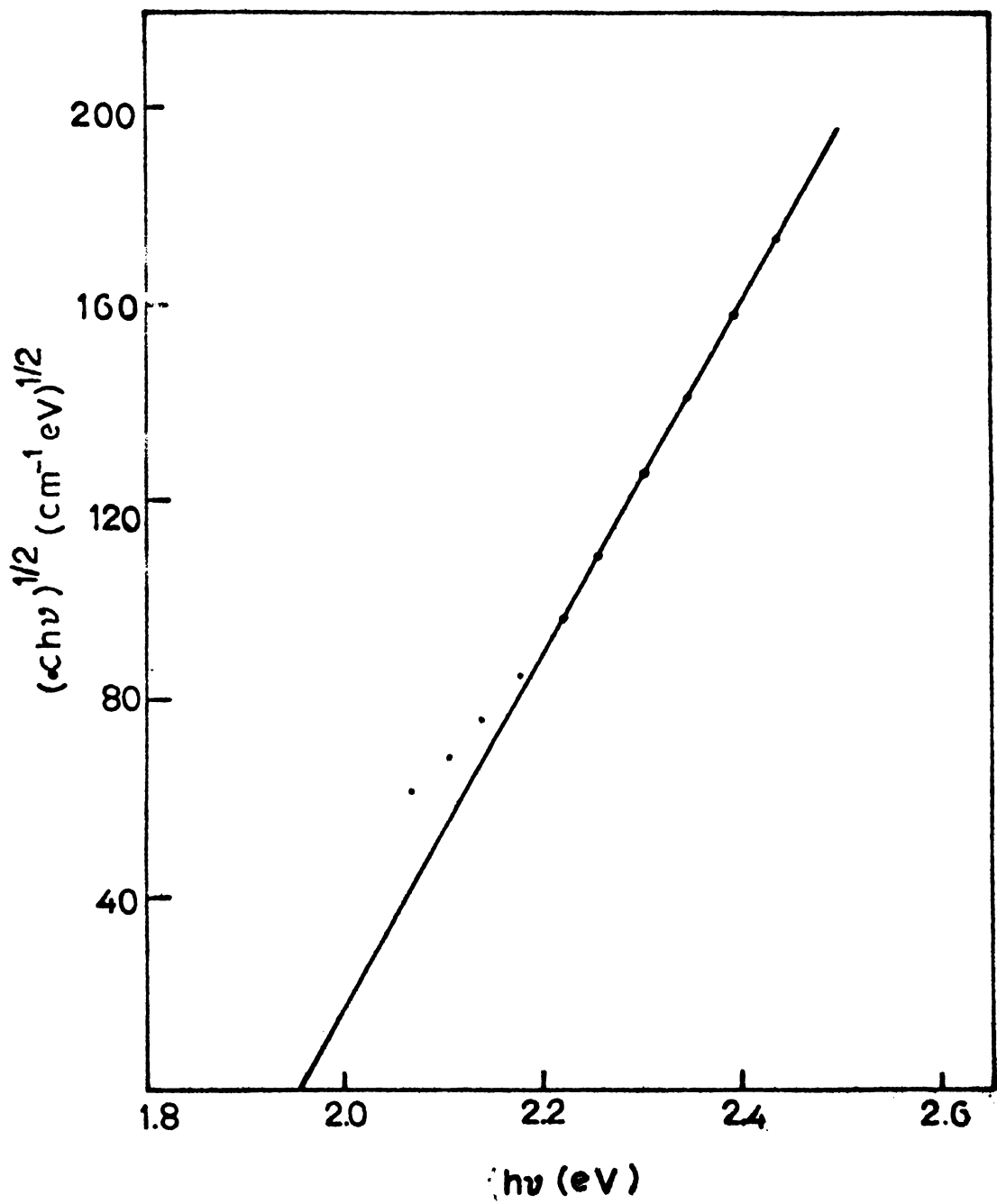


Figure 6: $(\alpha h\nu)^{1/2}$ versus photon energy.
Band gap is 1.95 ± 0.01 eV.

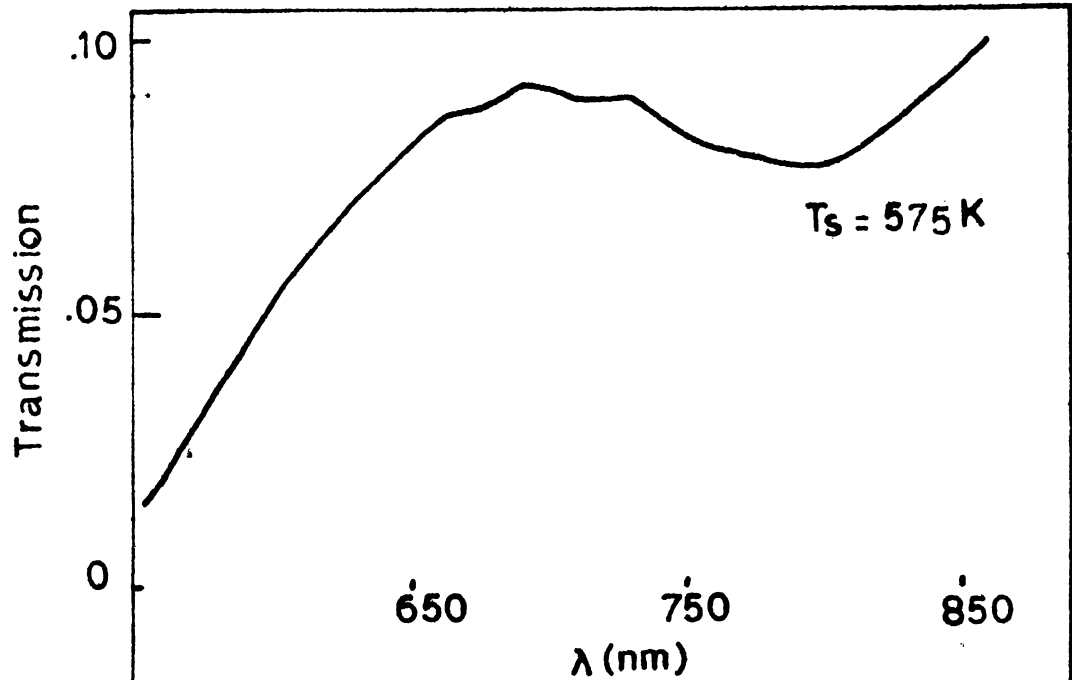


Figure 7(a): Transmission spectra of a film prepared at 575K. Thickness of the film is 2μ .

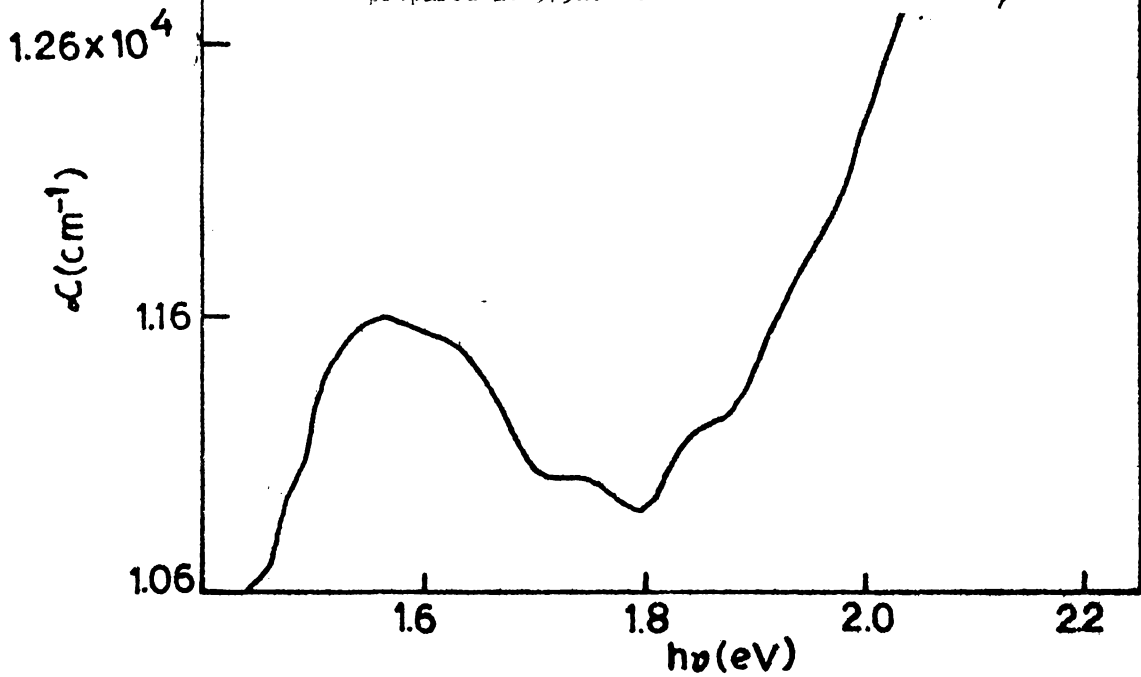


Figure 7(b): Variation of absorption coefficient as a function of photon energy.

that, films prepared below a substrate temperature of 350K are amorphous in nature, though no X-ray data is available at present.

Figure 7a shows the transmission spectra of a 2μ thick film prepared at 575K. The film obviously has a very low transmission. Figure 7b shows the variation of absorption coefficient as a function of photon energy. It may be seen that absorption coefficient show some structure which cannot be separated out into individual peaks. These absorption peaks can be due to different levels in the forbidden gap to which transitions may take place. Two defect levels may occur due to sulphur vacancies, which are doubly ionizable (two In outer electrons are left out from bonding due to a sulphur vacancy and these two electrons may be excited into the conduction band of the material with suitable activation). Another possibility is the formation of the disordered cubic phase (see beginning of this Chapter). More systematic low temperature optical absorption studies are needed to get information on the defect structure of In_2S_3 .

9.4 ELECTRICAL STUDIES

Electrical resistance measurements were carried out in the cell described in Chapter III. For resistance measurement a Hewlett Packard 3465A Digital Multimeter was used.

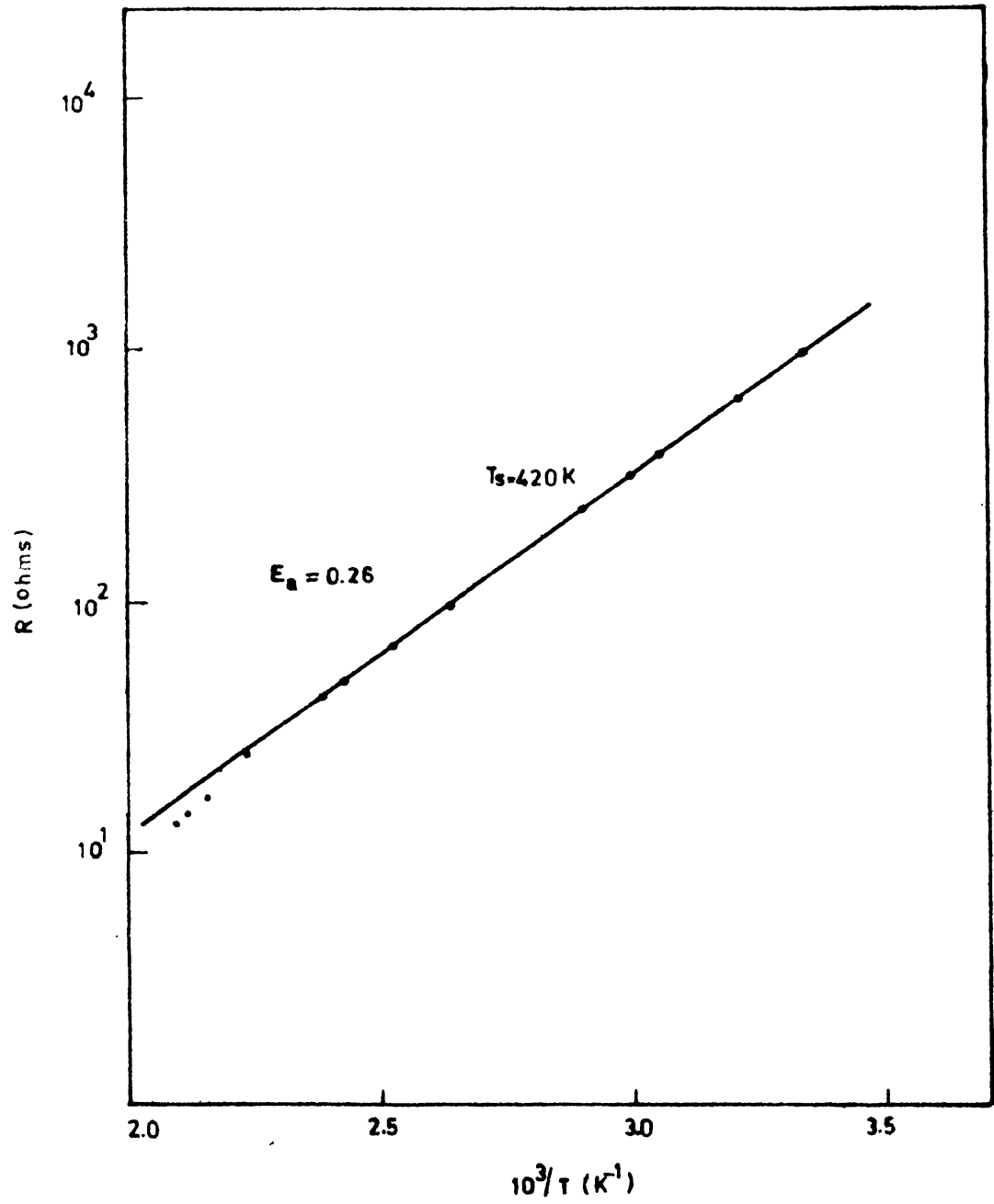


Figure 8: Temperature dependence of resistance of a film of thickness 600nm. Activation energy is 0.26 ± 0.02 eV.

Hot probe measurements showed that films are n-type. Electrically, the films could be classified into two groups according to the substrate temperature at which they are prepared. Films prepared above a substrate temperature of 350K were low resistivity films and indium made good ohmic contact to these films. Whereas films prepared below a substrate temperature of 350K showed high resistance and indium does not make ohmic contact to the films.

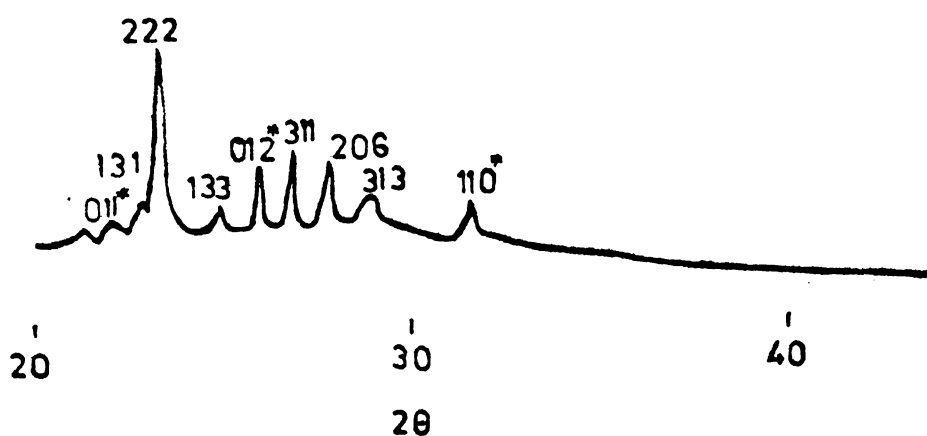
Figure 8 shows the temperature dependence of resistance of a film of thickness 600 nm prepared at a substrate temperature of 420K. Effective area of the film was 1cm^2 . It may be seen that data gives a good fit to the equation $\rho = \rho_0 \exp(E_a/k_B T)$. The activation energy for electronic conduction obtained in the present case is 0.26 ± 0.02 eV. Eventhough film resistivity decreased somewhat with increased substrate temperature, the activation energy obtained from electrical measurements for all films prepared at substrate temperatures greater than 350K were the same. The present result is in agreement with activation energy reported from Hall measurements in reference 4 on single crystals. However activation energy for electrical resistivity reported in reference 4 is slightly higher (0.34 to 0.41 eV). This indicates a temperature dependence of mobility in single crystals. But in thin films where the

mobility is controlled by grain boundaries, a temperature independent mobility is not unexpected and hence the agreement in the present activation energy value with that obtained from measurement of Hall effect in single crystals. It may be recalled that activation energy obtained from Hall measurements gives the depth of the level from the conduction (valence) band as it involves only the number of carriers; but resistivity measurements give a combined dependence on mobility and number of carriers.

Activation energy from electrical conduction obtained in reference 13 is 0.56 eV which is more than double that of the present value. This level cannot possibly be due to sulphur vacancies, because their samples were prepared at a sulphur pressure of the order of 5-10 atmosphere.

9.5 STABILITY OF β -In₂S₃ FILMS

It is found that β -In₂S₃ films prepared at substrate temperatures above 350K are very stable in the laboratory atmosphere. These films can be heated to 550K in air without the film getting oxidized. But films prepared below a substrate temperature of 350K are found to be unstable. These films deteriorated, upon storage in a desiccator for one month, into two phases. The X-ray diffraction pattern of such a deteriorated film is shown in figure 9. From the X-ray



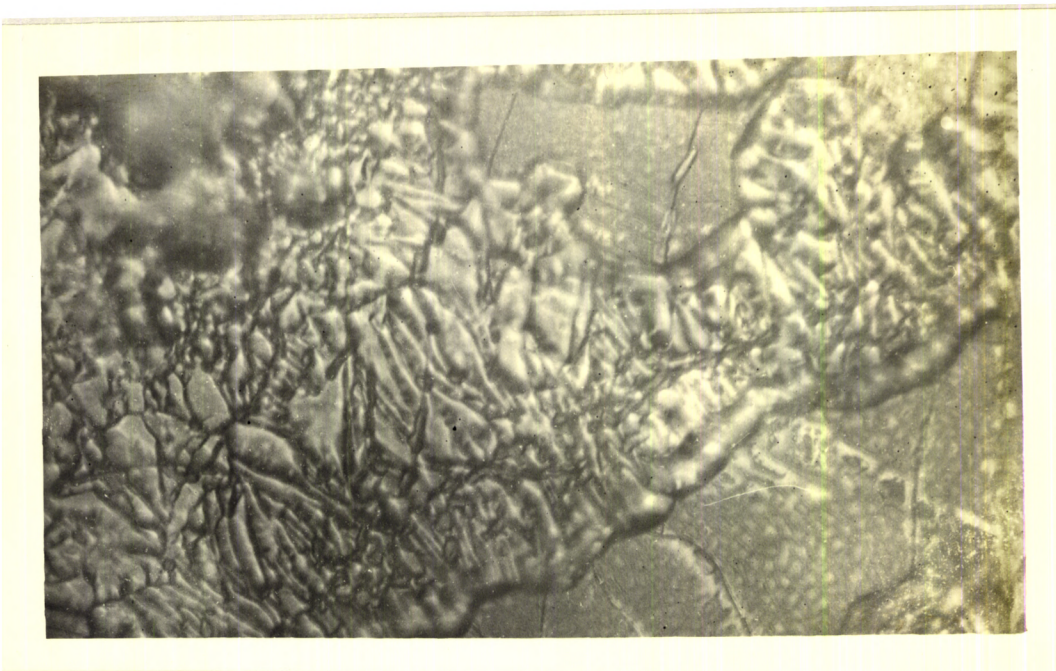
Orthorhombic Sulphur

InS

Present results

d (\AA°)	I/I_0	d (\AA°)	I/I_0	d (\AA°)	I
4.19	2	4.10	25	4.168	3
4.06	11			4.019	8
3.91	12			3.888	9
3.85	100			3.822	47
		3.70	50		
3.44	40	3.41	70	3.545	4
3.33	25			3.424	16
3.21	60			3.305	17
3.11	25			3.201	14
3.08	17			3.097	8
		2.951	100	3.066	8
2.842	18	2.843	40	2.842	18

Figure 9: X-ray diffraction pattern of a deteriorated film.



X100

Figure 10. Optical micrograph of a deteriorated film.

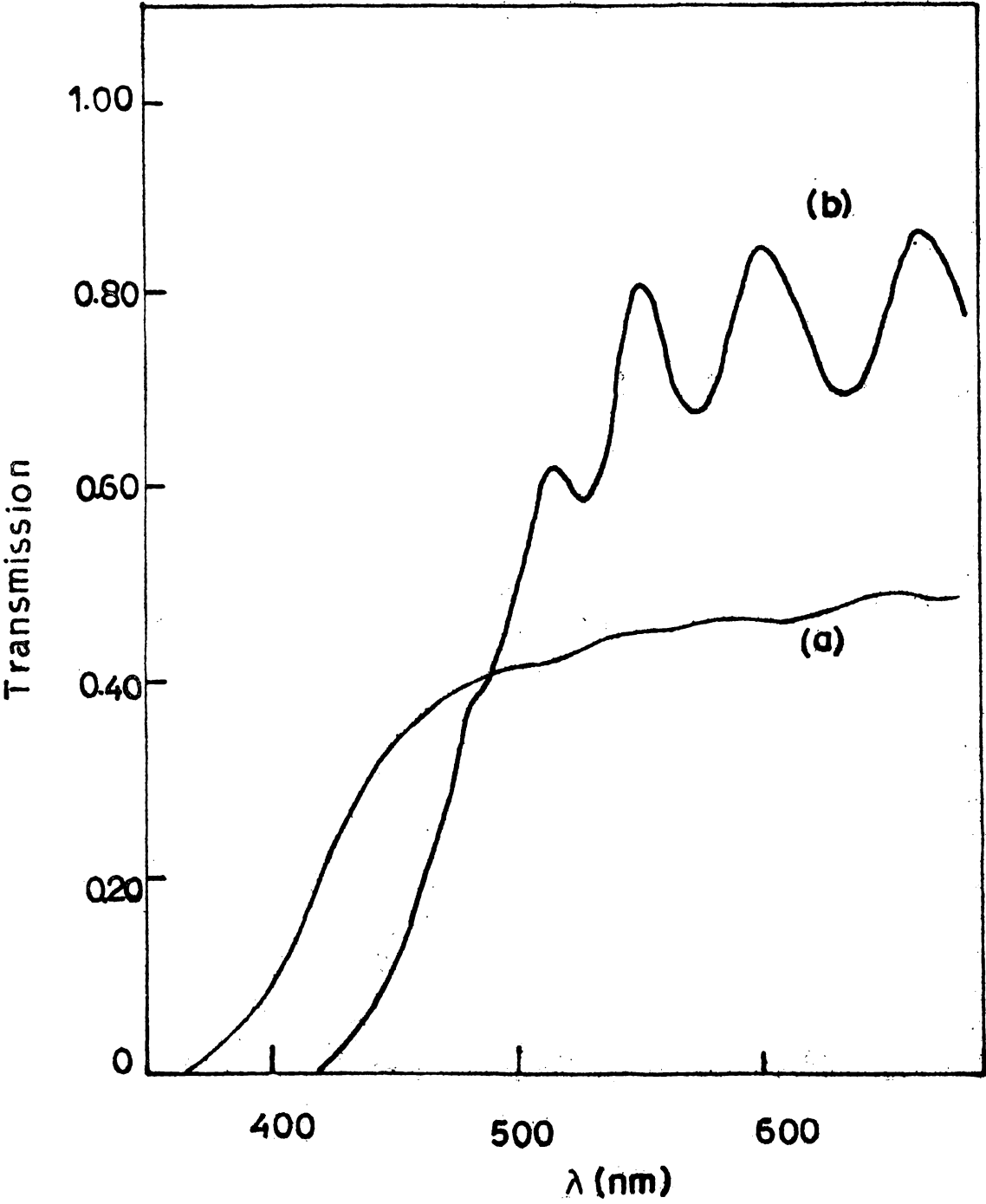


Figure 11: Transmission spectra of a deteriorated film together with that of a fresh film.

diffraction pattern it may be seen that the films have decomposed into InS and orthorhombic sulphur. Table I gives almost all the lines of orthorhombic sulphur together with lines of InS. We may here recall the decomposition of CuS into djurleite and rhombohedral sulphur described in Chapter VII, where because of the hexagonal symmetry of the underlying CuS layer, rhombohedral sulphur was formed. In the present case because of the cubic symmetry of the underlying β -In₂S₃, the most closely related sulphur structure (orthorhombic-three unequal axes inclined at 90°) is formed. This too is possibly an epitaxial nucleation and growth. Optical micrograph of a deteriorated film is shown in figure 10. Small sulphur crystallites may be easily identified. Transmission spectra of such a film is shown in figure 11 together with that of a fresh film. It may be seen that transmission is reduced considerably and the absorption edge is shifted to shorter wavelengths.

CONCLUSIONS

When indium is evaporated in an atmosphere of sulphur, In₂S₃ films are formed, rather than InS. This is different from other phase systems investigated in the present study, where the most sulphur rich phase is formed. Films prepared below a substrate temperature of 350K are amorphous in nature and have a band gap of

1.95 ± 0.01 eV. Films prepared above a substrate temperature of 350K are crystalline in nature and have a band gap of 2.01 ± 0.01 eV. Properties of the crystalline films obtained (surface smoothness, optical transmission, and refractive index) ~~goes~~ through an optimum at a temperature of 425 ± 50 K, in agreement with Vincett's concept of Critical Optimization.

References:

1. H. Welker, *Ergeb. d. exakt. Naturwissenschaften* 29 (1956) 275.
2. L. Pauling, *The Nature of Chemical Bond*, p 58, Cornell University Press, Ithaka, N.Y. (1948).
3. V.P. Zhuze and V.M. Sergeeva, *Sov. Phys. Solid State*, 2 (1961) 2562.
4. W. Rehwald and G. Harbeke, *J. Phys. Chem. Solids*, 26 (1965) 1309.
5. S. Dushman, *Scientific Foundations of Vacuum Technique*, p 697-699, Wiley, New York (1962).
6. R.H. Bube and W. McCaroll, *J. Phys. Chem. Solids* 10 (1959) 333.
7. H. Hahn and W. Klinger, *Z. Anorg. Allg. Chem.* 260 (1949) 97.
8. C.J. Rooymans, *J. Inorg. Nucl. Chem*, 11 (1959) 78.
9. J.V. Landuyt, H. Hatwel and S. Amelinckx, *Mater. Res. Bull.* 3 (1968) 59.
10. R. Diehl and R. Nitsche, *J. Cryst. Growth*, 20 (1973) 38.
11. R. Diehl and R. Nitsche, *J. Cryst. Growth*, 28 (1975) 306.
12. E. Kauer and A. Rabenau, *Z. Naturforschung* 13a (1959) 551.

13. J.M. Gilles, H. Hatwel, G. Offerfeld and
J. Van Cakenberghe, Phys. Status. Solidi
2 (1962) K73.
14. G.F. Garlick, M. Springford and H. Chęcinska,
Proc. Phys. Soc 82 (1963) 16.
15. P.S. Vincett, Thin Solid Films, 100 (1983)
371.

CHAPTER-X

FILMS PREPARED BY ACTIVATED REACTIVE EVAPORATION

Activated Reactive Evaporation is a versatile technique for depositing compound semiconductors. The main advantages of the process are, as discussed in Chapter II, (a) increased chemical reactivity of particles making it possible to use a low partial pressure of the reactive gas and consequent low wastage of the reactive gas (b) possibility of high deposition rates without abnormally increasing the partial pressure of the reactive gas and the consequent low probability of the entrapment of the unreacted gas as well as ambient gas in the growing film which will adversely affect film properties.

10.1 EXPERIMENTAL

In order to activate the reactive gas, an electric discharge must be produced in the reactive atmosphere. The usual ways of producing a low pressure electric discharge are (a) bombardment of reactive gas with electrons of suitable energy (b) using an RF or microwave source. The first method because of its simplicity and adaptability to the existing vacuum coating unit was chosen in these studies to activate the

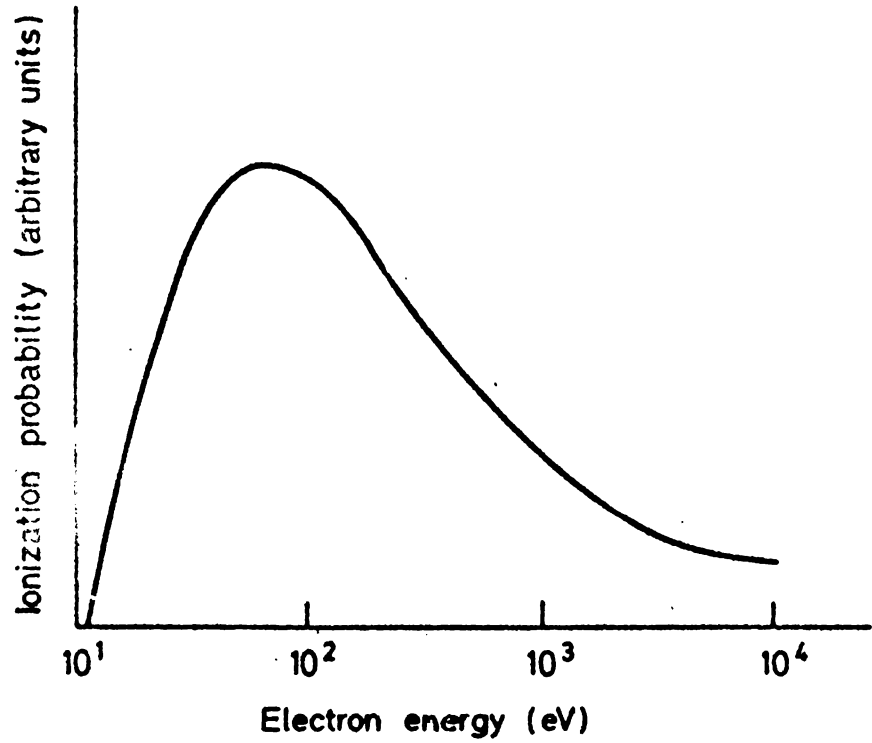


Figure 1: Ionization probability of a gas molecule on electron energy.

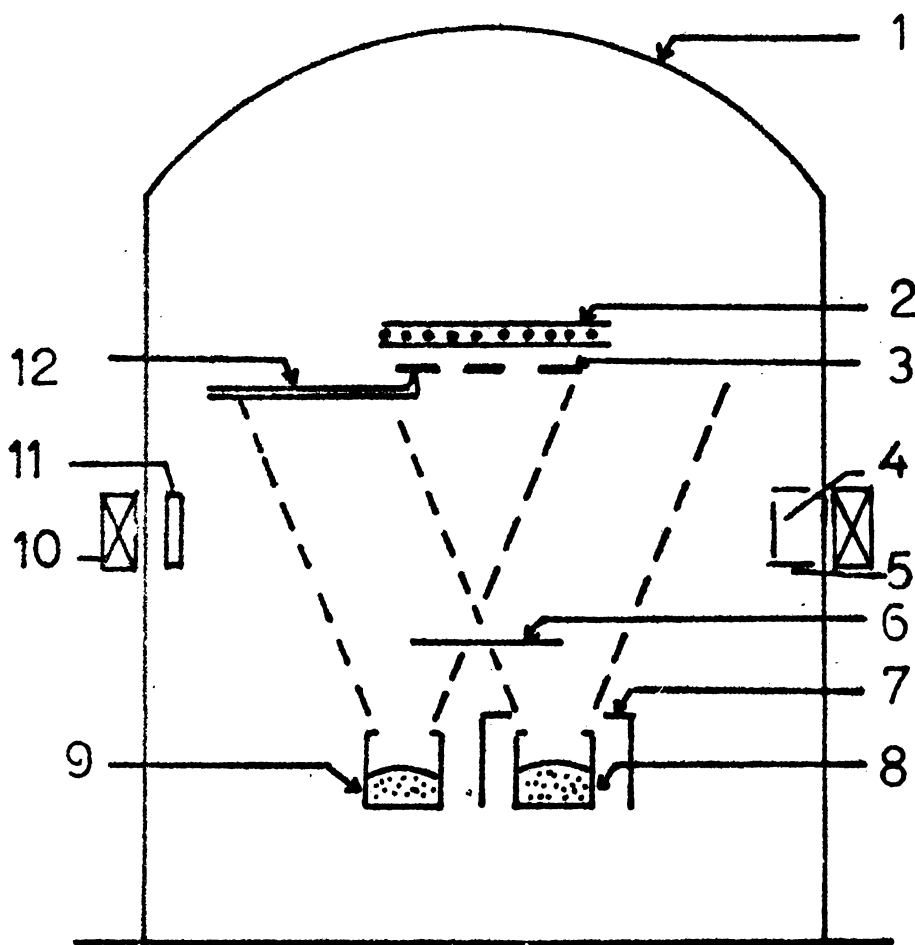


Figure 2: Set-up used for Activated Reactive Evaporation. 1. Bell jar, 2. substrate heater, 3. substrates, 4. electron emitter, 5. shield, 6. shutter, 7. heat shield, 8. metal source, 9. sulphur source, 10. field coil, 11. anode, 12. thermocouple.

suitable partial pressure was achieved in the chamber and after that, the electron emitter, magnetic field, and the anode supply was switched on. Within a short time, the filament emitted enough electrons and the discharge was established in the chamber. The electron filament current or the anode potential was then adjusted so that a suitable glow was maintained in the chamber. The metal was then evaporated at a suitable rate and the shutter over the metal source was withdrawn to allow film deposition on the substrates to take place. The discharge current was always kept constant at 1.5A.

The colour of the glow produced by sulphur vapours was blue.

10.2 FILMS OF TIN DISULPHIDE

The films of tin disulphide were prepared with the metal atom flux, sulphur partial pressure etc. the same as that used in the case of ordinary reactive evaporation. When tin atoms were ionized in the glow discharge it gave a pale blue colour. Films prepared by this technique had a golden yellow colour which is characteristic of tin disulphide and were more transparent than films prepared by ordinary reactive evaporation for a given thickness. Transmission spectra of such a film prepared on a room temperature substrate is shown in figure 3.

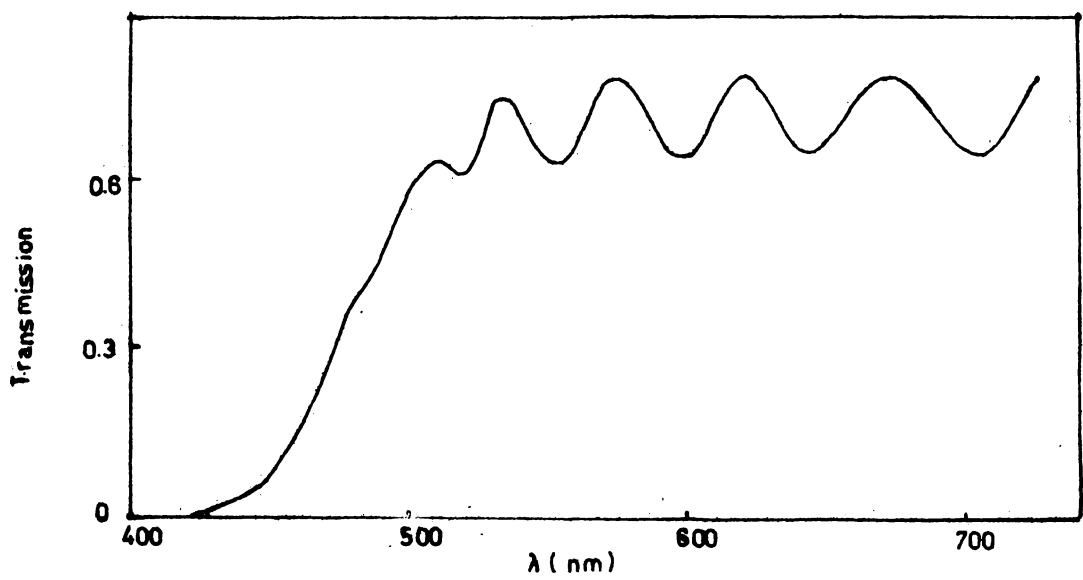


Figure 3. Transmission spectra of tin disulphide film prepared by ARE.

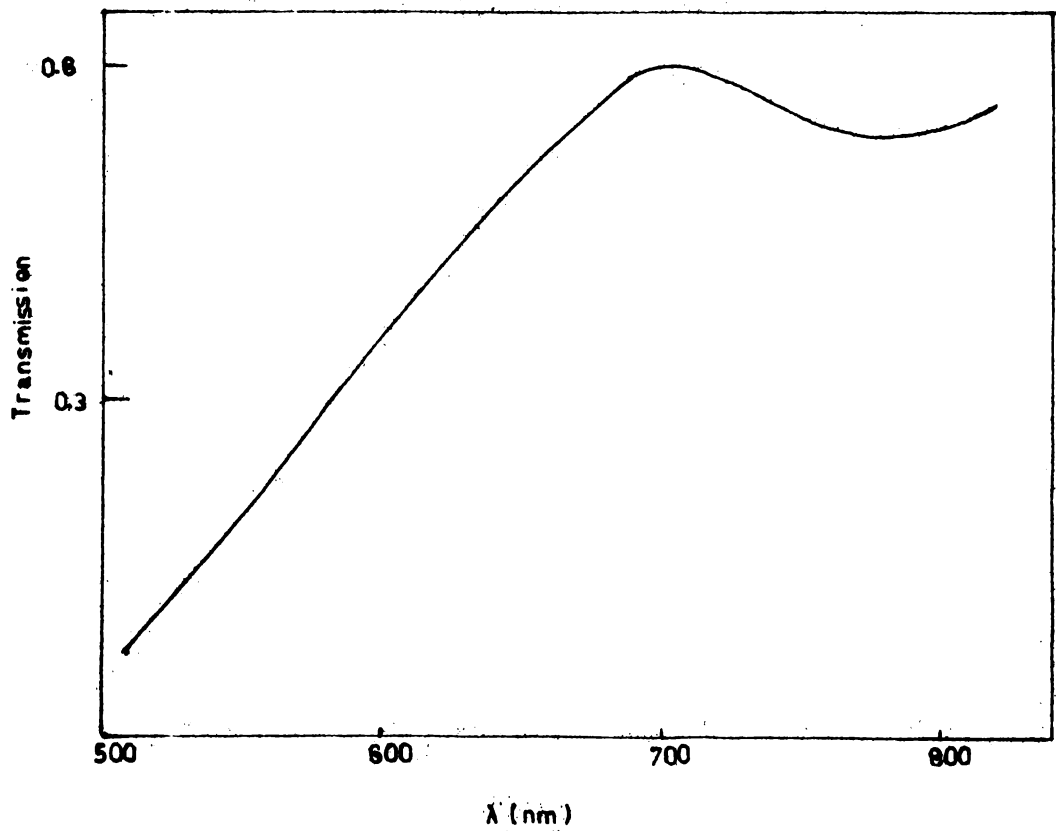


Figure 4. Transmission spectra of an amorphous SnS film prepared by ARE.

When substrate temperature was increased to more than 340K, a dust-like coating was found on the films and the transmission became poor as was found in the case of tin disulphide prepared by ordinary reactive evaporation.

10.3 FILMS OF COPPER SULPHIDE

For the deposition of copper sulphide also, the particle flux was the same as that used for ordinary reactive evaporation of copper in sulphur atmosphere. Copper when ionized in the glow gave a green colour. The phase formed using this deposition was the same as that formed due to ordinary reactive evaporation (CuS). Below a substrate temperature of 315K, as in the case of ordinary reactive evaporation, the films were amorphous and above a substrate temperature of 320K, the films were crystalline in nature. Transmission spectra of amorphous and crystalline films prepared using ARE is shown in figure 4.

It is reported by Bunshah /1/ that when copper is evaporated in a glow produced using H_2S , Cu_2S (chalcocite) phase is formed. But in the present case because sulphur itself is evaporated to achieve the reactive atmosphere, the sulphur rich phase CuS, is formed. Bunshah's result may be due to the lesser sulphur content of his plasma.

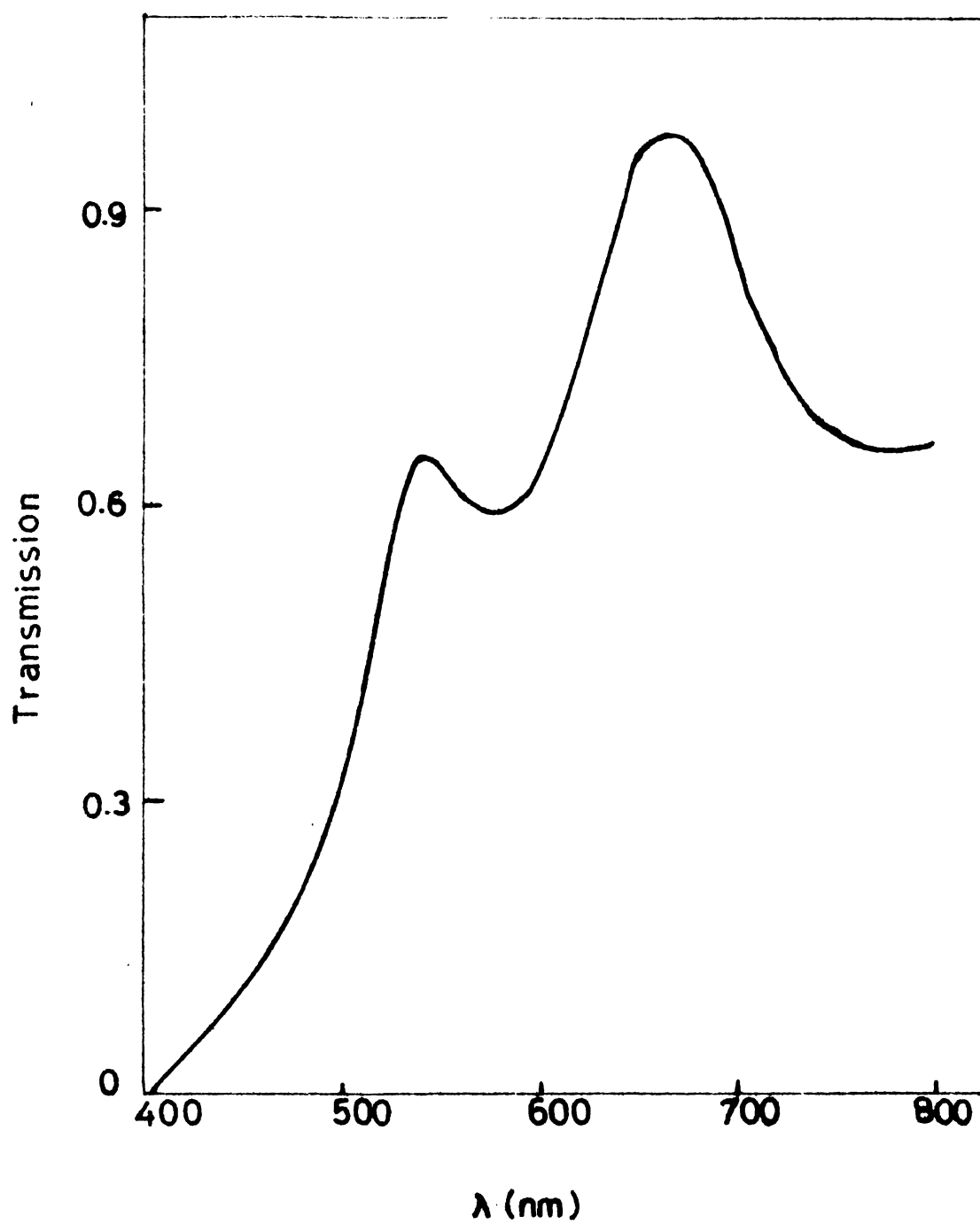


Figure 5. Transmission spectra of β - In_2S_3 film prepared by ARE. Note the quality of the film.

10.4 FILMS OF INDIUM SULPHIDE

Indium sulphide films was also prepared by ARE with the same flux and substrate temperature used for ordinary reactive evaporation. Indium when ionized gave a violet colour to the glow. In this case also there was no difference in the colour of the films formed from that of ordinary reactive evaporation except for a slightly higher optical transmission. Transmission spectra of such a film is shown in figure 5.

CONCLUSION

Films of SnS_2 , CuS and In_2S_3 are prepared by ARE. These films show more optical transmission than films prepared by ordinary reactive evaporation for the same thickness.

References:

1. R.F.Bunshah, Sol.Energy.Mater, 6 (1982) 445.

CHAPTER-XI

FORMATION OF COMPOUND FILMS IN
EVAPORATION TECHNIQUES

Kinetic energy of the ejected particles play an important role in the formation of compound films /1/. These include improvement of adhesion, removal of adsorbed impurities from substrate surface, enhancement of the growth of the nuclei at the early stages of film formation, enhancement in surface diffusion, increased chemical activity and change of morphology /2/. The presence of ions also increase film forming activity and chemical reaction. It greatly influences the critical parameters of the condensation process even when only a few percent of the atoms are ionized /3/. The most important phenomena observed in ion enhanced film growth can be divided into preferential orientation along a particular axis and growth at low substrate temperatures compared with other film growth techniques. As ions are electrically charged they can be given additional kinetic energy by accelerating them in electric fields. These accelerated ions when colliding with neutral particles effectively transfer some of these kinetic energies to them and this increased kinetic energy assist in the formation of good quality films. Ion Plating /4/, Activated Reactive evaporation /5/, and Ionized Cluster Beam Deposition /6/ are the

deposition techniques which utilize these increased kinetic energy^{and} ionization effects.

All these methods use some means to ionize the particles, usually electron bombardment or in some cases an RF discharge. There will also be some mechanism to accelerate the ions to give them the required kinetic energy. But the fact that kinetic energy and ionization effects also play an important role in ordinary 'non-ionized' techniques like flash evaporation and electron gun evaporation has not been taken into consideration in the earlier literature. In fact there is not much discussion in the literature about compound formation or the occurrence of epitaxy using these techniques. It will be shown here that one has to take into consideration increased kinetic energy and ionization effects in order to explain the formation of the compound film and the occurrence of epitaxy in these techniques. It will also be shown that Three Temperature Method (TTM) requires its high volatile to less-volatile flux ratios because of the low kinetic energies of the particles used.

11.1 EFFECT OF KINETIC ENERGY AND IONIZATION

Three Temperature Method (TTM) /7/

This method is based on the fact that continuous condensation of a given vapour on a substrate

at a given deposition rate is possible only if the substrate temperature drops below a critical temperature. Differences in magnitude of these critical values, which are functions of the interfacial energies, make it possible to condense a given vapour type or a combination (i.e., a compound) preferentially. These critical fluxes and temperatures act as some kind of limits and in general by a judicious selection of the fluxes and the substrate temperature, any particular compound/alloy of a multicomponent system can be condensed on the substrate. The basic ideas regarding this technique were put forward by Günther and he could deposit many technologically important III-V and II-VI compounds with bulk like properties. Here the individual components are evaporated separately and the compound made to form on the substrate by adjusting the individual fluxes and substrate temperature. In case the compound as well as the less-volatile element also deposit on the substrate at the particular substrate temperature chosen, the flux of the volatile element is increased so that in the growing film no unreacted less-volatile element remains. For this it is known that about ten to forty times excess of the volatile component flux is needed to get stoichiometric films /8,9/. If the volatile component is a gas at room temperature, the method is known as reactive evaporation.

We will now examine what is actually taking place in the process of film formation taking a typical example of a compound, say Bi_2Te_3 , containing a volatile element and a less-volatile element. Here bismuth is less-volatile and tellurium, volatile. Stoichiometric films of Bi_2Te_3 were obtained by Hänlein and Günther /8/ with a tellurium flux about ten to forty times more than what was needed. A high substrate temperature of $400\text{--}500^\circ\text{C}$ was used and apparently this high substrate temperature does not enhance chemical reaction. In the deposition of Bi_2Te_3 by TTM, tellurium was evaporated from crucibles maintained at low temperatures (temperature just enough to give the required vapour pressure) and the ejected particles will have only low energies. Because of their low energies these particles will have only low surface mobilities and the probability of these particles colliding with an adsorbed atom of a less-volatile element with sufficient energy for chemical reaction (to be discussed) will be low. After a finite time (called the 'dwell time'), as the substrate temperature is such that the formation of the film of the volatile element is not possible, the volatile atoms which are not chemically bound will be desorbed.

For any chemical reaction to take place a certain activation energy is necessary /10/. This is the height of the energy barrier which has to be overcome in order for

chemical reaction to occur. In most cases reaction does not invariably occur when two reactant molecules collide with each other and even if the relative orientations are suitable, the molecules must possess between them a certain amount of energy. A schematic potential energy diagram for the system $A + B \rightarrow C + D$ is shown in figure 1. The reactants must possess between them an energy equal to E_a (the activation energy for chemical reaction) to reach the activated state which is the maximum of the potential energy barrier. These activated complexes are transient species passing from the initial to the final state. Thus once the particles together get the required energy, they will react to form the compound. The reaction rate is temperature dependant and always obeys a law of the form /11/

$$r_a = A_a \exp(-E_a/kT) \quad (11.1)$$

where A_a is a constant. From this equation it can be seen that the reaction rate increases as the temperature is increased. This is due to the increase in kinetic energy of the particles with temperature. It is evident that if we increase the kinetic energy of the particles, keeping the substrate temperature constant, the reaction rate should increase. It is not possible to increase the particle energies without increasing the temperature in chemical reactors, but is readily possible in vacuum

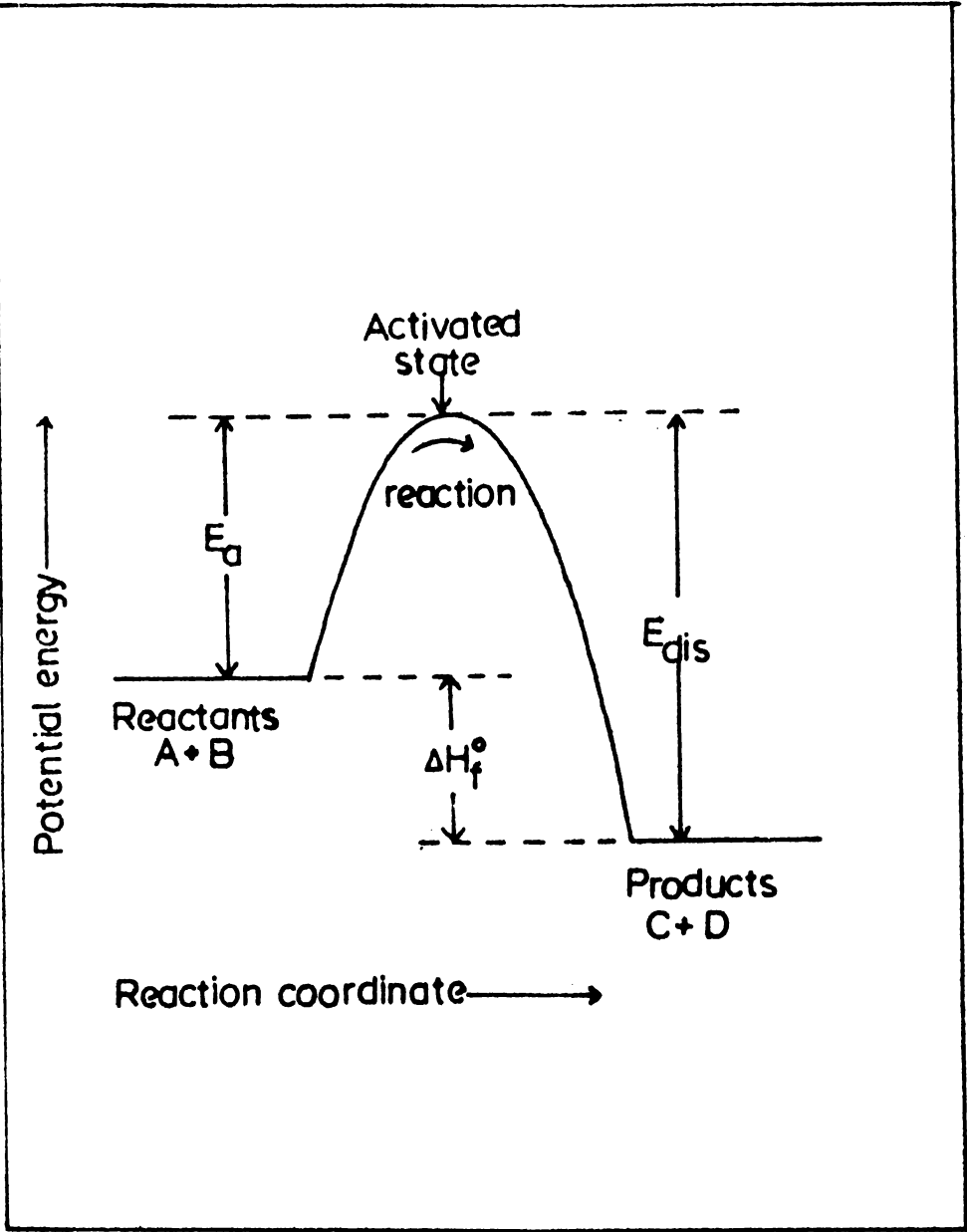


Figure 1: Schematic potential energy diagram for the system $A+B \rightleftharpoons C+D$ with ΔH_f° , the heat of formation of the compound, negative. E_a is the activation energy needed for chemical reaction, E_d the energy needed to dissociate the compound into component elements.

techniques by increasing the source temperature or by ionizing the particles and accelerating them in electric fields.

Activation energy for most surface process are always almost greater than 0.5eV, usually varying from 1 to 5 eV /12/. If we assume that the ejected particles cannot lose their energies once they are ejected from the boat, we can take the reaction being effectively taking place at the source temperature (or mean of the source temperature in TTM) on the substrate surface. This involves the assumption that the particles on impinging the substrate surface do not transfer energies to it. This assumption is somewhat justified, because, usually the substrate is heated to a certain extent and particles will not lose much of their energies on impingement to the substrate surface. This assumption, though crude, will allow us to equate T in the denominator of (11.1.1) to source temperature (or mean particle energies if we take $k_B T$) rather than to substrate temperature. Figure 2 shows the dependence of relative reaction rate on the mean source temperature for systems with activation energy equal to 1 eV and 3 eV. From the curve for $E_a = 3\text{eV}$, it can be seen that for a change in source temperature from 900°C to 1000°C , there is an order of magnitude change in reaction rate.

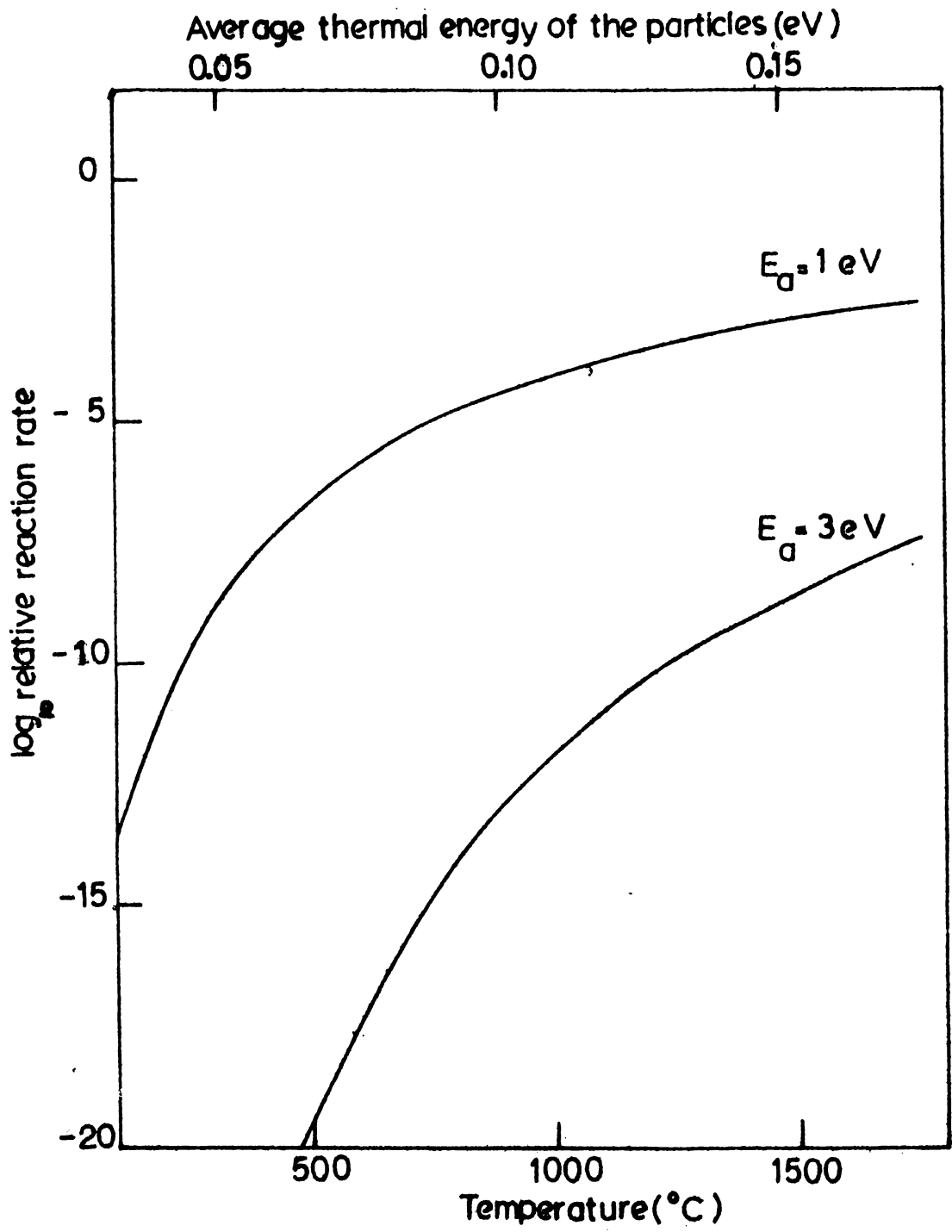


Figure 2: \log_{10} relative reaction rate Vs. temperature of the source.

Because of the low temperature at which particles are evaporated in TTM ($T_{\text{Bi}} = 750^{\circ}\text{C}$, $T_{\text{Te}} = 350^{\circ}\text{C}$, in the case of Bi_2Te_3), the ejected particles are not energetic. As the particles are of low average energy (less than 0.1eV) only a small fraction ($1/10$ to $1/40$ in the case of Bi_2Te_3 as found experimentally) of them will be able to cross over the potential barrier and form the compound. All the other particles which could not form chemical bond are reevaporated and hence we need the large flux ratios.

In many cases where TTM has been used, the substrate temperature was not high enough to supply the required activation energy. But if one increases the substrate temperature arbitrarily to get high reaction rates and epitaxial ordering, the dissociation rate of the formed compound will also increase rapidly, and hence it is necessary to condense the compound at a substrate temperature as low as possible. The substrate temperature should be such that the condensation of the individual components are prevented and is more or less fixed for a particular compound.

One more factor is that chalcogens tend to evaporate as molecular aggregates rather than monomers or dimers [13, 14]. These molecular aggregates are chemically less active [15]. Table I shows the vapour species observe

TABLE I*

Vapour species observed in the case of Sulphur at different temperatures.

Temperature, °C	Molecular composition of sulphur vapour		
	S ₆ + S ₈	S ₂	S
445	96.1	3.8	0.1
800	3.0	96.7	0.3
1000	-	98.6	1.4
1400	-	85.7	14.3

*From reference 13.

in the case of sulphur at different temperatures /13/. It can be seen that sulphur evaporates as S_6 and S_8 molecules at the low temperatures used in TTM (around 150°C). It is evident that unless these aggregates are broken into monomers or dimers, chemical reaction will not take place and consequently a large proportion of the chalcogens will be rejected from the substrate surface.

It is clear from the above discussion that in the TTM if one of the components is volatile, about ten to forty times excess of the volatile component flux will be necessary to get good stoichiometric films. But in the special case where both the components are volatile, apparently 1:1 flux ratios have been reported /16/, and it may be at the cost of reevaporation of both the components. Unfortunately no work has been done to correlate the amount of material evaporated and film thickness to determine how much material has been lost from the substrate surface.

Flash Evaporation /17/.

In flash evaporation the powder of fine grains of the evaporant is fed into a boat which is hot enough to vapourize all the components of the powder instantaneously. A grain of the powder striking the boat decomposes and gives off the more volatile component first, and the final composition of the vapour consist of the less volatile element. If the powder delivery is slow, a grain which is

dropped into the boat is completely vapourized before the next one arrives and the film which would be formed on the substrate under these conditions would consist of alternate layers of the constituent elements. If the alternate layers can be made less than one monolayer in thickness, i.e., by using smaller grains and large source to substrate distance, the impinging atoms will recombine on the substrate surface to form the compound. In practice since the feed of the material is continuous, there will be grains at different stages of evaporation on the boat and as no material accumulates on the boat during evaporation, the vapour which is produced has almost the same composition as the evaporant. If the substrate temperature is not high enough so that reevaporation does not take place, stoichiometric compound films will be formed. Thus it can be seen that, after the dissociation of the compound on the surface of the boat, the vapour species travel independently to the substrate surface with the stoichiometric flux ratio and the process may be viewed as analogous to TTM. As such if the flash evaporated material contained a volatile element, it can be seen that there will absolutely be no possibility of forming the compound film on the substrate surface. But this is not true. As an example where flash evaporation has been used successfully in the formation of good quality films we will discuss the case of CuInSe_2 .

This is a sufficiently complicated molecule where Cu and In are less-volatile and Se volatile. Strelchenko et al /18/ has reported that the compound dissociates when heated and they have detected vapour species of In_2Se_3 and Se_2 in the temperature range $600\text{--}860^\circ\text{C}$ and no copper or copper binaries were detected at this temperature range. It has also been reported that with a source temperature of 1200°C , the films contain excess In /19/. The copper liberated due to the dissociation of the compound will not evaporate at a fast rate and hence an apparent indium excess in the films obtained. Copper will reach the required vapour pressure for evaporation (10^{-2} Torr) only at 1270°C /20/. Using a source temperature in excess of 1300°C and a substrate temperature of 400°C stoichiometric films of CuInSe_2 were obtained by many authors /21,22/. At this substrate temperature, Se will be having a vapour pressure of 10 Torr /20/ and it is known that Se will not form a film by itself on the substrate with a reasonable rate of impingement /7/. The vapour pressures of Cu and In at this substrate temperature are negligible and it can be safely assumed that all the Cu and In atoms impinging on the substrate will stick. Because of its large vapour pressure, almost all the Se atoms should reevaporate and no compound films should be formed without ten to forty times excess of Se flux. But Newmann et al report the epitaxial growth of CuInSe_2 using flash evaporation on GaAs where twin free layers were obtained at a substrate temperature of 600°C /23/.

For epitaxial growth on Germanium (III) surfaces the same authors give a substrate temperature of 450-550°C /25/.

The formation of good quality films at these substrate temperatures can only be explained if we take into consideration the increased kinetic energy of the ejected particles consequent to evaporation from high temperature sources. All the elements present in the compound after dissociation is evaporated with an effective kinetic energy corresponding to this high source temperature. The increased kinetic energy of the ejected particles gives them increased mobility on the substrate surface and there is a good chance that these atoms may collide with another adsorbed atom of the less-volatile element with sufficient energy for the chemical reaction to take place and to form the compound. Referring to figure 1 it can be seen that the dissociation energy is greater than the activation energy necessary for chemical reaction. After the dissociation of the compound in the boat, as the components travel independantly to the substrate surface without transferring their kinetic energy to any medium, it must be possible to form the compound once again when they mutually collide on the substrate surface, the excess energy being taken up by the substrate. It is evident that the compound will be formed so long as the components travel in stoichiometric ratio to the substrate surface. The only requirement on the source temperature being that it should be such that

evaporation of all the components liberated due to dissociation take place almost simultaneously, unlike the case of CuInSe_2 with a source temperature of 1200°C , when copper will remain in the boat after dissociation.

The guaranteed recombination of the components on the substrate surface as discussed above is based on the earlier assumption that the components do not lose any energy when they impinge independently on the substrate surface. If some energy is lost to the substrate surface, the chemical reaction may suffer, but this can be taken care of adequately by increasing the evaporation source temperature which in turn will give the particles more energy. If epitaxial growth at a low substrate temperature is required, the source temperature should be further increased to give the particles additional kinetic energy which in turn will give them sufficient mobility on the substrate surface for epitaxial ordering. These requirements cannot be met in ordinary single source evaporation unless one uses a high source temperature and short deposition time. This is not usual and only rarely one come across such a deposition. As an example let us look into the case of the epitaxial deposition of AgSbSe_2 on alkali halide substrates using single source evaporation by Patel and Lakshminarayana /25/. They rapidly evaporated the whole charge at a deposition rate of $100\text{\AA}/\text{sec}$. Epitaxial films were obtained at a substrate temperature of 200°C . Considering the deposition

rate, which is rather high for epitaxy to occur in vacuum evaporation techniques, where thermodynamical equilibrium is not maintained, it must be concluded that the high source temperature used to get the high deposition rate and the resulting enhanced kinetic energy of the ejected particles must be responsible for epitaxial growth at such high rates of deposition. It is certain that the compound will be formed when evaporated from high temperature sources whether the material dissociated or not during evaporation. It may here be mentioned that the authors have not considered these aspects of the formation of the epitaxial film. The only drawback is one cannot get thick films by this method and as the time taken for evaporating large quantities of material will be long, all the defects of single source evaporation will be present there.

Evaporation at high temperature and consequently high kinetic energy of the ejected particles is precisely what is happening in flash evaporation. Since flash evaporation is a 'pulsed process', the average deposition rate can be kept rather low by adjusting the frequency of the vibrator or by adjusting the feed rate. This will give enough time for the adsorbed particles to react and also to orient themselves favourable with any underlying crystallographic orientation. Thus if flash evaporation is used with a high source temperature and slow powder delivery, it must be

possible to grow high quality epitaxial films without much difficulty on oriented substrates. It does not mean that epitaxial growth will be possible at any arbitrarily low substrate temperature. The effect of substrate temperature on epitaxial growth is not yet clearly understood. But in vacuum systems where pressure is rather high ($p > 10^{-6}$ Torr) in which flash evaporation is usually practiced, substrate heating will be necessary to keep the substrate clean of ambient molecules which may inhibit epitaxial growth.

Electron Beam Evaporation

Effect of increased kinetic energy and ionization is also manifested in the electron beam evaporation of compounds. It is to be expected that compounds will dissociate in electron beam evaporation as in conventional resistance heating. The only difference being, in the electron beam evaporation, the charge is heated at the point where the electron beam strikes, whereas in resistance heating the charge is heated as a whole and decomposition of the compound occurs in both cases. In the latter case dissociation occurs in the bulk and the more volatile element may evaporate away first leaving a residue, rich in the less-volatile element. Ionization of ejected particles is well known as a nuisance in electron beam evaporation as they affect the performance of most ionization gauges and also crystal monitors /26/. As the elemental

vapours travel independantly after dissociation in electron beam evaporation, the process may also be viewed analogously to TTM, in which case there is not much chance of compound formation as already pointed out. But electron beam evaporation, due to the shallow penetration depth of the electron beam into the material, is a 'point by point' evaporation technique and also the electron beam imparts high kinetic energy to the ejected particles. We have seen that if the compound dissociates and the components evaporate simultaiously, the formation of the compound on the substrate is not difficult. This is achieved in electron beam evaporation. The high kinetic energy imparted by the electron beam gives the particles additional energy for taking up any preferred orientation on substrate surface. Let us consider the epitaxial growth of CdS films on alkalie halide substrates by Holt and Wilcox using electron beam evaporation /27/. These authors could grow epitaxial films on BaF substrates from 0°C to 550°C (Substrate temperature) at a growth rate of $10\text{\AA}/\text{sec}$ and polycrystalline films down to -100°C . The occurance of epitaxy, apparently without any energy being supplied by the substrate, must be due to the enhanced kinetic energy and ionization of the particles. This will also explain how it is possible to form the compound even at substrate temperature of -100°C where it is certain that the components will stick independantly without any reaction being taking place had they

been evaporated from low energy sources as in the case of TTM. Even if any reactions took place, the deposits should have been amorphous in nature. The formation of polycrystalline films at these low substrate temperature suggest, that the particles themselves contain energy for chemical reaction and also for epitaxial ordering. The formation of the compound at the high temperature of 550°C may be due to the increase in sticking coefficient of the particles due to ionization /3/, otherwise both Cd and S would have reevaporated because of their highly volatile nature.

11.2 GENERAL REMARKS

From these discussions it is seen that TTM is a low energy process in the sense that the particles used for film formation are of very low energy and these particles will have only low mobilities on the substrate surface. Substrate temperature is more or less fixed due to considerations regarding the condensation and the dissociation pressure of the volatile element. It was hoped that by using TTM any particular compound of a binary or ternary system can be deposited by varying the substrate temperature. Eventhough stoichiometry can be varied to some extent, the formation of different compounds of a particular system by varying the substrate temperature has not so far been reported. If the

TABLE II

Comparison of the different evaporation techniques for the deposition of compound films

Method	Whether ionization and accelerated particles exists	Kinetic energy of the particles	Source temperature	Substrate temperature	Remarks
1	2	3	4	5	6
THM	No	Low	Just enough to get the required vapour pressure	Dependant on the condensation temperature of the more volatile element	Epitaxial films possible, but more suitable for the deposition of amorphous films
Flash Evaporation	No	Medium	Should be high to evaporate all the dissociated components at a high rate	Independent	More suitable for the deposition of polycrystalline and epitaxial layers
Electron gun Evaporation	Ionization present	Medium	-	Independent	Same as above

(Contd.)

1	2	3	4	5	6
Ion Plating	Ionization and acceleration of ejected per- ticles	High	Dictated by the rate of chemi- cal reaction at the substrate	Independent	Formation of compound films at a high rate. Suitable for the synthesis of high melting point Carbides, Nitrides and Oxides
Activated Reactive Eva- nents ionized poration	Both the compo- nents ionized	High	Same as above	Independent	Same as above
Ionized Clus- ter Beam	Components ionized	High	Same as above	Independent	Same as above

Particle energies - low: less than 0.1 eV; medium: less than 1 eV; high: less than 10 eV.

compound contain a volatile element (a chalcogen) the substrate temperature to be used will be usually low. Hence this method is best suited for the deposition of amorphous chalcogenide films. Another advantage is that the synthesis of the compound is not necessary.

In contrast, flash evaporation and electron gun evaporation are high energy processes. Formation of amorphous films using these techniques are difficult because of the high kinetic energies of ejected particles which favour crystalline phases. Hence these methods are more suited for the deposition of polycrystalline and epitaxial films. The advantage of these techniques is that the formation of the compound is independent of substrate temperature.

A comparison of the different techniques is summarized in table II.

CONCLUSIONS

To explain the formation of compound films and epitaxial growth in ordinary techniques like flash evaporation and electron gun evaporation, we have to take into consideration the increased kinetic energy of the evaporated particles. The formation of the compound depends on the collision of the adsorbed particles with sufficient energy to overcome the potential barrier for

reaction. After the dissociation of the compound in the boat, as the dissociated components travel independently to the substrate surface without transferring their kinetic energy to any medium, it will be possible to form the compound once again when they mutually collide on the substrate surface. If some energy of the particles is lost due to their impingement on the substrate surface, this can very well be compensated by increasing the source or substrate temperature in the case of flash evaporation. In electron gun evaporation the particles are so energetic that this problem does not arise. But in TTM the components are evaporated from low temperature sources and they have only low kinetic energies. Because of their low kinetic energy these particles will not be mobile on the substrate surface and the probability of these particles colliding with enough energies to form the compound will be low. Hence the need for a large flux of the volatile element to form the compound. Because of the low energies of the ejected particles used in TTM, the method is best suited for the preparation of amorphous layers if a low enough substrate temperature can be used. This is practically impossible with flash evaporation and electron gun evaporation, because of the inherent kinetic energies of the ejected particles. Hence flash evaporation and electron gun evaporation are more suitable for the deposition of polycrystalline layers.

References:

1. T. Takagi, Thin Solid Films, 92 (1982) 1 and references therein.
2. M. Marinov, Thin Solid Films, 46 (1977) 267.
3. F. Kitagawa and K. Takahashi, Thin Solid Films, 77 (1981) 273.
4. D.M. Mattox, Electrochem. Technol, 2 (1964) 295.
5. R.F. Bunshan and A.C. Raghuram, J. Vac, Sci. Tech, 9 (1972) 1389.
6. T. Takagi, I. Yamada, M. Kunori and S. Kobiyama, Proc. 2nd Int. Conf, on Ion Sources, Vienna 1972, Österreichische Studien - Gesellschaft für Atomenergie, Vienna, 1972, p. 790.
7. K.G. Günther in Use of Thin Films in Physical Investigations ed. J.C. Anderson, Academic Press, London, 1966, p.213.
8. W. Haenlein and K.G. Günther, Naturwissenschaften 46, 319 (1959).
9. J. George and K.S. Joseph, J. Phys. D.15, 1109 (1982).
10. S. Arrhenius, Z. Physik. Chem. 4, 226 (1889).
11. K.J. Laidler, Theories of Chemical Reaction, McGraw Hill; New York 1969, Chapters 1, 2 and 3.
12. D.W. Shaw in Crystal Growth, Theory and Techniques; ed. C.H.L. Goodman, Plenum Press, New York, 1974, Vol 1, p.11.

13. A. Volsky, E. Sergievskaya, Theory of Metallurgical Processes, Mir Publishers, Moscow, 1978 p.299.
14. R. Yamdagni and R.F. Porter, J. Electrochem. Soc. 115, 601 (1968).
15. V.N. Kondrat'ev, Chemical Kinetics of Gas Reactions, Pengamon Press: London 1964, Chapter 7.
16. N. Romeo, G. Sberveglieri and L. Tarricone, Thin Solid Films, 55 (1978) 413.
17. E.M. Seigel and L. Harris, J. Appl. Phys. 19 (1948) 739.
18. S.S. Strel'chenko, S.A. Bondan, A.O. Molodyk, L.I. Berger and A.E. Balanevskaya, Izv. Akad. Nauk SSR Neorg Matter, 5 (1969) 563.
19. R.D. Tomlinson, D. Omezi, J. Parkes and M.J.Hampshire, Thin Solid Films, 65 (1980) L3-L6.
20. S. Dushman, Scientific Foundations of Vacuum Technology, John Wiley: New York 1962, Chapter 10.
21. B. Schumann, C. Georgi, A. Tempel, G. Kuhn, N.V. Nam, H. Newmann and W. Horig, Thin Solid Films 52 (1978) 39.
22. E. Elliot, R.D. Tomilson, J. Parkes and M.J.Hampshire, Thin Solid Films 20 (1974) 525.
23. H. Newmann, E. Nowak, B. Schumann and G. Kühn, Thin Solid Films 74 (1980) 197.
24. B. Schumann, A. Tempel, C. Georgi and G. Kühn, Thin Solid Films 70 (1980) 319.

25. A.R. Patel and D. Lakshminarayana, Thin Solid Films 98 (1982) 59.
26. R. Glang in Handbook of Thin Film Technology ed. L.I. Maissel and R. Glang, McGraw Hill; New York 1970 p.150.
27. D.B. Holt and D.M. Wilcox, Journal of Crystal Growth, 9 (1971) 193.